Human mononuclear phagocytes and their control by IL-10 in health and inflammatory bowel disease

Inva Hoti

Submitted to the University of London for the degree of Doctor of Philosophy

August 2018

Centre for Immunobiology

Blizard Institute

Barts and The London School of Medicine and Dentistry

Queen Mary, University of London

Statement of originality

I, Inva Hoti, confirm that the research included within this thesis is my own work or that where it has been carried out in collaboration with or supported by others, that this is duly acknowledged below, and my contribution indicated. Previously published material is also acknowledged below.

I attest that I have exercised reasonable care to ensure that the work is original, and does not to the best of my knowledge break any UK law, infringe any third party's copyright or other Intellectual Property Right, or contain any confidential material.

I accept that the College has the right to use plagiarism detection software to check the electronic version of the thesis.

I confirm that this thesis has not been previously submitted for the award of a degree by this or any other university.

Signature:

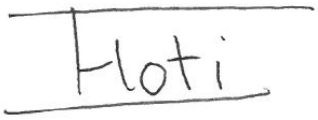

Date: 16/08/2018

Abstract

Intestinal macrophages, derived in part from monocytic precursors, are critical targets of IL-10, which prevents the development of colitis in mice. In humans, loss-of-function IL-10R mutations cause early-onset inflammatory bowel disease (IBD). We aimed to test the hypothesis that IL-10 responsiveness in monocyte/macrophages is suboptimal in adult IBD patients even in the presence of functional IL-10 signalling. A novel assay was developed to measure the ability of IL-10 to inhibit LPS-induced TNFα production by monocyte from blood or extracted from colonic biopsies. In healthy donors, monocyte subsets differed in their sensitivity to IL-10: classical monocytes were most sensitive and non-classical monocytes least, most likely due to lower levels of STAT3 availability and phosphorylation in response to IL-10. In IBD, circulating numbers of classical and intermediate monocytes were comparable to controls but non-classical monocytes were reduced. IL-10 was significantly less effective at inhibiting TNFα production by classical monocytes from IBD patients than controls (p=0.026), despite increased expression of IL-10Rα and IL-10-induced STAT3 phosphorylation. To determine the significance of this suboptimal response to IL-10 for monocyte-derived cells in the intestine, colonic CD14+ cells were analysed. Two populations were identified: $CD14^{hi}$ (P1) and $CD14^{lo}$ (P2) the latter of which were significantly increased in active Crohn's disease but not ulcerative colitis. Both populations produced TNFα in unstimulated cultures, and this response was significantly enhanced following LPS stimulation. The increase in TNFα production upon LPS stimulation was greater in P1 cells. Intestinal CD14+ cells were more sensitive to IL-10, in contrast to classical blood monocytes, TNFα production by P1 and P2 cells, from non-IBD and inflamed IBD mucosa, was completely inhibited by 2ng/ml IL-10. Since inhibition was complete under these conditions it was not possible to draw conclusions about differences between health and disease; further studies with less IL-10 may be informative.

Acknowledgements

Andy Stagg has provided continuous and constructive support throughout my PhD, and I am very grateful to him. I would also like to thank James Lindsay for his encouragement and invaluable input. I could not have asked for two better supervisors to guide me through this process. I want to thank the gastroenterology team for helping with patient recruitment, and I want to especially thank Paul Harrow, Hanna Gorden, and Ibrahim Ayada for their help with sample collection and patient data. Neil McCarthy has provided great advice and light-hearted banter. Last but not least, Eve Hornsby has been a positive person to turn to and share ideas with. It has been a pleasure to be part of the team.

I want to thank Ambika Kumar and Stefania Martin for keeping me laughing and providing a silver lining to every situation. My PhD experience would not have been as enjoyable without them. I am also grateful to the Blizard community for building a place that I was privileged to study at.

I cannot express how grateful I am to my mum and dad for the sacrifices they have made. They have challenged me to strive to be my best and believed in me when I needed it most. I hope I have made them proud. Milena thank you for always being there for me, I am lucky to have a sister and a best friend all in one, and Sam thank you for taking her off our hands.

Table of Contents

List of Figures

Chapter 4:

Chapter 5:

Chapter 6:

List of tables

Chapter 2:

Abbreviations

ADAM17	ADAM metallopeptidase domain 17
ADCC	Antibody dependent cellular cytotoxicity
AGM	Aorta–gonad–mesonephros
AMPs	Antimicrobial proteins
APCs	Antigen presenting cells
ARE	AU-rich elements
BM	Bone marrow
CCR2	C-C chemokine receptor type 2
CD	Cluster of differentiation
CD	Crohn's disease
CD8+	Cytotoxic T cell
CDP	Common DC precursor
cMoP	Common monocyte progenitors
COX2	Cyclooxygenase 2
CSF	Colony stimulating factor
CT	Cycle threshold
CTV	Cell trace violet
CX_3CR1	CX3C chemokine receptor 1
DCs	Dendritic cells
DNase I	Deoxyribonuclease I
dsRNA	Double-stranded RNA
DSS	Dextran sulphate sodium
DTT	Dithiothreitol
ED50	Effective dose 50
EDTA	Ethylenediaminetetraacetic acid
EIM	Extraintestinal manifestations
ESR	Erythrocyte sedimentation rate
FBC	Full blood counts
FcR	Fc receptor

FCS	Fetal calf serum
FL	Foetal liver
FLT3	FMS-like tyrosine kinase 3 ligand
FSC	Forward scatter
gDNA	genomic DNA
GF	Germ-free
GIT	Gastrointestinal tract
GWAS	Genome wide association studies
HBSS	Hank's balanced salt solution
HSCs	Hematopoietic stem cells
IBD	Inflammatory bowel disease
IC	Indeterminate colitis
IECs	Intestinal epithelial cells
IFN	Interferon
IL	Interleukin
ILCs	Innate lymphoid cells
IQR	Interquartile rage
JAK1	Janus kinase 1
KO	Knock out
LFT	Liver function test
LoF	Loss of Function
LP	Lamina propria
LPS	Lipopolysaccharide
Ly6C	Lymphocyte antigen 6C
MDP	Muramyl dipeptide
MFI	Mean flourescence intensity
MHC	Major histocompatibility complex
MLNs	Mesenteric lymph nodes
Mo	Monocytes
moDCs	Monocyte-derived DCs
moMϕ	Monocyte-derived Mϕ

MP	Mononuclear phagocyte
Mϕ	Macrophage
NFκB	Nuclear factor kappa B
NKT	Natural killer T
NLR	NOD-like receptor
NOD2	Nucleotide-Binding Oligomerization Domain Containing 2
Pam_3CSK_4	Pam3-Cys-Ser-Lys4
PBMC	Peripheral blood mononuclear cell
PBS	Phosphate buffered saline
PFA	Paraformaldehyde
PGE2	Prostaglandin E2
Poly(I:C)	Polyinosinic:polycytidylic acid
PP	Peyer's patch
pre-cDC	Pre-classical DC
pre-pDC	Pre-plasmacytoid DC
PRR	Pattern-recognition receptor
p-STAT3	Phosphorylated STAT3
RBC	Red blood cell
RM	Repeated measures
ROS	Reactive oxygen species
SCID	Severe combined immunodeficiency
SD	Standard deviation
SOCS	Suppressor of cytokine signalling
SSC	Side scatter
STAT	Signal transducer and activator of transcription
TGFβ	Transforming growth factor β
Th	T helper
TLR	Toll-like receptor
TNBS	Trinitrobenzene sulfonic acid
TNFα	Tumor necrosis factor α
Tr1	T regulatory cell type 1

Treg	Regulatory T cell
T-STAT3	Total STAT3
TYK2	Tyrosine kinase 2
UC	Ulcerative colitis
UV	Ultraviolet
VEO-IBD	Very early-onset IBD
WT	Wild-type
YS	Yolk sac
λmax	Maximum absorption

Chapter 1: Introduction

1.1 Overview

The gastrointestinal tract (GIT) is made up of the small and large intestine, which are distinct in their function and morphology. The small intestine is the site of food digestion and absorption, while the large intestine is involved in absorption of water and electrolytes. The overarching function of the intestine is the digestion and absorption of nutrients from ingested food. To help achieve this function, the intestine is colonised by a diverse community of microorganisms, including bacteria, fungi, and viruses, forming the microbiota, which aids in the breakdown and release of nutrients from food molecules that are indigestible by the enzymes present in the intestine as well as restricting access to invasive pathogens (reviewed by Backhed *et al.*, 2005; Abraham & Medzhitov, 2011). Therefore, the intestinal immune system must distinguish between beneficial microbiota and pathogens to maintain a balance between regulatory and pro-inflammatory responses. This balance is disturbed in IBD, leading to immune reactivity against commensal bacteria in genetically susceptible individuals, which results in chronic inflammation and damage to surrounding tissue (reviewed by Baumgart & Carding 2007). The pathogenesis of IBD is not fully understood.

This thesis will investigate the contribution of monocytes and intestinal macrophages (Mϕs) to the pathogenesis of IBD in humans. More specifically, the involvement of IL-10 in the role of monocytes and monocyte-derived Mϕs (Mo/moMϕ) during intestinal inflammation.

The introduction will begin with a broad overview of the mechanisms that maintain steady-state in the intestinal immune system, and how dysregulation of immune responses may give rise to IBD. There will then be a focus on understanding the roles of resident Mϕs in the intestine and how these functions are influenced by IL-10 during steady-state and in the context of intestinal inflammation, with supporting evidence from experimental mouse models. Finally, this chapter will introduce the aim of the project and a summary of the principal aims.

1.2 The immunological challenges of the intestine

The intestine and colonising microbiota have co-evolved to establish a symbiotic relationship; the host provides a favourable environment for the bacteria with access to nutrients, and in return, the bacteria aid in the digestion and release of nutrients from food that would be otherwise indigestible to the host (reviewed by Backhed et al. 2005). These bacteria also occupy a niche in the intestine, providing strong competition for the available nutrients and restricting access to invasive pathogens (reviewed by Hooper & MacPherson 2010). The dominant bacteria can be classified into the phyla gram-positive Firmicutes and gram-negative Bacteroidetes (reviewed by Hooper & MacPherson 2010). However, there is large diversity in the microbiota between individuals, making it difficult to distinguish between a healthy microbiome and microbial imbalance (dysbiosis).

Despite the symbiotic relationship between the intestine and microbiota, their close proximity poses an immunological challenge. The intestinal immune system must protect against invasive pathogens without responding to beneficial bacteria. Therefore, intestinal immune cells are required to distinguish between helpful and harmful bacteria to maintain a balance between regulatory and pro-inflammatory responses. There are multiple layers of protection against pathogens, which will be detailed in this section.

1.2.1 Barrier function

The first line of defence against invading pathogens in the GIT is the physical barrier formed from intestinal epithelial cells (IECs) connected by tight junctions (reviewed by Peterson & Artis 2014), and the layers of mucus that protect this barrier. The mucus is made up of two distinct layers: an inner stratified layer that that excludes bacteria and is adherent to the epithelium, and a looser outer layer that is not attached to the epithelium and is inhabited by bacteria (reviewed by Johansson et al. 2011). Goblet cells produce highly glycosylated MUC2 mucin, which are organised into large net-like polymers that form the mucus layers (reviewed by Johansson et al. 2011). MUC2 deficient mice display

enhanced susceptibility to invasive pathogens, and reduced MUC2 is associated with the onset of intestinal inflammation (Heazlewood et al. 2008; Johansson et al. 2008; Van der Sluis et al. 2006; Wenzel et al. 2014). This highlights the important role of mucus in maintaining immune regulation in the intestine. Also present in the mucus layers are antimicrobial proteins (AMPs), including defensins, lysozymes, and IgA, which further restricting access to bacteria (reviewed by Johansson et al. 2011).

The intestinal epithelium is made up of a single layer of IECs linked tightly together by tight junction proteins (Peterson & Artis 2014). This acts as a physical barrier to the microbiota colonising the intestine. There are distinct types of IECs present along the epithelium: enterocytes that assist in the absorption of nutrients, goblet cells that produce mucins, Paneth cells that produce AMPs, and tuft cells that defend against parasites (reviewed by Hooper & MacPherson 2010). IECs can sense and respond to pathogens via pattern recognition receptors (PRRs), including Toll-like receptors (TLRs) and NOD-like receptors (NLRs); upon activation of these pathways, IECs participate in the coordination of an appropriate immune response (reviewed by Abreu 2010). Therefore, IECs have an important role in regulating immune responses in the GIT.

As described above, Paneth cells produce AMPs, including defensins, cathelicidins, and C-type lectins, which provide additional protection against invading pathogens. Alpha-defensins are produced constitutively, whereas the production of C-type lectins is induced upon exposure to environmental microbes (reviewed by Hooper & MacPherson 2010). Germ-free mice (GF) mice maintain their capacity to produce defensins (Pütsep et al. 2000). In contrast, mice deficient in MyD88 (an adaptor molecule involved in TLR signalling) showed undetectable levels of RegIIIγ (C-type lectin), which was associated with impaired clearance of *Listeria monocytogenes* infection, and reconstitution with recombinant RegIIIγ restored bacterial clearance (Brandl et al. 2007). This highlights the role of AMPs in protecting intestinal mucosa against invasive pathogens.

As mentioned earlier, IgA is present in the mucus layers and aids in controlling bacterial access. IgA is the dominant antibody in the intestinal barrier and is secreted by terminally differentiated B cells

(plasma cells) upon exposure to environmental microbes, as demonstrated in GF mice and neonates, which display significantly fewer plasma cells (reviewed MacPherson et al. 2008). Secretory IgA (sIgA) is transported across the epithelial barrier by polymeric Ig receptor (pIgR)-mediated transcytosis (reviewed by MacPherson et al. 2008). The functions of sIgA include neutralising toxins, limiting bacterial attachment to the epithelium, and promoting agglutination (clumping) of bacteria to increase the efficiency of microbial elimination by phagocytosis (reviewed MacPherson et al. 2008). sIgA deficient mice display an expansion of segmented filamentous bacteria, which induce inflammatory responses, and reconstitution with sIgA recovered the normal composition of the microbiota and prevented further activation of immune responses (Suzuki et al. 2004). This demonstrates an important role of sIgA in regulating the composition of microbiota.

1.2.2 Innate immunity

If the epithelial barrier is breached, innate immune cells resident in the intestinal mucosa are the next line of immune defence against invading bacteria. The innate immune system is made up of a network of cells that can elicit a rapid immune response against pathogens recognised using TLRs and other PRRs. Innate immune cells include granulocytes, Mϕ and dendritic cells (DCs). Granulocytes include neutrophils, eosinophils, basophils, and mast cells, which contain granules in their cytoplasm composed of different active agents, for example neutrophils contain potent antimicrobial agents that aid in bacterial killing by phagocytosis (reviewed by Fournier & Parkos 2012). Granulocytes do not reside in the intestine during steady-state, instead they are recruited during inflammatory responses. They have an important role in eliminating invasive pathogens that gain access to the intestinal mucosa. However, in the context of IBD, these cells can perpetuate the intestinal inflammation, consistent with the observation that neutrophils are enriched in the mucosa of IBD patients (reviewed by Fournier & Parkos 2012).

Mϕs and DCs are antigen presenting cells (APCs) that interact with and influence the adaptive immune response, and therefore bridge the gap between the innate and adaptive immune system. These APCs

sample the luminal microbes using several methods. M cells translocate antigens from the lumen into the Peyer's patch (PP), where DC reside (Verrier et al. 2006). However, invasive pathogens can exploit M cells as a means of accessing the intestinal mucosa. It was believed that DCs could protrude their dendrites between epithelial cells to sample directly from the lumen but more recent studies have revealed that the cells that do this are Mϕ, which take up soluble antigens and transfer them to DCs (Mazzini et al. 2014; Rescigno et al. 2001). However, Mϕ and DCs also have distinct roles within the intestine. Resident Mϕs can phagocytose and clear bacteria detected in the lamina propria (LP), and also display the degraded regions of the bacteria on major histocompatibility complex (MHC) receptors to present to local effector cells (discussed in section 1.5). Mice deficient in the two major mechanisms of bacterial killing by phagocytes formed abscesses containing commensal organisms, demonstrating the important role of intestinal Mϕ in bacterial clearance (Shiloh et al. 1999). DCs sample the luminal microbiota and have the unique ability to migrate to the mesenteric lymph nodes (MLNs) (Schulz et al. 2009), where they present the antigens to naïve T cells (Th0) (reviewed by Mowat & Bain 2011). These interactions are critical in training the adaptive immune cells to elicit the appropriate response when presented with beneficial bacteria or invasive pathogens.

Innate lymphoid cells (ILCs) are enriched in the intestinal mucosa, where they play a protective role against pathogens (reviewed by Geremia & Arancibia-Cárcamo 2017). This population respond to environmental stress signals as they lack an antigen-specific receptor typical to lymphocytes but reflect functional characteristics of T helper subsets (reviewed by Geremia & Arancibia-Cárcamo 2017). ILCs have been implicated in the pathogenesis of colitis in murine models, and accumulate in the inflamed mucosa of patients with IBD (reviewed by Geremia & Arancibia-Cárcamo 2017).

1.2.3 Adaptive immunity

In many cases, components of the innate immune stem are sufficient to control intestinal pathogens. If this does not occur, innate immune cells can alert the adaptive immune system to generate a highly targeted response.

As mentioned earlier, DCs in PPs, or those that migrate to draining MLNs or iliac nodes (Schulz et al. 2009) present antigens sampled from the lumen to Th0 CD4+ T cells, leading to the activation and proliferation of the responding T cell (reviewed by Mowat & Bain 2011). The activity of the responding T cell is determined at least in part by cytokines produced by the DC (Figure 1.1). Type 1 T helper (Th1) cells are important in eliminating intracellular pathogens, and display characteristic cytokine production, including IFNγ, TNFα and IL-2 (reviewed by Szabo *et al.*, 2003). IFNγ activates Mϕs, resulting in increased phagocytosis by induction of nitric oxide (NO) and superoxide for the elimination of intracellular pathogens (reviewed by Boehm *et al.*, 1997). Th2 cells are involved in the defence against parasites (e.g. helminth infection), and display characteristic cytokine production, including IL-4, IL-5, and IL-9 (reviewed by Paul and Zhu, 2010). Th2 cells recruit mast cells and eosinophils to the intestine through the production of IL-9 and IL-5 respectively (reviewed by Paul and Zhu, 2010). IL-4 is critical in the defence against parasites through induction of B cell production of IgE (explained below), which activates eosinophils and mast cells, causing degranulation and release of pro-inflammatory mediators involved in parasite clearance (reviewed by Paul and Zhu, 2010). Th17 cells produce IL-17A, IL-17F, IL-22 and GM-CSF (Annunziato et al. 2007; Wilson et al. 2007). IL-17A and IL-17F are critical in the defence against extracellular bacterial and fungal pathogens through the induction of stromal cell production of IL-8 and GM-CSF, which recruits neutrophils and induces neutrophil development in the BM respectively (reviewed by Witowski, Ksiązek and Jörres, 2004). IL-22 production promotes the production of antimicrobial peptides by epithelial cells, and therefore enhances epithelial barrier function during intestinal infection (Zheng et al. 2008). The evidence that intestinal inflammation in CD patients is Th1/Th17-mediated but Th2-mediated in UC patients will be discussed in section 1.3.3.3, as well as the critical role of regulatory T cells (Tregs) regulating immune responses in the intestine.

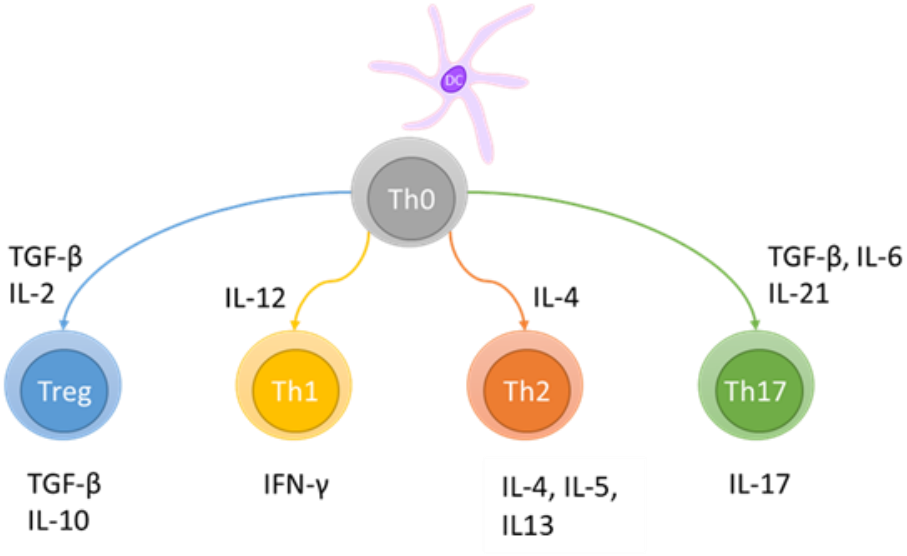

Figure 1.1: Th0 cell differentiation. DCs present antigens on MHC-II receptors Th0 cells. Differentiation of Th0 cells into effector CD4+ T cells is determined in part by their interactions with DC Figure adapted from Bailey et al., 2014.

Naïve CD8+ T cells can only be primed by DCs displaying its respective antigen on MHC class I receptors and costimulatory molecules in the presence of IL-12 (Joffre et al. 2012). CD8+ T cells contain pre-formed granules comprised of perforin, granzyme B, and granulysin. The granules are released in a focused manner into virally infected or malignant cells expressing the corresponding antigen, which then undergo apoptosis.

Naïve B cells bear B cell receptors, which in essence are antibodies anchored to their surface. These antibodies have two variable regions, which can recognise antigens without the need for APCs, and also enable B cells to present antigens. Upon activation, B cells mature into plasma cells, which produce their corresponding soluble antibodies. Soluble antibodies have five functions: agglutination, neutralisation, opsonisation, and antibody-dependent cellular cytotoxicity (ADCC). Antibodies come in 5 different forms: IgA, IgG, IgE, IgM, and IgD. These antibodies stimulate different effects on immune cells, which is determined by their Fc region. The Fc region is recognised by Fc receptors (FcR) present on the surface of specific immune cells, which elicit distinct immune responses, as described earlier, IgA is the dominant antibody in the intestinal barrier.

1.3 Inflammatory Bowel Disease

IBD is a chronic, relapsing inflammatory disorder affecting the GIT caused by a breakdown in immune regulation, which leads to reactivity against commensal bacteria that reside in the intestine. As a gross simplification, the breakdown in immune tolerance against commensal bacteria is the result of overactive pro-inflammatory activity or insufficient regulatory signals. IBD is mainly comprised of Crohn's disease (CD) and Ulcerative Colitis (UC), which manifest with distinct patterns of inflammation. Although CD and UC are accepted as clinically distinct conditions, 10-15% of cases cannot be diagnosed definitively, and are referred to as indeterminate colitis (IC) (reviewed by Guindi & Riddell 2004); this indicates a spectrum of disease instead of distinct conditions.

Despite extensive research into genetic and environmental predisposing factors, it is still unclear what triggers IBD in patients. The number of individuals with IBD is increasing with the highest incidence rates in industrialised countries; importantly, people who migrate from low to high prevalence areas acquire the new incidence rates of the background population with a generation, which is too rapid to be accounted for by genetic change (Molodecky et al. 2012). This indicates that there are lifestyle and environmental impacts on IBD. However, it has long been known that there are also genetic factors. This has been revealed through observing familial aggregation and results from concordance studies in twins and Ashkenazi Jewish descendants (Halfvarson et al., 2003; Kenny et al., 2012), and more recently through genome-wide association studies (GWAS) that have identified over 163 genetic variants influencing susceptibility to IBD (Anderson et al. 2011; Franke et al. 2010a; Jostins et al. 2012; McGovern et al. 2010). Thus, a complex picture is emerging, where genetic susceptibility to environmental factors, and immune interaction with gut microbiota are all interrelated.

1.3.1 Characteristics of IBD

CD is a transmural inflammatory disorder that can affect any region of the GIT. The inflammation occurs in segments and can be associated with granulomas (collections of Mϕs which are able to form a barrier between potential pathogens and host tissues), strictures where the intestine narrows causing bowel obstruction, and fistulae where inflammation forms abnormal connections between the bowel and the vagina, bladder or skin (reviewed by Baumgart & Sandborn 2012). In UC, inflammation occurs continuously, extending proximally from the rectum, and can spread through the entire colon; the inflammation is restricted to the mucosal surface, causing extensive superficial ulceration (reviewed by Ordás et al. 2012). A serious complication of UC is toxic megacolon, which can lead to mortality if not recognised early, and may require a colectomy (removal of the whole colon) if drug treatment is unsuccessful (reviewed by Bouma & Strober 2003). Patients with CD or UC present with similar symptoms such as recurring diarrhoea, rectal bleeding, abdominal pain, and fatigue. Approximately 25% of IBD patients will also develop extraintestinal manifestations (EIM) that can affect particularly the skin, eyes, or joints. EIMs may be a result of an overreactive immune system associated with intestinal inflammation or a genetic link causing multiple pathologies (reviewed by Baumgart & Sandborn 2012; Vavricka et al. 2015).. Endoscopy is used to examine the interior of the GIT, which enables imaging of the intestinal inflammation and diagnosis of CD or UC based on the characteristics of the inflammation. As well as aiding diagnosis, the extent of inflammation is monitored using biomarkers, including C-reactive protein, erythrocyte sedimentation rate (ESR), and faecal calprotectin (reviewed by Vermeire et al. 2004). In addition to this, full blood counts (FBC), liver function test (LFT), and a host of other measures of blood composition are measured. Collectively, the information is used to determine treatment response and inform therapy regimens.

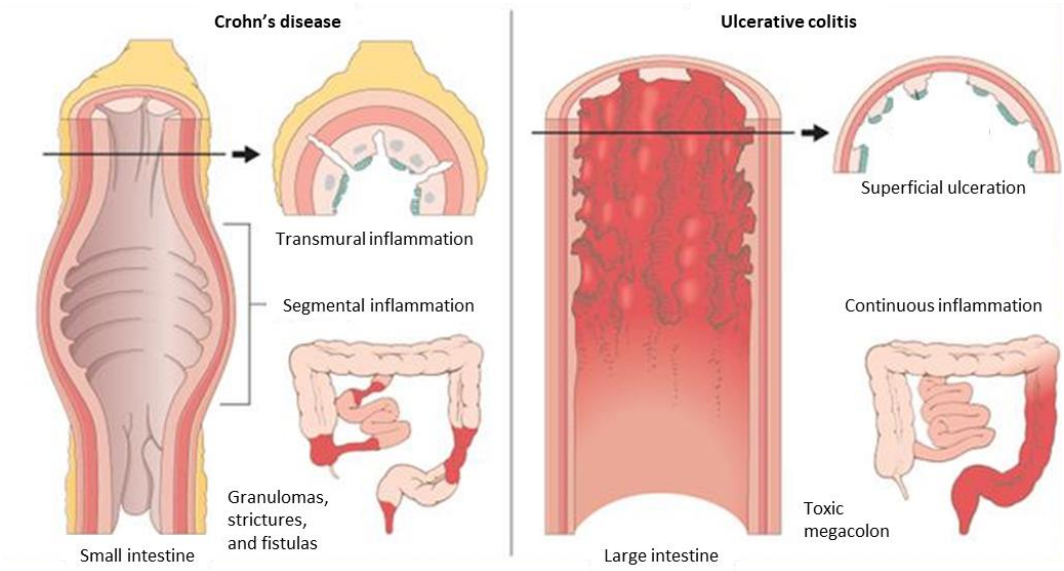

Figure 1.2: Summary of characteristics of CD vs UC. Although CD and UC patients present with similar symptoms, the inflammation differ in location, depth of inflammation, and complications (Mirza Muhammad Adnan 2011).

1.3.2 Epidemiology

The number of IBD cases is growing in industrialised countries, which implicates environmental factors. In addition, people who migrate from low to high prevalence areas acquire the new incidence rates with a generation, which is too rapid to be accounted for by genetic change (Molodecky et al. 2012). There are 322 cases of CD per 100,000 people and up to 12.7 new cases per 100,00 people per year in Europe alone (Molodecky et al. 2012). UC is more common than CD, with prevalence rates of up to 505 cases per 100,000 people and up to 24.3 new cases per 100,00 people per year in Europe (Molodecky et al. 2012). The majority of UC patients are diagnosed between 20-30 years, with a smaller population of patients being diagnosed between 50-70 years (reviewed by Ordás et al. 2012); disease onset later in life indicates a greater environmental cause (Polito et al. 1996). CD and UC both display a bimodal pattern of incidence. However, the main onset peak of CD is on average ten years earlier then UC (reviewed by Duricova et al. 2014), which may reflect a greater influence of genetic factors in CD than UC. This interpretation is supported by concordance studies in twins, where monozygotic twins had 50% concordance rates for CD but only 19% for UC, while dizygotic twins had concordance rates of 4% for CD and 0% for UC (Halfvarson et al. 2003).

1.3.3 Aetiology

1.3.3.1 Genetic predisposition

Early observations of familial aggregation in IBD patients initiated research into genetic predispositions. Nucleotide oligomerisation domain 2 (*NOD2*) was an early susceptibility gene identified in CD patients (Hugot et al. 2001; Ogura et al. 2001). NOD2 is an intracellular PRR expressed in monocytes, epithelial cells, and Paneth cells that detects muramyl dipeptide (MDP), which enables recognition of intracellular bacteria, leading to activation of nuclear factor kappa B (NFκB) and production of pro-inflammatory cytokines (Girardin et al. 2003; Inohara et al. 2003). NOD2 deficient mice presented with enhanced TLR2 activation and greater interleukin-12 (IL-12) production, leading to Th1-mediated intestinal inflammation, characteristic to CD (Watanabe et al. 2004; Yang et al. 2008). Human monocyte-derived DCs (moDCs) derived from CD patients with NOD2 mutations display a reduced capacity to process and present antigens (Cooney et al. 2010). This demonstrates the importance of the ability of the intestinal immune system to recognise and respond to invasive pathogens.

GWAS is a method of identifying associations between common genetic variants (loci that are usually single nucleotide polymorphisms (SNPs)) and traits (usually diseases); 215 susceptibility loci have been associated with IBD (Franke et al. 2010; McGovern et al. 2010; Anderson et al. 2011; Jostins et al. 2012; De Lange et al. 2017). This has provided insights into the potential pathways that are involved in the pathogenesis of IBD, which will be detailed below. The increased risk associated with each susceptibility loci is very small, and there is no association with prognosis (Lee et al. 2017). There are limitations of GWAS: it covers common genetic variants within the population and may fail to capture rare variants, the identity and function of many of the genes bearing the genetic variants remain unknown, and the majority of the genetic variants reside in noncoding regions of the genome (Graham & Xavier 2013).

Out of the 163 susceptibility loci, 30 are exclusively associated with CD and 23 are specific to UC (Jostins et al. 2012). This indicates that there are distinct pathways that lead to intestinal inflammation characterised as CD or UC, although the majority of genes are common to both diseases. The genes that are associated with CD susceptibility include autophagy related 16 like 1 (*ATG16L1*), which is associated with the NOD2 pathway. Upon NOD2 activation, the bacteria undergo autophagy with the help of recruited ATG16L1 machinery (Cadwell et al. 2008; Travassos et al. 2009). When there is a breakdown in this system, bacterial replication becomes uncontrollable inducing an overwhelming inflammatory response (Caprilli et al. 2010). This indicates that defects in recognition and response to bacterial encroachment is important in CD pathogenesis.

The genes that are associated with susceptibility to UC include hepatocyte nuclear factor-4α (*HNF4α*) which regulates expression of tight junction proteins, cadherin-1 (*CDH1*) which form adherens junctions, and laminin-β1 (*LAMB1*) which is a component of the basement membrane (McGovern et al. 2010). All three genes are involved in maintaining the integrity of the epithelial barrier, highlighting the importance of the mucosal barrier function in UC pathogenesis. However, it cannot be certain whether epithelial barrier integrity is impaired due to inflammatory damage caused by a pathogenic infection that is exacerbated by the genetic variants, or whether the genetic variants give pathogenic bacteria the opportunity to establish an infection that will cause inflammation and further damage to the epithelial barrier.

The susceptibility genes that are associated with both CD and UC impact on regulatory pathways such as IL-10R signalling, including *IL-10*, signal transducer and activator of transcription 3 (*STAT3*), and tyrosine kinase 2 (*TYK2*) (Franke et al., 2010). In addition, a comparison of genes responsible for monogenic disease with IBD-like pathology and risk loci associated with IBD revealed that genes related to IL-10 (IL-10, IL-10RA, and IL-10RB) were the only common variants (Uhlig 2013). Susceptibility genes involved in Th17-mediated immunity, including *IL-23* and *IL-12*, are also

associated with both CD and UC (Anderson et al. 2011; Granlund et al. 2013). This supports the concept that inflammation in IBD arises from excessive effector function and/or failure in regulation.

Individuals with IBD are genetically predisposed to have dysregulated immune responses. However, known genetic variants account for only ~20% of all IBD cases (13.6 % CD and 7.5 % UC) demonstrating the role of environmental or non-genetic factors in the pathogenesis of IBD (Jostins et al. 2012). This is highlighted in the twin studies mentioned earlier, where monozygotic twins had only 50% concordance rates for CD (Halfvarson et al. 2003). It has been proposed that one possibility for the unaccounted heritability could be an epigenetic modification that results from the interaction between genes and the environment (reviewed by Ventham et al. 2013).

1.3.3.2 Environmental factors

epidemiological studies of IBD implicate environmental factors in determining the progression of IBD in genetically predisposed individuals. Increased incidence in developing countries suggests that the environmental factors are related to the 'western lifestyle' and industrialisation (reviewed by Ng et al. 2013). The 'western lifestyle' is associated with changes in diet, antibiotic use, hygiene status, and pollution. These environmental factors might all converge on their impact on the microbiota.

A breakdown in immune regulation, which leads to reactivity against commensal bacteria is considered to be the basis of IBD (reviewed by Baumgart & Sandborn 2007). The intestinal microbiota has a critical role in training the intestinal immune system to recognise commensal bacteria and establish regulatory systems that help maintain immune tolerance (reviewed by Belkaid & Harrison 2017). Therefore, the nature of the microbiota itself an important environmental factor. The composition and diversity of commensal bacteria is determined by diet and environmental exposure, which may explain the greater incidence in industrialised regions, where there is greater consumption of processed food and exposure to pollution. The overuse of antibiotics and hygiene products is a risk factor for developing IBD because they have a negative effect on the diversity of the microbiota (Hviid et al. 2011), and are also a common feature in westernised societies.

Metagenomic studies have revealed a reduced diversity in the commensal bacteria of IBD patients (reviewed by Manichanh et al. 2012). The Firmicute *Faecalibacterium prausnitzii* has shown anti-inflammatory effects in mouse models of colitis (refer to section 1.3.3.5)(Sokol et al. 2008). Reduced diversity in the Firmicutes is a signature of the dysbiosis in patients with CD (Manichanh et al. 2006). In contrast, an increased *F. prausnitzii* was observed in paediatric CD patients, challenging the concept of a beneficial role of Firmicutes in CD (Hansen et al. 2012). An increased prevalence of *Escherichia coli* has been observed in CD and UC patients, which may contribute to disease pathogenesis through the invasion of the intestinal epithelium (Boudeau et al. 1999; Darfeuille-Michaud et al. 2004; Knoll et al. 2016; Martin et al. 2004). UC patients display a reduced abundance of bacteria that are considered to promote gut homeostasis, including *Eubacterium rectale* and *F. prausnitzii* (Knoll et al. 2016). UC patients display lower levels of major anaerobic bacteria (*Bacteroides* and *Clostridium* subcluster XIVab) (Nemoto et al. 2012). This dysbiosis is considered to enhance the ability of opportunistic pathogens to establish an infection. Whether dysbiosis of the microbiota is a cause or a consequence of intestinal inflammation remains to be elucidated.

The pathogenesis of IBD varies between patients, and the trigger of inflammation is usually unidentifiable. In some cases, infection by pathogens can be the initiator of inflammation, supported by seasonal variations in onset of disease (reviewed by Hanauer 2006). This is consistent with an infection triggering a breakdown in immune regulation that results in an uncontrolled immune response against the commensal bacteria. CD and UC have common environmental risk factors. However, smoking has been observed to have a protective effect in UC patients, whereas it is a risk factor for developing CD (Benjamin et al. 2012; Mahid et al. 2006). It has been shown that there is an increase in the number of sulfate-reducing bacteria in UC patients and that a build-up of sulfide becomes toxic. The cyanide from smoke neutralises the sulfide produced by these bacteria into non-toxic thiocyanate, which could account for the reported beneficial effect (Levitt et al. 1999). This is consistent with the concept that CD and UC patients display distinct dysbiosis in their commensal bacteria.

1.3.3.3 Immune-mediated intestinal inflammation

As previously mentioned, IBD is considered to result from a loss of tolerance against commensal bacteria leading to overwhelming inflammation and collateral damage to the surrounding tissue. This immune dysregulation is caused by an imbalance between pro-inflammatory and regulatory pathways. There is evidence that IBD patients display excessive effector T cell function, which form part of the pro-inflammatory system, these include CD8+ T cells, Th1, Th2, and Th17 cells. An early observation was that LPMCs showed enhanced capacity to produce pro-inflammatory cytokines, including tumour necrosis factor α (TNFα), IL-6, and IL-1β, from the inflamed mucosa of IBD patients compared to healthy controls (Reinecker et al. 1993). Anti-TNFα therapy is effective in treating ~50% of IBD cases, suggesting a significant role of TNFα in the pathogenesis of IBD (Molander et al. 2013). In support of this, over-expression of TNFα in mice leads to mucosal inflammation resembling IBD patients (Kontoyiannis et al. 1999). IL-6 and IL-1β are likely to propagate inflammation in the intestine by inducing T cell proliferation and promoting the production of interferon γ (IFNγ) and IL-17A (Huff et al. 2011). Elevated IFNγ production in CD4+ T cells has also been observed in CD patients, which promotes recruitment of innate immune cells, including neutrophils and monocytes, found to be enriched at inflammatory sites, leading to further production of pro-inflammatory cytokines (reviewed by Boehm et al. 1997). Overall, a higher abundance of pro-inflammatory cytokines is implicated in the pathogenesis of IBD.

Mϕs isolated from the inflamed mucosa of CD showed enhanced production of IL-12, which promotes IFNγ production by Th1 cells (Liu et al. 1999; Monteleone et al. 1997; Parronchi et al. 1997). Consistent with this, T cells isolated from the inflamed mucosa of CD display enhanced STAT4 (indicative of IL-12 signalling) and IL-12R expression, likely to contribute to their increased capacity to produce IFNγ (Parrello et al. 2000), suggesting that intestinal inflammation in CD patients is Th1-mediated. In addition, anti-IL-12p40 therapy was shown to be effective in treating CD, suggesting a role of IL-12 or IL-23 in the pathogenesis of CD (Mannon et al. 2004; Sandborn et al. 2008). IL-12 and IL-23 are

heterodimers, meaning anti-IL-12p40 can neutralise both IL-12 and IL-23 (Oppmann et al. 2000). More recent studies have shown that the development of intestinal inflammation was more dependent on IL-23 than IL-12. RAG-deficient mice (lack mature lymphocytes) also deficient in IL-23 did not develop colitis upon *H. Hepaticus* infection, whereas the same mice deficient in IL-12 developed colitis (Hue et al. 2006; Holm H. Uhlig et al. 2006). Therefore, it has been proposed that CD is mediated by a combination of Th1/Th17 responses (reviewed by Bouma & Strober 2003; Strober & Fuss 2011). However, the role of IL-17A in the pathogenesis of CD remains unclear because anti-IL-17A therapy lead to worsening of symptoms (Hueber et al. 2012), suggesting a protective role in the intestine.

Th2-mediated inflammation has been suggested to play a role UC because elevated levels of IL-13 and IL-5 detected (Fuss et al. 2004). However, there is no evidence of elevated levels of IL-4, a Th2 cytokine. Therefore, it has been proposed that natural killer T cells (NKT) cells are the predominant producers of IL-13, which causes altered expression of tight junctions and induces apoptosis (programmed cell death) in IECs (Heller et al. 2002); defective barrier function is characteristic to UC.

A recent study showed elevated levels of IL-17A and IFNγ production in CD4+ T cells, which did not differ between CD and UC patients (Rovedatti et al. 2009). In addition, whole genome expression meta-analysis has not revealed convincing differences between CD and UC (Granlund et al. 2013). These challenge the concept that CD and UC can be categorised into Th1 or Th2-mediated inflammation.

On the opposing side, inflammation in IBD is considered to arise from failure to regulate inflammatory responses. Tregs and Mϕs are important components of the regulatory pathway in the intestine. Tregs (FOXP3+CD4+CD25+) are crucial in regulating intestinal inflammation as demonstrated in the T cell transfer model of colitis, in which the intestinal inflammation that develops after the transfer of CD4+ T cells into mice with severe combined immunodeficient (SCID; absence of lymphocytes) can be prevented by co-transferring Tregs (Hori et al. 2002). The protective effect of Tregs can be reversed by administering a transforming growth factor β (TGFβ)-specific antibody, suggesting that the

suppressive effects of Tregs are mediated through TGFβ. However, Tregs from TGFβ-deficient mice still mediates suppressor activity in vitro, demonstrating that additional mechanisms exist (Piccirillo et al. 2002). A population of IL-10 producing Tregs that are CD25- have been defined and termed T regulatory type 1 (Tr1) cells (Brockmann et al. 2017). The critical role of IL-10 in regulating intestinal inflammation will be discussed in section 1.8.

Counterintuitively, more Tregs are present in the mucosa of IBD patients than healthy controls (Makita et al. 2004; Maul et al. 2005; H. H. Uhlig et al. 2006). However, effector T cells from inflamed mucosa display enhanced expression of SMAD7, which provides resistance to TGFβ-mediated suppression (Fantini et al. 2009). Therefore, Tregs are unable to suppress effector T cells within this context, consistent with a failure to regulate inflammatory responses in IBD.

A population of Tregs with the capacity to produce IL-17A has been reported in the inflamed mucosa of CD patients but not UC patients or healthy controls (Hovhannisyan et al. 2011). This population is absent in the blood, suggesting that their development occurs in the intestine, and it is dependent on local mediators that are distinct to CD. It is unclear whether this population have a pro or anti-inflammatory effect.

Intestinal Mϕs display a regulatory phenotype at steady-state; their features include resistance to TLR activation, removal of pathogens without producing pro-inflammatory cytokines, and constitutive production of IL-10 (reviewed by Mowat & Bain 2011). These properties have been shown to be critical in maintaining immune homeostasis in the intestine. The role of intestinal Mϕs during steady-state and inflammation will be discussed further in section 1.6.

1.3.3.4 Treatment

The goals of IBD treatment have shifted in recent years from a focus on relief from symptoms alone towards normalisation of inflammatory biomarkers and mucosal healing. There is increasing evidence that this approach improves outcomes in the longer term (Colombel et al. 2018).

Most treatments used in IBD have anti-inflammatory effects, and the commonly prescribed agents are described below. There is overlap between the phenotypes of CD and UC and similar treatments are used in both conditions with important differences highlighted. Treatments are often divided into agents to induce remission (treatments which lead to rapid resolution of symptoms) and agents which maintain remission.

Aminosalicylates, such as mesalazine, balsalazide and sulfasalazine, are the first line of treatment for UC to both induce and maintain remission. These drugs contain an active moiety (mesalazine) bound to a carrier molecule or encapsulated in a variety of coatings (e.g. MMX®, ethylcellulose) to ensure the majority of the active drug is delivered to the colon. Aminosalicylate anti-inflammatories are known to modulate the expression of genes involved in the NFκB pathway and cyclooxygenase 2 (COX2) (which is important in the generation of prostaglandins associated with inflammation). Recent meta-analysis suggest these agents do not lead to a significant benefit in CD (Ford et al. 2011).

Prednisolone and budesonide are corticosteroids commonly used to treat IBD. Corticosteroids bind to glucocorticoid receptors available in the cytoplasm of immune cells, which then translocate to the nucleus where they bind to the glucocorticoid response element and regulate gene expression. Inflammation can be suppressed using multiple targets, including the inhibition of NFκB (reviewed by Rhen & Cidlowski 2005). NFκB is involved in the production of pro-inflammatory cytokines, including TNFα, IL-1β, and IL-6 (reviewed by Lawrence 2009). Corticosteroid treatments are frequently used to induce remission but long-term use is ineffective and associated with multi-systemic side effects.

Immuno-modulators including thiopurines (azathioprine and mercaptopurine) and methotrexate are often used to maintain remission in CD and UC. Although recent evidence suggests methotrexate is not effective in UC (H. Herfarth 2018 abstract MERITUC). Thiopurines and methotrexate exert their anti-inflammatory effects by interfering with DNA synthesis, which proliferating immune cells are sensitive to. Metabolites of thiopurines are incorporated into DNA causing apoptosis (programmed cell death) as well as inhibiting purine synthesis (reviewed by Cara et al. 2004). Methotrexate is a folate analogue that interrupts the production of tetrahydrofolic acid and the synthesis of thymidine, which impairs RNA and DNA synthesis, and consequently white cell proliferation (reviewed by Tian & Cronstein 2007).

Biological agents have transformed the treatment of IBD in the past 20 years, and this remains an evolving field. In the UK a number of anti-TNF agents and vedolizumab are licenced for the treatment of both CD and UC. While recently ustekinumab has been licenced for the treatment of CD. Anti-TNF agents like infliximab and adalimumab are monoclonal antibodies that exert their anti-inflammatory effect by binding to and neutralising TNFα as well as inducing apoptosis in activated T cells and monocytes (reviewed by Levin et al. 2016). Infliximab is a chimeric antibody that needs to be administered intravenously, while adalimumab is humanised monoclonal antibody that can be administered subcutaneously. Vedolizumab is a humanised monoclonal antibody that blocks entry of pro-inflammatory T cells into the intestine by binding α4β7 integrin, a homing receptor on the surface of immune cells, that interacts with MAdCAM-1 on the vascular endothelium (Singh et al. 2016). Ustekinumab binds the p40 subunit common to the cytokines IL-12 and IL-23. The IL-23 inflammatory pathway has been implicated in the aetiology of IBD (Hue et al. 2006; Holm H. Uhlig et al. 2006). These agents are used as long-term treatments to maintain remission and are sometimes used to induce remission alone or in combination with corticosteroids.

Unfortunately, despite increased options for medical therapy, a significant minority of IBD patients do not respond or stop responding to medical interventions leading to recurring inflammation. Surgery

remains an important option for these patients. Surgery for UC involves a colectomy, which permanently removes the diseased colon. However, the patient will necessarily either have a stoma or internal pouch which does not function the same as a healthy colon. CD can affect anywhere in the gastrointestinal tract. Surgery for CD usually involves only removing the affected part of the bowel. Most patients experience a significant improvement in symptoms after surgery. However, recurrent inflammation affecting the anastomosis or a different part of the intestine is common in the long term (reviewed by Baumgart & Sandborn 2012).

In some individuals, the combination of genetic factors and environmental exposures leads to dysregulation of the intestinal immune system, loss of control of the response to commensals and chronic T cell inflammation driven by bacterial antigens. Section 1.6 will discuss the role of Mϕs in the intestine during steady-state and inflammation.

1.3.3.5 Mouse models of colitis

Much of what we understand about the immunological mechanisms underpinning intestinal inflammation come from animal models. This section will provide an overview of the animal models and their drawbacks.

There are four main types of IBD models: inducible colitis, spontaneous colitis, transgenic, and adoptive transfer. The most widely used mouse model of IBD is the dextran sulphate sodium (DSS)-induced colitis. DSS causes defects in the epithelial barrier by altering the expression of tight junction proteins, which causes enhanced epithelial cell apoptosis in concurrence with reduced proliferation (Poritz et al. 2007). Collectively, this causes an increase in gut permeability, which provides the opportunity for commensal bacteria to enter the mucosa and trigger an overwhelming inflammatory response. This reveals the critical role of the epithelial barrier in providing a protective barrier against external pathogens, helping maintain immune homeostasis in the intestine. In support of this, mice deficient in Muc2, which normally forms the mucous barrier that protects the epithelium, develop

spontaneous colitis upon exposure to commensal bacteria resembling UC (Heazlewood et al. 2008; Van der Sluis et al. 2006; Wenzel et al. 2014).

DSS treatment can be used to induce an acute, chronic, or relapsing model of colitis by administrating one high dose or multiple smaller doses via the drinking water, which can be easily monitored; the molecular weight is critical in determining the severity and location of the inflammation (reviewed by Perše & Cerar 2012). Mice in the chronic phase of DDS-induced colitis display colonic dysplasia, which resembles changes in the intestinal mucosa reported in human UC (reviewed by Perše & Cerar 2012). Dysbiosis of the intestinal microbiota has also been reported in the acute and chronic phase of DSS-induced colitis, which again is a feature of IBD in humans (Okayasu et al. 1990). Although there are histopathological features in common with UC, features that characterise CD, including transmural inflammation and granulomas, are rare in DDS-induced colitis, therefore, this model is recognised as more representative of UC (Alex et al. 2009).

Environmental exposure can be controlled in mouse models enabling a definitive effect of the intervention. However, differences in susceptibilities and progression between mouse strains have been reported, e.g. DSS-treated C57BL/6 progress to chronicity but not BALB/c mice (Melgar et al. 2005), much like humans. This has been attributed to the genetic makeup of the mouse strains revealing the critic role of genetics in susceptibility. The role of microbiota in intestinal inflammation was revealed in DSS-treated mice reared in GF conditions, where colitis was not induced (Hudcovic et al. 2001). However, conflicting results showed intestinal microflora was not necessary for intestinal pathology but DSS itself is destructive to the intestine (Kitajima et al. 2001). In support of Hudcovic et al. 2001, antibiotic treatment was shown to improve the outcomes of DSS-treated mice (Hans et al. 2000). A study testing current therapeutic agents on DSS-treated mice showed efficacy in treating the colitis, arguing that DSS-induced models are relevant for the translation of mouse data to human disease (Melgar et al. 2008). Models of DSS-induced colitis have already helped identify inflammatory mediators that have provided therapeutic targets, such as anti-TNFα therapy.

Less commonly used mouse models of inducible colitis are trinitrobenzene sulfonic acid (TNBS)-induced colitis and oxazolone-induced colitis. TNBS is dissolved in ethanol to disrupt the intestinal barrier and enable the interaction of TNBS with colon proteins (locally administered). TNBS acts as a hapten, when coupled with colonic proteins, makes them immunogenic eliciting an acute Th1-mediated immune response; chronicity can be achieved by repeated administration. However, Balb/c mice appear to develop Th2 inflammation, which provides another demonstration of the variation between mouse strains (reviewed by Antoniou et al. 2016). The pathophysiological properties of TNBS-treated mice reflect human CD, including transmural inflammation and granulomas (reviewed by Antoniou et al. 2016). In addition, the involvement of NOD2 (a key CD susceptibility gene) has been shown to be important in the pathogenesis of TNBS colitis (Yang et al. 2008). Current therapeutic agents showed efficacy in treating TNBS-induced colitis, which emphasises its similarity with human disease (Selve & Wöhrmann 1992). Oxazolone is also a hapten but it elicits a Th2-mediated immune response instead of Th1. The pathophysiological properties of oxazolone-treated mice reflect human UC, including superficial ulceration in the distal colon (Heller et al. 2002; Wang et al. 2004). Current therapeutic agents also showed improvement in oxazolone-induced colitis, which again suggests that the model is a good representation of human disease and provides a way to test the efficacy of therapeutic agents (Kojima et al. 2004).

Genetically modified mice have provided an invaluable resource for studying the interactions between microbiota, genetic, and immunogenic factors in IBD. Models based on genetic modifications can be grouped into depletion/deficiency, adoptive transfer, and transgenic. Mice deficient in IL-2, IL-10, or TGF-β develop spontaneous colitis, which reflects the critical role of immune-regulatory signals (Berg et al. 1996; Kühn et al. 1993). Loss of any one of these immune-regulatory molecules can alone induce intestinal inflammation, indicating important non-redundant roles of each molecule.

The contribution of the microbiota in training intestinal immune cells towards regulatory responses is highlighted in the adaptive transfer model where CD4+ T cells collected from mice reared in GF or

conventional conditions were transferred into SCID mice, and mice receiving CD4+ T cells from the GF reared mice developed colitis (Strauch et al. 2005). This was shown to be due to the lack of Tregs detected as a consequence of not being exposed to commensal bacteria. The role of pro-inflammatory immune cells has also been explored using the adoptive transfer model briefly mentioned. CD45RB+ cells (naïve CD4+ T cells) are transferred into SCID mice inducing a Th1-mediated response, which can be prevented by co-transferring Tregs (Morrissey et al. 1993), which again highlights the importance of balancing pro-inflammatory and regulatory responses.

TNFα is a pro-inflammatory cytokine detected at elevated levels in IBD patients. In mice, deletion of AU-rich elements (ARE) enhances the stability of mRNA encoding TNFα resulting in an increase in production in these mice, which develop spontaneous colitis as well as arthritis (Kontoyiannis et al. 1999). Transgenic mice have enabled the identification of important components of the pro-inflammatory pathway, including IL-7 and STAT4. Overexpression of IL-7, which is important for differentiation and proliferation of T cells, leads to pathophysiological outcomes that resemble UC, and STAT4 favours the differentiation of Th0 cells into Th1 cells, whereby overexpression of STAT4 leads to an increase in IL-12 production and as a consequence elevated levels of IFNγ, which favours a Th1-mediated inflammation (reviewed by Jurjus et al. 2004).

Studies in IBD patients and animal models of colitis have identified mononuclear phagocytes (MPs) as key players. This next section will define the origins of these populations before going on to discuss their role in intestinal inflammation.

1.4 Origin of MPs

1.4.1 Origin of MPs in the mouse

All tissue-resident Mϕs were once believed to be solely derived from monocytes. However, fate-mapping experiments have provided a better insight into the heterogeneity of the ontogeny of tissue-resident Mϕs. Yolk sac (YS)-derived myeloid progenitors seed the brain, liver, and skin giving rise to microglia, Kupffer cells, and Langerhans cells respectively. Microglial and Kuppfer cells are maintained through self-renewal during adult life (Ginhoux et al. 2010; Hashimoto et al. 2013; Hoeffel et al. 2012; Mass et al. 2016; Yona et al. 2013). The first hematopoietic stem cells (HSCs) emerge from the YS and aorta–gonad–mesonephros (AGM) region, which then seed the foetal liver (FL) and finally colonise the bone marrow (BM), where they are responsible for the maintenance of haematopoiesis thenceforth (reviewed by Kleer et al. 2014).

FL-derived monocytes contribute to the Langerhans cell and intestinal Mϕ pool (Hoeffel et al. 2012). They also form pre-alveolar Mϕs in the lung prenatally that subsequently differentiate into alveolar Mϕs after birth, which are able to self-maintain (Guilliams et al. 2013). Langerhans cells derived from FL monocytes proliferate after birth making up the majority of the Mϕ pool in the epidermis, and are also able to self-maintain (Hoeffel et al. 2012). In contrast, it has been shown the intestinal Mϕs pool requires constant replenishment by circulating blood monocytes (Yona et al. 2013; Bain et al. 2014). One explanation for the requirement of continuous monocyte recruitment could be that maintaining immune plasticity in the intestine becomes important due to the constant exposure to commensal bacteria. However, the Mϕ pool in the heart, a sterile environment, also requires the recruitment of circulating monocytes (Epelman et al. 2014; Molawi et al. 2014). A more recent study has shown that the intestinal Mϕ pool is made up of three distinct populations with heterogeneous ontogeny (Shaw et al. 2018). The key findings from Bain et al., 2014 and Shaw et al., 2018 will be discussed in section 1.6.

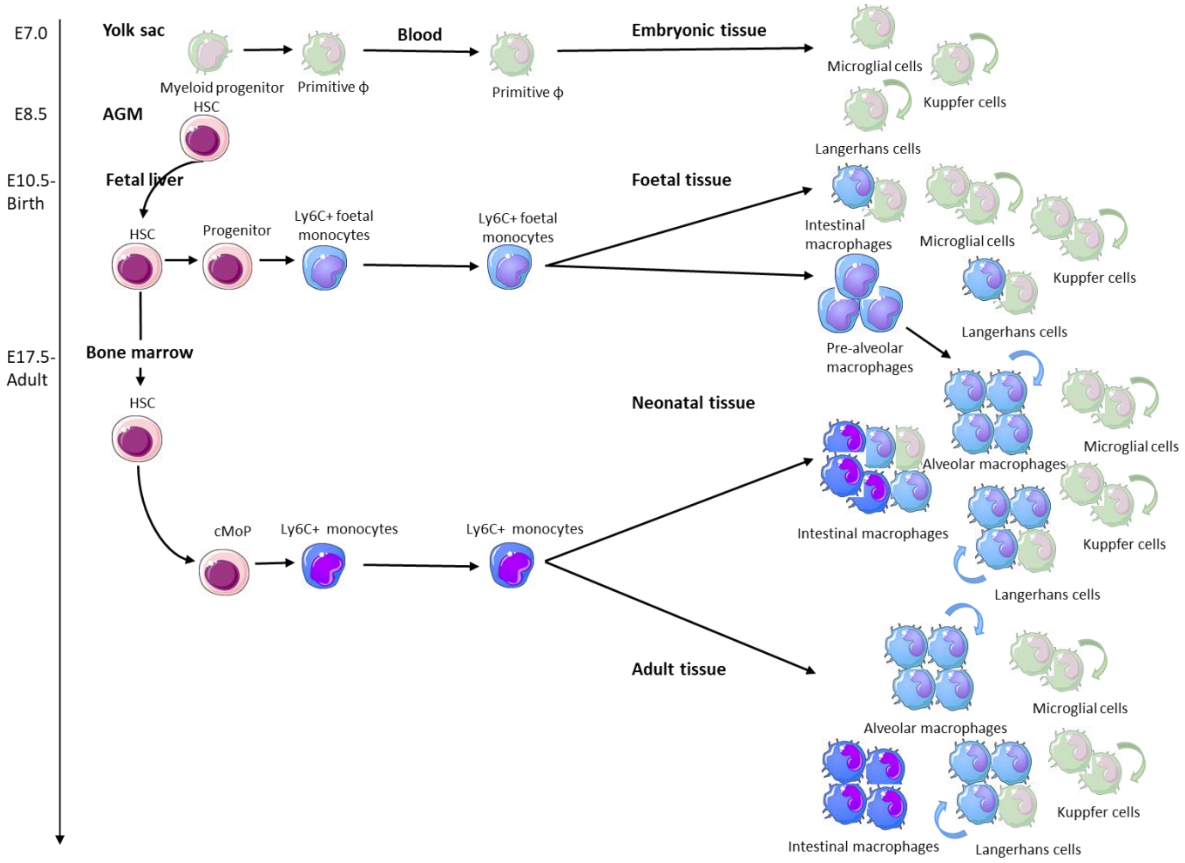

Figure 1.3: Summary of the ontogeny of tissue-resident Mϕs. Tissue-resident Mϕs arise at different stages of development and are derived from different sources of progenitor cells. Adapted from Kleer et al., 2014.

HSCs give rise to progressively more committed common monocyte progenitors (cMoP) and common DC precursor (CDP). cMoP differentiate into monocytes in the BM, which is dependent on colony stimulating factors (CSF1&2) (refer to figure 1.4), and are then released into the blood where they patrol for pathogens or can be readily recruited to most tissues during inflammation (detailed in section 1.7). Upon arrival to the tissue, monocytes have the capacity to differentiate into a variety of monocyte-derived cells (MDC) that include different types of tissue Mϕs and moDCs (Guilliams et al. 2014). MDCs can express F4/80 and CD64, are highly phagocytic and poor at migration like Mϕs (Tamoutounour et al. 2012; Tamoutounour et al. 2013), but can also express CD11c and induce naive T cells like DCs (Cheong et al. 2011; Plantinga et al. 2013). In support of this, irradiated mice given MDCs were able to form cDCs and several tissue-resident Mϕs (Fogg et al. 2006). Although monocytes

have the ability to differentiate into both Mϕs and DCs, weather moDCs occur in a physiological setting remains controversial

The majority of DCs are believed to be derived from CDPs. CDPs are subdivide into pre-classical DCs (pre-cDCs) and pre- plasmacytoid DCs (pre-pDCs). Pre-cDCs leave the BM and give rise to cDCs types 1&2 in peripheral tissues, while pre-pDCs terminally differentiate into pDCs in BM before seeding tissues (Guilliams et al. 2014). Initially, DC development relies on the cytokine FMS-like tyrosine kinase three ligand (FLT3), differentiation into DC subtypes is then controlled by a distinct set of transcription factors (refer to Figure 1.4) (Guilliams et al. 2014).

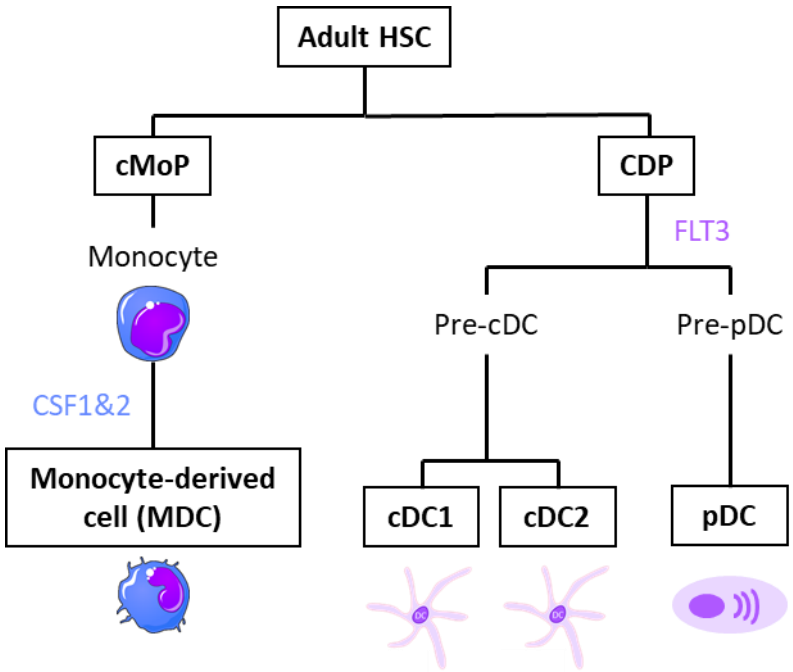

Figure 1.4: Summary of Monocyte and DC development. cMoP and CDP develop from HSCs and terminally differentiate in the BM or tissue. Adapted from Guilliams et al. 2014.

1.4.2 Origin of MPs in humans

The ontogeny of MPs occurs in humans via a similar progression to mice (Tavian & Peault 2005) but with a different time course as there is a difference in length of the gestational period. Studies on embryonic samples have furthered our understanding of haematopoiesis in humans, which will be described in this section. Embryos can be obtained at different gestational stages immediately after

voluntary terminations, and the foetal age estimated based on anatomic structures (Tavian & Peault 2005). Human embryos are rare and difficult to acquire, therefore, the findings have been verified in avian and mouse embryos, demonstrating the conservation in higher vertebrate (Godin & Cumano 2005).

Studies of these embryos revealed that haematopoiesis begins with the YS by week three and lasts for three to six weeks, during which myeloid progenitors develop into embryonic Mϕs in tissues of the brain, liver, and skin (Tavian & Peault 2005). Generation of HSC occurs in the AGM at around week six, before they seed the FL between 10 and 22 weeks (Tavian & Peault 2005). In support of this, proliferative Mϕs have been identified in extravascular mesenchymal tissue and intravascular spaces before BM formation (Enzan 1986). However, it is not clear when the transition between FL and BM-derived myeloid progenitors occurs. HSC begin to seed the BM by week 15 (Hann et al. 1983). High levels of circulating HSCs are observed before 32 weeks, which may reflect the active transfer of HSC from FL to BM (Clapp et al. 1989). The HSCs present in the BM are then responsible for the maintenance of haematopoiesis throughout adult life.

There is evidence that tissue-resident Mϕs in humans show similar self-renewing properties as in mouse. Patients with limb transplantations still present with the donors Langerhans cells ten years after the procedure (Kanitakis et al. 2011). In addition, patients with loss-of-function (LoF) mutations in GATA2 (a regulator of gene expression in HSCs) lack monocytes and DCs but display normal Langerhans cells and alveolar Mϕs (Bigley et al. 2011). The blood-brain barrier restricts access of monocytes to the brain, therefore, microglial cells must have the capacity for self-renewal at steady state. The origin of intestinal Mϕs in humans remains elusive without the applicability of fate-mapping techniques. A study assessing turnover of intestinal Mϕs in donor-derived small intestinal segments transplanted along with pancreas tissue revealed that all donor-derived Mϕ subsets were completely replaced by recipient cells over time (Bujko et al. 2017), consistent with findings by Bain et al., 2014.

However, distinct populations with different rates of replacement were identified, reflecting the findings by Shaw et al., 2018 in mice.

Parallel DC cell populations characterised in mice have been defined in humans based on transcriptional, phenotypical, and functional homology, therefore, their ontogeny is inferred from mouse studies (reviewed by Guilliams et al. 2014). Human cMoP have recently been identified that give rise to monocyte but not DCs, which is consistent with the separation of moDCs from the ontogeny of CDP (Kawamura et al. 2017).

1.5 Tissue-resident Mϕs and their functions

There are specialised Mϕs that reside in every tissue of the body, including microglia in the brain, Kupffer cells in the liver, and alveolar Mϕs in the lungs. As described earlier, these tissue-resident Mϕ are derived from primitive YS or FL progenitors, which are self-maintained during steady-state (Ginhoux et al. 2010; Guilliams et al. 2013; Hashimoto et al. 2013; Hoeffel et al. 2012; Mass et al. 2016; Yona et al. 2013). Classically and alternatively activated Mϕ give rise to M1 and M2 Mϕ respectively (reviewed by Italiani & Boraschi 2014). M1 Mϕ are activated by signals, such as IFNγ and TNFα, and display inflammatory properties including TNFα and NO production, whereas M2 Mϕ are activated by signals such as IL-4 and IL-13, and display reparative properties, including efferocytosis (phagocytosis of dead/dying cells) and IL-10 production (reviewed by Italiani & Boraschi 2014). In the context of inflammation, monocytes are recruited to the tissue, where they undergo maturation via a series of intermediaries and eventually acquiring the typical properties of M1 or M2 Mϕs, through a process sometimes referred to as the "monocyte waterfall" (Tamoutounour et al. 2013). The direction of maturation is determined by the environment. This demonstrates that monocytes are plastic cells which can give rise to populations with distinct functions depending on local signals

Tissue-resident Mϕs have distinct functions, which are considered to be influenced by the local environment but the determining factors remain largely unknown. Microglial cells are important during development of the brain and neural circuitry, as well as preserving synapses. Mutations in the

CSFR in humans leads to the loss of myelin sheaths and axonal destruction (reviewed by Wynn et al. 2013). Kupffer cells are involved in iron recycling when clearing old red blood cells (RBCs), lipid metabolism, and toxin removal (reviewed by Wynn et al. 2013). Alveolar Mϕs are important in surveillance, maintaining homeostasis, and clearing surfactants (reviewed by Davies et al. 2013). A common feature of tissue-resident Mϕs is that they are critical in the development and maintenance of normal organ function. However, Mϕs have also been associated with the pathogenesis of inflammatory and degenerative diseases, such as multiple sclerosis (MS) and liver fibrosis (reviewed by Wynn et al. 2013). Intestinal Mϕs have distinct specialisations for their microbe-rich environment, which will be discussed in more detail below.

1.5.1 Intestinal Mϕs in the mouse

Historically, studying the role of intestinal Mϕs has proven challenging due in part to overlapping in expression of surface markers with DCs, making it uncertain how to differentiate between the two populations. As a result, findings can be ambiguous when interpreting the literature. This has driven the use of multi-parameter analysis combining expression of surface markers with functional characteristics. Surface markers used to identify Mϕs include F4/80+, CD64+, and high levels of CX3C chemokine receptor 1 (CX_3CR1^{hi}), in combination with MHCII and CD11b, while DCs are defined by $CD11c^{hi}$, CD103+, and $MHCII^{hi}$ expression in the absence of CD64 (reviewed by Joeris et al. 2017). Mϕs are phagocytic and bactericidal, while DCs have the capacity to migrate to the MLNs and activate naïve T cells (Rivollier et al. 2012; Schulz et al. 2009). It is unclear why Mϕs highly express MHCII when they lack the capacity to migrate to MLNs and activate naïve T cells. A possible role is presenting antigens to local T cells; the IL-10 produced by Mϕs may contribute to the secondary expansion and maintenance of Tregs and inhibition of effector T cell responses (Hadis et al. 2011; Kayama et al. 2012). This suggests a role of intestinal Mϕs in inducing tolerance, which is consistent with their capacity to capture and present antigens and their regulatory properties.

Intestinal Mϕs in the mucosa are positioned directly under the epithelium, making them the first line of defence and ideal to capture and destroy invading pathogens. Upon activation, Mϕs initiate bacterial killing via the production of reactive oxygen species (ROS) (reviewed by Nathan & Cunningham-Bussel 2013). As described previously, mice deficient in ROS formed abscesses containing commensal organisms, highlighting the role of intestinal Mϕs in controlling the intestinal microbiota (Shiloh et al. 1999). In addition, CX_3CR1+ Mϕ sample the intestinal lumen for soluble antigens and transfer them to CD103+ DCs (Mazzini et al. 2014), which have the unique ability to prime naive T cells (Schulz et al. 2009). These interactions are critical in training the adaptive immune cells to elicit the appropriate response when presented with beneficial bacteria vs invasive pathogens.

At steady state, intestinal Mϕs constitutively produce IL-10 (Bain et al. 2013; Rivollier et al. 2012), which has an important regulatory role (Denning et al. 2007; Krause et al. 2015). Moreover, intestinal Mϕs downregulate their expression of TLRs and are able to mediate bacterial killing without the production of pro-inflammatory cytokines (Platt et al. 2010). Intestinal Mϕs do produce IL-1β, which supports the development of pro-inflammatory Th17 cells in the mucosa (Shaw et al. 2012). Th17 cells are enriched in the LP at steady-state, and there is increasing evidence that they contribute to the defence against invading bacteria by their production of a number of signature cytokines, such as IL-17, IL-22, and IL-21 (Annunziato et al. 2007; Wilson et al. 2007). IL-17 plays an important role in coordinating a response against pathogenic insults (reviewed by Witowski et al. 2004). IL-22 is a member of the IL-10 cytokine family, and it stimulates epithelial cells to enhance antimicrobial defence and epithelial barrier integrity (Zheng et al. 2008). However, Th17 cells are associated in the pathogenesis of IBD based on GWAS studies (e.g. CPEB4 loci is a transcriptional target of RORγt, a key determinant of Th17 cell differentiation), elevated levels of IL-17 production found in both CD and UC patients, and models of experimental colitis (reviewed by Wei et al. 2017).

As mentioned earlier, tissue-resident Mϕs have commonly been characterised as M1 or M2 based on mediators they produce. However, this method of characterisation is increasingly regard as too rigid

particularly for intestinal Mϕs because subsets have been identified that display overlapping properties, which may reflect a developmental continuum (with the continuous recruitment of monocytes) that is progressively imprinted by their local environment giving rise to heterogeneous populations that cannot be classified into the simplistic M1-M2 paradigm (reviewed by Biswas & Mantovani 2010; Mosser & Edwards 2009).

Consistent with the functions of other tissue resident Mϕs, intestinal Mϕs also perform a housekeeping role. Intestinal Mϕs expression of CD36 (a scavenger receptor), which is involved in the clearance of dead cells and debris (reviewed by Smith et al. 2011). Prostaglandin E2 (PGE2) production by intestinal Mϕs promotes the proliferation of epithelial progenitors in the intestinal crypts (Pull et al. 2004; Grainger et al. 2013), which highlights their role regulating the integrity of the epithelial barrier, involved in the pathogenesis of UC. Counter-intuitively, intestinal Mϕs constitutively produce a low level of TNFα at steady-state (Bain et al. 2013), which indicates that this level of TNFα does not induce pro-inflammatory responses. It has been shown that the TNFα has a role in promoting enterocyte growth, regulating the permeability of the epithelium, and stimulating the production of tissue remodelling enzymes (Ma et al. 2004).

Collectively, intestinal Mϕ provide a critical defence against invading pathogens while maintaining their regulatory properties, and carrying out housekeeping roles that are important in preserving a stable environment and may promote local regulatory responses. All things considered, it is not surprising that selective depletion of intestinal Mϕs results in increased susceptibly and severity of DDS-induced colitis (Qualls 2006). However, consistent with the other tissue Mϕs, intestinal Mϕs have also been implicated in intestinal inflammation. This will be discussed in detail in section 1.6.

1.5.2 Intestinal Mϕs in humans

Human intestinal Mϕs do not express F4/80 but do express CD64, CX_3CR1^{hi} and $MHCII^{hi}$ (reviewed by Mowat & Bain 2011; Smith et al. 2011; Smith et al. 2005). CD64 expression on human Mϕs can also be used to distinguish between intestinal Mϕs and DCs (Langlet et al. 2012; Tamoutounour et al.

2012). Intestinal Mϕs in humans are highly phagocytic and bactericidal but resistant to TLR stimulation and poor producers of pro-inflammatory cytokines, much like in mouse (Smythies et al. 2005). The bactericidal properties of human intestinal Mϕs are independent of ROS (Mahida et al. 1989), and the mechanisms by which intestinal Mϕs execute bacterial killing are unknown. There is conflicting data on the constitutive production of IL-10 in human intestinal Mϕs depending on the anatomical site examined. Bujko et al., 2017 did not detect IL-10 production by human jejunal Mϕs at baseline or upon TLR activation, which is in support of previous studies reporting a lack of IL-10 production by human jejunal Mϕs (Smythies et al. 2005; Smythies et al. 2010), whereas human colonic Mϕs have been shown to produce IL-10 (Kamada et al. 2008; Ogino et al. 2013). IL-10 producing Mϕs have also been shown to be more frequent in the large intestine compared with small intestine in the mouse (Krause et al. 2015).

The resistance of human intestinal Mϕs to TLR stimulation can be partly explained by the downregulation in expression of TLRs or other molecules involved in microbial recognition, for example during the differentiation of blood monocytes into intestinal Mϕs there is a downregulation of CD14 expression (Smith et al. 2001; Smythies et al. 2005). However, intestinal Mϕs express TLR3 and TLR5–9 but do not respond to stimulation with the corresponding TLR agonists (Smythies et al. 2010), which indicates that there are other mechanisms facilitating their resistance to TLR stimulation. NFκB is a transcription factor that is activated upon TLR stimulation. During steady state, NFκB is retained in the cytosol by its association with the protein IκBα. Upon stimulation of TLRs, IκBα is phosphorylated and targeted for degradation, freeing NFκB to translocate into the nucleus where it promotes the transcription of pro-inflammatory cytokines (reviewed by Baldwin 1996). Intestinal Mϕs have a reduced ability to phosphorylate IκBα in response to microbial stimulation and down-regulated adapter proteins MyD88 and TRIF (Smythies et al. 2010). Collectively, these components contribute to the regulatory properties of intestinal Mϕs. The signals required to promote these regulatory properties during monocyte differentiation are discussed in section 1.6.

1.6 The role of Mϕs in health and disease

1.6.1 The role of Mϕs in health and disease in the mouse

A study by Bain et al., 2014 showed that self-renewing Mϕ (embryonic precursors) are replaced by monocyte-derived Mϕ during the neonatal period. In the absence of inflammation, newly recruited monocytes lose their inflammatory properties as they mature into 'regulatory Mϕs', however, during inflammation this process is disrupted, and the recruited monocytes retain their inflammatory properties resulting in the accumulation of 'inflammatory Mϕs' (refer to Figure 1.5). This phenomenon has previously been reported but the inflammatory Mϕs were labelled as DCs (Rivollier et al. 2012; Zigmond et al. 2012). Bain et al. 2013 were also able to demonstrate a context-dependent differentiation of Ly6C^{hi} monocytes. It was first shown that resident Mϕs did not change their properties during inflammation and that there was no distinct population of inflammatory Mϕs carrying out a separate function. Instead, recruited monocytes were the source of both Mϕ phenotypes (Weber et al. 2011; Bain et al. 2013). The data showed the transition of Ly6C^{hi} monocytes into resident Mϕs via intermediary phases, where the cells still retained their pro-inflammatory properties. During colonic inflammation, there was an accumulation of cells in the intermediate phase (Weber et al. 2011; Bain et al. 2013). This suggests that during inflammation the full maturation of Ly6C^{hi} monocytes into non-inflammatory Mϕs is disrupted, which results in an accumulation of inflammatory Mϕs that further contribute to the inflammation. This context-dependent differentiation of Ly6C^{hi} monocytes provides the plasticity for intestinal Mϕs to respond to pathogenic insults. However, during chronic intestinal inflammation, there is a breakdown in the feedback mechanisms required to return to steady-state and begin repairs.

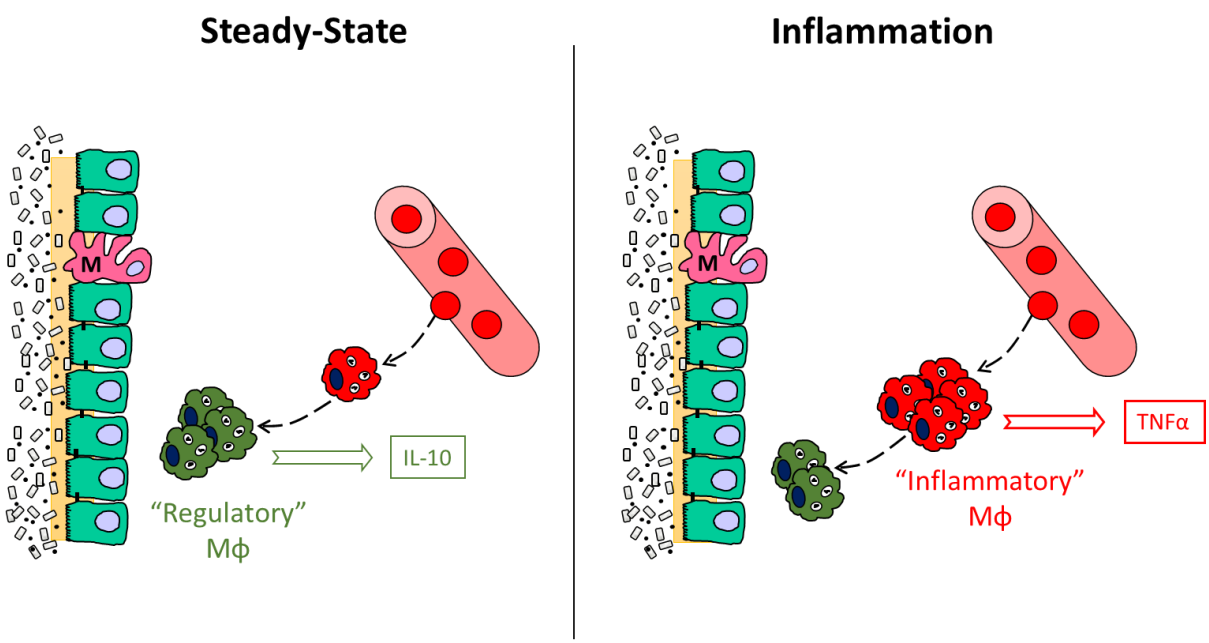

Figure 1.5: Monocyte recruitment to the intestine. In the absence of inflammation, Ly6C^{hi} monocytes are continuously recruited to the intestine where they replenish the Mϕ pool. These monocytes lose their inflammatory properties as they mature into regulatory Mϕs. However, during inflammation, this process is disrupted, and the monocytes retain their inflammatory properties to mature into pro-inflammatory Mϕs. The figure is based on data from Bain et al. 2013.

A recent study by Shaw et al., 2018 described three similarly sized intestinal Mϕ populations, based on expression of Tim-4 (apoptotic cell uptake receptor) and CD4, with distinct replenishment rates. Tim-4+CD4+ Mϕ were self-maintained, Tim-4-CD4+ Mϕ displayed slow turnover from blood monocytes, and Tim-4-CD4- Mϕ showed rapid replacement. In support of this, Tim-4+CD4+ cells were dominant in CCR2 KO mice (Shaw et al. 2018). These recent findings suggest there are locally maintained intestinal Mϕ in addition to the monocyte-derived Mϕ described by Bain et al., 2014, which may have been overlooked due to not being able to discriminate them from the monocyte-derived population. Interestingly, exposure to commensal bacteria was required for the development of all three populations, independent of ontogeny (Shaw et al. 2018). This highlights the role of environmental cues in determining Mϕ function. In support of this, a key study showed that YS-derived Mϕ (YS-Mϕ), FL monocytes, and adult monocytes could all colonise an empty alveolar niche and differentiate into functional and self-maintaining AM (Van de Laar et al. 2016).

The environmental conditions that determine monocyte differentiation into regulatory or inflammatory Mϕs are poorly understood but there are data to support a role for both IL-10 and TGFβ in the generation of the regulatory population. Conditional knock out (KO) mice were created in which the IL-10R was selectively deleted from Mϕs using CX_3CR1 to direct Cre recombinase enzymes to cut at LoxP sites on the IL-10R gene (Zigmond et al. 2014). These mice developed severe enterocolitis driven by exposure to commensal bacteria, with a phenotype similar to that observed in mice with IL-10 deficiency. Immunofluorescence analysis showed an accumulation of Mϕs with an inflammatory phenotype in the LP, which resembled the intermediate inflammatory cells previously described. This highlights that the ability of intestinal Mϕs to respond to IL-10 is critical to maintaining immune homeostasis. In part, the role of IL-10 may be to directly promote the differentiation of newly arrived monocytes into regulatory Mϕs. Alternatively, the accumulation of inflammatory Mϕs may be a consequence of the inflammation that develops in IL-10R deficient animals rather than a direct consequence of the inability of these cells to respond to IL-10. In support of IL-10 being the critical signal, Shouval et al. 2014 showed IL-10Rβ KO mutations targeting innate immune cells impaired the generation and function of regulatory intestinal Mϕs.

TGFβ has also been shown to be a crucial signal in promoting monocyte differentiation into regulatory Mϕs, as well as regulating the accumulation of monocytes in the intestine (Schridde et al. 2017). Importantly, Schriddle et al., 2017 showed that TGFβ and IL-10 imprint the distinct properties of intestinal Mϕs by comparing the global transcriptome of TGFβR-deficient Mϕs with that of published transcriptome from IL10R-deficient Mϕs: TGFβ shapes their tissue repair and scavenging functions, and IL-10 downregulates their capacity to produce pro-inflammatory mediators. There is evidence that TGFβ is also important in the development and self-maintenance of alveolar Mϕ and microglial cells (Butovsky et al. 2014; Yu et al. 2017). This is consistent with the concept that environmental cues, and not the developmental origin, are the major determinants of Mϕ function.

Collectively, these studies show TGFβ and IL-10 act synergistically to control the inflammatory activity of newly arrive monocytes and imprint the regulatory phenotype of intestinal Mϕ (refer to Figure 1.6).

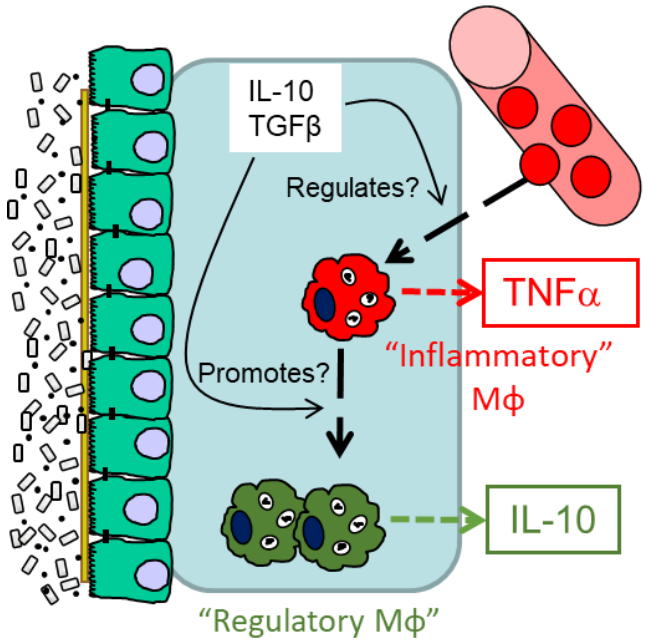

Figure 1.6: Mediators of intestinal Mϕ development. The local signals required for monocyte differentiation into 'regulatory' Mϕs during steady-state are unclear; IL-10 and TGFβ have both been shown to have important non-redundant roles. The figure is based on a collection of data from Zigmond et al., 2014, Shouval et al., 2014, and Smythies et al., 2005.

1.6.2 The role of Mϕs in health and disease in humans

Bujko et al. 2017 identified four Mϕ populations (Mf1-4) in human small intestine and tracked their turnover in patients who underwent a pancreatic transplant with an associated small intestinal segment; Mf1 and Mf2 showed rapid turnover and were phenotypically similar to blood monocytes, whereas Mf3 and Mf4 showed significantly slower replacement and displayed progressively similar properties typical of intestinal Mϕ, which suggests a developmental relationship between monocytes and intestinal Mϕs. The study by Bain et al., 2013 characterised Mϕs isolated from the human ileum, and suggested a pattern of maturation from $CD14^{hi}$ cells to $CD14^{lo}$ cells through intermediate stages, similar to that found in mice. The distribution of these cell populations was compared in healthy ileum and ileum from a CD patient. An accumulation of CD14+ cells was observed in the ileum of the CD patient, reflecting the murine model of colonic inflammation (Bain et al. 2013). Multiple studies have

observed the same increase in the proportion of CD14+ cells isolated from the mucosa of CD patients in comparison to healthy controls (M. C. Grimm et al. 1995; Kamada et al. 2008; Lissner et al. 2015; Rugtveit et al. 1997; Thiesen et al. 2014; Magnusson et al. 2016; Jones et al. 2018). This suggests that the same disruption in monocyte differentiation into resident Mϕsreported in mice may also occur in humans; the increase in the number of CD14+ cells in IBD may result in increased production of inflammatory mediators, and therefore perpetuating the intestinal inflammation. A study mapping transcriptional changes during monocyte differentiation in vitro, in the presence of CSF-1, showed that LPS-inducible genes were strongly enriched for those identified as IBD susceptibility loci in GWAS (Baillie et al. 2017). This indicates that dysregulation of monocyte differentiation in the intestine is a key process in the pathogenesis of IBD. However, the local signals that cause this disruption in monocyte maturation are unclear.

There have been few studies on the factors that control the differentiation of Mϕs within the human intestine but murine data suggest a potential role for TGFβ and IL-10. TGFβ produced by stromal cells has been shown to drive downregulation of both TLR expression and cytokine production in monocytes, resembling intestinal Mϕs, during in vitro culture (Smythies et al. 2005). The induction of these regulatory properties is partly due to a reduced capacity to phosphorylate NFκB as a result of TGFβ signalling (Smythies et al. 2010). As mentioned earlier, enhanced SMAD7 expression has been observed in T cells extracted from inflamed mucosa (Fantini et al. 2009), which provides resistance to Treg-mediated suppression by interfering with SMAD2/3 mediated TGFβ signalling. A similar effect on signalling could also be true in monocytes, where a reduced TGFβ signal would favour their differentiation into inflammatory Mϕs but this has yet to be tested. In mice, IL-10 has been shown to be important during monocyte differentiation into resident Mϕs(Zigmond et al. 2014; Shouval et al. 2014). If this is true in humans, then a reduced response of monocytes to IL-10 would shift the favourability of monocyte differentiation towards inflammatory Mϕs. Accumulation of inflammatory Mϕs in the intestine of IBD patients could be the exacerbating factor that sustains inflammation in these patients.

1.7 Monocyte subsets in health and disease

Monocytes are highly plastic cells that can be imprinted by the environment and rapidly respond to inflammatory cues. Monocytes themselves are made up of heterogeneous populations that have distinct functions. Monocytes were considered to simply be progenitors of tissue-resident Mϕs and some DCs. However only some tissue Mϕs, including those in the intestine, are monocytes derived. This has driven investigations into the roles and characteristics of monocytes in as effector cells in their own right, and these will be detailed in this section.

1.7.1 Monocyte subsets in the mouse

Two main monocyte subsets have been characterised in mice based on their expression of lymphocyte antigen six complex locus C1 (Ly6C) (Geissmann et al. 2003). The function of Ly6C is poorly understood but it is known to be expressed in a lineage-specific manner, and therefore it is often used as a marker of differentiation (reviewed by Lee et al. 2013). Ly6C^{hi} monocytes leave the BM and enter the bloodstream, where a small proportion down-regulate their Ly6C expression to mature into Ly6C^{lo} monocytes (Sunderkotter et al. 2004; Yona et al. 2013). C/EBPb drives Ly6C^{hi} differentiation into Ly6C^{lo} by promoting NR4A1, a master regulator of differentiation and survival of Ly6C^{lo} monocytes (Hanna et al. 2011; Mildner et al. 2017). In a recent publication on monocyte nomenclature, the addition of an intermediary subset was proposed (Ziegler-heitbrock et al. 2014). However, this intermediary subset has not been well characterised in mice.

Ly6C^{hi} monocytes highly express C-C chemokine receptor type 2 (CCR2), which mediates monocyte release from the BM as demonstrated in CCR2 KO mice (Boring et al. 1997; Jia et al. 2008; Serbina & Pamer 2006; Tsou et al. 2007). However, the contribution of CCR2 in recruiting monocytes to sites of inflammation is unclear and may be tissue-specific. Through the use of fate-mapping, Bain et al. 2014 showed that Ly6C^{hi} monocytes are continuously recruited to the intestine in a CCR2-dependent manner. In support of this, CCR2-sufficient Ly6C^{hi} monocytes fail to enter CCL2-deficient intestine

(Takada et al. 2010). During inflammation CCL2 expression is increased, indicating enhance recruitment of Ly6C^{hi} monocytes (Nenci et al. 2007). The newly recruited monocytes differentiate into intestinal Mϕ in a context-dependent manner, demonstrating their capacity to respond to environmental cues and that Ly6C^{hi} monocytes are highly plastic cells (Schridde et al. 2017; Bain et al. 2013). In addition, monocytes can enter tissues in steady-state and then recirculate to the lymph nodes (LNs) without differentiation into Mϕs, challenging the concept that monocytes become tissue-resident Mϕ by default (Jakubzick et al. 2013).

The main role of Ly6C^{lo} monocytes is to remain in the bloodstream and patrol the endothelium, which is dependent on the integrin LFA-1 (Auffray et al. 2007). CX_3CR1 is highly expressed in Ly6C^{lo} monocytes, which mediates patrolling and rapid tissue invasion at the site of an infection, making them a part of the early inflammatory response (Auffray et al. 2007; Ancuta et al. 2003). Auffray et al., 2007 showed in the first two hours of infection, Ly6C^{lo} monocytes are the major source of TNFα, which was transiently produced and genes involved in tissue repair were turned on. The half-life of Ly6C^{hi} monocytes is relatively short (20 hours), consistent with the concept that they are readily recruited to tissues, while Ly6C^{lo} monocytes have a half-life of two days (Yona et al. 2013).

1.7.2 Monocyte subsets in humans

There are three major monocyte subsets in humans, which can be characterised based on their expression of CD14 and CD16 (FcγIII): classical (CD14++CD16-), intermediates (CD14++CD16+), and non-classical (CD14+CD16++) monocytes (Passlick et al. 1989; Ziegler-heitbrock et al. 2014). CD14 acts with TLR4 as a co-receptor for lipopolysaccharides (LPS), in the induction of pro-inflammatory responses (reviewed by Dobrovolskaia & Vogel 2002). CD16 is a low-affinity Fc receptor for IgG, which is expressed on a number of immune cells, including neutrophils and NK cells (Lisi et al. 2011).

A study in macaques showed that the three monocyte subsets are not isolated populations, instead they represent a maturation pathway: classical monocytes are released from the BM into the bloodstream, where a proportion mature via an intermediate monocytes phase into non-classical

monocytes (Sugimoto et al. 2015). A more recent study, using in vivo deuterium labelling to follow monocytes in response to endotoxemia (LPS in the blood) and by analysis of humanised mice have identified a maturation pathway for human blood monocytes that is similar to mice (refer to Figure 1.7) (Patel et al. 2017). Healthy volunteers were given deuterium-labelled glucose (incorporated into the DNA of dividing cells but not carcinogenic) drink at short intervals, and their monocyte subsets were then flow-sorted at sequential time points and analysed for deuterium incorporation. The sequence in which the monocyte subsets with deuterium incorporation appeared in the blood was used to predict their maturation using mathematical modelling. Healthy volunteers received a low dose of LPS intravenously, which causes monocytopenia and the sequence of recovery of the monocyte subsets in the blood was then followed. Finally, humanised mice were injected with classical monocytes, and their development was then tracked. The relative lifespan of human monocyte subsets are consistent with mice: classical monocytes have a short half-life (one day), while non-classical monocytes have a half-life of seven days. Intermediate monocytes also display a short half-life (four days), supporting the concept that they represent a transition between classical and non-classical monocytes.

Gene expression analysis comparing the monocyte subsets in humans and mice indicate that the classical monocytes resemble Ly6C^{hi} monocytes, while non-classical monocytes resemble Ly6C^{lo} monocyte (Figure 1.6)(Ingersoll et al. 2010). CCR2 is highly expressed on classical monocytes, drawing parallels with the mouse data discussed above, this is consistent with the concept that this subset is readily recruited to the intestine. Classical monocytes have also been labelled as 'inflammatory' monocytes because they display robust production of pro-inflammatory cytokines in response to various TLR agonists (Belge et al. 2002; Boyette et al. 2017; Cros et al. 2010; Thiesen et al. 2014).

The intermediate subset was not recognised in mice until recently, and as a result, relatively little is known about this subset. Gene expression profiling revealed that 87% of genes and surface proteins in intermediate monocytes were expressed at levels between classical and non-classical monocytes,

consistent with their proposed intermediary nature (Wong et al. 2011). However, analyses of their transcriptome using SuperSAGE revealed unique identifiers of intermediate monocytes involving antigen presentation, activation, and angiogenesis, which provides genetic evidence for distinct roles (Zawada et al. 2011). Studies have shown that intermediate monocytes display a high capacity to produce pro-inflammatory cytokines in response to various TLR agonists *in vitro* (Belge et al. 2002; Boyette et al. 2017; Cros et al. 2010; Thiesen et al. 2014). In addition, an expansion in intermediate monocytes has been reported in acute infections, such as sepsis, as well as chronic inflammation, including IBD, rheumatoid arthritis (RA), and atherosclerosis (Fingerle et al. 2018; Nockher et al. 1998; Rossol et al. 2012; Schlitt et al. 2004; Thiesen et al. 2014). Collectively, these indicate that intermediate monocytes may not simply be a population transiting between classical and non-classical monocytes but may have functional activities distinct from either of the other subsets.

Non-classical monocytes highly express CX_3CR1, resembling $Ly6C^{lo}$ monocytes, which is consistent with the concept that this subset patrol the endothelium as CX_3CR1 was shown to be critical in this role in mouse (Auffray et al. 2007; Thiesen et al. 2014). Studies have shown that non-classical monocytes respond poorly to various TLR agonists and have a low capacity to produce pro-inflammatory cytokines (Belge et al. 2002; Boyette et al. 2017; Thiesen et al. 2014; Cros et al. 2010). However, non-classical monocytes display a robust response to TLR7/8 (viral recognition) agonists, which suggest that this subset has the capacity to be pro-inflammatory in certain contexts (Cros et al. 2010).

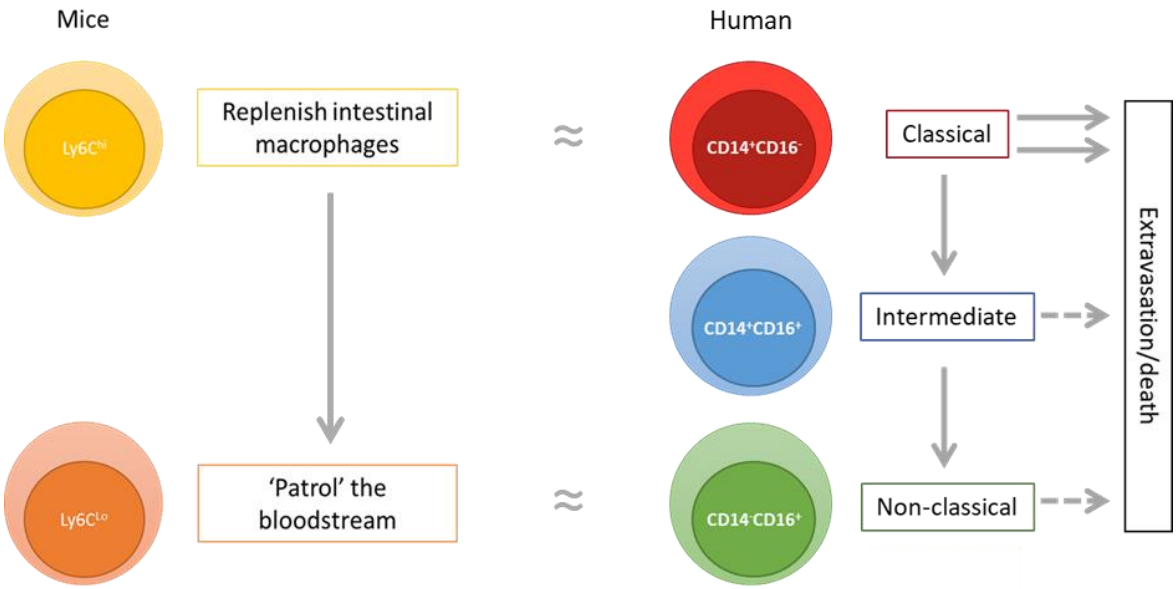

Figure 1.7: Monocyte subsets and their function. Ly6C^{hi} monocytes replenish the intestinal Mϕ pool, while Ly6C^{lo} monocytes remain in the bloodstream and patrol for pathogens. Gene expression analysis revealed similarities between Ly6C^{hi} and classical monocytes, while Ly6C^{lo} monocytes showed similarities to non-classical monocytes. These are not isolated populations but represent stages of differentiation. The figure is based on a collection of data from Bain et al., 2014, Auffray et al., 2007, Yona et al., 2013, Ingersoll et al., 2010, Patel et al.,. 2017.

1.7.3 Role of monocytes in intestinal inflammation in the mouse

An increase in CCL2 expression has been observed in mucosal inflammation indicating enhance recruitment of Ly6C^{hi} monocytes, which may contribute to the persisting inflammation (Nenci et al. 2007). In support of this, CCR2 KO mice display reduced susceptibility to DSS-induced colitis (Platt et al. 2010). A recent study further implicates monocytes in gut inflammation: Schippers et al. 2015 showed that β_7 integrin deficiency in mice was protective against DSS-induced colitis in Rag-deficient mice due to reduced monocyte recruitment. Injecting WT Ly6C^{hi} monocytes but not β_7 integrin-deficient monocytes, caused an aggravation of the colitis in these mice. This again indicates that monocytes are a critical contributor of inflammation in already inflamed conditions. However, there has been no evidence yet that monocytes are the trigger of inflammation.

Alternatively, studies have shown that monocytes have a regulatory role during inflammation. As mentioned previously, NOD2 mutations are associated with CD pathogenesis considered to be due to

the impaired clearance of pathogenic bacteria (Cooney et al. 2010; Kim et al. 2011). Stromal cells produce CCL2 in a NOD2-dependent manner, demonstrated by the reduced production of CCL2 in NOD2 KO mice (Kim et al. 2011). The subsequent reduction in monocyte recruitment results in impaired clearance of pathogens as adoptive transfer of Ly6Chi monocytes restored the clearance of pathogens (Kim et al. 2011). In addition, orally inoculated with *Toxoplasma gondii*, a parasite, showed that monocytes were primed for regulatory function in the BM by systemic inflammatory signals received from the intestine and relayed by NK cells (Askenase et al. 2015). This study demonstrates that the function of intestinal Mϕs can be regulated at two levels: locally by the environment and systemically via the BM, and these can interact i.e. systemic signals from the intestine during inflammation can cause functional changes in progenitors in the BM, termed 'trained immunity'. The concept of 'trained immunity' was considered to apply to mature myeloid cells but it is now evident that myeloid progenitors are also involved. Myeloid progenitors expand in the BM in response to β-glucan (a component of the cell wall of bacteria and fungi), and these progenitors displayed functional changes, including elevated IL-1β, which coincided with a more robust response to secondary LPS challenge (Mitroulis et al. 2018). These observations demonstrate the benefits of 'trained immunity' for the host's defence against pathogens. Another study observed the same expansion of myeloid progenitors with greater capacity to produce pro-inflammatory cytokines in response to a high-fat diet (Christ et al. 2018). Thus, there is evidence that reprogramming of myeloid cell development in BM can both promote inflammatory activity (Christ et al., 2018; Mitroulis et al., 2018) and regulatory properties (Askenase et al., 2015) with the outcome likely to vary between different contexts and experimental models. The implication of trained immunity identified in the context of acute inflammation for chronic inflammatory diseases like IBD remains to be explored.

1.7.4 Role of monocytes in intestinal inflammation in humans

There is direct evidence that there is enhanced monocyte recruitment to inflamed mucosa: peripheral blood mononuclear cells (PBMCs) isolated from IBD patients were radiolabelled and re-injected before

abdominal scanning, which demonstrated monocyte uptake at actively inflamed regions (Grimm et al. 1995). In addition, enhanced expression and production of CCL2 has been observed in IBD patients (Grimm et al. 1996), reflecting observations by Nenci et al., 2007 in the mouse.

There is also evidence in humans that systemic signals from the intestine during inflammation cause functional changes to circulating cells. One study showed that the BCG vaccine given to volunteers improved their symptoms of viremia when a second vaccine with the live attenuated yellow fever vaccine (YFV) was given four weeks later compared to placebo, and PBMCs isolated from volunteers given the BCG displayed greater capacity to produce proinflammatory cytokines (Arts et al. 2018). Another study showed that monocyte-derived Mϕ (moMϕ) from CD patients displayed reduced TNFα production in response to *E.coli* compared to healthy controls (Smith et al. 2009). Furthermore, monocytes showed reduced retinaldehyde dehydrogenase (RALDH) activity in CD patients, which favours the differentiation of Mϕ with an inflammatory phenotype in vitro (Sanders et al. 2014). The concept that systemic signals from the intestine during inflammation cause functional changes to circulating cells formed the rationale for studying blood monocytes, as the likely precursors of intestinal Mϕ. The rationale for studying IL-10 response will be covered in the subsequent section.

1.8 The importance of IL-10 in regulating intestinal inflammation

IL-10 is mainly produced by leukocytes, including monocytes, Mϕs, and Tregs (reviewed by Kole & Maloy 2014). The production of pro-inflammatory cytokines is inhibited by IL-10, and therefore, is considered an anti-inflammatory cytokine. IL-10 acts on both myeloid cells and lymphoid cells to suppress innate and adaptive inflammatory responses. It has been over 20 years since the observation that IL-10 deficient mice developed colitis upon exposure to commensal gut bacteria (Kühn et al. 1993), which revealed an essential role for IL-10 in maintaining immune homeostasis in the intestine. The role of IL-10 in the steady-state and inflamed intestine will be examined in this section.

1.8.1 IL-10R signalling

IL-10 signals through the IL-10R, which is a tetramer consisting of two α and two β chains; the α chain is specific to the IL-10R, while the β chain appears in other cytokine receptors, including IFNλ and IL-22 receptors (reviewed by Moore et al. 2001). The α chain has been shown to be important in mediating high-affinity binding and signal transduction, while the β chain is mainly required for signalling (Kotenko et al. 1997). Upon binding of IL-10 onto IL-10Rα, IL-10Rβ is recruited, and the receptor becomes activated (reviewed by Mosser & Zhang 2008). The activation of the receptor triggers a phosphorylation cascade involving Janus kinase 1 (JAK1), TYK2, and STAT3 (Riley et al. 1999). Phosphorylated STAT3 molecules dimerise and translocate to the nucleus where they modify gene expression to bring about immune regulation but the events following DNA binding are poorly understood. Suppressor of cytokine signalling 3 (SOCS3) transcription is induced by STAT3, and is a key regulator of the activity of IL-10, including inhibition of the NFκB pathway, as well as negative feedback to suppress further IL-10 signalling (refer to Figure 1.8)(Mosser & Zhang 2008). The role of IL-10 in regulating intestinal inflammation will be discussed further in this section.

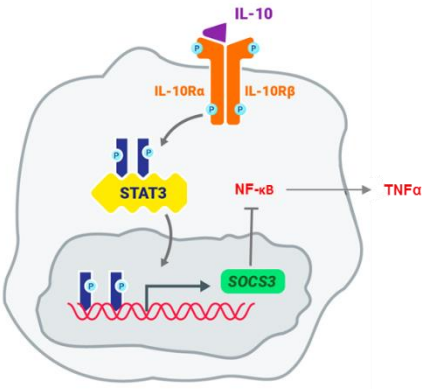

Figure 1.8: IL-10R signalling pathway. Upon activation of the IL-10R, phosphorylated STAT3 undergoes dimerisation and is translocated to the nucleus where it promotes the transcription of SOCS3. SOCS3 inhibits the NFκB pathway, which prevents the release of inflammatory cytokines, including TNFα, IL-6, and IL-1β. The figure is based on a collection of data from Moore et al., 2001, Mosser & Zhang, and Riley et al., 1999

1.8.2 The role of IL-10 in the murine intestine

IL-10 is a critical cytokine in preventing excessive inflammatory responses to innocuous agents, as demonstrated in murine models. IL-10 deficient mice developed chronic enterocolitis (inflammation of the small intestine and colon) driven by exposure to pathobiome (Berg et al. 1996; Kühn et al. 1993). Mice that are selectively deficient in MyD88 in Mϕs, and therefore lack bacterial sensing do not develop colitis in an IL-10 deficient setting (Hoshi et al. 2012). These findings demonstrate that IL-10 is important in preventing inflammatory responses against commensal bacteria. Treatment with IL-10 prevents the development of colitis in IL-10 deficient mice and DSS-treated mice (Lindsay et al. 2003; Steidler et al. 2000). This further supports the importance of IL-10 in regulating inflammation even in the setting of induced inflammation. A recent study showed that IL-10-deficiency contributes to a loss of intestinal Mϕ tolerance to bacteria as assessed by chromatin alterations mimicking inflammation, which is an initiating event in chronic intestinal inflammation (Simon et al. 2016). IL-10 has also been shown to be involved in promoting mitophagy (mitochondrial autophagy) that eliminates dysfunctional mitochondria; in IL-10 deficient mice and IL-10R-deficient patients, Mϕs accumulate damaged mitochondria resulting in enhanced activation of the inflammasome and subsequent production of IL-1β (Ip et al. 2017). These provide mechanisms by which Mϕs contribute to intestinal inflammation in the absence of IL-10 signalling.

IL-10 has the potential to act on myeloid and lymphocyte populations to control inflammation, and until recently it was unclear which is the critical population whose response to IL-10 is essential in preventing the development of intestinal inflammation. Two studies by Shouval et al. 2014 and Zigmond et al. 2014, in which the IL-10R was selectively deleted in Mϕs, support the concept that these cell populations are the critical targets of IL-10 as the mice developed spontaneous colitis. These studies also highlight the important role of Mϕs in regulating inflammation in the intestine.

IL-10 has been shown to be critical in the ability of Mϕs to regulate adaptive immune responses. One study showed that the ability of CX_3CR1^{hi} cells, likely to be Mϕs, to inhibit T cell responses and prevent

intestinal inflammation was abrogated in myeloid-specific STAT3-deficient mice, and the transfer of WT CX_3CR1^{hi} cells prevented the development of colitis in these mice (Kayama et al. 2012). In addition, CCR2 KO mice have a significantly depleted intestinal Mϕ population and display more severe DDS-induced colitis due to impaired IL-10 production (Takada et al. 2010). This highlights the importance of intestinal Mϕs in maintaining homeostasis, and that both their production of IL-10 and their control by IL-10 are a crucial feature of their regulatory properties.

1.8.3 The role of IL-10 in the human intestine

Naturally occurring LoF mutations in the IL-10R gene are rare but have been identified in patients with very early-onset IBD (VEO-IBD), who display enhanced production of pro-inflammatory cytokines, including TNFα and IL-1β, from their PBMCs. VEO-IBD patients have a severe treatment-refractory phenotype and often require treatment by allogeneic BM transplantation (Begue et al. 2011; Glocker & Kotlarz 2009; Mao et al. 2012). This demonstrates the important non-redundant role of IL-10 signalling in preventing inflammation in the human intestine. Patients with VEO-IBD also commonly suffer from auto-immune diseases, including psoriasis and RA, which highlights the importance of IL-10 in establishing tolerance to self-antigens. In addition, a comparison of genes responsible for monogenic disease with IBD-like pathology and risk loci associated with IBD revealed that genes related to IL-10 (*IL-10*, *IL-10RA*, and *IL-10RB*) were the only ones common to both groups of patients (Uhlig 2013).

GWAS have found IBD susceptibility variants in the genes for *IL-10* and *STAT3* (Franke et al. 2010; McGovern et al. 2010). However, the majority of IBD patients do not have LoF mutations or functionally significant variants in their IL-10R genes. Begue et al. 2011 investigated the concept of defective anti-inflammatory responses in IBD patients and showed patients with a severe relapse at the time of analysis displayed a reduced response to IL-10 inhibition of LPS-induced IL-8 production, which was restored once the patients achieved remission (Begue et al. 2011). However, immune populations were not specifically examined. Therefore, the possibility that these patients have

reduced responsiveness to IL-10 in critical populations has not been fully explored. There is evidence for a similar concept in T cells where cells from IBD patients are resistant to TGFβ-mediated suppression due to enhanced expression of SMAD7.

IL-10 therapy showed promise in murine models of intestinal inflammation but did not show significant benefits in IBD patients (reviewed by Marlow et al. 2013). There are a number of explanations proposed for the failure of IL-10 therapy (reviewed by Marlow et al. 2013) but a sub-optimal ability of critical cells to respond to IL-10 in IBD could contribute. Analogous to the targeting of SMAD7, with the anti-sense drug Mongersen, in order to enhance T cell responses to TGFβ (Monteleone et al. 2015), understanding the IL-10 response of IBD patients could lead to therapeutic interventions involving the IL-10 signalling pathway.

1.9 Hypothesis and Aims

1.9.1 Hypothesis

A sub-optimal response to IL-10 in critical populations gives rise to inflammatory cells that initiate or sustain inflammation in IBD.

According to this hypothesis, individuals in the population fall within a spectrum of MP responsiveness to IL-10. At one end, healthy individuals with an optimal IL-10 response and at the other end, rare individuals with LoF mutations in their IL-10R who develop VEO-IBD. The majority of IBD patients lie in-between and are capable of responding to IL-10 but their response is suboptimal.

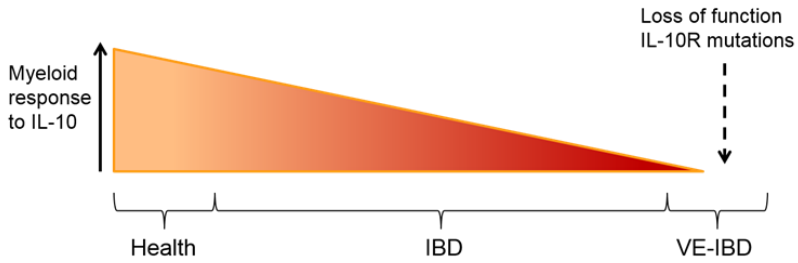

Figure 1.9: Illustration of the spectrum of IL-10 response in the population.

1.9.2 Aims

The overall aim of the project is to compare IL-10 responses of Mo/moMϕ in health and IBD and define mechanisms underlying any differences. Specifically, the objectives of this project are:

1. Determine the ability of IL-10 to inhibit LPS-induced TNFα production in the monocyte subsets of healthy individuals; identify the mechanistic basis of the differences between monocyte subsets by investigating components along the IL-10 signalling pathway.
2. Determine the ability of IL-10 to inhibit LPS-induced TNFα production in the monocyte subsets of healthy controls and IBD patients; assess differences in signalling components along the IL-10 signalling pathway between health and IBD.
3. Identify intestinal Mo/moMϕs in health and IBD and determine their responsiveness to IL-10.

Chapter 2: Materials and Methods

2.1 Materials

2.1.1 Chemicals and Reagents

- **Ficoll-Paque Plus:** is a high-density isotonic polysaccharide solution, which is used to separate PBMCs from whole blood on the basis of their densities (GE Healthcare, UK).
- **RPMI-1640 Medium (Dutch modification):** is a tissue culture medium containing two buffering agents, sodium bicarbonate and 20mM HEPES, for maintaining optimal pH conditions (Sigma, USA).
- **HBSS (Hank's balanced salt solution):** is a tissue culture medium containing bicarbonate ions used as a buffer system (Sigma, USA).
- **FCS (fetal calf serum):** is a supplement for complete medium, and it is used in FACS buffer to inhibit non-specific binding of antibodies during labelling (PAA, Austria).
- **L-glutamine:** is an amino acid used as a supplement in complete medium (Sigma, USA).
- **Pen/Strep (Penicillin/Streptomycin):** are antibiotics used in complete medium to control bacterial contamination (Sigma, USA).
- **Gentamicin:** is an antibiotic used in complete medium to control bacterial contamination (Invitrogen, USA).
- **EDTA (ethylenediaminetetraacetic acid):** is a chelating agent used in FACS buffer to prevent clustering of the cells by binding calcium ions, which interferes with cadherins and integrins. Also used to disassociate epithelial cells from intestinal tissue during LPMC extraction (Sigma, USA).
- **Dithiothreitol (DTT):** is a reducing agent used to remove mucus and debris from intestinal tissue during LPMC extraction by disrupting disulfide bonds (Sigma, USA).
- **Deoxyribonuclease I (DNase I):** is used to degrade cell-free DNA in order to prevent clumping of LPMCs during extraction (Roche, Switzerland).

- **Collagenase D:** is an enzyme used to extract LPMCs by digesting the intestinal tissue (Roche, Switzerland).
- **Sodium azide:** is used in FACS buffer to prevent capping by inhibiting crosslinking, and therefore shedding or internalisation of the antibody-antigen complexes formed once the antibodies have bound to the surface marker during labelling (Sigma, USA).
- **Trypan blue solution (0.4%):** dead cells take up the stain due to their disrupted membrane allowing them to be distinguished. Used during cell counting (Sigma, USA).
- **CTV (cell trace violet):** is used for the labelling of cells to trace dividing populations using dye dilution by flow cytometry (ThermoFisher, USA).
- **LPS (lipopolysaccharide):** is an endotoxin found in the outer membrane of Gram-positive bacteria, and is a TLR4 agonist (*E. coli* 0111: B4 from Sigma, USA).
- **Flagellin:** is a protein that forms the filament in bacterial flagellum, and is a TLR5 agonist (Invivogen).
- **Pam3-Cys-Ser-Lys4 (Pam_3CSK_4):** synthetic bacterial lipopeptide, and is a TLR1/2 agonist (Invivogen, USA)
- **Polyinosinic:polycytidylic acid (Poly(I:C)):** a synthetic analogue of double-stranded RNA (dsRNA), and is a TLR3 agonist (Sigma, USA).
- **Monensin:** widely used to disrupt the Golgi apparatus and retain newly synthesised cytokines within the Golgi apparatus by blocking vesicle transport. The stock solution was prepared in ethanol at a concentration of 12mM and aliquots were stored at -80˚C (Sigma, USA).
- **PFA (paraformaldehyde):** is used as a fixative by creating covalent bonds between intracellular proteins (Sigma, USA).
- **Leucoperm A and B:** are used for intracellular cytokine staining. Leucoperm A is a fixative and Leucoperm B is a permeabilising agent (AbD Serotec, UK).
- **Methanol:** alcohol used as a permeabilisation agent for intracellular staining.

- **Flow-Count Fluorospheres:** are count beads used to calculate absolute cell numbers on the flow cytometer (Beckman Coulter, USA).
- **TMI-005 (Apratastat):** ADAM metallopeptidase domain 17 (ADAM17) inhibitor (Axon Medchem, Netherlands).
- **Fixable viability dye:** enables identification of dead cells (eBioscience, USA)
- **Annexin V:** binds to phosphatidylserine, which is a marker of apoptosis (Thermofisher, USA)
- **FcR blocking solution:** blocks FcR-involved unspecific staining (Biolegend, UK).
- **IL-10R blocking antibody:** blocks IL-10 signalling (Biolegend, UK).
- **Fluoresbrite® carboxylate microspheres:** fluorescent microspheres that have carboxylate groups on their surfaces, used in phagocytosis studies (Polysciences Inc, US).
- **OptilyseC:** used to lyse RBCs (Beckman Coulter, USA).

2.1.2 Media and Buffers

- **Complete medium:** RPMI-1640 Medium (Dutch modification) supplemented with 10% FCS, 100ug/ml of penicillin, 100µg/ml of streptomycin, and 20mM of L-glutamine (25µg/ml of gentamicin included in LPMC culture)
- **PBS (phosphate buffered saline):** a solution containing 137mM sodium chloride, 2.7mM potassium chloride, and 12mM phosphate in ultrapure water (Ca and Mg free).
- **FACS buffer:** PBS containing 2% FCS, 1mM EDTA, and 0.2% (w/v) sodium azide.
- **PFA solution:** PBS containing 1% PFA.
- **Brilliant stain buffer:** recommended by BD to add 50µl when staining with more than one of their antibodies at the same time (BD Bioscience, UK).

2.1.3 Antibodies

The antibodies used for flow cytometry are detailed below in Table 1. The corresponding isotype controls are also listed and were used to exclude unspecific binding.

Antigen	Fluorochrome	Clone	Isotype control	Supplier
HLA-DR	APC	L243	Mouse IgG2a	Biolegend
CD16	PerCP-Cy5.5	3G8	Mouse IgG1	Biolegend
T-STAT3	PerCP-Cy5.5	M59-50	Mouse IgG2a	BD
CD192 (CCR2)	PerCP-Cy5.5	K036C2	Mouse IgG2a	Biolegend
CD14	Pacific Blue	MFE2	Mouse IgG2a	Biolegend
CD16	PE	3G8	Mouse IgG1	Biolegend
IL-10Rα	PE	3F9	Mouse IgG1	Biolegend
TNFα	PE	MAb11	Mouse IgG1	Biolegend
CD45	PE	HI30	Mouse IgG1	Biolegend
IFNα [2b]	PE	7N4-1	Mouse IgG1	BD
pSTAT3 (pY705)	Alexa Fluor 488	4/P-STAT3	Mouse IgG1	BD
CD206	FITC	15-2	Mouse IgG1	Biolegend
IL-1β	FITC	JK1B-1	Mouse IgG1	Biolegend
CX_3CR1	FITC	2A9-1	Rat IgG2b	Biolegend
IL-10	PE-Cy7	JES3-9D7	Rat IgG1	Biolegend
TNFα	PE-Cy7	Mab11	Mouse IgG1	Biolegend
CD126 (IL-6Rα)	PE-Cy7	UV4	Mouse IgG1	Biolegend
CD64	APC-Cy7	10.1	Mouse IgG1	Biolegend

Table 2.1: List of antibodies used for flow cytometry.

2.1.4 Cytokines

- **IL-10 (interleukin-10):** is a regulatory cytokine used to inhibit production of pro-inflammatory cytokines. The stock concentration was 50µg/mL, and the solution was prepared in sterile PBS containing 0.1% BSA and stored at -80˚C (R&D systems, UK).
- **IL-6 (interleukin-6):** is a pro-inflammatory cytokine used to stimulate immune responses. The stock concentration was 100µg/mL, and the solution was prepared in sterile PBS containing 0.1% BSA and stored at -80˚C (R&D systems, UK).

2.1.5 Kits

- PCR (Qiagen, Germany)
    - RNA extraction: RNeasy Micro Kit or Mini Kit
    - Reverse Transcription: QuantiTect Reverse Transcription Kit
    - SYBR Green real-time PCR: QuantiFast SYBR Green PCR Kit
    - QuantiTect primers: *SOCS3* (QT00244580), *SOCS1* (QT01157905), and *GAPDH* (QT00079247)

2.2 Methods

2.2.1 Patient recruitment and sample collection

IBD patients were recruited from The Royal London Hospital (ethical approval P/01/023 and 15/LO/2127), and healthy controls were recruited from Barts and the London School of Medicine and Dentistry (ethical approval 05/Q0405/71). All study participants gave informed written consent. In line with ethical principles for medical research involving human subjects (World Medical Association Declaration of Helsinki)

Intestinal biopsies were from patients attending The Royal London Hospital who were having a colonoscopy or a flexible sigmoidoscopy as part of their routine clinical care. Up to 8 biopsies were collected from either the colon or the ileum of IBD patients or non-IBD patients. Non-IBD patients were typically under investigation for altered bowel habit or rectal bleeding, with no previous diagnosis of IBD and no evidence of macroscopic or histological intestinal inflammation. The tissue was collected in RPMI-1640 Dutch Modification (Sigma-Aldrich) and placed on ice.

Peripheral blood was collected by venipuncture into 10ml sodium heparin Vacutainer tubes (BD) and mixed gently to prevent clotting.

For detailed demographic information collected by a clinical fellow refer to the Appendix.

2.2.2 Extracting lamina propria mononuclear cells (LPMCs) from intestinal tissue

LPMCs extraction methods have been previously described (Hart et al. 2005). Briefly, the biopsies were added to a T25 tissue culture flask (BD) containing 1mM DTT (Sigma-Aldrich) in a total volume of 15ml made up with calcium and magnesium-free HBSS (Sigma-Aldrich) to incubate for 20 minutes at room temperature (RT). The flask was then manually shaken at regular intervals. A Pasteur pipette was used to aspirate the HBSS. The biopsies were then washed twice in 10ml of fresh HBSS, using a Pasteur pipette to aspirate the HBSS between each wash. The biopsies were incubated with 1mM EDTA (Sigma-Aldrich) in a total volume of 25mL made up with HBSS for 30 minutes in a heated shaker (37^{o}C).

The EDTA was aspirated, and the biopsies were washed twice in HBSS followed by a further EDTA incubation and HBSS washes. The biopsies were then added to a new T25 flask containing 1 mg/ml collagenase D (Roche Applied Science), 2% FCS, and 20 µg/ml deoxyribonuclease I (Roche Applied Science) in a total volume of 15mL made up with HEPES buffered RPMI 1640 medium (Sigma-Aldrich) to incubate for a 1 hour in a heated shaker (37^{o}C). The flask was then manually shaken at 5 minutes intervals for a further 15 minutes. The cell suspension was passed through a 70 µm cell strainer (Fisher Scientific) and washed with HBSS, centrifuging for 5 minutes at 300g at RT before discarding the supernatant. The cell pellet was then resuspended in complete medium (with the addition of 25µg/ml gentamicin).

2.2.3 PBMC separation

Whole blood was diluted 2:1 using RPMI-1640 Dutch Modification (Sigma-Aldrich). The diluted blood was layered onto 15ml of Ficoll-Paque Plus in a 50ml Falcon tube. The Falcon tube was centrifuged for 20 minutes at 650g with the break off at RT. The interface containing PBMCs was collected into two 15ml Falcon tubes, using a Pasteur pipette, and diluted 1:1 using RPMI-1640 Dutch Modification. The 15ml Falcon tubes were then centrifuged for 10 minutes at 650g with the brake on. The cells were rewashed with complete medium, centrifuging for 5 minutes at 300g at RT before discarding the supernatant. The pellet was then resuspended in complete medium.

2.2.4 Cell counting

50µl of Trypan Blue (0.4%), 150µl of RPMI-1640 Dutch modification base medium, and 50µl of the cell suspension were mixed giving a 1:5 dilution to the cell suspension. The diluted cell suspension was then applied onto a Neubauer hemocytometer with a coverslip. The cells were counted three times in a four by four grid, and the average was taken to calculate the overall concentration of the cell suspension using the following equation:

$$5 \times (\text{Average cell number of the three counts} \times 10^{4}) = \text{cells/ml}$$

2.2.5 Monoclonal antibody staining and flow cytometry

2.2.5.1 Whole blood labelling

Anti-coagulated whole blood was added at a volume of 100µL to FACS tubes (BD) for labelling. Fluorescent antibodies were used to label cell surface markers, as indicated in individual experiments. Each antibody was added at a predetermined optimal concentration directly onto the whole blood, gently mixed and left for 15 minutes at RT in the dark. To lyse the RBCs and fix the sample, OptilyseC (Beckman Coulter) was then added at a volume of 500µL to each FACS tube before mixing vigorously and leaving for 15 minutes at RT in the dark. The samples were washed twice in FACS buffer, centrifuging for 5 minutes at 300g at RT and the supernatant discarded between each wash. The cell pellet was then resuspended in 300µL of 1% paraformaldehyde (PFA). To determine absolute cell numbers, 20µL of Flow-count fluorospheres (Beckman Coulter) were added just before acquiring the samples on the flow cytometer (BD FACSCanto II). Method of calculation is described in section 2.2.5.5.

2.2.5.2 Labelling of PBMC and LPMC

Following PBMC or LPMC culture, the cells were harvested and washed once in FACS buffer. The samples were centrifuged for 5 minutes at 300g at RT, and the supernatant was discarded. The cell pellet was then resuspended in 100µl of FACS buffer for cell surface staining. Fluorescent antibodies were used to label cell surface markers required to identify cell populations. Each antibody was added at a predetermined optimal concentration and left for 20 minutes on ice in the dark. The cells were then washed with FACS buffer, centrifuging for 5 minutes at 300g at RT before discarding the supernatant. The cells were either staining for intracellular cytokines (Section 2.2.5.3) or resuspended in 300µL 1% PFA buffer and acquired on the flow cytometer (BD FACSCanto II) on the same day. To determine absolute cell numbers, 20µL of Flow-count fluorospheres (Beckman Coulter, USA) were added just before acquiring the samples on the flow cytometer (BD FACSCanto II). Method of calculation is described in section 2.2.5.5.

2.2.5.3. Intracellular cytokine staining

Following cell surface staining (Section 2.2.5.2), cells were fixed in 100µL of Leucoperm A at 4°C for 20 minutes in the dark. The cells were washed once in FACS buffer, centrifuging for 5 minutes at 300g at RT, and the supernatant discarded before permeabilising with 100µL Leucoperm B at 4°C for 30 minutes in the dark, while simultaneously staining for intracellular cytokines using fluorochrome-conjugated antibodies (Table 1). The cells were washed once in FACS buffer, centrifuging for 5 minutes at 300g at RT, and the supernatant discarded. The cell pellet was resuspended in 300µL 1% PFA buffer, and the samples were acquired on the flow cytometer (BD FACSCanto II) on the same day. To determine absolute cell numbers, 20µL of flow-count fluorospheres (Beckman Coulter, USA) were added just before acquiring the samples on the flow cytometer (BD FACSCanto II). Method of calculation is described in section 2.2.5.5.

2.2.5.4 PhosFlow

One million PBMCs, suspended in 500µl of complete medium, were added to FACS tubes (BD) and washed with FACS buffer, centrifuging for 5 minutes at 300g at RT before discarding the supernatant. The cell pellet was then resuspended in 100µl of FACS buffer for cell surface staining (Section 2.2.5.2). The cells were then washed with FACS buffer, centrifuging for 5 minutes at 300g at RT before discarding the supernatant. The cell pellet was resuspended in 500µL FACS buffer before placing the FACS tubes (BD) in a 37°C water bath and stimulated for 15 minutes with IL-10 (100ng/ml), IL-6, (100ng/ml) or with phosphate buffered saline (PBS) as a control. 500ul of 4% PFA was then added to each tube to fix the cells rapidly, and left for a further 15 minutes in the 37°C water bath. The cells were washed once with PBS, centrifuging for 5 minutes at 300g at RT before discarding the supernatant. The cell pellet was resuspended in 1mL of cold 70% methanol to permeabilise the cells and kept on ice for 30 minutes. The cells were then washed twice with FACS buffer, centrifuging for 5 minutes at 300g at RT and discarding the supernatant between each wash. The cell pellet was resuspended in 100µl of FACS buffer and 50µl of brilliant stain buffer (BD) for intracellular staining.

Fluorescently labelled antibodies against STAT3 proteins or specific for phosphorylated forms of STAT3 were added to the cells and left to incubate on ice in the dark for 30 minutes. The cells were washed once in FACS buffer, centrifuging for 5 minutes at 300g at RT before discarding the supernatant. The cell pellet was resuspended in 300µL 1% PFA buffer, and the samples were acquired on the flow cytometer (BD FACSCanto II) immediately.

2.2.5.5 Flow-count fluorospheres

Flow-Count Fluorospheres (Beckman Coulter, USA) are a suspension of fluorescent microbeads used to determine absolute cell numbers on the flow cytometer. A known volume of the beads (20µL) with a known concentration (Lot specific concentration: 1013 beads/µL of stock suspension) are added to the cell suspension just before acquiring the samples on the flow cytometer (BD FACSCanto II). The calculation is detailed below.

$$\frac{\text{Vol of original cell suspension}}{\text{Vol of beads}} = \mathbf{A}$$

$$\left(\frac{\text{No. of cell events}}{\text{No. of bead events x } \mathbf{A}}\right) \times 1013 \text{ beads}/\mu L = \text{cells per } \mu\text{L}$$

2.2.5.6 Flow Cytometry

Labelled cells were acquired on BD FACSCanto II using the BD FACSDiva software. Single colour compensation controls were generated by labelling PBMCs with fluorochrome-conjugated anti-CD3 or anti-CD4 monoclonal antibodies (Biolegend), which created positively and negatively stained populations for each fluorochrome used in a particular experiment. No less than 100,000 events were acquired for each sample. Once the data were collected as FSC files, they were analysed using Winlist 3D version 8.0 (Verity Software House, Maine). Compensation was applied before data analysis using the WinList algorithm. Positive staining was determined by comparison with populations within samples stained with corresponding isotype control antibodies.

2.2.6 Cytokine production by blood monocytes and intestinal Mo/moMϕs

Two million PBMCs suspended in 1mL of complete medium, or a variable number of LPMCs suspended in 1mL of complete medium (with the addition of 25µg/ml gentamicin) were added to a 24 well plate (flat-bottom, VWR). Monensin at a concentration of 3µM was added to all wells. PBMCs were cultured for 3 hours at 37^{o}C in medium alone or with several TLR ligands at variable concentrations as indicated in individual experiments. The ADAM17 inhibitor TMI-005 (Axon Medchem) was added 30 minutes before stimulation at a concentration of 50µM in some experiments (see below).

To test the inhibitory effects of IL-10 on cytokine production, recombinant human IL-10 (0.016ng/ml-10ng/ml) was added 30 minutes prior addition of TLR agonists in some experiments. At the end of incubation, cells were transferred to FACS tubes and washed with FACS buffer, centrifuging for 5 minutes at 300g at RT and the supernatant discarded. The cell pellet was then resuspended in 100µl of FACS buffer. Cell surface staining with fluorochrome-conjugated monoclonal antibodies (Section 2.2.5.2) was used to identify blood monocyte populations and intestinal Mo/moMϕs as detailed in individual experiments. The cells were then washed with FACS buffer, centrifuging for 5 minutes at 300g at RT before discarding the supernatant. Cytokines, including TNFα, IL-1β, and IFNα, were detected by intracellular staining (Section 2.2.5.3).

2.2.7 Cell sorting of blood monocyte populations

Monocyte subset populations were cell sorted using the FACS Aria flow cytometer (Becton Dickinson) with the assistance of Gary Warnes, Flow Cytometry Core Facility, Blizard Institute. Before cell sorting, whole PBMCs were collected from up to 50ml of blood and combined into one FACS tube (BD). The cells were washed with FACS buffer, centrifuging for 5 minutes at 300g at RT before discarding the supernatant. The cell pellet was then resuspended in 100µl of FACS buffer for cell surface staining (Section 2.2.5.2). The cells were then washed with FACS buffer, centrifuging for 5 minutes at 300g at RT before discarding the supernatant. The cell pellet was resuspended in FACS buffer at a concentration of 20 million cells per ml for cell sorting. Single colour compensation tubes were

generated by labelling PBMCs with anti-CD3 or anti-CD4 antibodies (Biolegend) conjugated to the relevant fluorochromes. Compensation was applied in the cytometer before setting the sort gates and collecting monocyte populations. Classical monocytes (HLA-DR+CD14++CD16-), intermediate monocytes (HLA-DR+CD14++CD16+) and non-classical monocytes (HLA-DR+CD14+CD16++) were collected into separate FACS tubes (BD) and washed with FACS buffer, centrifuging for 5 minutes at 300g at RT and then the supernatant was discarded. The cell pellets were resuspended in FACS buffer and divided into aliquots of 100,00 cells each to compare SOCS3 expression between subsets, and $1x10^6$ classical cells to compare SOCS3 expression between healthy controls and IBD patients. The 1.5ml Eppendorf tubes were then centrifuged for 5 minutes at 400g before aspirating the supernatant. The cell pellets were resuspended in 350µL RTL lysis buffer and vortexed for 1 minute before placing in -80^{o}C until further processing.

2.2.8 Tracking phenotypic changes in monocyte subsets *in vitro*

Monocyte subset populations were cell sorted using the FACS Aria flow cytometer (Becton Dickinson) with the assistance of Gary Warnes, Flow Cytometry Core Facility, Blizard Institute. Before cell sorting, whole PBMCs were collected from up to 50ml of blood and combined into one FACS tube (BD). The cells were washed with sterile PBS, centrifuging for 5 minutes at 300g at RT before discarding the supernatant. The cell pellet was resuspended in 500µl of warmed cell trace violet (CTV) dye and incubated at 37^{o}C for 20 minutes. To stop the reaction, 500µl of cold FCS was added. The cells were washed with sterile FACS buffer (prepared with sterile PBS and EDTA, minus the sodium azide), centrifuging for 5 minutes at 300g at RT before discarding the supernatant. The cell pellet was then resuspended in 100µl of FACS buffer for cell surface staining (Section 2.2.5.2). The cells were then washed with sterile FACS buffer, centrifuging for 5 minutes at 300g at RT before discarding the supernatant. The cell pellet was resuspended in sterile FACS buffer at a concentration of 20 million cells per ml for cell sorting. Single colour compensation tubes were generated by labelling PBMCs with anti-CD3 or anti-CD4 antibodies (Biolegend) conjugated to the relevant fluorochromes. Compensation

was applied in the cytometer before setting the sort gates and collecting monocyte populations. Classical monocytes (HLA-DR+CD14++CD16-), intermediate monocytes (HLA-DR+CD14++CD16+) and non-classical monocytes (HLA-DR+CD14+CD16++) were collected into separate FACS tubes (BD) and washed with complete medium, centrifuging for 5 minutes at 300g at RT and then the supernatant was discarded. The cell pellet of classical monocytes was resuspended in complete medium at a concentration of 2 million cells per mL. The cell pellets of intermediate and non-classical monocytes were resuspended in 1mL of complete medium (100,000 cells). 500µL of each subset was added to two separate wells and topped up with 500µL of unlabeled PBMCs (suspended in complete medium at a concentration of 2 million cells per mL). Monensin at a concentration of 3µM was added to all wells. PBMCs were cultured for 3 hours at 37^{o}C in medium alone or with 1ng/ml LPS. At the end of incubation, cells were transferred to FACS tubes and washed with cold FACS buffer, centrifuging for 5 minutes at 300g at RT and the supernatant discarded. The cell pellet was then resuspended in 100µl of FACS buffer. Cell surface staining with fluorochrome-conjugated monoclonal antibodies (Section 2.2.5.2) to identify blood monocyte populations as detailed in individual experiments. The cells were then washed with FACS buffer, centrifuging for 5 minutes at 300g at RT before discarding the supernatant. The cell pellet was resuspended in 300µL 1% PFA buffer and acquired on the flow cytometer (BD FACSCanto II) on the same day.

2.2.9 Measuring cell viability

Two million PBMCs suspended in 1ml of complete medium were added to a 24 well plate (flat-bottom, VWR). Monensin at a concentration of 3µM was added to all wells. PBMCs were cultured for 3 hours at 37^{o}C in medium alone or with 1ng/ml LPS. One million PBMCs, suspended in 500µl of complete medium, were added to FACS tubes (BD) and washed with FACS buffer, centrifuging for 5 minutes at 300g at RT before discarding the supernatant. The cell pellet was then resuspended in 100µl of FACS buffer for cell surface staining (Section 2.2.5.2). The cells were then washed with FACS buffer, centrifuging for 5 minutes at 300g at RT before discarding the supernatant. The cell pellet was

resuspended in 200µL PBS and placed on ice to prevent endocytic uptake. The viability dye was added to a final dilution of 1:10,000 and incubated for 30min in the dark. The cells were then washed with binding buffer, centrifuging for 5 minutes at 300g at RT before discarding the supernatant. The cell pellet was resuspended in 200µL PBS, and 10µL of the annexin V stain was added and incubated for 15 minutes at RT. The cells were then washed twice with binding buffer, centrifuging for 5 minutes at 300g at RT before discarding the supernatant. The cell pellet was resuspended in 300µL 1% PFA buffer and acquired on the flow cytometer (BD FACSCanto II) on the same day. For the compensation controls, two FACS tubes were prepared with PBMCs suspended in PBS. One tube was placed in a water bath at 55°C for 10 minutes. Once cooled, the two tubes were combined to provide a sample with both viable and dead cells. The sample was then divided into two FACS tubes. One tube was stained with fixable dye only, and the other tube with annexin V only.

2.2.10 Measuring phagocytosis capacity

One million LPMCs suspended in 1mL of complete medium (with the addition of 25µg/ml gentamicin) were added to two separate 24 well plates (flat-bottom, VWR). One plate was incubated at 4°C (control) and the other at 37°C for 15 minutes before adding the FITC-labelled microspheres 2.00µm (Polysciences Inc.) at a concentration of 10 microspheres per cell to incubate for a further 1.5 hours. One million LPMCs, suspended in 1mL of complete medium, were added to FACS tubes (BD) and washed with FACS buffer, centrifuging for 5 minutes at 300g at RT before discarding the supernatant. The cell pellet was then resuspended in 100µl of FACS buffer for cell surface staining (Section 2.2.5.2). The cells were then washed with FACS buffer, centrifuging for 5 minutes at 300g at RT before discarding the supernatant. The cell pellet was resuspended in 300µL 1% PFA buffer, and the samples were acquired on the flow cytometer (BD FACSCanto II) immediately.

2.2.11 Quantitative real-time PCR

2.2.11.1 RNA extraction

The RNeasy Micro Kit (Qiagen) was used in accordance with the manufacturer's instructions. The samples stored at -80°C were defrosted at RT and vortexed. 350µL of 70% Ethanol was then added and the samples vortexed again. The solution was transferred to a spin column placed in a 2ml collection tube, which was centrifuged for 15 seconds at 8000g before discarding the flow through. 700µL of RW1 buffer was then added and centrifuged again for 15 seconds at 8000g before discarding the flow through. The spin column was transferred to a new 2ml collection tube before adding 500µL of RPE buffer, centrifuging for 15 seconds at 8000g and discarding the flow through. 500µl of 80% ethanol was then added and centrifuged for 2 minutes at 8000g before discarding the flow through. The spin column was transferred to a new 2ml collection tube and centrifuged at 1600g for 5 minutes with the lids open to evaporate the alcohol. The spin column was then transferred to a new 1.5ml collection tube; 14µl of RNase-free water was added directly to the membrane and then centrifuged at 1600g for 1 minute to elute the RNA, which was used immediately for reverse transcription.

The RNeasy Mini kit (Qiagen) was used in accordance with the manufacturer's instructions. The samples stored at -80°C were defrosted at RT and vortexed. The homogenised lysate was transferred to a genomic DNA (gDNA) Eliminator spin column placed in a 2ml collection tube, and centrifuged for 30 seconds at 8000g. The column was discarded, and 350µL of 70% Ethanol was added to the flow-through. The suspension was then transferred to a spin column placed in a 2ml collection tube and centrifuged for 15 seconds at 8000g before discarding the flow through. 700µL of RW1 was then added and centrifuged again for 15 seconds at 8000g before discarding the flow through. 500µL of RPE buffer was added and centrifuged for 15 seconds at 8000g before discarding the flow through. 500µl of RPE buffer was added again and centrifuged for 2 minutes at 8000g before discarding the flow through. The spin column was transferred to a new 2ml collection tube and centrifuged at 1600g for 1 minutes to further dry the membrane. Finally, the spin column was then transferred to a new 1.5ml collection

tube; 30µl of RNase-free water was added directly to the membrane and then centrifuged at 8000g for 1 minute to elute the RNA. The RNA was quantified using Nanodrop. The RNA was used immediately for reverse transcription.

2.2.11.2 Measurement of RNA concentration

NanoDrop uses the properties of RNA to measure concentration and purity. RNA absorbs ultraviolet (UV) light with a maximum absorption (λmax) wavelength of 260nm. The 260/280 ratio is used to assess RNA purity and should ideally be around 2.0. Each base has a characteristic λmax, therefore, the ratio will depend on the base composition of the RNA. However, a ratio that is much lower than 2.0 may indicate the presence of contaminants, such as phenol that absorbs UV light at 230 nm and can contribute to an overestimation of DNA concentration in addition to inhibiting downstream reactions. The 260/230 ratio is a secondary measure of purity and should ideally be around 2.2. Using λmax and a known path length, the concentration of RNA can be calculated. However, very dilute samples lead to inaccurate ratios due to little differences between 260 nm and 280 nm absorbance and the similarity in absorption between RNA and DNA (λmax = 280) makes it challenging to determine DNA contamination (Desjardins et al. 2009). Therefore, nanodrop was used for RNA samples extracted using the RNeasy Mini kit (Qiagen). RNA-40 was selected on the NanoDrop software. 1µl of RNase-free water was pipetted onto the lower measurement pedestal, and Blank was selected on the software. 1µl of the RNA sample was then pipetted onto the lower measurement pedestal, and the sample was measured.

2.2.11.3 Reverse transcription

The QuantiTect Reverse Transcription Kit (Qiagen) was used in accordance with manufacturer's instructions. 12µl of the RNA samples extracted using the RNeasy Micro Kit (Qiagen) was transferred to a 200µl tube; 2µl of gDNA Wipeout Buffer was then added and mixed before incubating for 2 minutes at 42°C to degrade the gDNA. The RNA samples extracted using the RNeasy Mini kit (Qiagen)

were diluted with RNase-free water to a normalised concentration (section 2.2.9.2), and 2µl of gDNA Wipeout Buffer was added before incubating for 2 minutes at 42°C. A reverse transcription master mix was made containing 1µl Quantiscript Reverse Transcriptase, 4µl Quantiscript RT Buffer, and 1µl RT primer mix per dose. 6µl of the master mix was added to the 14µl of RNA and mixed. This was incubated for 15 minutes at 42°C for the reverse transcription of the RNA into cDNA. The sample was then incubated for 3 minutes at 95°C to inactivate the Quantiscript Reverse Transcriptase. The cDNA was either used immediately for quantitative real-time PCR (qRT-PCR) or stored at -20 °C for future use.

2.2.11.4 SYBR Green qRT-PCR

This technique uses a highly specific, dsDNA binding dye to detect PCR product as it accumulates during PCR cycles. During the PCR, DNA Polymerase amplifies the target sequence that creates PCR product. The dye then binds to each new copy of dsDNA, which increases in fluorescence intensity proportionate to the amount of PCR product produced (Arya et al. 2005). The dye will detect all dsDNA, including non-specific reaction products, therefore, a well-optimised reaction is essential for accurate results.

A master mix was made for each primer containing 12.5µl of SYBR Green PCR Mix, 2.5µl of the primer, and 8µl of RNase free water. 23µl of this master mix was added to a 96-well PCR plate in triplicates followed by 2µl of cDNA (replaced with RNase free water for no template control). The plate was sealed with Advanced Polyolefin StarSeal (Star Lab) and then centrifuged briefly to combine the liquids at the bottom of the well. The plate was then run immediately on the 7500 Real-Time PCR Systems (Applied Biosystems, USA), which used the 7,500 Software version 2.0.6. (Applied Biosystems, USA). The program was set in accordance with the manufacturer's instructions (Table 2).

Step	Temperature (°C)	Time (seconds)	Repeats
1. Activation	95	300	1x
2. Denaturing	95	10	40x
3. Annealing & Extension	60	30	
4. Melt Curve	95	15	1x
	60	60	
	95	30	
	60	15	

Table 2.2: PCR program

Data was collected of the cycle threshold (C_T) values (the cycle number at which there's a detectable signal). Relative gene expression of the genes of interest can be calculated using a reference gene (*GAPDH*), which are highly conserved and constitutively expressed, therefore, are used to normalise gene expression of target using the $2^{-deltaCt}$ method (Livak & Schmittgen 2001), where deltaCt is the difference in C_T number for target and reference gene.

The samples run through qRT-PCR included RNA extracted from relatively few cells using the RNeasy Micro kit (Qiagen) in which exact quantification of RNA concentration using nanodrop was not possible. Therefore, a titration of classical monocytes was carried out to determine the lowest cell number that allows calculation of a reliable deltaCT, after which GAPDH expression is no longer linear These cells were titrated down past the cell number present in the experimental samples to be analysed and showed a reliable deltaCT could be calculated (refer to Appendix 1). The concentration of the RNA extracted with the RNeasy Mini kit (Qiagen) could be measured using Nanodrop and was normalised to 19.4ng/µL in subsequent experiments. Before this, titration of a known concentration of RNA was carried out to determine the lowest RNA concentration that allows calculation of a reliable deltaCT, and 19.4ng/µL was within this range (refer to Appendix 2)

The purity and specificity of the amplified product was determined using melt curves. SYBR Green dye only fluoresces when bound to dsDNA, therefore can be used to determine the melting point of the PCR product. At the end of synthesis, all of the DNA is double-stranded, and SYBR Green is maximally bound producing the maximal relative fluorescence, as temperature increases, the DNA is denatured, and the fluorescence decreases following the same curve as the melting temperature. If the PCR product is pure, there will be a single peak (refer to Appendix 3). The appearance of an earlier peak is a sign of primer dimer formation (smaller fragments), while a peak later indicates genomic contamination (larger size). These samples were excluded because it affects the accuracy of the gene expression analysis.

The primers were ordered from Qiagen, typically designed to be exon spanning to prevent amplification of contaminating gDNA. However, the SOCS genes consist of only two exons so the primers were within one axon, therefore, effective gDNA wipeout was critical. This was tested by replacing the reverse transcriptase with water during the RT-PCR reaction, and no signal was detected during the qRT-PCR reaction.

2.3 Statistics

Statistical analyses were performed using Prism 6 (GraphPad Software, USA). t-tests were used to compare two groups of normally distributed data (paired and unpaired), with Welch's correction for unequal standard deviations (SD) for unpaired data. A Mann-Whitney test was used to compare two groups of unpaired data that were non-normally distributed. A Wilcoxon tests was used to compare two groups of non-normally distributed paired data. Datasets containing more than two groups of unpaired and normally distributed data were compared using a one-way ANOVA with a Tukey test to correct for multiple comparisons. More than two groups of data that were unpaired and non-normally distributed were compared using a Kruskal-Wallis test with a Dunn's test to correct for multiple comparisons. Paired datasets containing more than two groups of normally distributed data were compared using a repeated measures (RM) one-way ANOVA with the Greenhouse-Geisser correction and a Tukey test to correct for multiple comparisons. More than two groups of paired data that were non-normally distributed were compared using a Friedman test with Dunn's test to correct for multiple comparisons. Paired datasets containing more than three groups of normally distributed data were compared using an RM Two-way ANOVA with a Tukey test to correct for multiple comparisons. Mean and SD are displayed for normally distributed data sets, while median and interquartile range (IQR) are displayed for non-normally distributed data sets. The normal distribution of the datasets was verified using three normality tests: D'Agostino-Pearson omnibus, Shapiro-Wilk, and Kolmogorov-Smirnov. P-values were regarded as statistically significant when $p < 0.05$.

Chapter 3: Developing an assay to measure IL-10 response

3.1 Chapter summary

This chapter focusses on the development of an assay that could be used to measure IL-10 responsiveness in human monocyte subsets. First, the monocyte subsets were defined based on CD14 and CD16 expression: classical (CD14++CD16-), intermediate (CD14++CD16+), and non-classical (CD14+CD16++) monocytes, pre-gated on HLA-DR positive cells. Additional markers were used to confirm the identity of the monocyte subsets. To carry out functional experiments, PBMCs had to be separated from whole blood. However, culturing PBMCs ex vivo may impact monocyte subset distribution. To test this, monocyte subset distribution was compared between cells labelled in whole blood and PBMCs cultured for three hours. The data show little effect of short-term culture on monocyte subset distribution.

The optimal stimulation conditions and cytokine readout with which to measure IL-10 response where then determined. Whole PBMCs were stimulated with LPS in the presence of increasing amounts of IL-10 to measure inhibition of TNFα production in the monocyte subsets. However, upon stimulation with LPS, there was an apparent loss of CD16+ cells that could not be dissociated from induction of TNFα production by adjusting LPS concentration or time course of stimulation or the use of alternative TLR agonists. The CD16+ cells did not show enhanced cell death or adherence to culture plates with LPS. A cell tracking experiment revealed a downregulation CD16 expression on the intermediate and non-classical monocytes. This downregulation was not due to internalisation of CD16 so was likely to be due to cleavage. In the presence of an ADAM17 inhibitor (TMI-005), CD16+ monocytes were still identifiable following LPS stimulation suggesting that CD16 is cleaved from the monocyte surface by this enzyme. The ADAM17 inhibitor was used in subsequent experiments to enable the IL-10 response to be determined in all three monocyte subsets in parallel.

3.2 Introduction

The critical role of IL-10 in preventing excessive inflammatory responses to innocuous agents was discussed in depth in the introduction. Briefly, IL-10 deficient mice developed chronic enterocolitis upon exposure to commensal bacteria (Berg et al. 1996; Kühn et al. 1993), and in humans, patients with naturally occurring LoF mutations in the IL-10R genes develop VEO-IBD (Begue et al. 2011; Glocker & Kotlarz 2009; Mao et al. 2012). These studies highlight that IL-10 has a non-redundant role in regulating inflammation, and is especially important in maintaining immune homeostasis in the intestine where there is continuous exposure to external antigens. However, the majority of IBD patients do not have LoF mutations. The concept of defective anti-inflammatory responses in IBD patients has been previously investigated and showed patients with a severe relapse at the time of analysis displayed a reduced response to IL-10, which was restored once the patients achieved remission (Begue et al. 2011). However, specific cell types were not identified in this study.

The critical target of IL-10 in regulating intestinal inflammation in humans was unclear. Recent murine studies by Shouval et al. 2014 and Zigmond et al. 2014 suggest that Mϕs play a non-redundant role in IL-10 signalling: selective deletion of the IL-10R in this population caused spontaneous colitis with an accumulation of inflammatory Mϕs (Shouval et al. 2014). These studies also highlight the critical role of Mϕs in regulating inflammation in the intestine. Monocytes maintain at least some of the intestinal Mϕ pool, therefore, regulating their inflammatory activity upon entry to the intestine would be critical.

There is increasing evidence that systemic signals from the intestine during inflammation can cause functional changes to circulating cells formed the rationale for studying IL-10 response in blood monocytes (Arts et al. 2018; Askenase et al. 2015; Christ et al. 2018; Mitroulis et al. 2018; Sanders et al. 2014; Smith et al. 2009). The capacity of IL-10 to inhibit pro-inflammatory cytokine induction in monocytes has previously been reported, without taking into account monocyte subsets (Gasche et al. 2003). The monocyte subsets have distinct roles and characteristics, which should be considered

when investigating their response to IL-10. There was a need to develop an assay that could be used to measure IL-10 responses in the individual monocyte subsets in parallel to ensure the same culture environment.

The aim of the work described in this chapter was to develop an assay that could be used to measure IL-10 responsiveness in human monocyte subsets.

3.3 Aims

1. Develop a gating strategy for the identification of well-defined human classical, intermediate, and non-classical monocytes.
2. Establish stimulation conditions for the induction of cytokine responses in the monocyte subsets.
3. Optimise methodology and analytical approach to quantify the impact of IL-10 on cytokine production by the monocyte subsets.

3.4 Results

3.4.1 Identification of human monocyte subsets

First, a robust gating strategy had to be defined to identify the monocyte subsets. Monocytes were labelled for HLA-DR, CD14, and CD16 in healthy donor whole blood. PBMCs were gated based on their forward scatter (FSC) and side scatter (SSC) properties (Figure 3.1 A). Doublet discrimination was carried out (Figure 3.1 B, C). HLA-DR labelling was then used to distinguish APCs (Figure 3.1 D). Finally, using an isotype control (Figure 3.1 E), CD14 and CD16 marker expression was used to distinguish the three monocyte subsets: CD14++CD16- (classical), CD14++CD16+ (intermediate), and CD14+CD16++ (non-classical) (Figure 3.1 F).

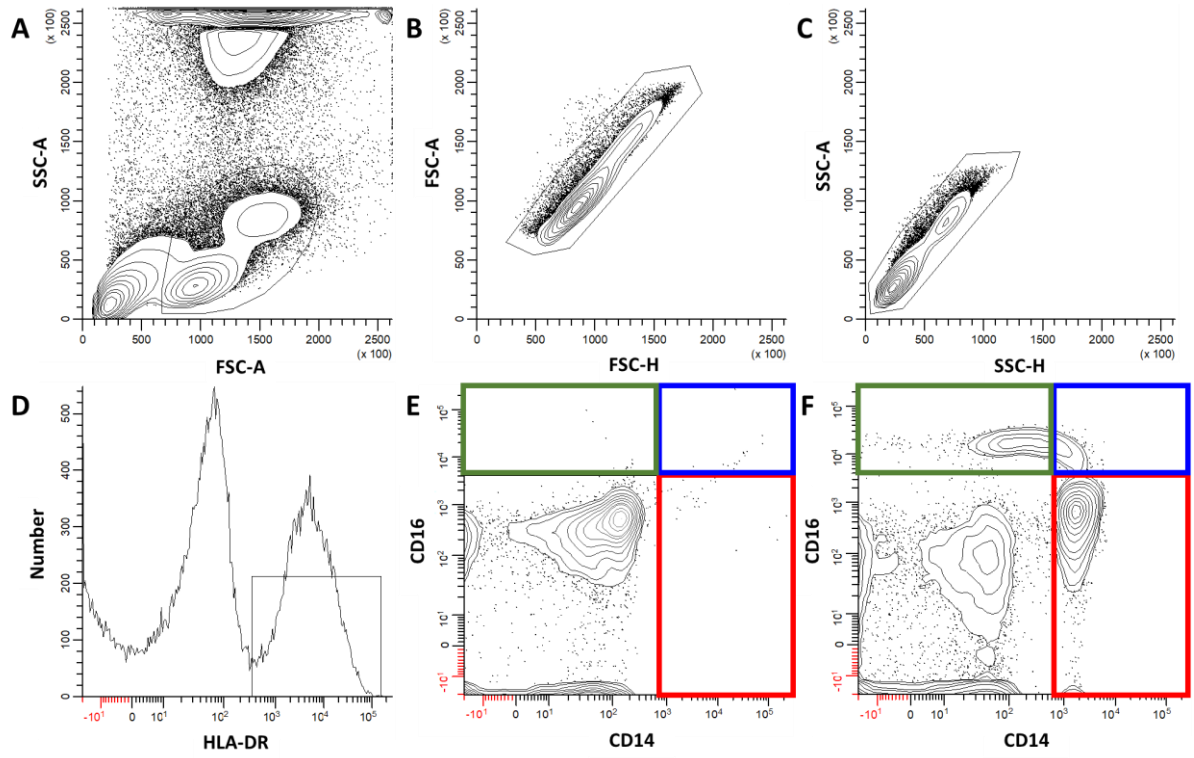

Figure 3.1: Gating strategy for the identification of human monocyte subsets. Whole blood from a healthy donor was labelled with anti-HLA-DR, anti-CD14, and anti-CD16 antibodies; monocyte subsets were then identified using a flow cytometer. **A)** PBMCs were gated based on FSC and SSC. **B and C)** doublet discrimination was carried out. **D)** HLA-DR labelling was then used to distinguish APCs. **E)** isotype control for CD14 and CD16. **F)** the three monocyte subsets were distinguished based on their CD14 and CD16 expression: CD14++CD16- (classical), CD14++CD16+ (intermediate), and CD14+CD16++ (non-classical).

The phenotype of the monocytes was investigated further using additional subset-associated markers as well as markers of potential contaminating cell types (e.g. CD16+ NK cells) to confirm the identity of the gated monocyte subsets. Healthy donor PBMCs were labelled for HLA-DR, CD14, and CD16 to distinguish the monocyte subsets and the following markers: CD33 (expressed on monocytes), NKp46 (used to exclude NK cells), CCR2 and CX_3CR1 (hierarchy of expression is well characterised in the monocyte subsets). Expression levels of each marker in relation to the isotype control for the total monocytes were compared between the monocyte subsets using overlaid histograms. All three monocyte subsets were positive for CD33 but negative for NKp46, which confirmed the identity of the monocytes and ensured that the gating strategy excluded CD16+ cell populations that were not monocytes, e.g. NK cells. Expression of CCR2 (a chemokine receptor that facilitates monocyte release from the BM) was highest in classical monocytes and lowest in non-classical monocytes. In contrast, CX_3CR1 (a chemokine receptor that facilitates endothelial adhesion, rolling, and migration) expression was lowest on classical monocytes and highest in non-classical monocytes. These findings are in agreement with previous reports on the hierarchy of expression of these markers in the human monocyte subsets (Boyette et al. 2017; Patel et al. 2017; Wong et al. 2011), therefore, the gating strategy can robustly identify monocyte subsets for further analysis.

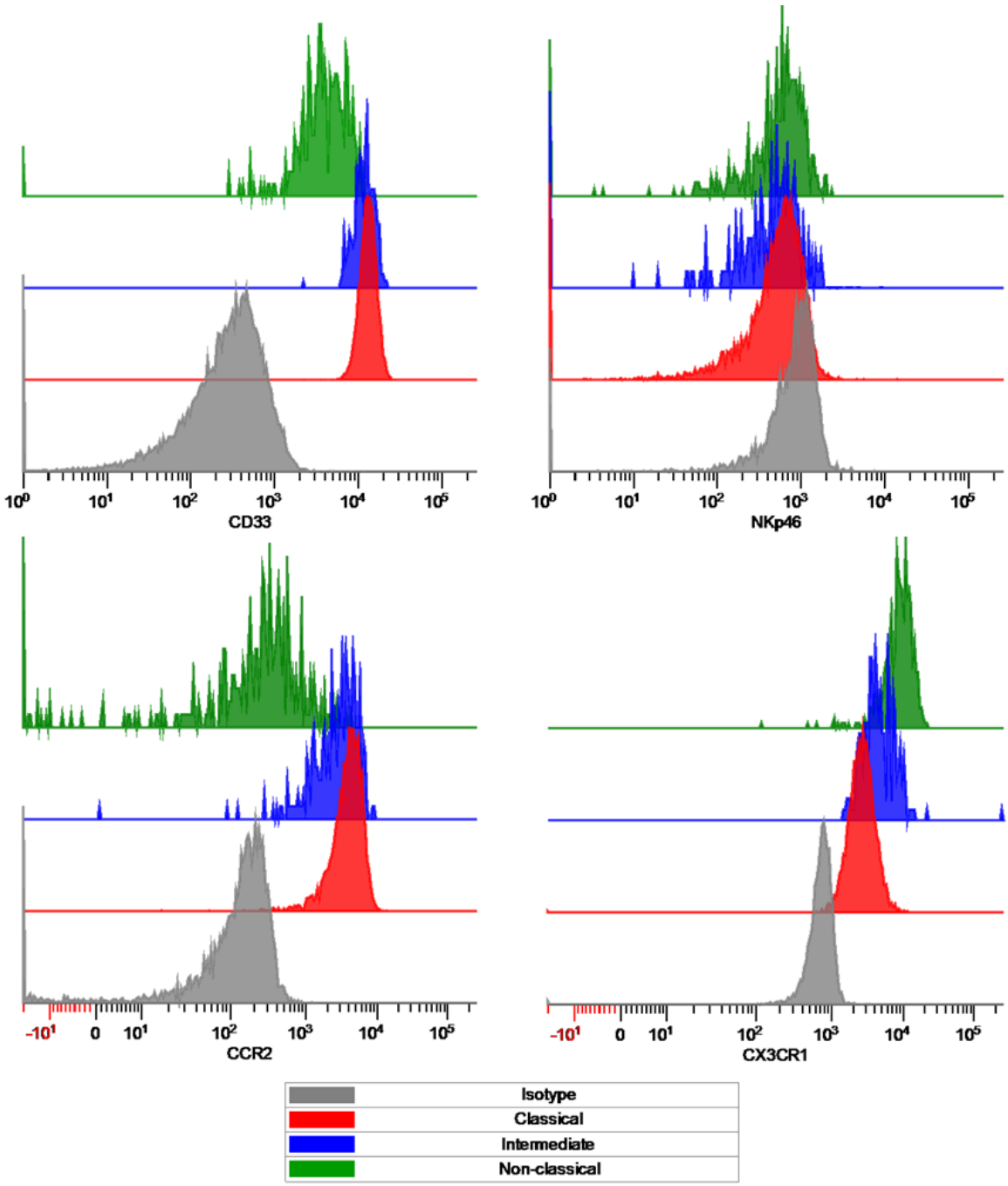

Figure 3.2 Characterisation of the human monocyte subsets. Healthy donor PBMCs (n=1) were labelled with anti-HLA-DR, anti-CD14, and anti-CD16 antibodies to distinguish the monocyte subsets. Additional markers were used to further characterise the monocyte subsets, including CD33, NKp46, CCR2, and CX_3CR1. The sample was then acquired on the flow cytometer. The overlays represent the expression levels of each marker in relation to the isotype control for the total monocytes (grey histogram) and each monocyte subset (classical, intermediate, and non-classical).

Whole blood labelling minimises potential isolation-related changes to marker expression, making it highly suitable for phenotyping experiments but it is not suitable for many functional experiments, where separated PBMC are required. The assay for measuring IL-10 responsiveness would require separation of PBMCs from whole blood. To determine if all subsets are recovered equally well, monocyte labelling was compared between whole blood and separated PBMCs, cultured for three hours, from a healthy donor. The ratio of the monocyte subsets was similar whether determined in whole blood or PBMC.

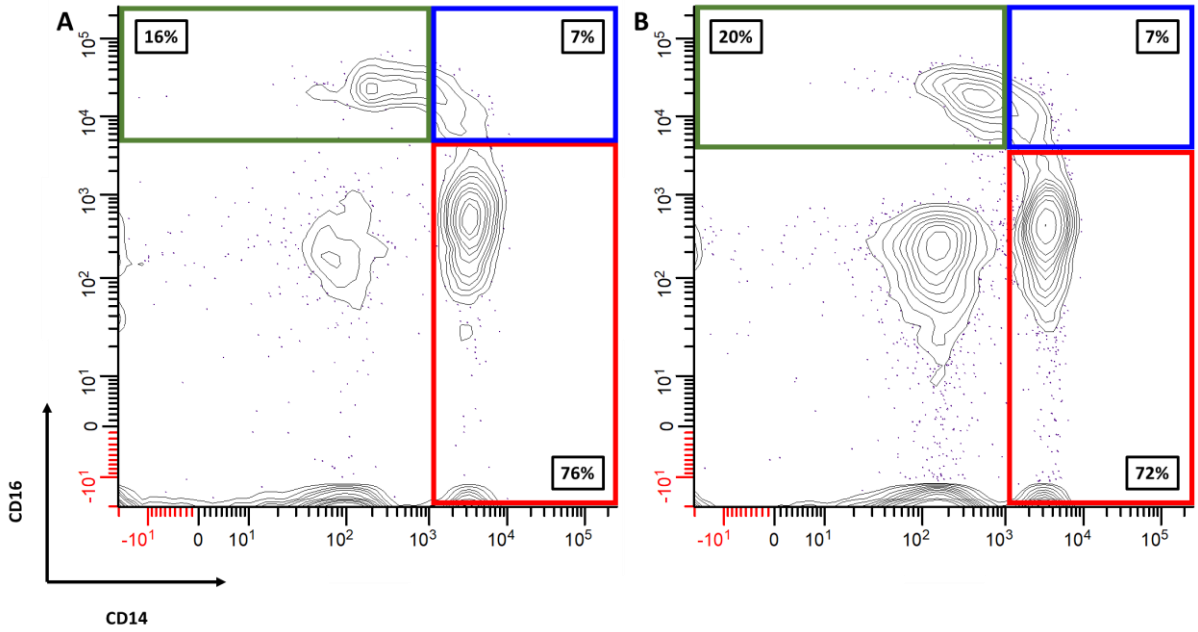

Figure 3.3: Comparing monocyte subset labelling in whole blood and separated PBMCs. A) whole blood from a healthy donor (n=1) was labelled with anti-HLA-DR, anti-CD14, and anti-CD16 antibodies to distinguish the monocyte subsets. **B)** PBMCs from the same donor were extracted, cultured for three hours, and labelled with the same set of antibodies before acquiring both samples on the flow cytometer.

3.4.2 Establishing stimulation conditions for induction of cytokine responses in monocytes subsets

3.4.2.1 LPS induces apparent loss of CD16+ monocyte subsets

Having confirmed the gating strategy, the next step was to define the stimulation conditions and cytokine readout. TNFα was chosen as the readout because it is clinically relevant in IBD, and LPS is known to stimulate a robust TNFα response in monocytes (Beutler 2000; Kontoyiannis et al. 1999). In order to establish a workable assay, the optimal LPS concentration for stimulation was determined by the ability to induce a robust TNFα response that could be measurably inhibited by IL-10 but not reach maximal TNFα production in all monocyte subsets that would diminish the sensitivity of the assay. To define this concentration, healthy donor PBMCs were stimulated with various concentrations of LPS (0.001-1000ng/mL) for three hours in the presence of monensin before staining for intracellular TNFα. TNFα production was quantified as a percentage of cells positive for TNFα above the unstimulated condition (Appendix 4a). Absolute cell numbers were calculated using Flow-Count Fluorospheres added to each sample immediately before acquisition. CD14 and CD16 expression was measured as mean fluorescence intensity (MFI) for staining with anti-14 or anti-CD16 antibody.

Following culture for three hours in medium alone all three monocyte subsets remained identifiable, and there was little or no production of TNFα (Figure 3.4 A). In contrast, following stimulation with 1ng/mL LPS, there was an apparent loss of CD16+ monocytes; the classical monocytes showed robust production of TNFα, the remaining intermediate cells were TNFα positive, and a small proportion of the remaining non-classical monocytes were also TNFα positive (Figure 3.4 B).

To determine whether TNFα production and the apparent loss of specific monocyte populations could be dissociated by varying the concentration of LPS used for stimulation, LPS was titrated between 0.001-1000ng/mL (Figure 3.4 C, D). The absolute number of classical monocytes was remained constant at lower concentrations of LPS but showed a gradual reduction above 1ng/mL, the concentration at which TNFα production was first detectable (Figure 3.4 C). The intermediate

monocytes showed maximal TNFα production at 1ng/mL but induction of TNFα production was closely associated with the apparent loss of this population (Figure 3.4 C). In non-classical monocytes, TNFα production increased with increasing concentrations of LPS and was greatest at to 100ng/mL. Although this response was less robust, it was again closely associated with the apparent loss of these cells from the cultures (Figure 3.4 C). The intermediate and non-classical cells remaining after stimulation showed a reduced level of CD16 expression with increasing LPS concentration (Figure 3.4 D). There was little impact of LPS stimulation on CD14 expression by classical monocytes (Figure 3.4 D). Figure 3.4 displays representative data; for pooled numerical data from repeated experiments refer to appendix 4b.

TNFα production was detectable in all three subsets at LPS concentrations of 100pg/mL and above. Approximately 10-100-fold more LPS was required for maximal TNFα production by non-classical monocytes than by classical and intermediate monocytes (1-10ng/mL), and fewer non-classical monocytes were TNFα positive at this optimal LPS concentration than classical and intermediate monocytes (see also Chapter 4). A reduced proportion of monocytes were TNFα positive at super-optimal concentrations of LPS in all three subsets.

These data indicate that it is not possible to dissociate the apparent loss of CD16-expressing monocytes from stimulation of TNFα production by adjusting LPS concentration as the two phenomena are too tightly linked.

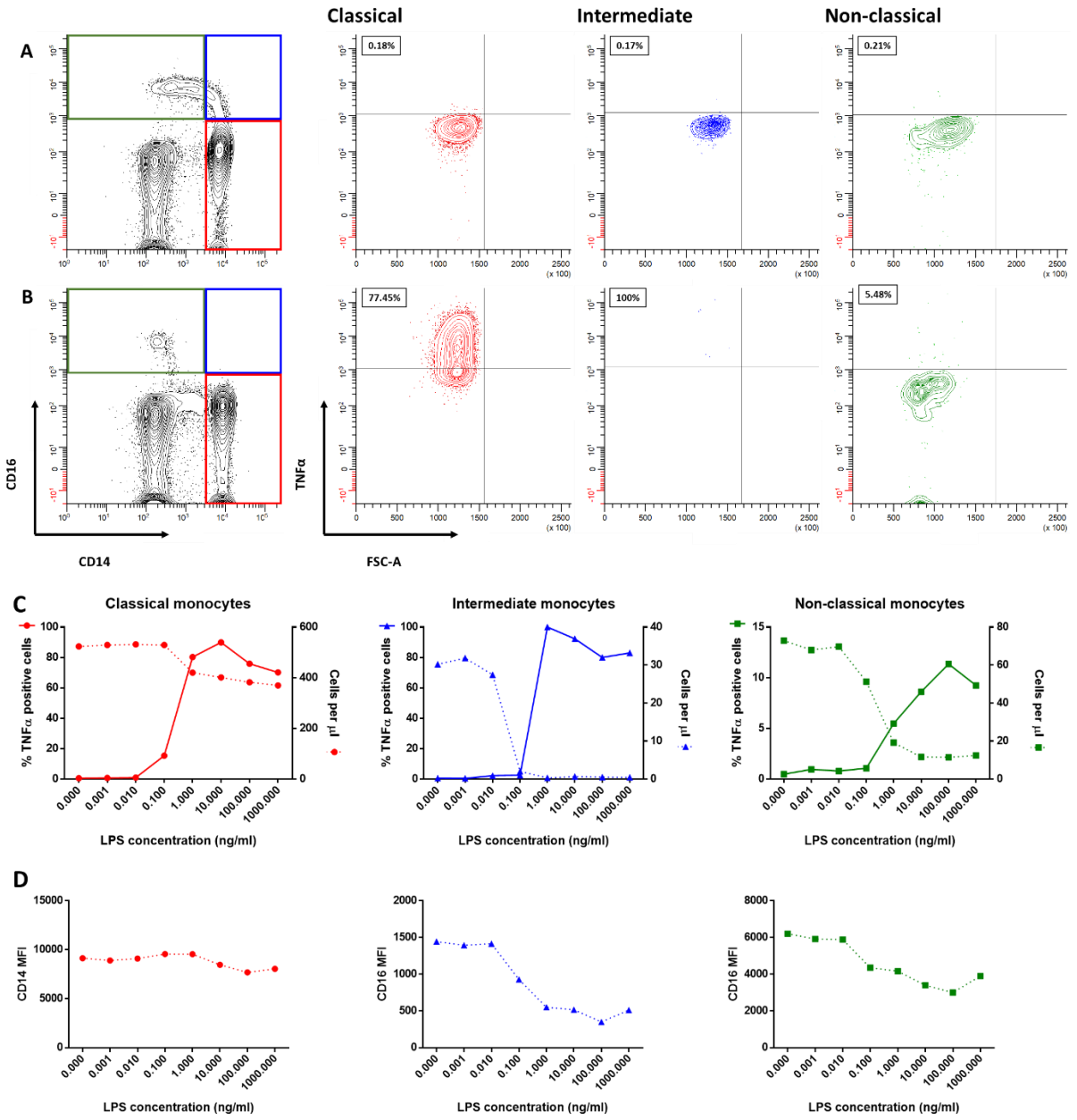

Figure 3.4: A representative of the effect of stimulation with LPS on the monocyte subsets. Healthy donor PBMCs were stimulated with increasing concentrations of LPS (0.001-1000ng/mL) for three hours in the presence of monensin. The PBMCs were then labelled for anti-HLA-DR, anti-CD14, and anti-CD16 antibodies to distinguish the monocytes subsets, fixed, permeabilised and labelling intracellularly with anti-TNFα antibody before acquiring on the flow cytometer. **A)** representative flow cytometry plots of monocyte subset distribution and TNFα production in unstimulated cultures. **B)** representative flow cytometry plots of monocyte subset distribution and TNFα production in cultures stimulated with 1ng/mL LPS. TNFα production was quantified as a percentage of cells positive for TNFα. Absolute cell number calculated using Flow-Count Fluorospheres. **C)** LPS-induced TNFα production with increasing concentration of LPS, and absolute numbers of the monocyte subsets. **D)** the level of CD14 and CD16 expression, measured as MFI, on monocyte subsets with increasing concentration of LPS.

A time course of LPS stimulation was also carried out to determine the kinetics of TNFα production and the 'loss' of CD16+ cells, and to assess whether these two effects of stimulation can be dissociated by careful selection of time points for analysis. Whole PBMCs from a healthy donor were stimulated with 1ng/mL LPS for one, three, six and 24 hours in the presence of monensin before staining for TNFα intracellularly. TNFα production was quantified as a percentage of cells positive for TNFα. Absolute cell number was calculated using Flow-Count Fluorospheres. CD14 and CD16 expression was measured as MFI for staining with anti-14 or anti-CD16 antibody.

In unstimulated culture, the CD16+ cells displayed a gradual decline in CD16 expression over the first six hours of incubation but, interestingly, at 24 hours there was an increase in the double positive population (Figure 3.5 A). Upon stimulation, CD16+ cells were lost at all time points (Figure 3.5 B). In classical monocytes, TNFα production increased between one and six hours, but the response at 24 hours was diminished; absolute numbers of classical monocytes showed a gradual reduction over the time course (Figure 3.5 C). TNFα production by intermediate monocytes increased between one and six hours but again was diminished at 24 hours; absolute numbers of intermediate monocytes were gradually lost over the six-hour stimulation but at 24 hours there was an apparent increase in the number of intermediate monocytes (Figure 3.5 C). In contrast, TNFα production by non-classical monocytes increased over the time course and was maximal at 24 hours; a loss in their cell numbers closely mirrored the production of TNFα (Figure 3.5 C). Time-dependent loss of CD16+ cells was mirrored by a reduced level of CD16 on the surface of the remaining cells (Figure 3.5 D).

These data reveal a change in the phenotype of the monocyte subsets over a 24-hour culture reflected in marker expression and TNFα producing capacity. These data demonstrate that it is not possible to dissociated TNFα production and the apparent-loss of CD16+ cells by adjusting the duration of LPS stimulation.

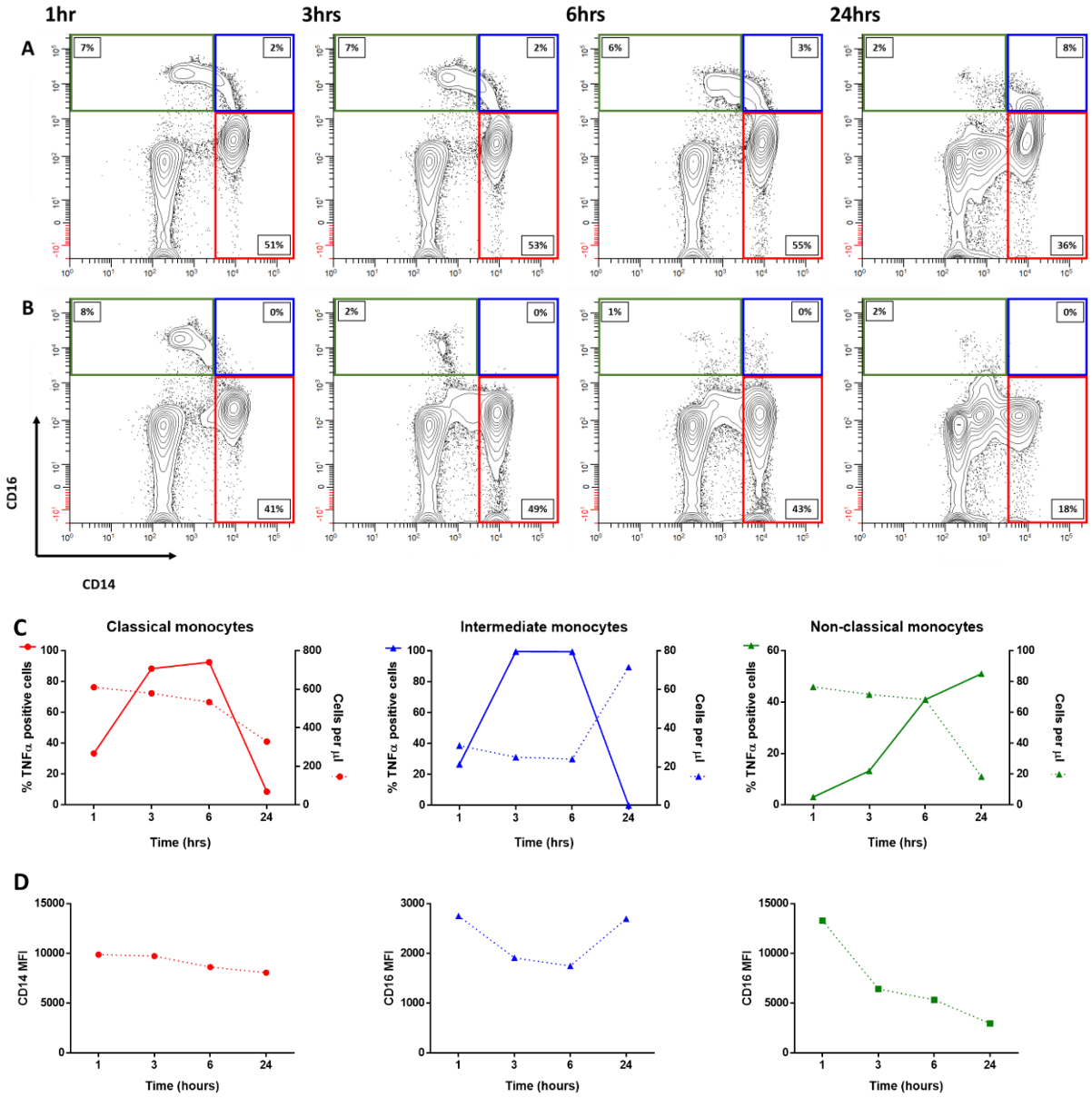

Figure 3.5: Time course for LPS stimulation. Healthy donor PBMCs (n=1) were stimulated with 1ng/mL LPS for one, three, six, or 24 hours in the presence of monensin. The PBMCs were then labelled for anti-HLA-DR, anti-CD14, and anti-CD16 antibodies to distinguish the monocytes subsets, fixed, permeabilised and labelling intracellularly with anti-TNFα antibody before acquiring on the flow cytometer. **A)** representative flow cytometry plots of monocyte subset distribution over the time course in unstimulated cultures. **B)** representative flow cytometry plots of monocyte subset distribution over the time course in cultures stimulated with 1ng/mL LPS. TNFα production was quantified as a percentage of cells positive for TNFα. Absolute cell number was calculated using Flow-Count Fluorospheres. **C)** LPS-induced TNFα production with increasing time course of stimulation, and absolute numbers of the monocyte subsets. **D)** expression of CD14 or CD16, measured as MFI, on monocyte subsets stimulated with 1ng/ml LPS for 1-24 hours.

To determine whether the loss of CD16+ cells was specific to stimulation with LPS, the effect of other TLR agonists was investigated. Whole PBMCs from a healthy donor were stimulated with LPS a TLR4 agonist (1ng/mL), Pam_3CSK_4 a TLR2 agonist (1000ng/mL), Poly(I:C) a TLR3 agonist (1000ng/mL), or Flagellin a TLR5 agonist (1000ng/mL) for three hours in the presence of monensin before staining for TNFα intracellularly. TNFα production was quantified as a percentage of cells positive for TNFα. Absolute cell number was calculated using Flow-Count Fluorospheres. CD14 and CD16 expression was measured as MFI for staining with anti-14 or anti-CD16 antibody.

There was an apparent reduction in the absolute number of intermediate monocytes and to a lesser extent non-classical monocytes, upon stimulation with the all of the TLR agonists tested (Figure 3.6 A). Like LPS, the other TLR agonists also caused a loss of CD16 expression on the residual intermediate and non-classical cells (Figure 3.6 B). There was a modest reduction in the absolute number of classical monocytes upon stimulation with the TLR agonists, but this seemed unrelated to the level of CD14 expression (Figure 3.6 A, B). When comparing different TLR agonists, the 'loss' of monocytes was not always related to the level of TNFα production they induced. For instance, TNFα production was greater with LPS and Poly(I:C) stimulation than with Pam_3CSK_4 or flagellin but their effects on numbers of intermediate and non-classical monocytes and the level of CD16 expression was similar (Figure 3.6 B, C).

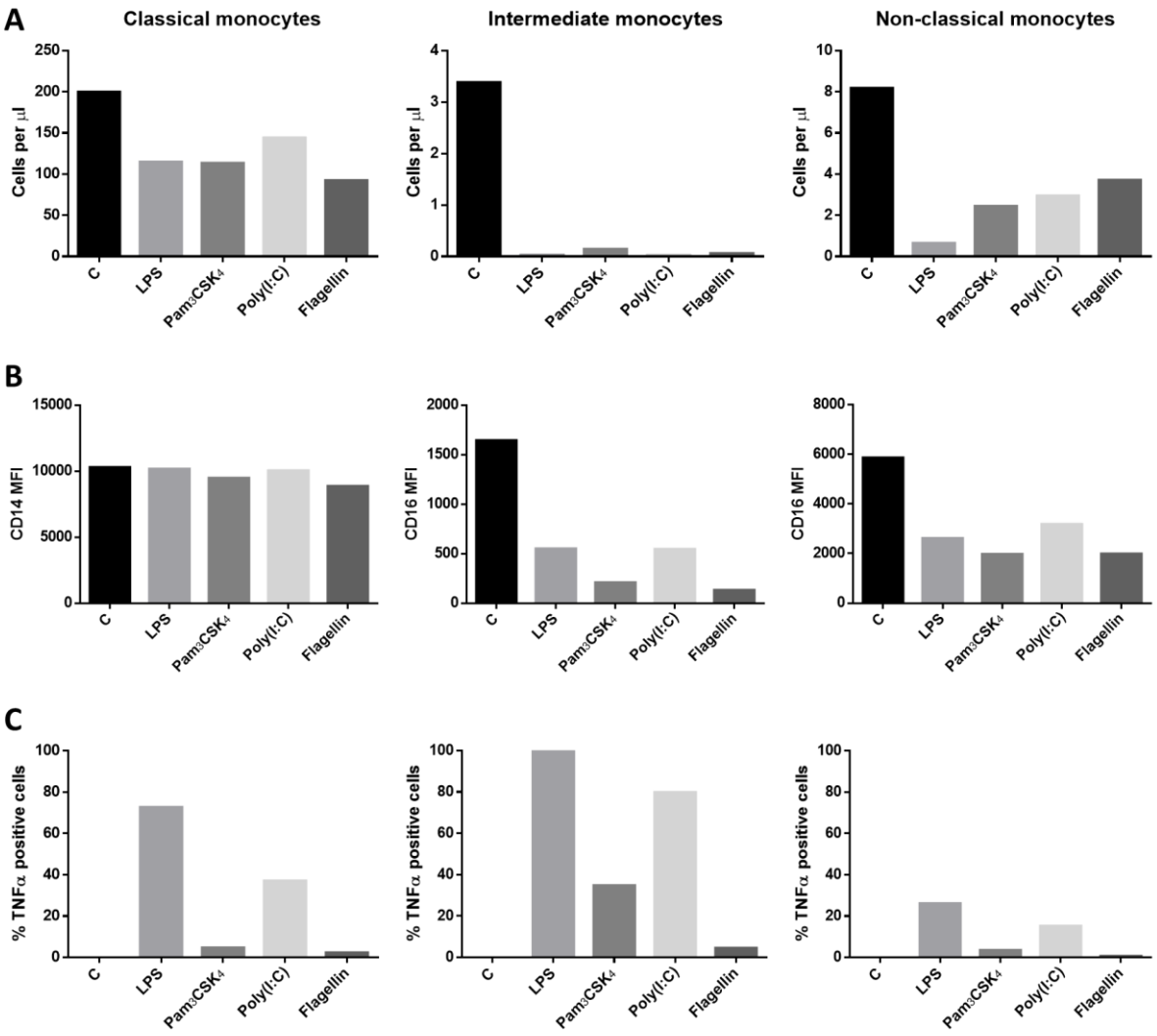

Figure 3.6: The effect of stimulation with various TLR agonists on the monocyte subsets. Healthy donor PBMCs (n=1) were stimulated with LPS (1ng/mL), Pam_3CSK_4 (1000ng/mL), Poly(I:C) (1000ng/mL), or flagellin (1000ng/mL) for three hours in the presence of monensin. The PBMCs were then labelled for anti-HLA-DR, anti-CD14, and anti-CD16 antibodies to distinguish the monocytes subsets before acquiring on the flow cytometer. **A)** absolute cell numbers, calculated using Flow-Count fluorospheres, of the monocyte subsets upon stimulation with the TLR agonists. **B)** expression of CD14 or CD16, measured as MFI, on the monocyte subsets upon stimulation with the TLR agonists. **C)** TNFα production, quantified as a percentage of cells positive for TNFα, in the monocyte subsets upon stimulation with the TLR agonists.

3.4.3.2 The apparent loss of CD16+ cells is not due to cell death or adherence

The apparent loss of CD16+ cells could be due to induced cell death upon TLR4 stimulation. To test this, the viability of the cells was investigated. Whole PBMCs from a healthy donor were stimulated or not with LPS (1ng/mL) for three hours in the presence of monensin and stained with fixable viability dye (enables identification of dead cells) and annexin V (binds to phosphatidylserine, a marker of apoptosis) to detect dead or dying cells within the three populations of monocytes.

There was no shift in staining for fixable dye or annexin V in any of the monocyte subsets between unstimulated and LPS stimulated cultures, indicating no difference in the viability of the cells (Figure 3.7). However, this approach can only assess the viability of the cells in the monocyte population remaining after stimulation and the viability of the cells that are 'lost' cannot be determined. Therefore, a contribution of cell death induced by TLR stimulation cannot be ruled out as an explanation for the loss of CD16+ cells.

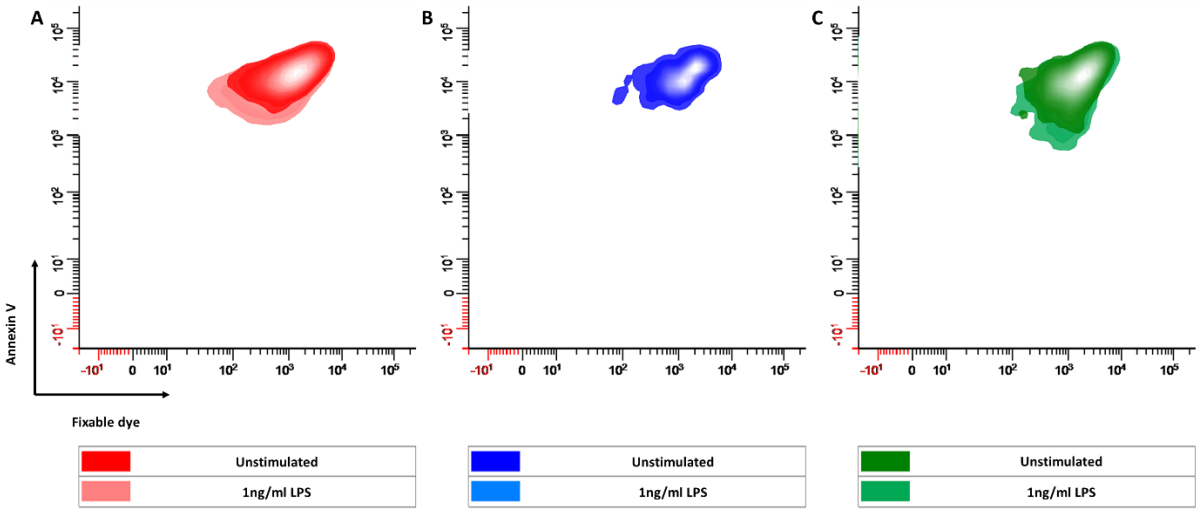

Figure 3.7: Viability of the monocyte subsets upon LPS stimulation. Whole PBMCs from a healthy donor (n=1) were stimulated or not with 1ng/mL LPS for three hours in the presence of monensin. The PBMCs were then labelled for anti-HLA-DR, anti-CD14, and anti-CD16 antibodies to distinguish the monocytes subsets, and stained with annexin V and fixable viability dye to identify dead or dying cells. The sample was then acquired on the flow cytometer. Graphs show annexin V and fixable dye staining in classical **(A; red)**, intermediate **(B; blue)**, and non-classical **(C; green)** monocytes overlaying unstimulated culture **(solid colour)** and stimulated cultures **(pale colour)**.

Upon activation, monocyte subsets may become adherent to tissue culture plastic to different extents. This raises the possibility that CD16+ monocytes could adhere to a greater degree leading to reduced recovery. To test this idea, stimulation assays were compared in low adhesive and standard tissue culture plates. Whole PBMCs from a healthy donor were stimulated with increasing concentrations of LPS (0.001-10ng/mL) for three hours in the presence of monensin. Absolute cell number was calculated using Flow-Count Fluorospheres. CD14 and CD16 expression was measured as MFI for staining with anti-14 or anti-CD16 antibody.

The apparent loss of CD16+ monocytes upon LPS stimulation did not differ substantially between cultures in low adherence and standard tissue culture plates (Figure 3.8 A). The residual intermediate and non-classical monocytes were characterised by their reduced levels of CD16 expression with increasing LPS concentration whether they were cultured on standard or low-adhesive plates (Figure 3.8 B). The modest loss of CD14+ classical monocytes in the absence of any effect on the level of CD14 expression, previously observed, was observed in both types of plates (Figure 3.8 A, B). Nonetheless, results obtained using low adherence and standard plates were not identical; the recovery of both classical and intermediate monocytes was marginally higher in the low adherence plates compared with standard culture plates, consistent with a loss of small numbers of cells by adherence to the standard plate (Figure 3.8 A). This was reflected in their expression levels of CD14 and CD16 (Figure 3.8 B).

Overall, these data indicate that although there was a minor loss of both classical and intermediate monocytes on the standard plate, most likely due to adherence. The apparent loss of CD16+ subsets following LPS stimulation could not be attributed to adherence to the culture plate.

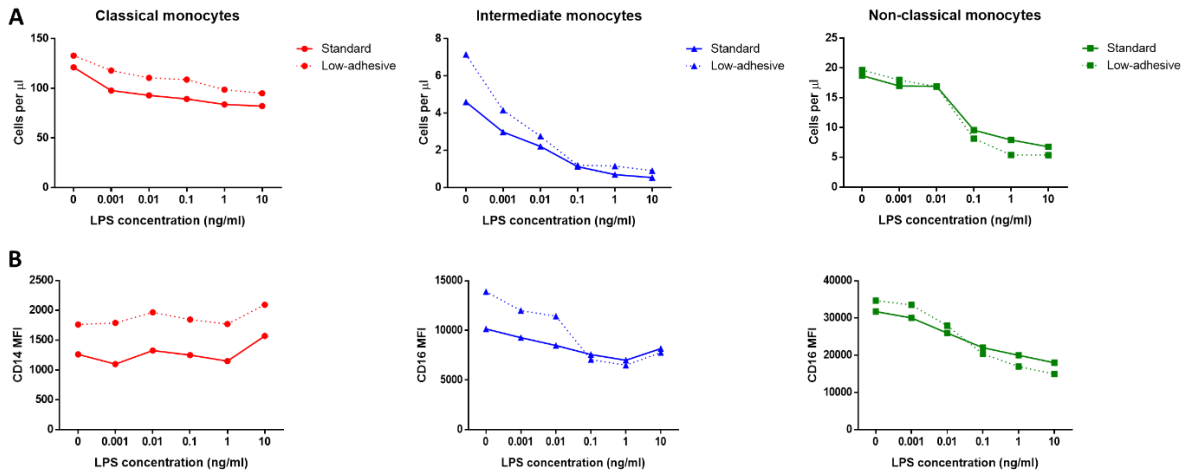

Figure 3.8: The effect of stimulation with LPS on the monocyte subsets cultured in standard or low-adhesive plates. Whole PBMCs from a healthy donor (n=1) were stimulated or not in standard or low-adhesive plates with increasing concentrations of LPS (0.001-10ng/mL) for three hours in the presence of monensin. The PBMCs were then labelled for anti-HLA-DR, anti-CD14, and anti-CD16 antibodies to distinguish the monocytes subsets before acquiring on the flow cytometer. **A)** absolute cell numbers, calculated using Flow-Count fluorospheres, of the monocyte subsets upon stimulation with the TLR agonists. **B)** expression of CD14 or CD16, measured as MFI, on the monocyte subsets upon stimulation with the TLR agonists.

3.4.3.3 LPS stimulation causes loss of CD16 expression

Thus far, the findings indicated that the loss of CD16+ cells upon LPS stimulation was unlikely to be explained by cell death or adherence to culture plates. Reduced expression of CD16 on the residual intermediate, and to a lesser extent non-classical monocytes following stimulation, suggested the alternative possibility that the CD16 marker was lost following stimulation. Thus, CD16+ monocytes may not be genuinely lost but instead undergo a phenotypic change upon stimulation such that they are no longer identifiable. To test this possibility, an approach was developed that allowed the fate of monocytes subsets to be tracked following stimulation independently of their continued expression of CD16 and CD14. Whole PBMCs from a healthy donor were stained with CTV and then labelled for HLA-DR, CD14, and CD16 to distinguish the monocytes subsets for cell sorting on the FACS Aria. The separated subsets were spiked into unlabelled PBMCs and stimulated or not with 1ng/mL LPS for three hours in the presence of monensin. The level of CD14 and CD16 expression on the purified, labelled monocyte subsets were measured before and after culture.

The level of CD14 expression on the classical monocytes was maintained after three hours of incubation with or without LPS stimulation (Figure 3.9 A, D). However, intermediate and non-classical monocytes showed a decline in CD16 expression after three hours of incubation even in the absence of LPS, and the level of CD16 expression was reduced further in LPS-stimulated cultures (Figure 3.9 B-D). These observations suggest that the process of antibody labelling and/or sorting of the cells led to activation of the cells and reduced expression of CD16, and that this effect was further promoted by the addition of LPS. Although moderate, there was a further reduction in CD16 expression on the intermediate and non-classical monocytes upon LPS stimulation (Figure 3.10 B-D).

Collectively, these data suggest that the apparent loss of CD16+ cells upon activation was due to changes in marker expression and not cell death or adherence.

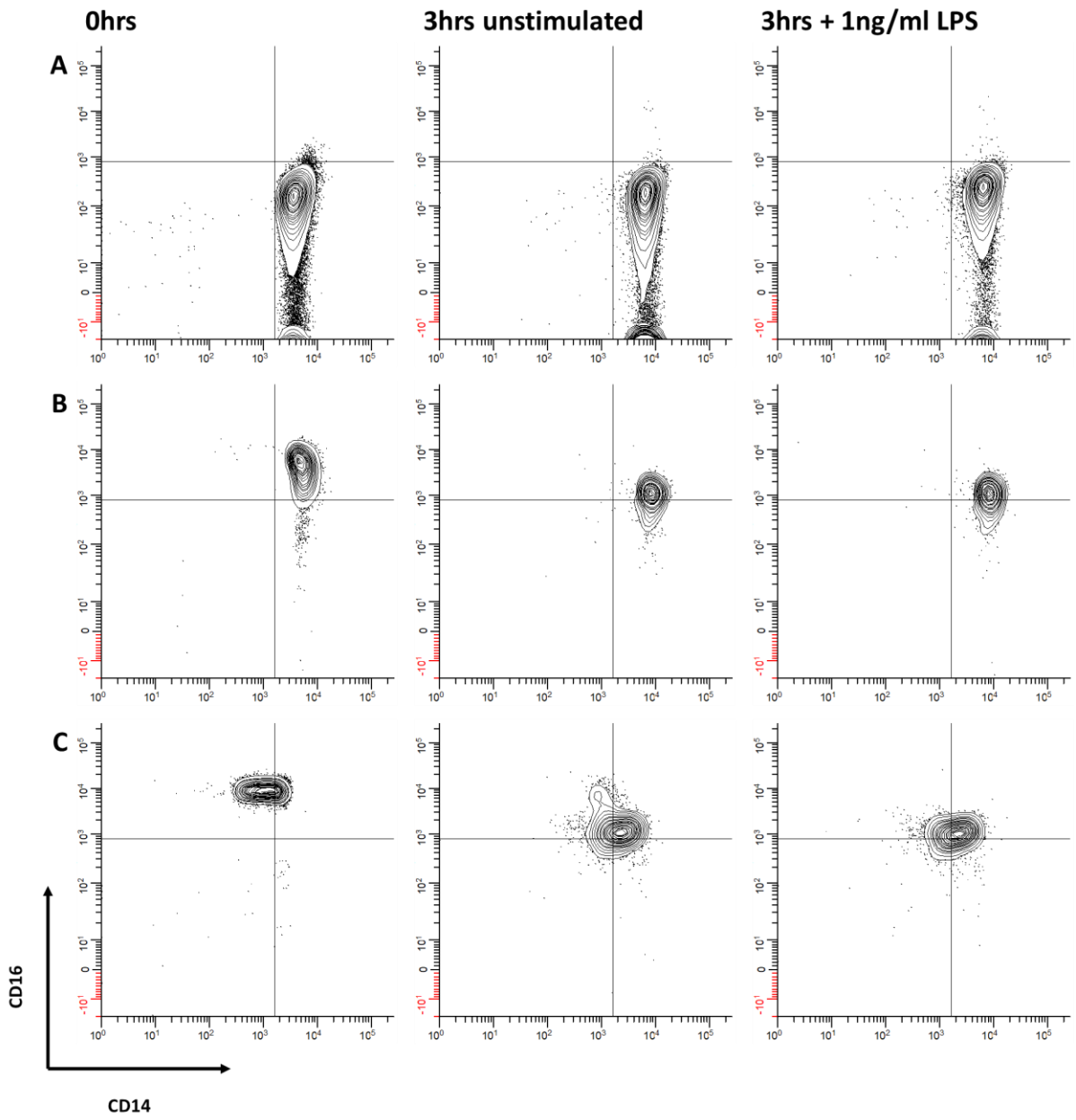

D

Time (hrs)	MFI		
	CD14 (Classical)	CD16 (Intermediate)	CD16 (Non-classical)
0	7170	4273	9911
3	7070	1387	1923
3 +1ng/ml LPS	7000	1096	1299

Figure 3.9: Tracking monocyte subsets upon LPS stimulation. Representative of healthy donor PBMCs (n=4) were stained with CTV and then labelled for anti-HLA-DR, anti-CD14, and anti-CD16 antibodies to distinguish the monocytes subsets before cell sorting on the FACS Aria. The separated subsets were spiked into unlabelled PBMCs and stimulated or not with 1ng/mL LPS for three hours in the presence of monensin. The cultured cells were harvested and then labelled for HLA-DR, CD14, and CD16 before acquiring on the flow cytometer. **A, B and C)** representative flow cytometry plots of individual subsets at 0hrs, 3hrs, and 3-hour LPS stimulation. **D)** expression of CD14 or CD16, measured as MFI, on the monocyte subsets at 0hrs, 3hrs, and 3-hour LPS stimulation.

3.4.3.4 Loss of CD16 expression is not due to internalisation

Tracking monocyte subsets as described above indicated that CD16 expression was rapidly lost from the cell surface upon activation. The possible mechanisms for this reduction in CD16 expression over a few hours are internalisation of CD16 or cleavage from the cell surface. First, the internalisation of the marker was investigated. Whole PBMCs from a healthy donor were stimulated with 1ng/mL LPS for three hours in the presence of monensin before staining for intracellular CD16 by permeabilising the cells before the addition of anti-CD16.

Permeabilisation of LPS-stimulated cells before addition of anti-CD16 did not reveal a population of CD16+ intermediate or non-classical monocytes (Figure 3.10 A, B). This suggests that CD16 is not internalised following LPS stimulation and indicates that it must be lost from the surface by an alternative mechanism.

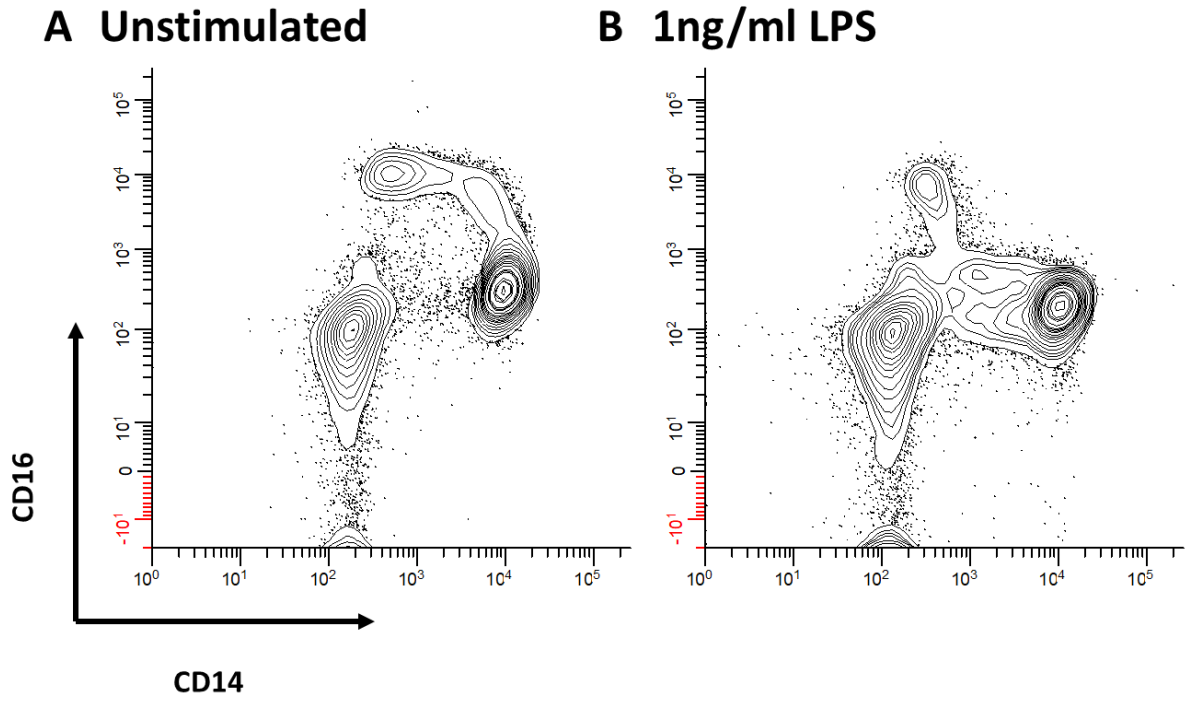

Figure 3.10: Monocyte subset distribution upon LPS stimulation with intracellular CD16 labelling. Whole PBMCs from a healthy donor (n=1) were stimulated with 1ng/mL LPS for three hours in the presence of monensin. The PBMCs were then labelled for anti-HLA-DR, anti-CD14, and anti-CD16 antibodies to distinguish the monocytes subsets, fixed, permeabilised and stained intracellularly for CD16 before acquiring on the flow cytometer. **A and B)** representative flow cytometry plots of monocyte subsets distribution under the two conditions.

3.4.3.5 LPS induces cleavage of CD16 via ADAM17

The next step was to investigate the possible cleavage of CD16 from the surface of monocytes upon LPS stimulation. There is a precedent for this in NK cells as Romee et al. (2013) showed that CD16 was cleaved from the surface of NK cells upon stimulation and that this effect could be blocked by inhibitors of the metalloprotease ADAM17. To test whether monocytes cleaved CD16 in the same way, a specific ADMA17 inhibitor (TMI-005) was used. Whole PBMCs from a healthy donor were stimulated with LPS (1ng/mL) for three hours in the presence of monensin, and with or without ADAM17 inhibitor (50µM TMI-005 added 30min before LPS).

Loss of CD16 expression was again observed upon LPS stimulation in the absence of the ADAM17 inhibitor (Figure 3.11 A). However, in the presence of the ADAM17 inhibitor, CD16+ monocytes, both intermediate and non-classical subsets, were maintained following LPS stimulation (Figure 3.11 B). These findings indicate that CD16 is cleaved off the cell surface by ADAM17 upon TLR4 activation. Blocking ADAM17 also prevented the loss of CD16 expression when stimulating with other TLR agonists, including Poly(I:C), Pam_3CSK_4, and Flagellin (data not included), which suggests the downregulation of CD16 expression upon activation by various TLR agonists work via the same mechanism.

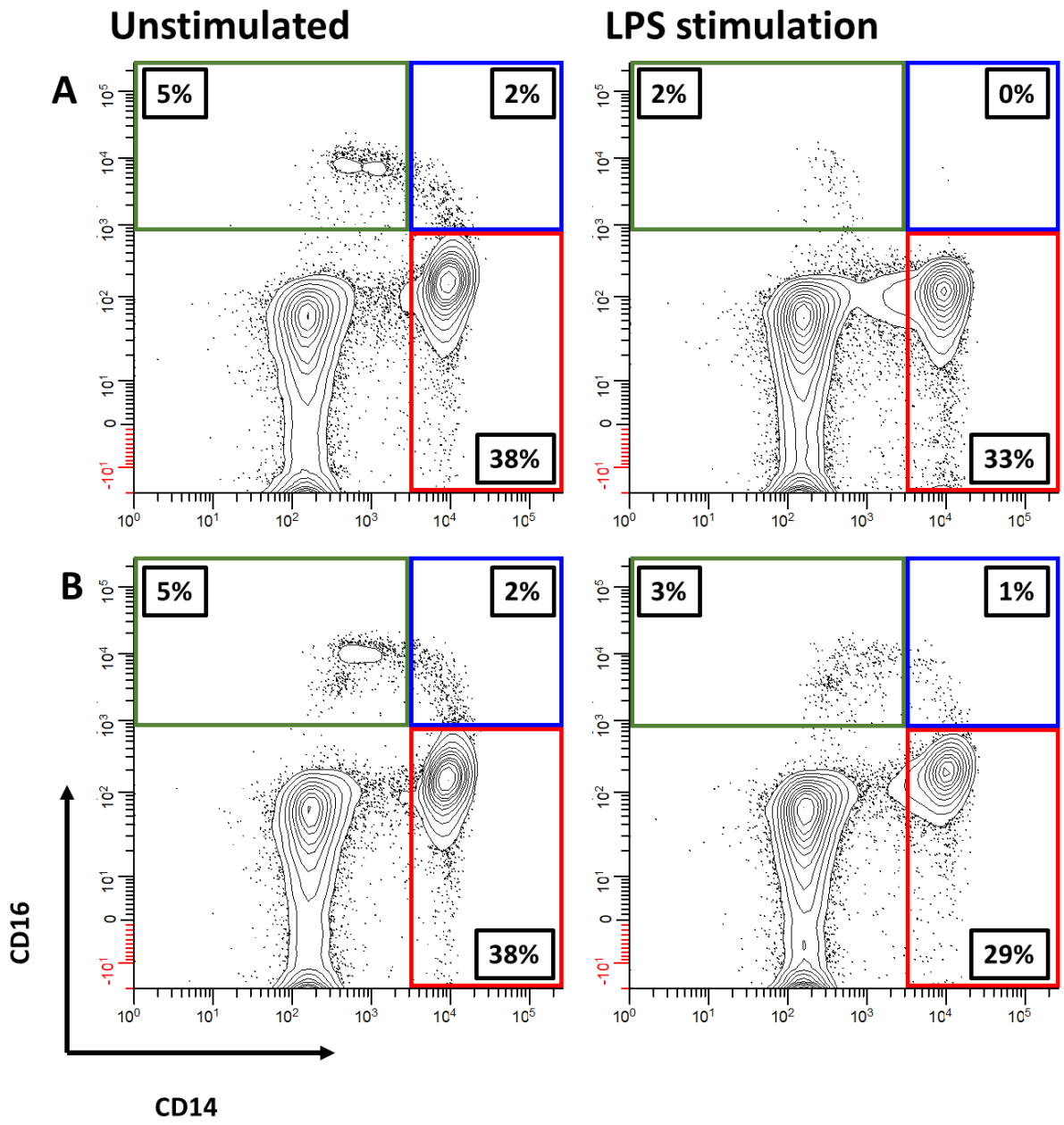

Figure 3.11: The effect of stimulation with LPS on the monocyte subsets cultured in the presence or absence of an ADAM17 inhibitor. Healthy donor PBMCs (n=1) were stimulated or not with LPS (1ng/mL), for three hours in the presence of monensin, and with or without ADAM17 inhibitor (TMI-005 at 50µM added 30min before LPS). The PBMCs were then labelled for anti-HLA-DR, anti-CD14, and anti-CD16 antibodies to distinguish the monocytes subsets before acquiring on the flow cytometer. Graphs show representative plots of monocyte subset distribution upon TLR stimulation **A)** without ADAM17 inhibitor **B)** with ADAM17 inhibitor.

3.4.3 Optimising the assay for measuring monocyte responsiveness to IL-10

Once the cleavage of CD16 could be blocked with an ADAM17 inhibitor, it was possible to reliably identify all monocyte subsets following LPS stimulation. ADAM17 is also involved in cleaving and release TNFα from the cell surface (Adrain et al. 2012), which could theoretically impact on the staining of cell-associated TNFα used as a readout for the response to LPS in this assay, therefore, it was important to ensure that that the addition of TMI-005 did not have a negative impact on the LPS-induced TNFα response. Whole PBMCs from a healthy donor were stimulated with increasing concentrations of LPS (0.001-1000ng/mL) for three hours in the presence of monensin and ADAM17 inhibitor (50μM TMI-005 added 30min before LPS) before staining for TNFα intracellularly. TNFα production was quantified as a percentage of cells positive for TNFα. Absolute cell number was calculated using Flow-Count Fluorospheres. CD14 and CD16 expression was measured as MFI for staining with anti-14 or anti-CD16 antibody.

In the presence of ADAM17 inhibitor LPS induced TNFα production with the same hierarchy of the monocyte subsets and LPS dose-dependence previously noted in its absence (Figure 3.12 A). Therefore, ADAM17 does not appear to have a negative impact on TNFα as a readout, most likely because intracellular rather than secreted TNFα was measured in this protocol.

The number of classical monocytes and CD14 expression was constant across the LPS concentrations (Figure 3.12 A, B). The number of intermediate and non-classical monocytes and CD16 expression was reduced at higher LPS concentrations even in the presence of TMI-005, suggesting that the protective effect of 50μM TMI-005 can be partially overcome if the strength of stimulation is sufficiently strong, but the magnitude of this effect was much lower than in the absence of ADAM17 inhibitor (Figure 3.12 A). On the basis of these findings, TMI-005 was included in the assays going forward.

Accordingly, 1ng/mL was determined as the optimal LPS concentration going forward as it was the minimum concentration required to produce a robust but sub-maximal TNFα response, measurable in all subsets, that should therefore provide sensitivity when assaying the inhibitory effects of IL-10.

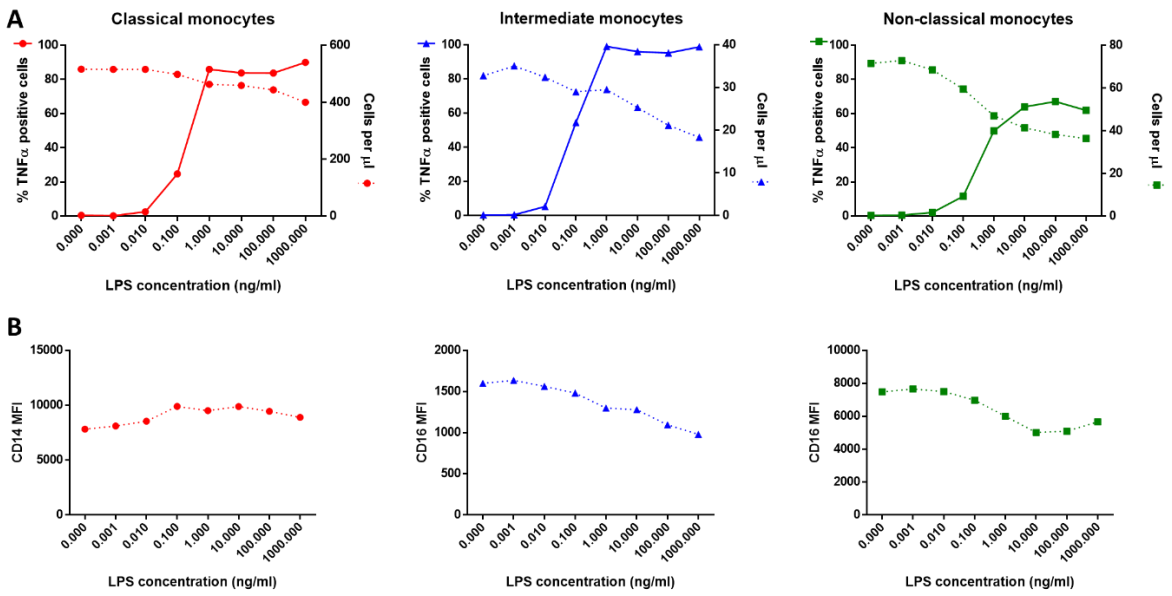

Figure 3.12: LPS titration in the presence of ADAM17 inhibitor. Healthy donor PBMCs (n=1) were stimulated with increasing concentrations of LPS (0.001-1000ng/mL added 30min before LPS) for three hours in the presence of monensin and ADAM17 inhibitor (TMI-005 at 50µM added 30min before LPS). The PBMCs were then labelled for anti-HLA-DR, anti-CD14, and anti-CD16 antibodies to distinguish the monocytes subsets, fixed, permeabilised and labelling intracellularly with anti-TNFα antibody before acquiring on the flow cytometer. TNFα production was quantified as a percentage of cells positive for TNFα. Absolute cell number calculated using Flow-Count Fluorospheres. **C)** LPS-induced TNFα production with increasing concentration of LPS, and absolute numbers of the monocyte subsets. **D)** the level of CD14 and CD16 expression, measured as MFI, on monocyte subsets with increasing concentration of LPS.

Finally, to confirm the suitability of the assay for measuring the ability of IL-10 to inhibit LPS-induced TNFα production by the monocyte subsets, IL-10 was titrated into the assay. Whole PBMCs from a healthy donor were stimulated with 1ng/mL LPS and increasing concentrations of IL-10 (0.016-10ng/mL added 30min before LPS) for three hours in the presence of monensin and ADAM17 inhibitor (50µM TMI-005 added 30min before LPS) before staining for TNFα intracellularly. TNFα production was quantified as a percentage of cells positive for TNFα.

A dose-dependent reduction in TNFα production was observed with increasing concentrations of IL-10 for each monocyte subset (Figure 3.13 A). The inhibition of TNFα production by IL-10 could be completely blocked by addition of an anti-IL-10R blocking antibody (Figure 3.13 B), confirming that the inhibitory action of IL-10 is a specific effect via the IL-10R.

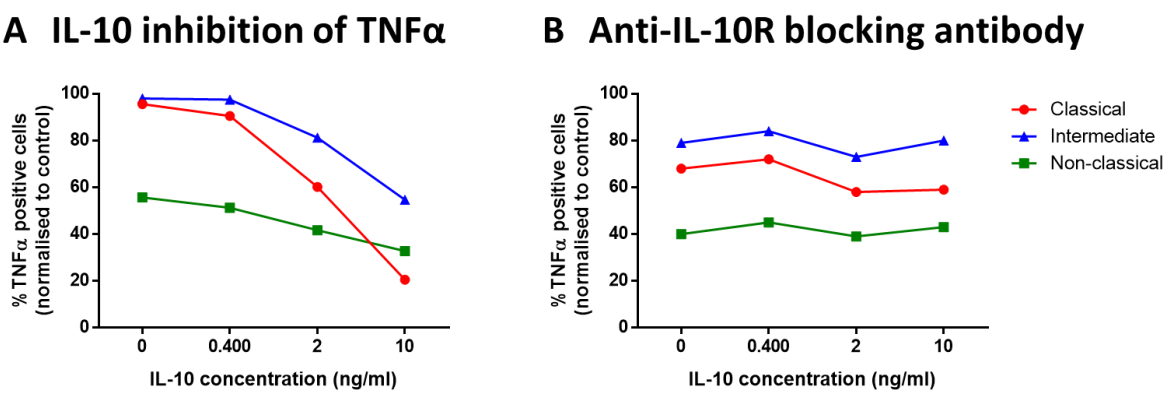

Figure 3.13: Inhibition of LPS-induced TNFα production with increasing concentration of IL-10. Whole PBMCs from a healthy donor (n=1) were stimulated with 1ng/mL LPS and increasing concentration of IL-10 (0.4-10ng/mL added 30min prior to LPS) for three hours in the presence of monensin and ADAM17 inhibitor (TMI-005 at 50µM added 30min prior to LPS), and with or without IL-10R blocking antibody (5µg/mL added 30min prior to IL-10). The PBMCs were then labelled for anti-HLA-DR, anti-CD14, and anti-CD16 antibodies to distinguish the monocytes subsets, fixed, permeabilised and labelling intracellularly with anti-TNFα antibody before acquiring on the flow cytometer. TNFα production was quantified as a percentage of cells positive for TNFα. **A)** LPS-induced TNFα production by monocyte subsets with increasing concentration of IL-10 in the absence of anti-IL-10R blocking antibody. **B)** LPS-induced TNFα production by monocyte subsets with increasing concentration of IL-10 in the presence of ant-IL-10R blocking antibody.

In summary, the final assay optimised in this chapter used unfractionated PBMCs stimulated with 1ng/mL LPS and increasing concentration of IL-10 (0.016-10ng/mL added 30min before LPS) for three hours in the presence of monensin and ADAM17 inhibitor (TMI-005 at 50µM mL added 30min before LPS). The hierarchy of response to IL-10 inhibition for each subset is discussed in more detail in the next chapter.

5.5 Discussion

The primary aim of this chapter was to develop an assay that could be used to measure IL-10 responsiveness in human monocyte subsets. First, a gating strategy for the identification of the human monocyte subsets was established. The assay for measuring IL-10 responses in the monocyte subsets involved induction of TNFα production with LPS. However, this led to an apparent loss of CD16+ cells. This effect could be inhibited by an ADAM17 inhibitor (TMI-005), which enabled the IL-10 response of the monocyte subsets to be determined in parallel in the same culture environment.

The method of monocyte subset identification was broadly based on previously published work by Thiesen et al. 2013. Importantly, CD33 and NKp46 labelling confirmed the identity of the monocytes and showed that CD16+ cell populations that are not monocytes (e.g. NK cells) were excluded from the non-classical monocyte gate as a result of pre-gating on HLA-DR+ cells. A recent study demonstrated in humans that the monocyte subsets are not isolated populations but represent stages of differentiation, along which the expression of various markers change (Patel et al. 2017). For instance, CCR2 is downregulated during the maturation of classical monocytes into non-classical monocytes, while CX_3CR1 is upregulated (Patel et al. 2017). This expression profile was reflected in the analysis of the monocyte subsets identified with the gating strategy described in this chapter.

The monocyte subsets could be identified using whole blood labelling, which was attractive for phenotyping because there is less manipulation of the cells. However, separated PBMCs had to be used for the functional experiments. The two methods were compared, and distribution of subsets within the monocyte population was similar in whole blood and separated PBMCs cultured short term, enabling the comparison of data produced from each method.

It was decided to measure IL-10 responsiveness of monocyte subsets by stimulating whole PBMCs with LPS in the presence of increasing amounts of IL-10 and determining inhibition of TNFα production. TNFα was chosen as the readout because it is clinically relevant in IBD, and LPS is known to stimulate a robust TNFα response in monocytes (Kontoyiannis et al. 1999). However, upon

stimulation with LPS there was an apparent loss of intermediate monocytes, and to a lesser extent non-classical monocytes, which may be due to the greater induction of TNFα in intermediate monocytes compared to non-classical monocytes. The expression of CD16 on the residual intermediate and non-classical monocytes was also reduced with increasing concentration of LPS. The loss of CD16 expression upon TLR stimulation has previously been reported on NK cells (Romee et al. 2013). The mechanism behind the apparent loss CD16+ cells will be discussed in more detail.

The loss of CD14 expression upon activation has been previously described in monocytes (Bazil & Strominger 1991). In the data presented in this chapter, there was only a small reduction in the number of CD14+ classical monocytes, and a modest reduction in the level of CD14 expression at higher concentrations of LPS. The study by Bazil & Strominger 1991 used purified monocytes, which may account for the greater loss of CD14 expression reported. In addition, their study concluded that the loss of CD14 expression was due to shedding from the cell surface as they detected an increase in soluble CD14 in stimulated cultures (Bazil & Strominger 1991). Another study showed that the downregulation of TLR4 expression on human aortic endothelial cells was due to cleavage (Yang et al. 2018). In contrast, a study by Kagan et al., 2008 showed that TLR4 activation induced CD14-dependent endocytosis of the TLR4 complex in Mϕs. However, Rajaiah et al. 2015 showed endocytosis is CD14-independent. Therefore, it appears that different cell types have different mechanisms for downregulating TLR4 expression. This phenomenon may demonstrate a negative feedback mechanism of endotoxin tolerance.

A number of experiments were carried out in an attempt to dissociate the induction of TNFα production from the impact of stimulation on CD16+ monocytes. A time course was used to investigate the kinetics of LPS induced loss of the monocyte subsets and induction of TNFα production but both outcomes were tightly associated in time between one and six hours after stimulation. Following overnight culture, there was an apparent loss of classical monocytes that shift towards intermediate monocytes, with both populations displaying a diminished response to LPS. The upregulation of CD16

expression with overnight culture has not been previously described. However, this does not reflect the 'monocyte waterfall' of the maturation of classical monocytes into intermediate monocytes because of other phenotypic features (diminished LPS response). There is evidence that RBCs have a role in regulating CD16 expression (Schakel et al. 2006), therefore, the separation of PBMCs from whole blood during overnight culture could be the cause of the upregulated CD16 expression. The 'loss' of non-classical monocytes was closely linked to TNFα production throughout the 24 hours of stimulated culture.

The experiments so far had focused on LPS stimulation, which raised the question whether the 'loss' of CD16+ cells was TLR4-dependent. LPS signals down two pathways: MyD88-dependent and TRIF-dependent (MyD88-independent) (Lu et al. 2008). Although there is cross-talk in these two signalling pathways, the former is associated particularly with activation of transcription factors such as NF-κB and production of pro-inflammatory cytokines including TNFα, whereas MyD88-independent signalling leads to the production of Type 1 interferons. To investigate the contribution of MyD88 signalling to the 'loss' of CD16+ cells, MyD88-dependent and -independent pathways were compared. LPS was compared with three other TLR ligands chosen to target these signaling pathways individually: Pam_3CSK_4 acts via TLR2 and Flagellin act via TLR5, both triggering the MyD88 pathway, whilst Poly(I:C) acts via TLR3 to activate TRIF (TLR3 is the only TLR not to activate MyD88-dependent signaling) (Akira & Takeda 2004). However, all the TLR agonists tested induced an equivalent 'loss' of the CD16+ cells, suggesting that both MyD88- and TRIF-dependent signalling are capable of inducing this effect. However, these two signalling pathways may not be completely independent as TNFα was induced by Poly(I:C) stimulation, indicating potential crosstalk between the two signalling pathways. The different TLR agonists induced variable levels of TNFα production but the 'loss' of the CD16+ cells was comparable, indicating that TNFα is unlikely to be solely responsible for the monocyte loss.

Importantly, the viability of the monocytes was measured upon LPS stimulation to ensure that the monocytes were not impaired under the stimulation conditions. It is not known how long monocytes

survive in vitro after stimulation or if it varies between subsets. LPS stimulation did not affect the viability of the subset with the caveat that this could only be measured in the remaining cells. There is evidence that monocytes become more adherent upon activation (Tzeng et al. 1985), therefore, low-adhesive plates were used to ensure the monocytes were not being lost during cell harvesting. Although the low adhesive plates did not reverse the 'loss' of CD16+ monocytes observed with increasing LPS concentrations, there was an overall improvement of cell recovery of classical monocytes, and of intermediate monocytes at lower concentrations of LPS confirming limited adherence to the standard plates. Non-classical monocytes did not show a noticeable difference in cell recovery with non-adherent plates. Although their role in patrolling the endothelium would suggest they are highly adherent, the surface of the plastic and the endothelium are not comparable (Auffray et al. 2007).

Thus far, the apparent loss of CD16+ cells upon LPS stimulation could not be explained by induced cell death or adherence to culture plates, therefore, an alternative explanation that the changes in surface marker expression on the monocyte subsets upon stimulation was investigated. Cell sorted monocyte subsets were labelled with CTV to enable tracking once they were placed into culture with whole PBMCs (to maintain a consistent culture environment), with or without LPS stimulation. Expression of CD14 on classical monocytes was unaffected during the three-hour culture or by LPS stimulation. However, intermediate and non-classical monocytes showed a decline in CD16 expression during the three-hour incubation in the absence of stimulation. This suggests that the process of antibody labelling and/or cell sorting causes activation of the cells. Although moderate, there is a further reduction in CD16 expression on the intermediate and non-classical monocytes upon LPS stimulation. The moderate loss of CD16 expression upon LPS activation could be due to negative feedback mechanisms primed by the initial activation, as endotoxin tolerance is a well-known phenomenon (reviewed by Biswas & Lopez-Collazo 2009). Overall, these data suggest that the apparent loss of CD16+ cells upon activation is due to reduced cell surface expression. The most likely explanations for a reduction in CD16 expression over a few hours are internalisation or shedding of the marker from

the cell surface. However, there was no increase in intracellular CD16 staining in permeabilised cells suggesting that cleavage from the cell surface is the most likely explanation.

Romee et al., 2013 showed that CD16 was shed from the surface of NK cells upon activation due to detecting an increase in soluble CD16 in stimulated culture, and this could be blocked by an ADAM17 inhibitor. Therefore, a specific ADAM17 inhibitor (TMI-005) was used to investigate whether the same mechanism was present in monocytes. ADAM17 (also called tumor necrosis factor converting enzyme/TACE) is a metalloprotease first recognised for releasing membrane-bound TNFα to its active form, and is now understood to play a broader role (Adrain et al. 2012). In the presence of ADAM17 inhibitor, CD16+ monocytes were still identifiable following stimulation, which indicates that CD16 is cleaved off the cell surface by ADAM17 upon TLR activation. There was still some cleavage of CD16 at higher LPS concentrations, which may suggest a suboptimal concentration of ADAM17 inhibitor or possibly that other protease could contribute to the loss of CD16. As mentioned, ADAM17 is also involved in cleaving TNFα, which is the readout for the LPS response, therefore, it was important to ensure that ADAM17 blockade did not have a negative impact on the LPS response. ADAM17 showed no negative impact on TNFα as a readout, which is most likely due to measuring intracellular TNFα production and not secretion.

The use of an ADAM17 inhibitor enabled the measurement of IL-10 responsiveness of the monocyte subsets in parallel ensuring the same culture environment, and removed the need for cell sorting that appeared to activate the monocytes. TNFα production was measured via intracellular staining, which may differ to secretion that is regulated by ADAM17. The implications of CD16 shedding upon TLR activation are unclear. Downregulation of CD16 expression may limit cross-linking by immune complexes that induce ADCC (Romee et al. 2013; Schmitz et al. 2002), with the aim to maintain immune homeostasis. Shedding of CD16 could also be an artefact of in vitro stimulation. However, Picozza Picozza, Batistini, and Borsellino 2013 showed that stimulating whole blood with LPS induced the same effect. The concentration of LPS used may not be physiological, therefore, CD16 shedding

due to high LPS exposure cannot be ruled out. An environment where immune cells are continuously exposed to external antigens includes the intestine, where the function and origin of intestinal Mϕs have been previously investigated. Although fate-mapping experiments in mice point to classical monocytes as the origin of intestinal Mϕ in steady state, there may be circumstances in which other populations could contribute. In humans, a contribution of CD16+ monocytes to the intestinal Mϕ pool may have been missed if CD16 is shed upon entry into the intestine making their identification challenging due to the lack of unique identifiers.

5.6 Conclusion

TLR stimulation leads to ADAM17 mediated cleavage of CD16 on monocytes and the apparent loss of intermediate monocytes, and to a lesser extent non-classical monocytes, from stimulated cultures. Addition of an ADAM17 inhibitor (TMI-005) to the cultures maintains CD16 expression and enables the responsiveness to IL-10 of the monocyte subsets to be determined in parallel in the same culture environment. The shedding of CD16 from the surface of populations of monocytes upon activation has important implications for the functions of these cells and also for the identification of moMϕs within the intestine and other tissues. Caution should be applied when in interpreting an absence of CD16 expression as an absence of cells derived from intermediate or non-classical populations.

Chapter 4: Human monocyte subsets differ in their response to IL-10 in healthy individuals

4.1 Chapter summary

In this chapter, the response of individual monocytes subsets to IL-10 was determined in healthy individuals. Response to IL-10 was measured using the ability of IL-10 to inhibit LPS-induced TNFα production. First, LPS-induced TNFα production was measured: intermediate monocytes showed greater TNFα production than classical monocytes, and non-classical monocytes showed the lowest TNFα production. IL-10 inhibition of this TNFα was greatest in classical monocytes, followed by intermediates, and least responsive were the non-classical monocytes despite low levels of TNFα production. Signalling components of the IL-10R signalling pathway were investigated to provide a possible explanation for the differences found in IL-10 response between monocyte subsets. These included IL-10Rα expression, STAT3 availability and phosphorylation, and *SOCS3* mRNA expression. IL-10Rα expression was highest in intermediate monocyte and lowest in classical monocytes, demonstrating that receptor expression was a poor indicator of the ability of IL-10 to inhibit pro-inflammatory cytokine production in the different subsets. Classical and intermediate monocytes displayed equally high levels of STAT3, while non-classical monocytes displayed lower levels of STAT3, which correlated well with levels of STAT3 phosphorylation upon IL-10 stimulation. This may explain why classical monocytes are more responsive to IL-10 than non-classical monocytes but does not explain the difference between classical and intermediate monocytes. Classical monocytes also expressed higher levels of *SOCS3* at steady-state than both intermediate and non-classical monocytes, as determined by qRT-PCR, which may provide another mechanism to explain their enhanced response to IL-10. This sensitivity to IL-10 may be particularly important in the intestine where regulatory signals must control recruited classical monocytes to limit their activation by commensal bacteria.

4.2 Introduction

Most of our current knowledge about the role of monocytes and their subsets come from studying mice. However, striking similarities shown in gene expression analysis and expression of surface markers between monocyte subsets in mice and humans suggests one can draw parallels between their functions (Ingersoll et al. 2010; Geissmann et al. 2003). In brief, Ly6C^{hi} cells in mice are analogous to classical monocytes (CD14++CD16+) in humans, as are Ly6C^{lo} cells to non-classical monocytes (CD14+CD16++). The equivalent of intermediate monocytes has had little interest in mice, and as a consequence, not much is known about the role of these cells. In mice and now humans, it has been convincingly shown that the subsets of monocytes are not isolated populations, instead they represent stages of differentiation, where a small proportion of classical monocytes differentiate into intermediate monocytes, and finally non-classical monocytes (Patel et al. 2017; Yona et al. 2013; Sunderkotter et al. 2004). Ly6C^{hi} cells at least in part maintain the intestinal Mϕ pool during steady-state, which has been shown to be CCR2-dependent (Bain et al. 2014; Takada et al. 2010; Yona et al. 2013). In humans, classical monocytes highly express CCR2, and therefore are likely to perform similar roles (Appleby et al. 2013; Thiesen et al. 2014; Patel et al. 2017). Ly6C^{lo} cells remain in the bloodstream and 'patrol' the endothelial wall, where CX_3CR1 expression is critical in this role as well as rapid tissue invasion at the site of an infection (Ancuta et al. 2003; Auffray et al. 2007); non-classical monocytes in humans express a high level of CX_3CR1 (Cros et al. 2010; Geissmann et al. 2003; Thiesen et al. 2014). Previous studies have shown that classical and intermediate monocytes are efficient producers of pro-inflammatory cytokines upon stimulation with LPS, which was not seen in non-classical monocytes (Belge et al., 2002; Cros et al., 2010; Thiesen et al., 2014). It is critical that the inflammatory properties of the newly arrived monocytes are controlled as they differentiate into regulatory Mϕs, which have been shown to play a critical role in maintaining steady-state in the intestine (Bain et al. 2013; Takada et al. 2010). The signals required for this process remain elusive but both IL-10 and TGFβ have been shown to have important non-redundant roles (Zigmond et al. 2014; Shouval et al. 2014; Smythies et al. 2005).

IL-10 is an important suppressor of inflammation. Mice and humans with deficiency in IL-10 or IL-10 signalling components develop severe inflammation early in life (Begue et al. 2011; Gasche et al. 2003; Glocker & Kotlarz 2009; Grundtner et al. 2009; Kühn et al. 1993; Shouval et al. 2014; Zigmond et al. 2014). The IL-10R is made up of two subunits: the alpha chain which facilitates specific binding of IL-10, and the beta chain which is important for signal transduction (Kotenko et al. 1997). Upon activation of the IL-10R, proximal signalling events trigger a phosphorylation cascade involving JAK1, TYK2, and STAT3 (Riley et al. 1999). The p-STAT3 dimerise and translocate to the nucleus, where they regulate gene expression to bring about immune regulation (Donnelly et al. 1999), and therefore STAT3 phosphorylation is often used as a marker of IL-10R activity.

STAT3 has been shown to be critical in both IL-10 and IL-6 signalling using Cre-loxP recombination systems to show that IL-10 and IL-6 fail to induce a response in cells deficient in STAT3 (Akira 2000). However, it is not clear how activation of STAT3 with IL-10 causes inhibition of inflammatory responses, while IL-6 induces pro-inflammatory responses. A study by Yasukawa et al. 2003 suggests that SOCS3, induced by IL-10, is a key regulator of the divergent actions by selectively blocking signalling via IL-6. SOCS3 performs suppressive roles, such as inhibiting the NFkB pathway, as well as establishing a feedback loop to suppress further IL-10 signalling. LoupeTM cell browser (10X genomics) enables easy visualisation and analysis of 10x ChromiumTM Single Cell 5' and 3' gene expression data. The monocyte subsets were identified on the basis of CD14 and CD16 gene expression. Expression levels of selective genes along the IL-10R pathway were analysed in the monocyte subsets. *SOCS3* was the only gene that showed significantly different expression levels between the monocyte subsets; classical monocytes showed the highest *SOCS3* expression, followed by intermediates, and finally non-classical monocytes (Appendix 5).

The aim of the work described in this chapter was to determine the IL-10 responsiveness of monocyte subsets in healthy individuals. Signalling components of the IL-10R signalling pathway were measured to examine their relationship with the functional response to IL-10.

4.3 Aims

To:

4. Determine the ability of IL-10 to inhibit LPS-induced TNFα production in the monocyte subsets of healthy individuals.
5. Identify the mechanistic basis of the differences between monocyte subsets by investigating the relationship between components of the IL-10 signalling pathway and TNFα inhibition.
6. Investigate the specificity of the subset difference in IL-10 response with respect to both modes of activation and cytokine read-out.

4.4 Results

4.4.1 Classical monocytes are most responsive to IL-10 inhibition in healthy individuals

The response of monocyte subsets to LPS stimulation was compared in eight healthy individuals. PBMCs were stimulated with 1ng/ml LPS for three hours before staining for intracellular TNFα. TNFα production was quantified as a percentage of cells positive for TNFα and as the level of expression on a per cell basis, assessed as MFI. A significantly ($p = 0.0183$) higher percentage of intermediate monocytes produce TNFα than classical monocytes (Figure 4.1 A). Fewer non-classical monocytes produced TNFα in response to LPS when compared to either classical ($p = 0.0002$) and intermediate monocytes ($p < 0.0001$). The level of TNFα production (MFI) in the TNFα positive cells was significantly higher in intermediate monocytes than classical ($p = 0.0132$) and non-classical ($p = 0.0063$) monocytes. The level of TNFα production in classical monocytes was significantly higher than non-classical monocytes ($p = 0.0457$) (Figure 4.1 B).

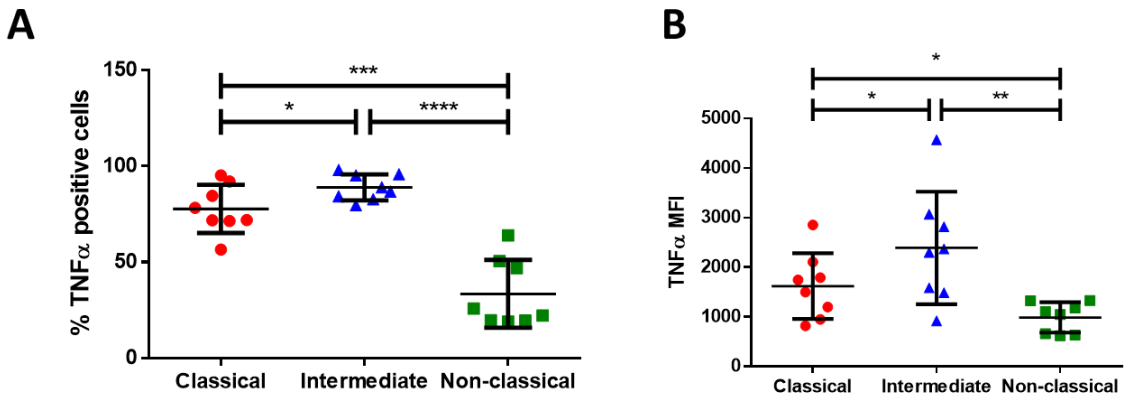

Figure 4.1: LPS-induced TNFα production in the monocyte subsets. PBMCs from healthy individuals (n=8) were stimulated with 1ng/ml LPS for three hours in the presence of monensin and ADAM17 inhibitor (TMI-005). The PBMCs were then labelled with anti-HLA-DR, anti-CD14, and anti-CD16 antibodies to distinguish the monocytes subsets, fixed, permeabilised and stained intracellularly for TNFα before acquiring on the flow cytometer. **A)** TNFα production was quantified as a percentage of cells positive for TNFα and **B)** level of expression on a per cell basis, assessed as MFI. Mean values and SD displayed. Data were analysed statistically by RM one-way ANOVA. $p < 0.05$* $p < 0.01$** $p < 0.001$*** $p < 0.0001$****.

The response of monocyte subsets to IL-10 was compared in eight healthy individuals. Responses to IL-10 were measured by determining the inhibitory effect of IL-10 on LPS-induced TNFα production. PBMCs were stimulated with 1ng/ml LPS in the presence or absence of increasing concentrations of IL-10 (0.016-10ng/ml IL-10), for three hours before staining for intracellular TNFα. Dose-response curves can be created, in which the percentage of cells positive for TNFα are reduced with increasing concentration of IL-10. These dose-response curves were compared between monocyte subsets (Figure 4.2A). A high proportion of classical and intermediate monocytes produced TNFα in response to LPS stimulation, whereas a smaller proportion of non-classical monocytes are stimulated to produce TNFα. Addition of between 0.016 and 0.4ng/ml IL-10 had no noticeable effect on TNFα production by all three subsets. With further increases in IL-10 concentration, TNFα production was inhibited. Visual inspection of dose-response curves indicated greater IL-10 inhibition of TNFα production by classical monocytes than by the intermediate cells, and non-classical monocytes showed the lowest response to IL-10. Although TNFα production by non-classical monocytes was lower than in the other two

subsets, this production was maintained in the presence of IL-10. As a result, TNFα production by non-classical monocytes was equivalent to that of the other two subsets at 10ng/ml IL-10.

These differences were quantified more formally in two ways. Firstly, the concentration of IL-10 at which the frequency of TNFα producing cells was inhibited by 50% (effective dose 50/ED50) was calculated for each subset using MyCurveFit software. By this measure, classical monocytes required the lowest concentration of IL-10 to reach 50% inhibition of TNFα producing cells, followed by intermediate monocytes, and non-classical monocytes required the greatest mean concentration (Figure 4.2 C). However, formal statistical analysis of these data was problematic because in non-classical and intermediate monocytes from some donors, 50% inhibition of TNFα production was not reached even at 10ng/ml IL-10, the highest concentration tested. Therefore, as an alternative approach, the percentage of inhibition at 2ng/ml IL-10 was used to compare monocyte subsets and carry out statistical analysis. At this concentration of IL-10, TNFα production by classical monocytes was significantly more inhibited than production by intermediate ($p = 0.0090$) and non-classical ($p < 0.0001$) monocytes. TNFα production by intermediate monocytes was significantly more inhibited than non-classical monocytes ($p = 0.0466$) (Figure 4.2 C).

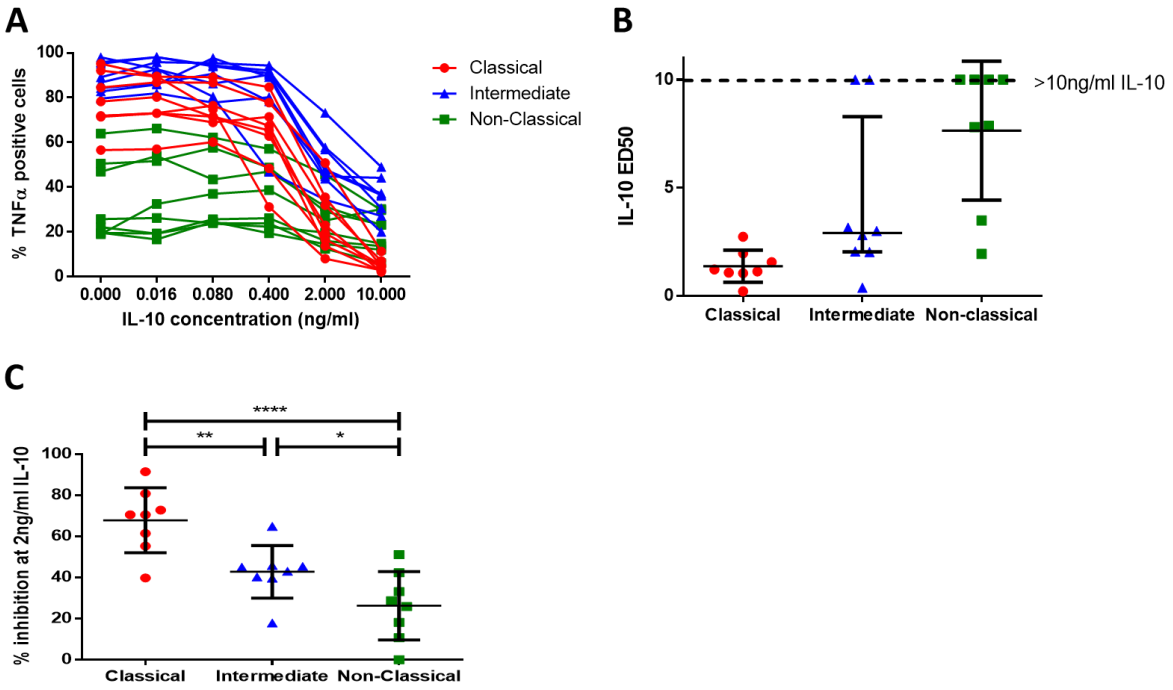

Figure 4.2: IL-10 responsiveness of monocyte subsets in health. PBMCs from healthy individuals (n=8) were stimulated with 1ng/ml LPS and increasing concentrations of IL-10 (0.016-10ng/ml) for three hours in the presence of monensin and ADAM17 inhibitor (TMI-005). PBMCs were then labelled with anti-HLA-DR, anti-CD14, and anti-CD16 antibodies to distinguish the monocytes subsets, fixed, permeabilised and stained intracellularly for TNFα before acquiring on the flow cytometer. The resulting dose-response curves were compared between the monocyte subsets. **A)** TNFα production was quantified as a percentage of cells positive for TNFα and plotted along increasing concentrations of IL-10. **B)** the ED50 was calculated for each monocyte subset. Intermediate and non-classical monocytes from some donors did not reach 50% inhibition of TNFα production at 10ng/ml IL-10, the highest concentration tested, therefore, statistical analysis of these data was not conducted. Median and IQR are displayed. **C)** percentage inhibition of TNFα production at 2ng/ml IL-10 was used to carry out statistical analysis on. Mean values and SD displayed. Data were analysed statistically by RM one-way ANOVA. $p < 0.05$* $p < 0.01$** $p < 0.001$*** $p < 0.0001$****.

Although all three subsets were assayed in parallel within whole PBMCs, and therefore exposed to the same assay environment, it was a theoretical possibility that autocrine IL-10 signalling could contribute to differences in IL-10 response by effectively increasing the local concentration active on some subsets. Indeed, endogenous IL-10 production and an increase in IL-10 production upon LPS stimulation in the monocytes has previously been observed (Malefyt et al., 1991) but individual subsets were not studied. To address this question in our system, endogenous as well as LPS-induced (1ng/ml for 3 hours) IL-10 production in the monocyte subsets was measured via intracellular staining in the same eight healthy individuals. IL-10 production was quantified as a percentage of cells positive for IL-10 and as the level of expression on a per cell basis, assessed as MFI.

A significantly higher proportion of classical monocytes produced IL-10 in steady-state than both intermediates ($p < 0.0001$) and non-classical ($p < 0.0001$) monocytes but there was no difference between intermediate and non-classical monocytes ($p = 0.3729$) (Figure 4.3 B). Upon LPS stimulation, IL-10 production was significantly increased in classical monocytes ($p = 0.0016$) and intermediate monocytes ($p = 0.0215$), but not non-classical monocytes ($p = 0.6355$) (Figure 4.3 C, D).

Taken together, these data suggest that IL-10 production by classical monocytes could contribute to their high responsiveness to the inhibitory effects of added cytokine by increasing the amount of IL-10 in the culture. However, a parallel assessment of monocyte subsets within the same culture and environment is likely to minimise the impact of subset-specific autocrine effects. Moreover, the differential effect of exogenous IL-10 on intermediate and non-classical monocytes cannot be explained by a difference in their ability to produce IL-10.

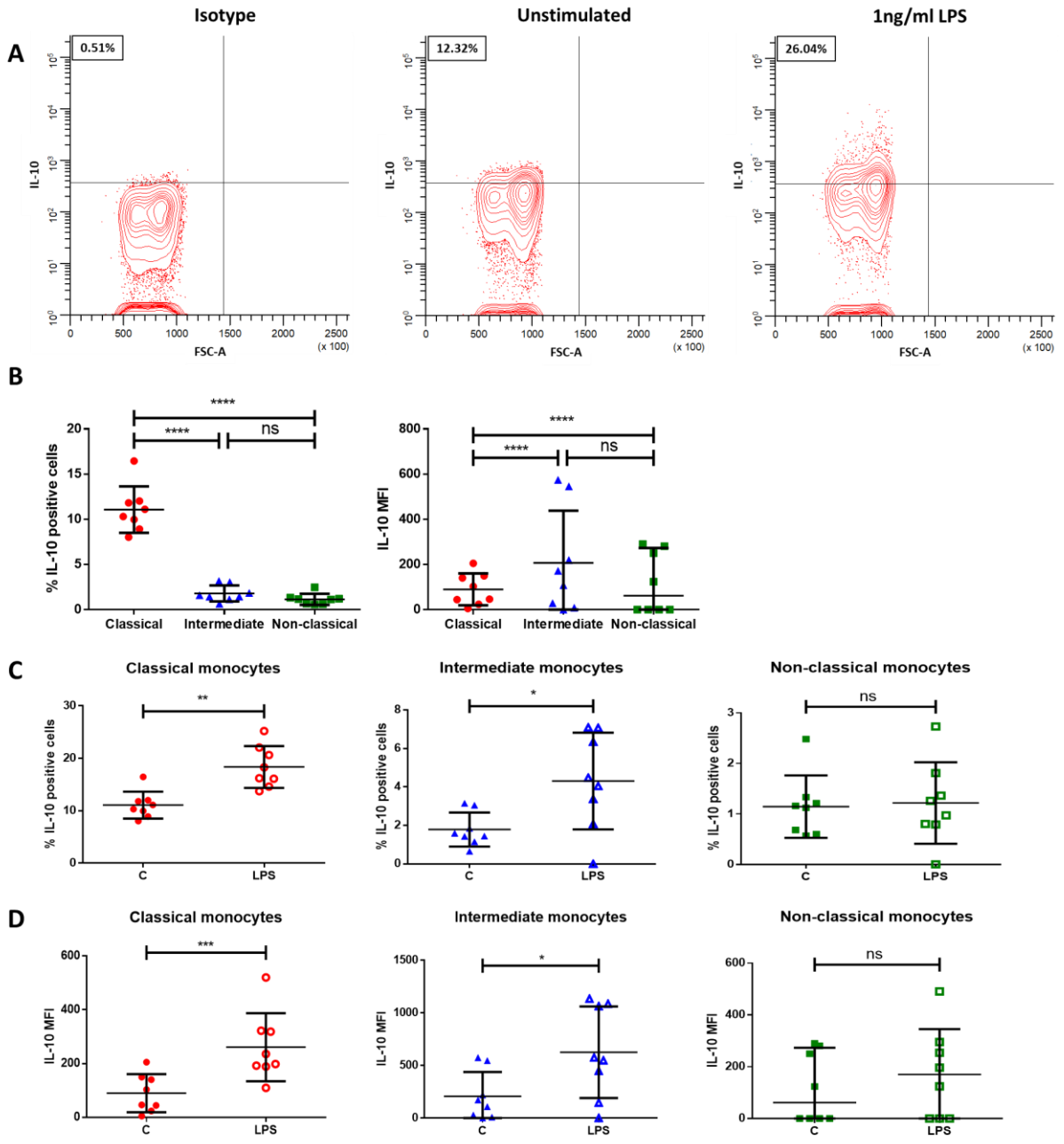

Figure 4.3: Endogenous and LPS-induced IL-10 production in the monocyte subsets in health. PBMCs from healthy individuals (n=8) were stimulated with 1ng/ml LPS for three hours in the presence of monensin and ADAM17 inhibitor (TMI-005). PBMCs were then labelled with anti-HLA-DR, anti-CD14, and anti-CD16 antibodies to distinguish the monocytes subsets, fixed, permeabilised and stained intracellularly for IL-10 before acquiring on the flow cytometer. **A)** representative flow cytometry plots of IL-10 production in classical monocytes. IL-10 production was quantified as a percentage of cells positive for IL-10 and as the level of expression on a per cell basis, assessed as MFI. **B)** IL-10 production by monocytes subsets in the absence of stimulation. Mean values and SD displayed. Data were analysed statistically by RM one-way ANOVA. **C, D)** IL-10 production by monocytes subsets in LPS-stimulated cultures. Mean values and SD displayed. Data were analysed statistically by paired t-test. $p < 0.05$* $p < 0.01$** $p < 0.001$*** $p < 0.0001$****.

4.4.2 Monocyte subset response to IL-10 is independent of TLR agonist and readout

The next step was to determine if the differences in IL-10 response between monocyte subsets was dependent on the stimulus and/or readout (cytokine) measured. LPS engagement with TLR4 results in signalling down two pathways involving distinct adaptor molecules: MyD88 and TRIF (Lu et al. 2008). LPS was compared with two stimulants chosen to target these pathways: Pam_3CSK_4 triggers the MyD88 pathway, while Poly(I:C) activates TRIF. TNFα production was also compared to two readouts: IL-1β and IFNα induced predominately by MyD88 and TRIF pathways respectively (Akira & Takeda 2004). Cytokine production was measured as a percentage of cells positive for the cytokine and as the level of expression on a per cell basis, assessed as MFI. Healthy PBMCs (n=7) were stimulated with 1ng/ml LPS, 1000ng/ml Pam_3CSK_4, or 1000ng/ml Poly(I:C) and increasing concentrations of IL-10 (0.4-10ng/ml IL-10) for three hours before staining for TNFα, IFNα, and IL-1β intracellularly. Percentage inhibition at 2ng/ml IL-10 was used to compare the responses as ED50 had limited sensitivity.

A significantly greater proportion of intermediate monocytes produced TNFα than classical and non-classical monocytes irrespective of the TLR agonist used for stimulation (Figure 4.4 A). Significantly more classical monocytes than non-classical monocytes produced TNFα in response to both LPS and Poly(I:C) stimulation but not in response to Pam_3CSK_4. LPS induced the greatest proportion of TNFα producing cells in all three monocytes subsets, despite using a concentration 1000x lower (Figure 4.4 A). Poly(I:C) induced a greater proportion of TNFα producing classical and intermediate monocytes, but not non-classical monocytes, than were induced by Pam_3CSK_4 at the same concentration.

Overall IFNα responses were low compared with production of the other cytokines. Upon LPS stimulation, more classical and intermediate monocytes than non-classical monocytes produced IFNα. The low level of IFNα production following Poly(I:C) and Pam_3CSK_4 stimulation was not sufficient to allow differences between subsets to be determined (Figure 4.4B). In contrast, almost all classical and intermediate monocytes produced IL-1β irrespective of the agonist used. Significantly fewer non-

classical monocytes produced IL-1β in response to all stimuli and the response to Poly(I:C) was significantly lower than to either LPS or Pam_3CSK_4 (Figure 4.4 C).

The per cell level of cytokine production (MFI) in the cytokine positive cells was also determined in an attempt to improve sensitivity when the percentage of cells producing cytokine approaches 100%. Although the frequency of classical and intermediate monocytes producing IL-1β was similar (Figure 4.4A), the MFI of intermediate monocytes was significantly higher irrespective of stimulus (Figure 4.4B). This approach also revealed that LPS induced a greater IL-1β response than either of the other two stimuli in all monocyte subsets (Figure 4.4B)

The degree to which each response was inhibited by addition of 2ng/ml IL-10 was calculated. The clearest differences between monocytes subsets with regard the inhibitory effects of IL-10 were observed when TNFα production was the read-out (Figure 4.4 C). Using this measure, IL-10 responsiveness of non-classical monocytes was significantly lower than that of classical monocytes for all three stimuli tested. The response of intermediate cells was more similar to that of non-classical monocytes with Poly(I:C), to classical monocytes with Pam_3CSK_4, or as previously noted, intermediate between the two other subsets with LPS. Differences between monocyte subsets with regard to response to IL-10 were less when measuring IL-1β or IFNα production as read-outs. This may because the there is less resolving power when cytokine production is very high (IL-1β) or very low (IFNα); the intermediate TNFα response offers a greater resolution. Nonetheless, when measuring IL-1β, the response of non-classical monocytes to IL-10 was significantly lower than either subset.

In summary, intermediate monocytes are the greatest producers of TNFα and IL-1β with the TLR agonists tested, followed by classical and then non-classical monocytes. IFNα production was too low using all agonists to enable clear conclusions about monocyte subsets to be drawn. When measuring TNFα production, the hierarchy of monocyte subset response to IL-10 inhibition was broadly similar irrespective of stimulation and consistently lower in non-classical monocytes. An intermediate level of cytokine production provides more sensitivity for resolving differences between subsets.

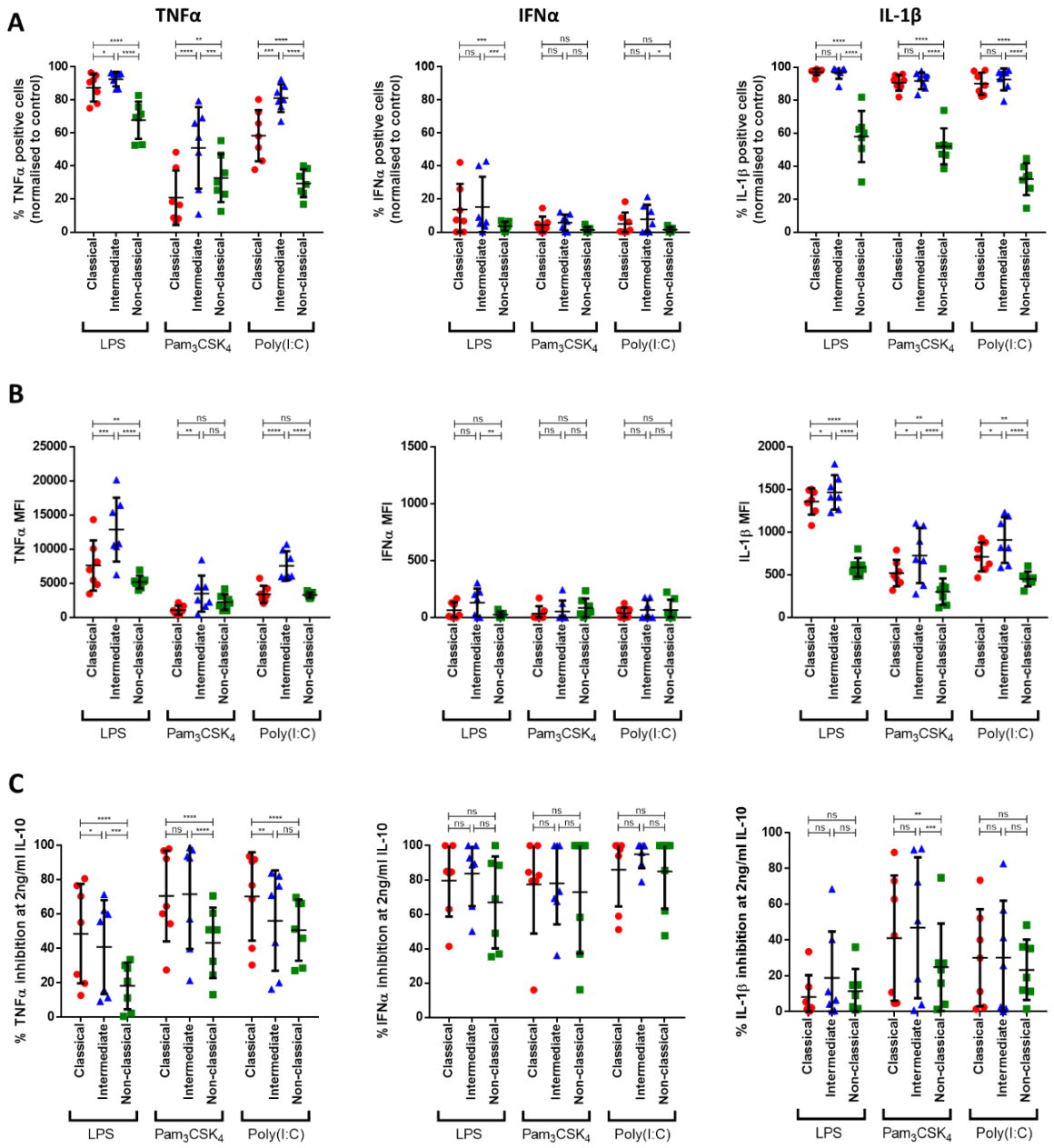

Figure 4.4: Monocyte subset responsiveness to IL-10 with various TLR agonists and readouts. PBMCs from healthy individuals (n=7) were stimulated with 1ng/ml LPS, 1000ng/ml Pam_3CSK_4, or 1000ng/ml Poly(I:C) and increasing concentrations of IL-10 (0.4-10ng/ml) for three hours in the presence of monensin and ADAM17 inhibitor (TMI-005). The PBMCs were then labelled with anti-HLA-DR, anti-CD14, and anti-CD16 antibodies to distinguish the monocytes subsets, fixed, permeabilised and stained intracellularly for TNFα, IFNα, and IL-1β before acquiring on the flow cytometer. **A)** the proportion of TNFα, IFNα, and IL-1β producing cells with various TLR agonists for each monocyte subset. **B)** the level of cytokine expression on a per cell basis (MFI) with various TLR agonists for each monocyte subset. **C)** inhibition of TNFα, IFNα, and IL-1β production at 2ng/ml IL-10 with various TLR ligand for each monocyte subset. Mean and SD is displayed. Data were analysed statistically by a Two-way ANOVA. $p < 0.05$* $p < 0.01$** $p < 0.001$*** $p < 0.0001$****.

4.4.3 Intermediate monocytes have the highest IL-10Rα expression

The IL-10R is made up of two subunits: the alpha chains that facilitate specific binding of IL-10, and the beta chains which are important in signal transduction. The beta chains appear in other cytokine receptors including IL-22 and IFN-λ (reviewed by Moore et al. 2001), therefore, labelling for IL-10Rα enables the measurement of IL-10R expression specifically. Expression of IL-10Rα, the specific ligand binding component of IL-10R was measured on the individual monocyte subsets to determine the relationship between receptor expression and functional response to IL-10. The monocyte subsets from 15 healthy donors were labelled for IL-10Rα in whole blood to minimise isolation related changes. Receptor expression was quantified as percentage positive cells and MFI calculated as MFI for staining with anti-IL-10Rα antibody minus MFI for staining with an isotype-matched control antibody.

Both the and proportion of IL-10Rα positive cells and level of IL-10Rα expression (MFI) differed between monocyte subsets (Figure 4.5 B, C). The proportion of IL-10Rα expressing cells was significantly higher in intermediate monocytes than in classical monocytes ($p < 0.0001$) and non-classical monocytes ($p < 0.0001$), and comparable between classical and non-classical monocytes ($p = 0.1994$) (Figure 4.5 B). The level of IL-10Rα expression was significantly higher on intermediate monocytes than on either classical ($p < 0.0001$) or non-classical ($p < 0.0001$) monocytes; non-classical monocytes expressed significantly higher levels of IL-10Rα than classical monocytes ($p = 0.0370$) (Figure 4.5 C). These data suggest that IL-10Rα expression level is a poor predictor of the ultimate functional response to IL-10 in the monocyte subsets.

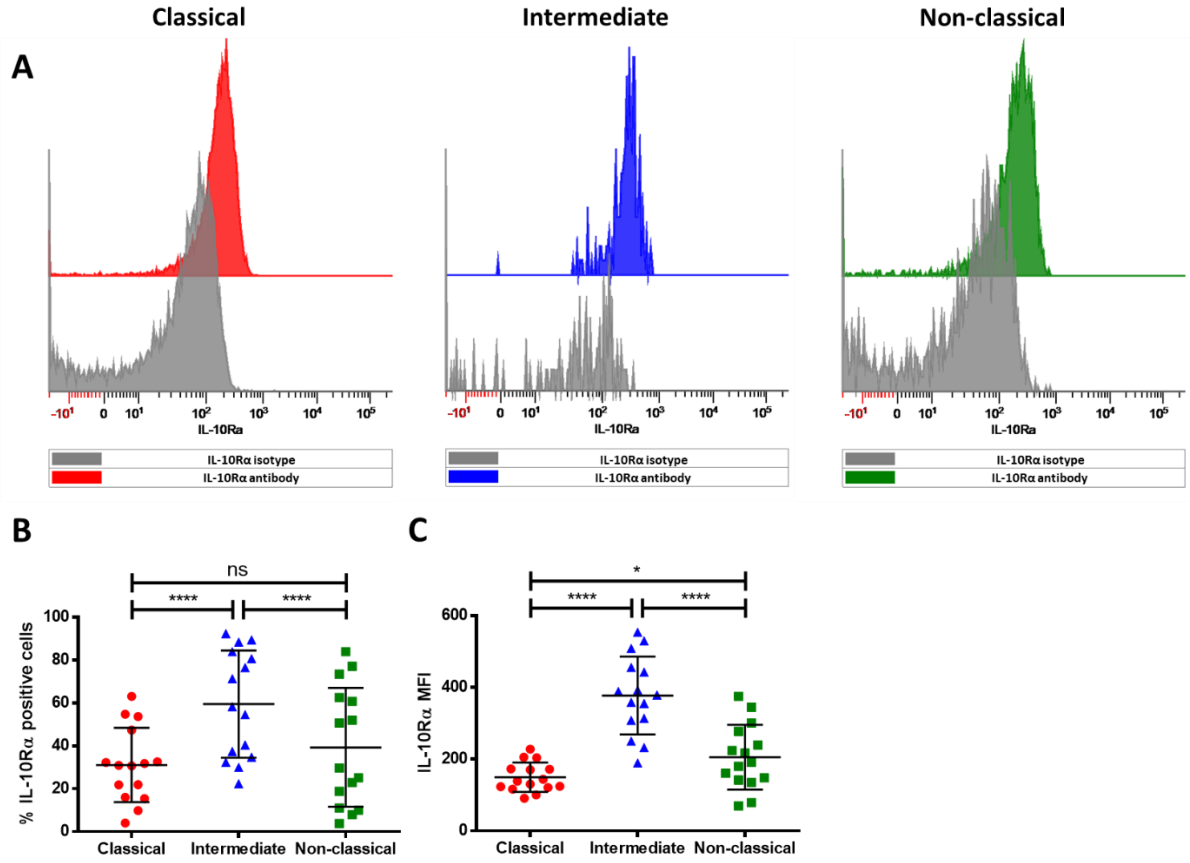

Figure 4.5: IL-10Rα expression on the monocyte subsets in health. Whole blood from healthy donors (n=15) were labelled with anti-HLA-DR, anti-CD14, and anti-CD16 antibodies to distinguish the monocyte subsets, and IL-10Rα before acquiring on the flow cytometer. **A)** representative histograms for the expression of IL-10Rα on each monocyte subset. The coloured histograms represent anti-IL-10Rα staining for each monocyte subset (classical, intermediate, and non-classical) in relation to the corresponding isotype-matched control (grey histogram). IL-10Rα expression was calculated as **B)** percentage of cells positive for IL-10Rα and **C)** MFI calculated as MFI for staining with anti-IL-10Rα antibody minus MFI for staining with an isotype-matched control antibody for each monocyte subset. Mean values and SD displayed. Data were analysed statistically by RM one-way ANOVA. $p < 0.05$* $p < 0.01$** $p < 0.001$*** $p < 0.0001$****.

4.4.4 STAT3 availability and STAT3 phosphorylation in response to IL-10 are lower in non-classical monocytes

As mentioned above, the response of monocytes subsets to IL-10 did not correlate with their IL-10Rα expression. This led to investigations into the relationship between the availability of STAT3 and level of STAT3 phosphorylation in the individual monocyte subsets and how this relates to the functional response to IL-10. PBMCs from 10 healthy donors were stimulated with 100ng/ml of IL-10 for 15min before fixing and staining intracellularly for total (T-STAT3) and for p-STAT3 (p-STAT3) p-STAT3 using an antibody that binds specifically to STAT3 phosphorylated on Y705. T-STAT3 and p-STAT3 was quantified as a percentage of cells positive and MFI calculated as MFI for staining with anti-STAT3 and -p-STAT3 antibody minus MFI for staining with an isotype-matched control antibody.

The percentage of cells positive for T-STAT3 and the level of STAT3 available (MFI) was comparable for classical and intermediate monocytes but lower in non-classical monocytes ($p < 0.0001$ versus classical monocytes; $p = 0.0022$ versus intermediate monocytes) (Figure 4.6 C). Reassuringly, there was minimal background STAT3 phosphorylation in cells not exposed to IL-10 (data not shown). Following IL-10 stimulation p-STAT3 was detected. The percentage of cells positive for p-STAT3 upon IL-10 stimulation was equally high in classical and intermediate monocytes but was significantly lower than both of these in non-classical monocytes ($p = 0.0016$ versus classical monocytes; $p = 0.0054$ versus intermediate monocytes) (Figure 4.6 D). These differences were reflected in MFI. Therefore, across the monocyte subsets, the level of p-STAT3 in response to IL-10 correlates with the availability of STAT3 within the cell but not IL-10 response.

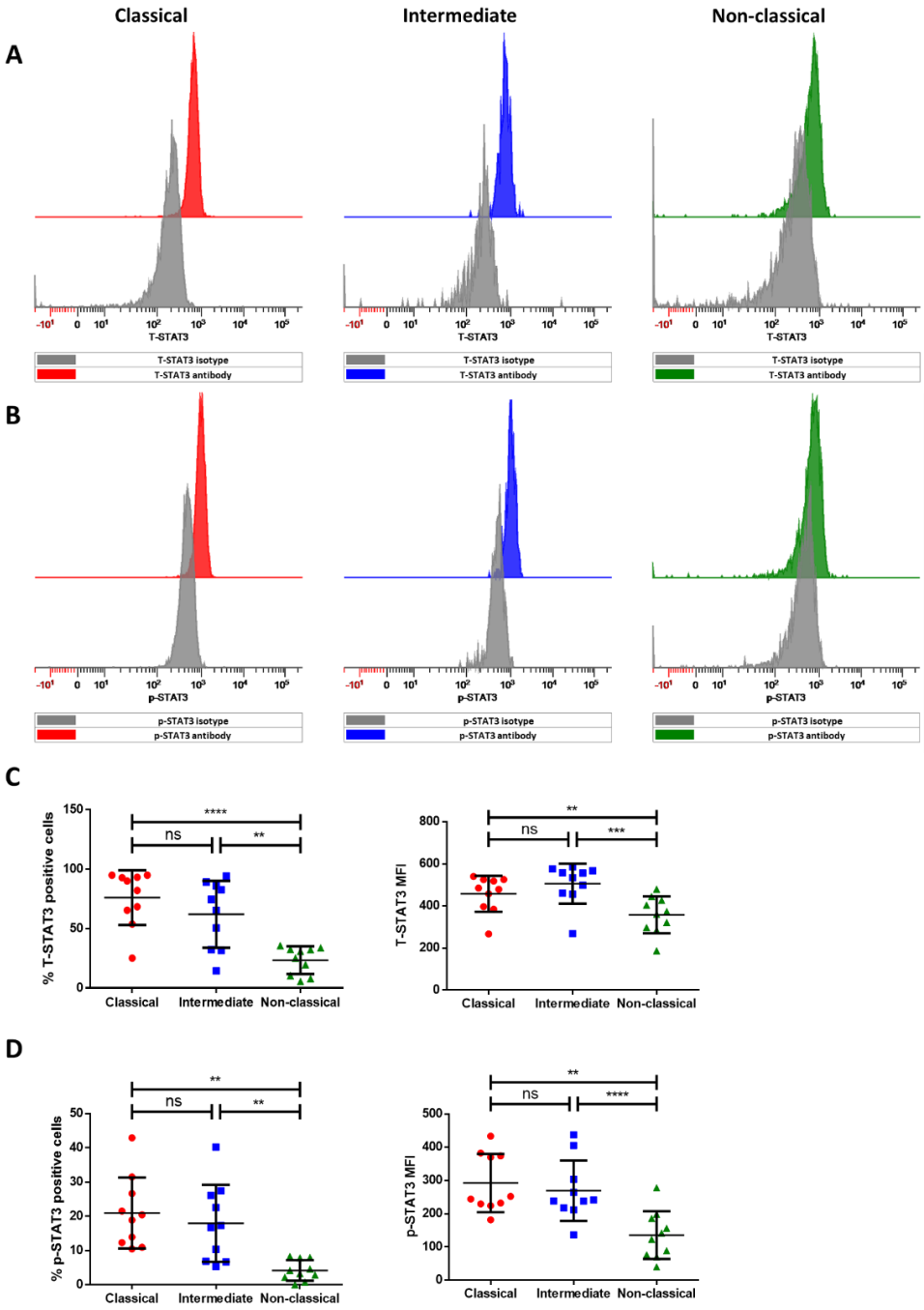

Figure 4.6: STAT3 availability and phosphorylation levels upon IL-10 stimulation in monocyte subsets in health. PBMCs from healthy donors (n=10) were labelled with anti-HLA-DR, anti-CD14, and anti-CD16 antibodies to distinguish the monocyte subsets. PBMCs were stimulated with 100ng/ml IL-10 before fixation, permeabilisation and intracellular staining for STAT3 and p-STAT3. Samples were then acquired on the flow cytometer. Representative histograms for the expression of **A)** T-STAT3 **B)** p-STAT3 for each monocyte subset. The overlays represent staining with anti-STAT3 and -p-STAT3 respectively for each monocyte subset (classical, intermediate, and non-classical) in relation to their corresponding isotype-matched control antibody (grey histogram). **C, D)** expression of STAT3 and p-STAT3 was calculated as a percentage of positive cells and MFI calculated as MFI for staining with anti-STAT3 and -p-STAT3 antibody minus MFI for staining with an isotype-matched control antibody. Mean values and SD displayed. Data were analysed statistically by RM one-way ANOVA. $p < 0.05$* $p < 0.01$** $p < 0.001$*** $p < 0.0001$****.

To further explore the relationship between low T-STAT3 in non-classical monocytes and their ability to phosphorylate STAT3 in responses to appropriate stimuli, their response to IL-6, a second cytokine that induces STAT3 phosphorylation, was tested. PBMCs from seven healthy donors were stimulated with 100ng/ml IL-6 for 15min before fixing and staining intracellularly for p-STAT3. STAT3 phosphorylation was quantified as a percentage of cells positive for p-STAT3 and MFI calculated as MFI for staining with anti-p-STAT3 antibody minus MFI for staining with an isotype-matched control antibody. Again, there was minimal background STAT3 phosphorylation in the absence of stimulation (data not shown). Following stimulation with IL-6, the proportion of p-STAT3 positive non-classical monocytes was significantly lower than both classical and intermediate monocytes ($p = 0.0011$ and $p = 0.0006$ respectively; Figure 4.7A), which was also reflected in MFI (Figure 4.7B). This is consistent with a causal link between low T-STAT3 in non-classical monocytes and low capacity to phosphorylate STAT3. Interestingly, although the ability to phosphorylate STAT3 in response to IL-10 was similar in classical and intermediate monocytes, they differed in their response to IL-6. There was greater p-STAT3 in response to IL-6 in classical than intermediate monocytes, despite similar levels of T-STAT3. This does not follow the same pattern of STAT3 phosphorylation induced with IL-10. Additional factors are likely to regulate IL-6 mediated STAT3 phosphorylation in these subsets.

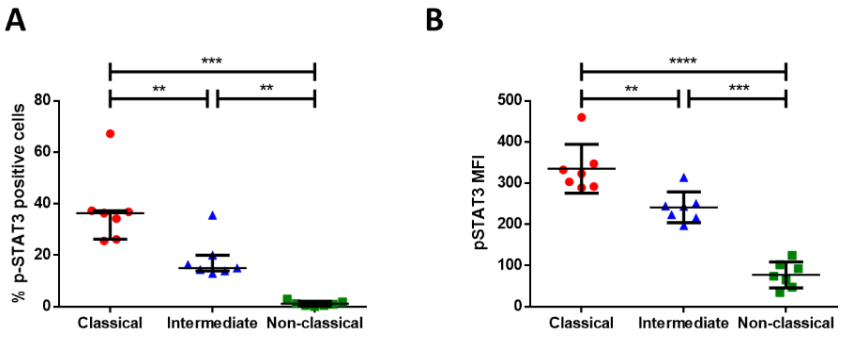

Figure 4.7: p-STAT3 upon IL-6 stimulation. Health PBMCs (n=7) were labelled with anti-HLA-DR, anti-CD14, and anti-CD16 antibodies to distinguish the monocyte subsets. PBMCs were stimulated with 100ng/ml IL-6 before fixation, permeabilisation and intracellular staining for STAT3 and p-STAT3. Samples were then acquired on the flow cytometer. **A)** STAT3 phosphorylation was calculated as a percentage of cells positive for p-STAT3. Median and IQR displayed. Data were analysed statistically by Friedman test. **B)** MFI calculated as MFI for staining with anti-p-STAT3 antibody minus MFI for staining with an isotype-matched control antibody. Mean values and SD displayed. Data were analysed statistically by RM one-way ANOVA. $p < 0.05$* $p < 0.01$** $p < 0.001$*** $p < 0.0001$****.

4.4.5 *SOCS3* expression is highest in classical monocytes

SOCS3 has been shown to be a critical component in the IL-10R signalling pathway (Yasukawa et al. 2003), and *SOCS3* was the only gene along the IL-10R pathway that showed significantly higher expression levels in classical monocytes in a recent single-cell RNA sequencing analysis (10X genomics). To verify this, expression levels of *SOCS3* mRNA were measured in the monocyte subsets. PBMCs from 14 healthy donors were labelled with anti-HLA-DR, anti-CD14, and anti-CD16 antibodies to distinguish the monocyte subsets before sorting on the FACS Aria (BD). 100,000 cells were sorted for each population, and the relative gene expression of *SOCS3* at resting level was measured using quantitative RT-PCR. *SOCS3* expression in classical monocytes was significantly higher than in both intermediate and non-classical monocytes ($p = 0.0422$ and $p = 0.0249$ respectively). Intermediate and non-classical monocytes did not differ in their expression of *SOCS3*. Higher expression of *SOCS3* in classical monocytes may contribute to their enhanced response to IL-10.

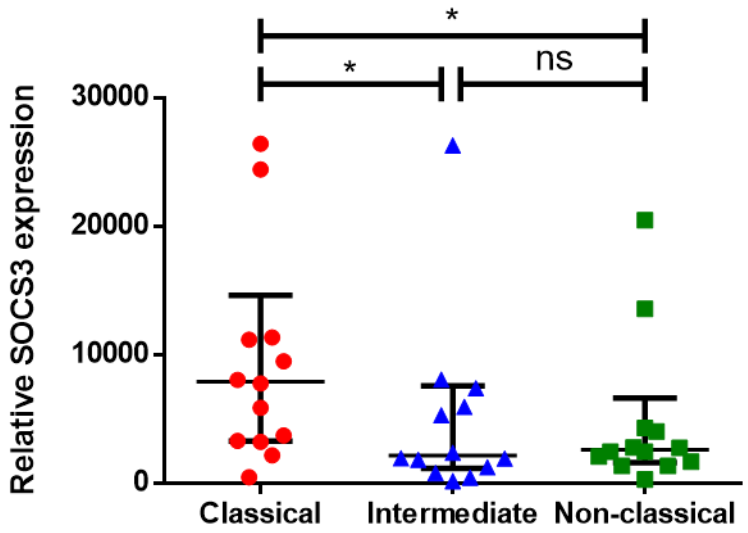

Figure 4.8: *SOCS3* mRNA expression in monocyte subsets in health. PBMCs from healthy donors (n=14) were labelled with anti-HLA-DR, anti-CD14, and anti-CD16 antibodies to distinguish the monocyte subsets before sorting on the FACS Aria (BD). 100,000 cells were sorted for each population, and the relative gene expression of *SOCS3* at baseline was measured using qRT-PCR. Median and IQR are displayed. Data were analysed statistically by Friedman test. $p < 0.05$* $p < 0.01$** $p < 0.001$*** $p < 0.0001$****.

4.5 Discussion

The primary aim of this chapter was to determine IL-10 responsiveness of monocyte subsets in healthy individuals. First, LPS-induced TNFα production was measured. Intermediate monocytes showed greater TNFα production than classical monocytes, and non-classical monocytes showed the least TNFα production. The ability of IL-10 to inhibit this TNFα response was greatest in classical monocytes, followed by intermediates, and least responsive were the non-classical monocytes despite low levels of TNFα production. Signalling components along the IL-10R signalling pathway were measured to examine their relationship with the functional response to IL-10.

In this chapter, there was no TNFα detected by intracellular staining in the unstimulated monocyte subsets. This is in agreement with the work of Cros et al., 2010, who reported a lack of secreted TNFα in unstimulated cultures of monocytes. However, Theisen et al., 2014 reported secretion of TNFα in unstimulated cultures of all three subsets. Cros et al., 2010 and Theisen et al., 2014 both measured TNFα secretion using supernatants, which requires separation of the subsets to enable the source of cytokines to be defined. Depending on the method of separation, this could result in unintended activation of the cells. Cros et al., 2010 used magnetic beads that are designed to avoid activation of monocytes, whereas Theisen et al., 2014 used FACS separation, which as described in the previous chapter can cause activation of the cells. Culturing the monocyte subsets separately also risks exposing them to distinct environments created by their own products. An additional limitation, culturing the monocytes subsets in the absence of other immune cells blocks their interactions, which is not representative of the immune diversity in the bloodstream.

LPS-induced TNFα production in monocytes subsets has been previously investigated. The results in this chapter show that intermediate monocytes have the highest TNFα production, followed by classical monocytes, and least responsive to TLR4 activation are the non-classical monocytes. CD14 is a co-receptor for TLR4 (Beutler et al., 2000), therefore, its expression may explain the more robust LPS response in $CD14^{hi}$ monocytes. A greater proportion of intermediate monocytes produce TNFα than

classical monocytes, which may be due to the synergistic role of CD16 in CD14 signalling (Shalova et al. 2017). Although non-classical monocytes are more refractory to LPS stimulation, they do still retain some capacity to respond. This may be partly because non-classical monocytes still express low levels of CD14 as they mature from classical monocytes and/or due to the soluble CD14 reported to be present in FCS (Yang et al. 1996). A study that also measured intracellular TNFα showed a hierarchy of LPS response in classical monocytes and intermediate monocytes that is similar to the findings in this chapter except no TNFα production was detected in non-classical monocytes (Belge et al., 2002). Theisen et al., 2014 reported comparable levels of TNFα secretion by classical and intermediate monocytes, which is not consistent with the findings in this chapter. There are a number of possible explanations for this difference. Cytokine secretion may not correlate with levels of production detected by intracellular staining as secretory pathways can be independently regulated, for example cleavage of TNFα from the cell surface by ADAM17 may be regulated independently of production. Theisen et al., 2014 also used a much higher concentration of LPS and stimulated for a longer time, which may have maximised the LPS response in both subsets. Variation in levels of soluble CD14 present in the culture may also contribute, and it is notable that Theisen et al., 2014 found no TNFα secretion by non-classical monocytes following LPS stimulation. Cros et al., 2010 reported yet another hierarchy of responses, with TNFα secretion being highest in intermediate monocytes, followed by non-classical monocytes, and finally classical monocytes. This diversity of findings demonstrates that the assay chosen to measure inflammatory properties can affect the outcome.

As mentioned previously, human classical monocytes resemble Ly6C^{hi} monocytes in mice based on gene expression profiles (Ingersoll et al. 2010). Ly6C^{hi} monocytes have been shown to replenish the intestinal Mϕ population in a CCL2-dependent manner in the steady-state intestine (Bain et al. 2014; Yona et al. 2013; Takada et al. 2010). High expression of CCR2 on classical monocytes supports the notion that they replenish intestinal Mϕs, which have been shown to have a regulatory role in the mouse intestine (Thiesen et al. 2014; Bain et al. 2013; Takada et al. 2010; Yona et al. 2013; Appleby et al. 2013; Patel et al. 2017). However, it is not fully understood how the inflammatory properties of

these newly arrived monocytes are controlled during their differentiation into regulatory Mϕs. A collection of studies described in the literature review indicate that IL-10 and TGFβ have important non-redundant roles (Zigmond et al. 2014; Shouval et al. 2014; Smythies et al. 2005).

It has long been known that IL-10 inhibits pro-inflammatory cytokine production in monocytes (Malefyt et al. 1991). However, the capacity of each monocyte subset to respond to IL-10 inhibition has not been previously explored. IL-10 responsiveness of monocytes subsets was measured using the assay described in the previous chapter. Classical monocytes are most responsive to IL-10 inhibition despite their robust response to LPS stimulation. This supports the idea that a strong response to IL-10 in classical monocytes is a critical mechanism by which their inflammatory properties can be controlled and may play an important role during their differentiation into regulatory intestinal Mϕs (Bain et al. 2013; Takada et al. 2010). However, in the event of pathogenic insults to the intestine, there is a need for inflammatory responses to aid pathogen clearance. There is evidence that newly recruited monocytes provide this inflammatory response (discussed in the subsequent chapters). This plasticity in immune responses is especially important in the intestine where there is constant exposure to foreign antigens.

As shown here and in previous studies (Belge et al. 2002; Cros et al. 2010; Thiesen et al. 2014) intermediate monocytes display a great capacity to respond to an inflammatory stimulus. Not only are these responses greater than those of classical monocytes but they are also less well controlled by IL-10. The role of intermediate monocytes is poorly understood in part because the lack of identified counterparts in the mouse has hampered research. It is believed that intermediate monocytes only represent a stage of differentiation from classical monocytes into non-classical monocytes and do not play a major role in immune function, which is supported by their short half-life (Patel et al. 2017). However, data reported here show that intermediates have distinctive properties such as greater cytokine production and higher expression levels of IL-10Rα than either of the other subsets. Consistent with a distinct role they have been associated with inflammatory disorders such as RA

(Belge et al. 2002; Rossol et al. 2012). Collectively, these observations challenge the view that they are merely transitioning cells. Like classical monocytes, intermediate cells express CCR2 (Thiesen et al. 2014; Appleby et al. 2013; Patel et al. 2017), and therefore may share the capacity to be recruited to the intestine. There has been no evidence of the existence of CD16+ Mϕ populations in the human intestine. However, as demonstrated in the previous chapter, CD16 is readily cleaved upon TLR activation, and in the intestine, there is high potential for exposure to microbial agonist that induce loss of CD16 expression. The combination of strong pro-inflammatory properties and a suboptimal response to IL-10 inhibition may make intermediate monocytes, activated by microbial TLR ligands, important potential contributors to inflammatory pathology in the intestine and other tissues, even under conditions where their classical counterparts are constrained by IL-10.

Non-classical monocytes have a poor response to IL-10 but as they produce low levels of TNFα in response to LPS, they may not be regarded as pro-inflammatory cells in many situations. This suggests that immune cell populations with a non-inflammatory phenotype have less restrictions on their activity. Although non-classical monocytes do not respond as aggressively to LPS stimulation as classical and intermediate monocytes in the absence of exogenous IL-10, when IL-10 is present, their response is maintained and can become equivalent to the other two subsets. Auffray et al., 2007 showed that non-classical monocytes undergo rapid extravasation at sites of infection, making them part of the initial inflammatory response, during which restrictions on their inflammatory activity would be undesirable. In IL-10 rich environments such as the intestine, non-classical monocytes may become relevant during inflammation. In addition, Cros et al., 2010 showed that TLR7 and TLR8 agonist are robust stimulators of pro-inflammatory cytokine production in non-classical monocytes, which suggests a capacity of these cells to contribute to inflammation under particular stimulatory conditions. Expression of CCR2 on non-classical monocytes is low (Thiesen et al. 2014; Patel et al. 2017), and therefore unlikely to contribute to CCR2-dependent monocyte recruitment to the intestine under steady state conditions. However, changes to the vascular endothelium and chemokine

production induced by intestinal inflammation may enable extravasation of patrolling non-classical monocytes by alternative pathways.

IL-10 production by LPS-stimulated monocytes has previously been observed (Cros et al. 2010; Malefyt et al. 1991; Thiesen et al. 2014). Malefyt et al., 1991 showed that the IL-10 produced had an auto-regulatory role on the monocytes as TNFα production was increased in the presence of anti-IL-10 neutralising antibody. However, this study did not identify the monocyte subsets individually. The findings in this chapter show that, under unstimulated conditions, IL-10 production is greatest in classical monocytes, while intermediate and non-classical monocytes display relatively low production of IL-10. Upon LPS stimulation, IL-10 production is increased in classical and intermediate monocytes but not in non-classical monocytes, which is in agreement with previous findings (Cros et al. 2010; Thiesen et al. 2014). LPS-induced IL-10 production by classical and intermediate monocytes may represent a negative feedback mechanism, restricting their activity, that is not active in non-classical monocytes. Thus, this mechanism of immune regulation is mainly focused on pro-inflammatory cells and is not necessary for the less inflammatory non-classical monocytes. It is possible that classical monocytes appeared more responsive to added IL-10 in the experiments reported here because there was an additive effect of the endogenous IL-10 production, which was less prominent in intermediate and non-classical monocytes. This is unlikely to be a major effect because the IL-10 produced by classical monocytes in the PBMC culture will diffuse freely with the potential to affect the other subsets in the same environment. However, in assays used by others, using purified cell populations, this effect would be particularly important. However, it is not possible to completely exclude some contribution of autocrine effects of IL-10 produced by classical monocytes.

To determine whether differences in monocytes subset responses to IL-10 were specific to the mode of activation (LPS) or functional readout (TNFα production), additional TLR agonists and cytokines were compared. LPS signals down two pathways depending on the involvement of additional adaptor molecules: MyD88-dependent signalling following engagement of TLR4 at the cell surface and MyD88-

independent TRIF-dependent signalling following triggering of endosomal TLR4 (Lu et al. 2008). Although there is cross-talk in these two signalling pathways, the former is associated particularly with activation of transcription factors such as NF-κB and production of pro-inflammatory cytokines, including TNFα and IL-1β, whereas MyD88-independent signalling leads to production of Type 1 interferons, especially IFNβ, via the transcription factor IRF3/7 (Honda et al. 2005). To investigate the contribution of the MyD88 dependent and independent pathways, LPS was compared with two other stimulants chosen to target these signalling pathways individually; Pam_3CSK_4 acts via TLR2 to trigger the MyD88 pathway, while Poly(I:C) acts via TLR3 to activate TRIF. TLR3 is the only TLR not to activate MyD88-dependent signalling. To determine whether the differences observed between monocytes subsets were specific for TNFα, two other cytokine readouts were assessed: IL-1β and IFNα (an alternative Type 1 interferon chosen on the basis that anti-IFNβ antibodies are not commercially available) induced by MyD88 and TRIF pathways respectively (Akira & Takeda 2004).

All three stimuli induced TNFα production but with different magnitudes of response. The hierarchy of response between monocyte subsets was broadly similar, which suggests that intermediate and classical monocytes are dominant responders to diverse TLR agonists regardless of the readout. The exception to this is that TNFα production by classical monocytes in response to Pam_3CSK_4 was relatively low. It has been previously reported that activating the MyD88 and TRIF pathways in isolation results in lower TNFα production suggesting that the two pathways act synergistically (Covert 2005) with a role for the TRIF and Type I interferons in maximising TNFα production by classical monocytes. Non-classical monocytes display poor response to the TLR agonists tested regardless of readout. However, Cros et al., 2010 showed that TLR7 and TLR8 agonist induce a robust inflammatory response in non-classical monocytes. Therefore, further analysis with TLR7 and TLR8 agonists is required to determine whether non-classical monocytes can be stimulated to produce a robust response with an appropriate activator.

LPS induced the greatest production of all three cytokines tested. Production of IFNα was low but the hierarchy of production across the monocyte subsets was similar to that observed for LPS-stimulated TNFα and IL-1β with a greater proportion of cytokine-positive intermediate monocytes. The low type 1 IFN response induced by Pam_3CSK_4 was expected as it does not signal through the TRIF pathway. However, Poly(I:C), which does signal down the TRIF pathway, also stimulated little IFNα production. As mentioned earlier, the TRIF pathway is mainly associated with IFNβ induction, and it is possible that IFNα, which was chosen because of the availability of reagents, is not a useful read-out for this pathway. Almost 100% of classical and intermediate monocytes were induced to produce IL-1β with all three TLR agonists, while non-classical monocytes again were less responsive to activation. MFI was used to overcome the limitations in sensitivity for detecting subset differences when the percentage of cytokine-positive cells approaches 100%. The level of IL-1β production in the cytokine positive cells is significantly higher in intermediate than classical monocyte irrespective of stimulus, consistent with the hierarchy of responses.

IL-10 inhibition of TNFα production induced by Pam_3CSK_4 and Poly(I:C) showed a similar hierarchy of response between the monocyte subsets as LPS. It is difficult to conclude with respect to differences in IL-10 inhibition of IFNα production between the monocyte subsets because the poor induction with all three TLR ligands means that the sensitivity of the assay is diminished. Conversely, IL-1β induction was very robust, and its inhibition by IL-10 inhibition was poor, again reducing the sensitivity of the assay and making it difficult to draw conclusions regarding differences between subsets. Overall, these data indicate that intermediate cytokine response gives the greatest ability to resolve differences between monocyte subsets. Both weak responses and very strong responses reduce the ability to resolve differences; weak responses (IFNα induction) are readily inhibited for all subsets, and very strong responses (IL-1β induction) are poorly inhibited even in classical monocytes. Of the read-outs tested, TNFα production fulfilled this criterion best and using this, differences between subsets with respect to inflammatory properties and response to IL-10 were not dependent on the TLR agonist used.

The relationship between IL-10Rα expression and the response to IL-10 was investigated with the aim of finding a possible mechanism for the differences in IL-10 response between the monocyte subsets. Intermediate monocytes had the highest expression of the IL-10Rα measured as either the percent of cells expressing the receptor or MFI. It has been suggested that intermediate monocytes are simply a collection of cells captured as they transition from classical to non-classical monocytes (Patel et al. 2017). Consistent with this view, expression of several markers, including CCR2 and CXCR1, intermediate monocyte falls between that of classical and non-classical monocytes. However, relatively high expression of IL-10Rα on intermediate monocytes in combination with their robust response to TLR activation suggests they are a distinct population. Classical monocytes expressed the lowest level of IL-10Rα even though they had the best functional response to IL-10. In summary, IL-10R expression level does not correlate with functional response to IL-10, indicating that the level of receptor expression is a poor predictor of response.

IL-10Rα expression could not explain the difference in IL-10 response between monocyte subsets, therefore, the relationship between proximal signalling events and response to IL-10 was investigated. As mentioned previously, STAT3 is phosphorylated upon IL-10R activation (Riley et al. 1999), and therefore STAT3 phosphorylation is commonly used as an indirect measure of IL-10R activity. The capacity of the individual monocytes subsets to phosphorylate STAT3 has not been previously examined. More classical and intermediate monocytes than non-classical monocytes were positive for T-STAT3, and the per cell level of T-STAT3 expression was also lower in non-classical cells. These levels correlate well with p-STAT3 in response to IL-10 and IL-6: classical and intermediate monocytes show comparable levels of p-STAT3 upon IL-10 stimulation, while non-classical monocytes display lower phosphorylation levels. At the monocyte population level, the relative level of receptor expression did not determine the degree of STAT3 phosphorylation in response to IL-10: p-STAT3 phosphorylation was high but receptor expression relatively low in classical monocytes. Again, this demonstrates that the level of IL-10Rα expression does not correlate well with the capacity of monocyte subsets to respond functionally to IL-10. Factors other than receptor expression that may influence the efficiency

of STAT3 phosphorylation are unclear. The relatively low availability of STAT3 and capacity to phosphorylate STAT3 in non-classical monocytes may explain their suboptimal response to IL-10 when compared to classical monocytes. However, intermediate monocytes were also less responsive to IL-10 than classical monocytes despite displaying comparable levels of T-STAT3 and capacity to phosphorylate STAT3. Intermediate monocytes displayed greater TNFα production making it intrinsically harder to be inhibited by a given amount of IL-10, which may explain the lower response to IL-10.

STAT3 does not directly suppress pro-inflammatory genes. Instead, *SOCS3*, as well as numerous other IL-10 regulated genes, are induced by p-STAT3 once it enters the nucleus. SOCS3 inhibits NFκB, blocking the production of pro-inflammatory cytokines such as TNFα and IL-6, as well as mitogen-activated protein kinases (MAPKs) involved in TLR signalling (reviewed by Mosser & Zhang 2008). As mentioned earlier, *SOCS3* was the only gene along the IL-10R pathway that showed significantly different expression levels between the monocyte subsets (10X genomics). In addition, Kontoyainnis et al., 2001 identified the existence of a pre-existing pool of SOCS3 available for rapid inhibition of inflammatory responses in the period during which STAT3 promotes gene expression and protein synthesis to generate new SOCS3 protein; differences in this pool could explain the differences found in IL-10 response between the monocyte subsets. This led to investigations into the expression of *SOCS3* in the monocyte subsets. Unfortunately, it was not possible to measure protein levels with the small number of cells available so gene expression was determined instead. There was a higher *SOCS3* expression in classical monocytes than intermediate and non-classical monocytes, and if reflected in increased *SOCS3* activity this could explain differences in their IL-10 response. In future work, it would be informative to also compare the level of IL-10 induced *SOCS3* expression between the monocyte subsets.

4.6 Conclusion

Classical and intermediate monocytes are robust producers of pro-inflammatory cytokines induced by diverse TLR agonists. The pro-inflammatory properties of classical monocytes can be effectively regulated by IL-10 which may be an important property of the cells that replenish the intestinal Mϕ pool, preventing the development of bacterially driven inflammation. Fewer, non-classical monocytes produced inflammatory cytokines but in contrast to classical cells, this response was poorly controlled by IL-10, most likely because low STAT3 availability in this population limits STAT3 phosphorylation and downstream signalling. Thus, non-classical cells may contribute to inflammation in IL-10 rich environments. Similarly, although intermediate monocytes are similar to classical monocytes in their expression of proximal IL-10 signalling molecules, they were also less responsive to IL-10 and may contribute to inflammation in the presence of this cytokine. In terms of cytokine production and its control by IL-10, the properties of intermediate monocytes were distinct from those of classical and non-classical cells, suggesting that the view of them as simply a population transiting between the latter types of cell, is likely to be over-simplistic.

Chapter 5: Monocyte subsets and their responsiveness to IL-10 are altered in IBD

5.1 Chapter summary

The focus of this chapter is to investigate the responsiveness of monocyte subsets to IL-10 in health and IBD. Responsiveness to IL-10 was measured using the assay described in the previous chapters. First, the inflammatory capacity of the monocyte subsets was compared between healthy controls and IBD patients to ensure that IL-10 response was measured against the same inflammatory activity. There was no difference in LPS-induced TNFα production or spontaneous IL-10 production between health and disease. Classical monocytes, but not other subsets, were found to have a reduced response to IL-10 in IBD patients compared with healthy controls. Signalling components of the IL-10R signalling pathway were investigated to explore the possible mechanisms behind this reduced response to IL-10 in classical monocytes. Despite this reduced response to IL-10, classical monocytes from IBD patients express more IL-10Rα, which may explain their enhanced capacity to phosphorylate STAT3 in response to IL-10 despite comparable levels of STAT3 available within the cell. Thus, the proximal signalling components investigated so far do not suggest a mechanism for the reduced response to IL-10 in classical monocytes found in IBD patients. Downstream *SOCS3*, a key regulator of the activity of IL-10, also showed a trend towards increased mRNA expression in IBD patients. Additional properties of the IL-10 signalling pathway need to be explored.

The distribution of the monocyte subsets in health and IBD was investigated, and a reduction was observed in both the number and proportion of non-classical monocytes in the circulating blood of two separate cohorts of IBD patients. There was no difference in numbers of classical or intermediate monocytes. This is in contrast to the previously reported increase in the proportion of intermediate monocytes as a percentage of total monocytes (Grip et al. 2006; Thiesen et al. 2014). The final section of this chapter will begin to explore the possible mechanisms for the loss of non-classical monocytes from the circulation.

5.2 Introduction

Bain et al., 2014 showed that monocytes are continuously recruited to the intestine to replenish the Mϕ pool. In addition, the same group showed that the newly recruited monocytes differentiate into Mϕs in a context-dependent manner (Bain et al., 2013). In healthy mice, newly recruited Ly6C^{hi} monocytes lose their inflammatory properties to give rise to regulatory Mϕs, which have been shown to be critical in maintaining steady-state in the intestine (Takada et al. 2010; Bain et al. 2014). However, during inflammation, this pathway is disrupted, and the monocytes retain their inflammatory properties giving rise to pro-inflammatory Mϕs that contribute to inflammation (Zigmond et al. 2012; Bain et al. 2013). The environmental cues that determine monocyte differentiation into regulatory or inflammatory Mϕs are poorly understood.

Numerous studies demonstrate the critical role of IL-10 in regulating inflammatory responses in the intestine (Begue et al. 2011; Kühn et al. 1993; Glocker & Kotlarz 2009; Gasche et al. 2003; Grundtner et al. 2009; Uhlig 2013). However, many immune cells can be influenced by IL-10, and until recently it was unclear which cell population(s) are the critical target of IL-10 for maintaining immune homeostasis in the intestine. There is growing evidence in mice that Mϕs can drive intestinal inflammation but that their response is normally controlled in a non-redundant way by the action of IL-10 (Shouval et al. 2014; Zigmond et al. 2014). TGFβ has also been shown to be a crucial signal in promoting monocyte differentiation into resident Mϕs (Smythies et al. 2010; Schridde et al. 2017). Importantly, Schriddle et al., 2017 showed that TGFβ and IL-10 imprint the distinct properties of intestinal Mϕs; TGFβ shapes their tissue repair and scavenging functions, and IL-10 downregulates their capacity to produce pro-inflammatory mediators.

There is evidence that systemic signals from the intestine during inflammation cause functional changes to circulating cells. For example, mice orally inoculated with *Toxoplasma gondii*, a parasite, showed that monocytes were primed for regulatory function in the BM by systemic inflammatory signals received from the intestine and relayed by NK cells (Askenase et al. 2015). In humans, moMϕ

from CD patients displayed reduced TNFα production in response to *E.coli* compared to healthy controls (Smith et al. 2009) but whether this is the result of altered haematopoiesis or modulation of circulating monocytes is not known. Nonetheless, these observations suggest that systemic changes in circulating monocytes occur when the intestine is inflamed, and that these changes have consequences for the mucosal populations that are derived from them, which formed the rationale for studying blood monocytes, as the likely precursors of intestinal Mϕ.

The aim of the work described in this chapter was to determine whether IL-10 responsiveness of monocyte subsets is altered in disease, enumerate monocyte subsets in health and IBD, and explore possible mechanisms related to components of the IL-10R signalling pathway.

5.3 Aims

7. Determine the ability of IL-10 to inhibit LPS-induced TNFα production in the monocyte subsets of healthy controls and IBD patients.
8. Assess differences in signalling components along the IL-10 signalling pathway between health and IBD.
9. Investigate monocyte subset distribution and gut homing capacity in health and IBD.

5.4 Results

5.4.1 The inflammatory capacity of monocytes subsets does not differ between health and disease

The pro-inflammatory capacity of the monocyte subsets, assessed as TNFα production, was compared between healthy controls and IBD patients to ensure that IL-10 response was measured against the same inflammatory activity. PBMCs from eight healthy controls and eight IBD patients with active disease (six CD and two UC) patients were stimulated with 1ng/ml LPS for three hours before staining for intracellular TNFα. TNFα production was measured as a percentage of cells positive for TNFα and as the level of expression on a per cell basis, assessed as MFI. The results show that there was no significant difference in TNFα production in any of the monocyte subsets of IBD patients compared with healthy controls (Figure 5.1). There were no detectable TNFα production in the monocyte subsets in unstimulated culture from healthy controls or IBD patients (data not shown).

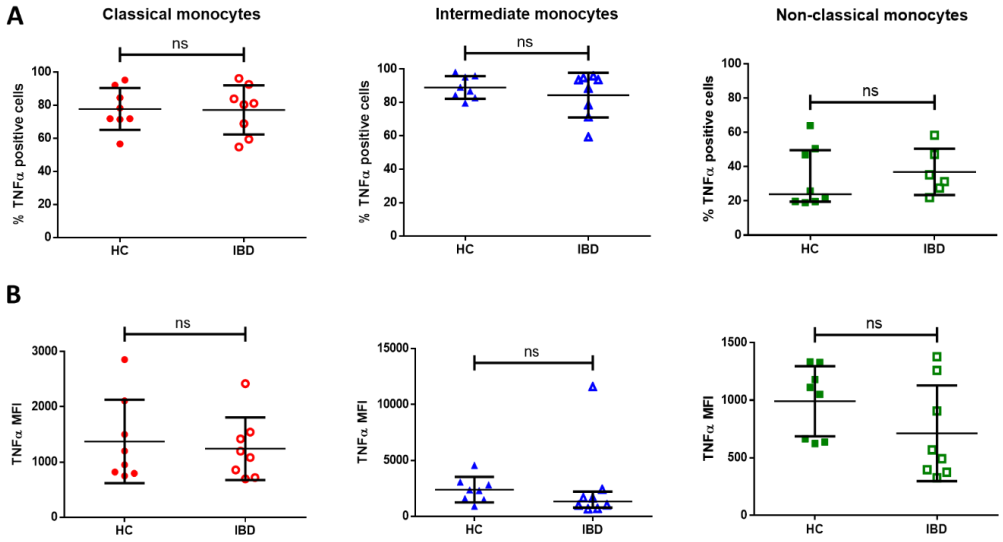

Figure 5.1: LPS-induced TNFα production by monocyte subsets in health and IBD. PBMCs were stimulated with 1ng/ml LPS for three hours in the presence of monensin and ADAM17 inhibitor (TMI-005). The PBMCs were labelled with anti-HLA-DR, anti-CD14, and anti-CD16 antibodies to distinguish the monocytes subsets, fixed, permeabilised, and stained intracellularly for TNFα before acquiring on the flow cytometer. TNFα production was compared between healthy controls (n=8) and IBD patients (n=8) with active disease. TNFα production was quantified as **A)** percentage of cells positive for TNFα and **B)** as the level of expression on a per cell basis, assessed as MFI, for each monocyte subset. Mean and SD are displayed for normally distributed data sets, while median and IQR are displayed for non-normally distributed data sets. An unpaired T-tests was used to compare two groups of normally distributed data, while a Mann-Whitney test was used to compare two groups of data that were non-normally distributed.

Next, the anti-inflammatory activity, assessed as IL-10 production, was compared between the same eight healthy controls and eight IBD patients with active disease. PBMCs were stimulated or not with 1ng/ml LPS for three hours before staining for intracellular IL-10. IL-10 production was measured as a percentage of cells positive for IL-10 and as the level of expression on a per cell basis, assessed as MFI. There was no significant difference in the production of IL-10 at baseline or with LPS stimulation in the monocyte subsets from healthy controls and IBD patients.

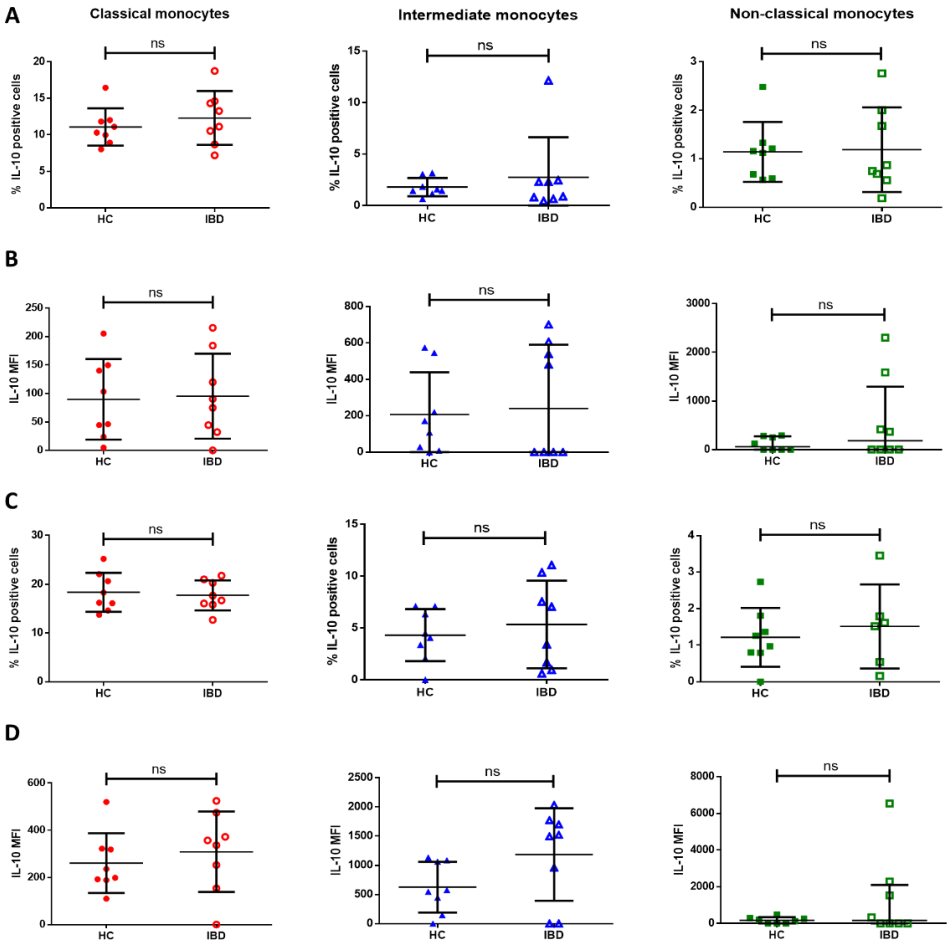

Figure 5.2: Endogenous and LPS-induced IL-10 production by monocyte subsets in health and IBD. PBMCs were stimulated or not with 1ng/ml LPS for three hours in the presence of monensin and ADAM17 inhibitor (TMI-005). The PBMCs were labelled with anti-HLA-DR, anti-CD14, and anti-CD16 antibodies to distinguish the monocytes subsets, fixed, permeabilised, and stained intracellularly for IL-10 before acquiring on the flow cytometer. IL-10 production was compared between healthy (n=8) and IBD patients (n=8) with active disease. IL-10 production was quantified as a percentage of cells positive for IL-10 and as the level of expression on a per cell basis, assessed as MFI, for each monocyte subset in **A, B)** unstimulated and **C, D)** LPS-stimulated cultures. Mean and SD are displayed for normally distributed data sets, while median and IQR are displayed for non-normally distributed data sets. An unpaired T-tests was used to compare two groups of normally distributed data, while a Mann-Whitney test was used to compare two groups of data that were non-normally distributed.

5.4.2 Classical monocytes are less responsive to IL-10 in IBD patients compared with healthy controls

The response of monocyte subsets to IL-10 was compared between the same eight healthy individuals and eight IBD patients with active disease. Responsiveness to IL-10 was measured using the assay described in Chapter 3, determining the ability of IL-10 to inhibit LPS-induced TNFα production. IL-10 dose-response curves were compared between healthy controls and IBD patients for each monocyte subset (Figure 5.3 A). IL-10 response was quantified as either ED50 or as the percentage of inhibition measured at an IL-10 concentration of 2ng/ml (Figure 5.3 B, C).

IL-10 at a concentration ≤0.08ng/ml had no significant impact on LPS-induced TNFα production by any monocyte subset (Figure 5.3 A). In classical monocytes, IL-10 at concentrations >0.08ng/ml caused a dose-dependent inhibition of TNFα production (Figure 5.3 A) but the inhibition was significantly lower in monocytes from IBD patients compared with healthy controls as assessed by ED50 ($p = 0.0379$) or by inhibition at 2ng/ml IL-10 ($p = 0.0264$) (Figure 5.3 B, C).

In intermediate monocytes, IL-10 at concentrations >0.4ng/ml caused a dose-dependent inhibition of TNFα production (Figure 5.3 A). As previously noted in non-classical monocytes from healthy controls (Chapter 4), non-classical monocytes from IBD patients were also relatively resistant to control by IL-10 despite poor TNFα production (Figure 5.1 A). It was not possible to accurately determine ED50 values for intermediate and non-classical monocytes because inhibition did not reach 50% in cells from some donors even at the highest concentration of IL-10 tested (Figure 5.3 B). However, as determined by the response to 2ng/ml, the inhibitory effect of IL-10 did not differ between health and IBD in either intermediate and non-classical monocytes (Figure 5.3 C).

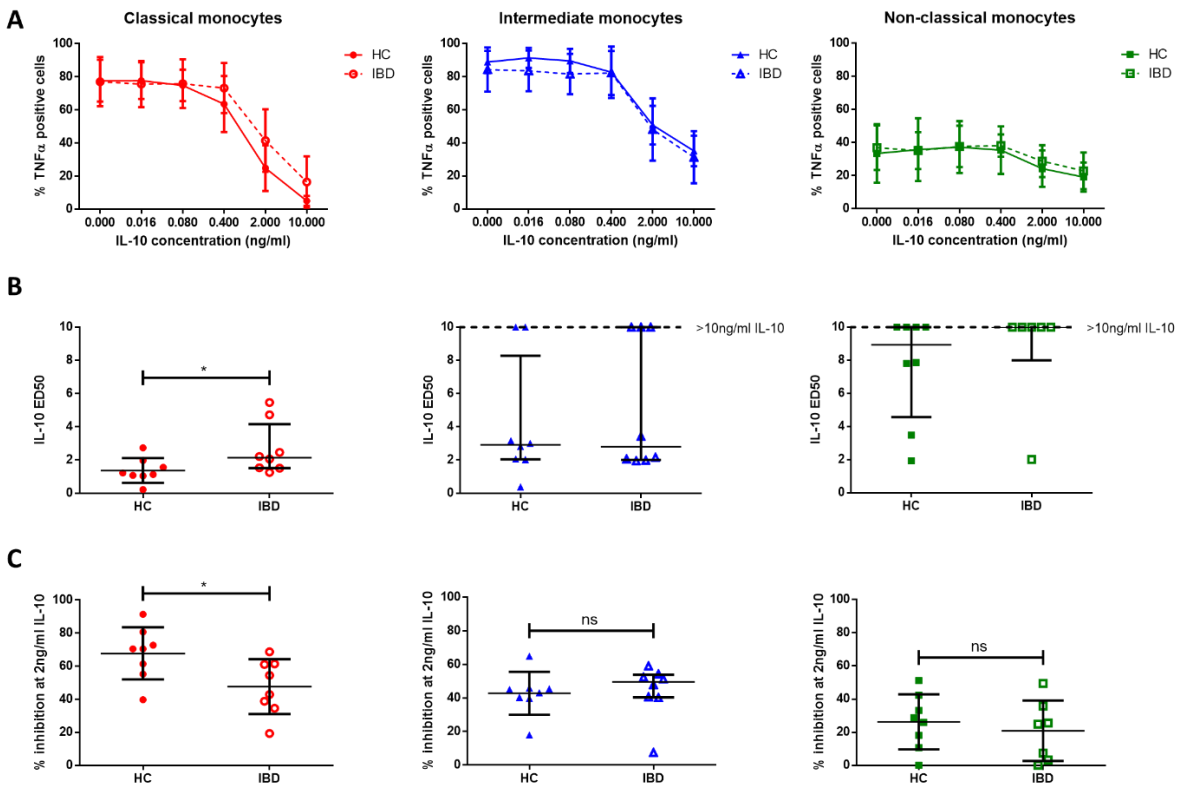

Figure 5.3: IL-10 responsiveness of monocyte subsets in health and IBD. PBMCs were stimulated with 1ng/ml LPS and increasing concentrations of IL-10 (0.016-10ng/ml) for three hours in the presence of monensin and ADAM17 inhibitor (TMI-005). The PBMCs were labelled with anti-HLA-DR, anti-CD14, and anti-CD16 antibodies to distinguish the monocytes subsets, fixed, permeabilised, and stained intracellularly for TNFα before acquiring on the flow cytometer. **A)** IL-10 dose-response curves were compared between healthy controls (n=8) and IBD patients (n=8) with active disease for each monocyte subset. IL-10 response was quantified as **B)** ED50 and **C)** percentage inhibition of TNFα at 2ng/ml IL-10 for each monocyte subset. Mean and SD are displayed for normally distributed data sets, while median and IQR are displayed for non-normally distributed data sets. An unpaired T-tests was used to compare two groups of normally distributed data, while a Mann-Whitney test was used to compare two groups of data that were non-normally distributed. $p \leq 0.05$* $p \leq 0.01$** $p \leq 0.001$*** $p \leq 0.0001$****.

5.4.3 IL-10Rα expression is increased in classical monocytes of IBD patients

The underlying mechanism behind the reduced response to IL-10 was then investigated by examining proximal signalling components, including IL-10R expression. Whole blood from 15 healthy donors and 31 IBD patients (15 active and 16 inactive; 21 CD, eight UC, and two IC) were labelled for IL-10Rα. Receptor expression was quantified as percentage positive cells and MFI calculated as MFI for staining with anti-IL-10Rα antibody minus MFI for staining with an isotype-matched control antibody.

There was no significant difference in the proportion of IL-10Rα expressing monocytes between healthy controls and IBD patients (Figure 5.4 A, B, and C). There was a significant increase in the level of IL-10Rα expression by the classical monocytes of IBD patients ($p = 0.0207$) (Figure 5.4 D). Therefore, the reduced response to IL-10 in classical monocytes from IBD patients cannot be explained by a reduced level of receptor expression. Instead, these data provide further evidence that the level of IL-10R expression is a poor predictor of functional response to the cytokine. There was no significant difference in the level of IL-10Rα expression on intermediate and non-classical monocytes in health and IBD (Figure 5.4 E and F). However, there was greater heterogeneity in the IBD group. Stratifying the IBD group into active and inactive, CD and UC, or treatment groups did not reveal any associations with IL-10R expression (Appendix 6).

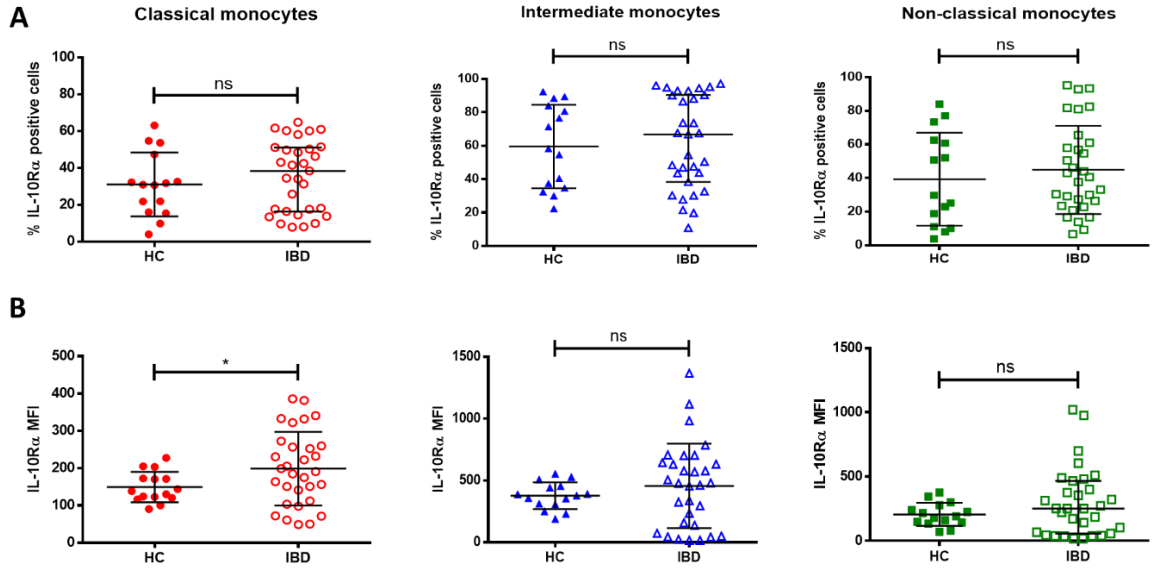

Figure 5.4: IL-10Rα expression on monocytes subsets in health and IBD. Whole blood from healthy donors (n=15) and IBD patients (n=31) were labelled with anti-HLA-DR, anti-CD14, and anti-CD16 antibodies to distinguish the monocyte subsets, and IL-10Rα before acquiring on the flow cytometer. IL-10Rα expression was quantified as **A)** percentage of cells positive for IL-10Rα and **B)** MFI calculated as MFI for staining with anti-IL-10Rα antibody minus MFI for staining with an isotype-matched control antibody for each monocyte subset. Mean and SD are displayed for normally distributed data sets, while median and IQR are displayed for non-normally distributed data sets. An unpaired T-tests was used to compare two groups of normally distributed data, while a Mann-Whitney test was used to compare two groups of data that were non-normally distributed. $p \leq 0.05$* $p \leq 0.01$** $p \leq 0.001$*** $p \leq 0.0001$****.

5.4.4 IL-10-induced STAT3 phosphorylation is more efficient in classical monocytes of IBD patients

To test whether the increased IL-10Rα expression in IBD patients impacts on phosphorylation of STAT3, the capacity to phosphorylate STAT3 was measured in the monocyte subsets of 10 healthy controls and 11 IBD patients with active disease (six CD and five UC). Whole PBMCs were stimulated with 100ng/ml IL-10 for 15min before staining intracellularly for p-STAT3. STAT3 phosphorylation was quantified as a percentage of cells positive for p-STAT3 and MFI calculated as MFI for staining with anti-p-STAT3 antibody minus MFI for staining with an isotype-matched control antibody. The percent of cells positive for p-STAT3 was significantly enhanced in classical monocytes of IBD patients in comparison to healthy volunteers ($p = 0.0029$), which is reflected in MFI ($p = 0.0032$) (Figure 5.5 D). The increase in p-STAT3 positive cells may be explained by the enhanced surface expression of IL-10Rα in classical monocytes of IBD patients but does not explain the reduced functional response to IL-10 in IBD patients. The proportion of p-STAT3 positive cells and the level of STAT3 phosphorylation did not differ between IBD patients and healthy controls in both intermediate and non-classical monocytes. However, as with IL-10R expression, there is greater heterogeneity in p-STAT3 expression the IBD group and elevated levels could be observed in some individuals.

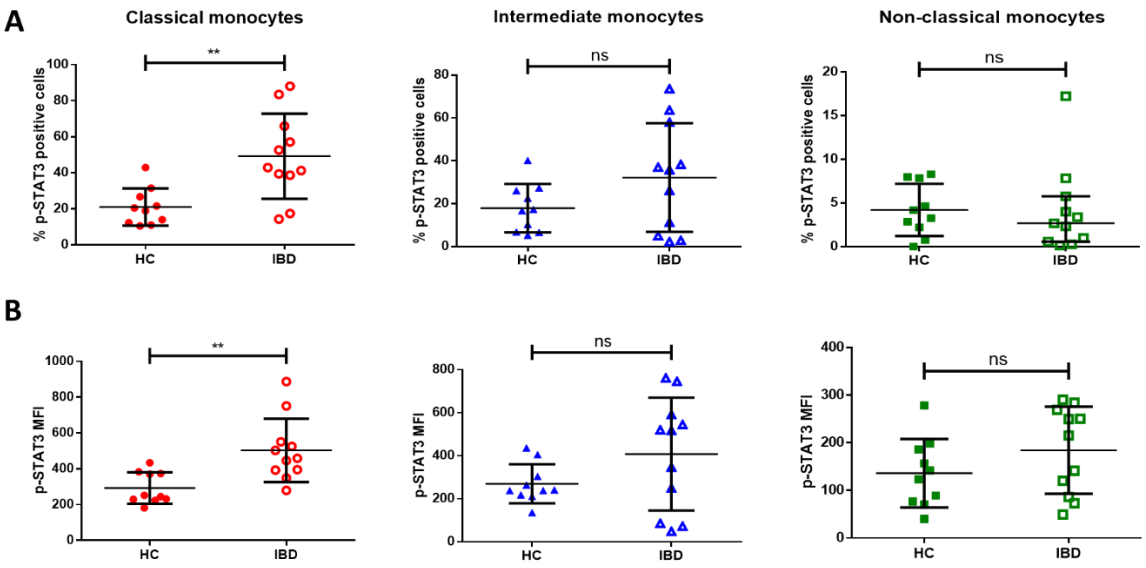

Figure 5.5: STAT3 phosphorylation in monocyte subsets in health and IBD. PBMCs were labelled with anti-HLA-DR, anti-CD14, and anti-CD16 antibodies to distinguish the monocyte subsets. The PBMCs were stimulated with 100ng/ml IL-10 before fixation, permeabilisation, and intracellular staining for p-STAT3. Samples from healthy donors (n=10) and IBD patients (n=16) with active disease were then acquired on the flow cytometer. STAT3 phosphorylation was calculated as **A)** percentage of cells positive for p-STAT3 and **B)** and MFI calculated as MFI for staining with anti-p-STAT3 antibody minus MFI for staining with an isotype-matched control antibody for each monocyte subset. Mean and SD are displayed for normally distributed data sets, while median and IQR are displayed for non-normally distributed data sets. An unpaired T-tests was used to compare two groups of normally distributed data, while a Mann-Whitney test was used to compare two groups of data that were non-normally distributed. $p \leq 0.05$* $p \leq 0.01$** $p \leq 0.001$*** $p \leq 0.0001$****.

In the analysis of STAT3 phosphorylation in the monocyte subsets in health, there was an association between with STAT3 availability and STAT3 phosphorylation in response to IL-10. To determine if the enhanced capacity to phosphorylation STAT3 observed in classical monocytes from IBD patients was also associated with a greater STAT3 pool, STAT3 availability was measured in the monocyte subsets of the same ten healthy controls and 11 IBD patients with active disease. STAT3 availability was quantified as a percentage of cells positive for STAT3 and MFI calculated as MFI for staining with anti-STAT3 antibody minus MFI for staining with an isotype-matched control antibody.

Figure 5.6 shows that there was no significant difference in the proportion of T-STAT3 positive cells or the level of T-STAT3 in any of the monocyte subsets in health and IBD. This suggests that STAT3 availability is not contributing to the enhanced STAT3 phosphorylation observed in classical monocytes of IBD patients.

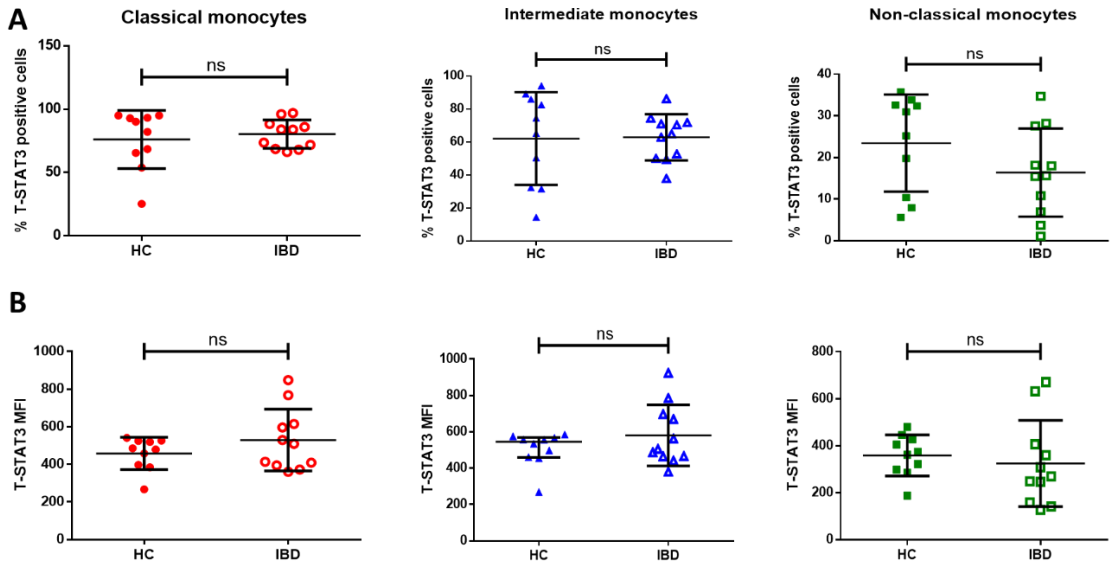

Figure 5.6: STAT3 availability in monocytes subsets in health and IBD. PBMCs were labelled with anti-HLA-DR, anti-CD14, and anti-CD16 antibodies to distinguish the monocyte subsets before fixation, permeabilisation, and intracellular staining for STAT3. Samples from healthy donors (n=10) and IBD patients (n=11) with active disease were then acquired on the flow cytometer. STAT3 availability was calculated as **A)** percentage of cells positive for T-STAT3 and **B)** and MFI calculated as MFI for staining with anti-STAT3 antibody minus MFI for staining with an isotype-matched control antibody for each monocyte subset for each monocyte subset. Mean and SD are displayed for normally distributed data sets, while median and IQR are displayed for non-normally distributed data sets. An unpaired T-tests was used to compare two groups of normally distributed data, while a Mann-Whitney test was used to compare two groups of data that were non-normally distributed.

5.4.5 *SOCS3* mRNA expression in classical monocytes is enhanced in IBD patients compared to healthy controls

The data presented so far in this chapter indicate that the reduced ability of IL-10 to inhibit LPS-induced TNFα production in classical monocytes of IBD patients cannot be explained by proximal signalling events. Therefore, the next step was to look further downstream at *SOCS3* mRNA expression. Investigating SOCS3 protein levels directly was hindered by low cell numbers, therefore, baseline transcription level was used as a surrogate. In addition, low recovery of purified subsets meant that it was not possible to compare the level of IL-10 induced *SOCS3* mRNA expression. PBMCs from 14 healthy donors and 16 IBD patients with active disease (eight CD, six UC, and two IC) were labelled with anti-HLA-DR, anti-CD14, and anti-CD16 antibodies to distinguish the monocyte subsets before purification by sorting on the FACS Aria (BD). $1x10^6$ classical monocytes were sorted, and the relative gene expression of *SOCS3* was measured using qRT-PCR. *SOCS3* mRNA expression in intermediate and non-classical monocytes was not compared between healthy individuals and IBD patients because sufficient cells could not be obtained from the volume of blood we were able to obtain under our ethical approval. However, the IL-10 response in these subsets did not differ in IBD patients (Figure 5.3), and therefore these subsets were unlikely to have been informative.

A trend towards increased expression of *SOCS3* mRNA expression in the classical monocytes of IBD patients was observed ($p = 0.0695$) (Figure 5.7), which is consistent with the increase in IL-10R expression and STAT3 phosphorylation reported above. However, a larger cohort is required to confirm this trend.

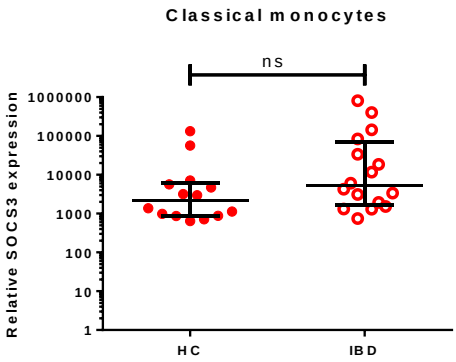

Figure 5.7: SOCS3 mRNA expression in classical monocytes in health and IBD. Whole PBMCs from healthy donors (n=14) and IBD patients (n=16) with active disease were labelled with anti-HLA-DR, anti-CD14, and anti-CD16 antibodies to distinguish the monocyte subsets before sorting on the FACS Aria (BD). $1x10^6$ classical monocytes were sorted, and the relative gene expression of SOCS3 was measured using qRT-PCR. Median and IQR displayed; a Man-Whitney test was used.

5.4.6 Fewer circulating non-classical monocytes are present in IBD patients

The findings above together with other published work (Arts et al. 2018; Askenase et al. 2015; Christ et al. 2018; Mitroulis et al. 2018; Sanders et al. 2014; Smith et al. 2009) showed changes in the properties of blood monocytes during intestinal inflammation. Next, the distribution of the monocyte subset was examined. A comparison of monocyte subset distribution was made between 24 healthy controls and 41 IBD patients (21 active and 20 inactive; 28 CD, 11 UC, and two IC) using whole blood labelling. Each monocyte subset was assessed as both the proportion of total PBMCs and total monocytes as well as absolute cell number using Flow-Count Fluorospheres. There was a significant reduction in non-classical monocytes in IBD patients in comparison with healthy controls (Figure 5.8). This was true whether measured as a percentage of total PBMCs ($p = 0.0202$), as a percentage of total monocytes ($p = 0.0025$), and as absolute cell numbers ($p = 0.0057$). There were no significant changes in the proportion or cell number of the classical and intermediate monocytes between IBD patients and healthy controls. Stratifying the IBD cohort into active and inactive, CD and UC, or treatment groups did not reveal any significant associations (Appendix 7). This finding was in contrast to previously reported increase in the proportion of intermediate monocytes as a percentage of total monocytes (Grip et al. 2006; Thiesen et al. 2014). Therefore, the investigation into monocyte subset

distribution in health and IBD was repeated in a separate cohort of 18 healthy controls and 19 IBD patients with active disease (nine CD and ten UC) who were about to start vedolizumab treatment (Appendix 8a). In agreement with the findings in the first cohort, a significant reduction in the proportion and absolute cell number of non-classical monocytes was observed, and there was no difference in the proportion or number of classical and intermediate monocytes (Appendix 8b).

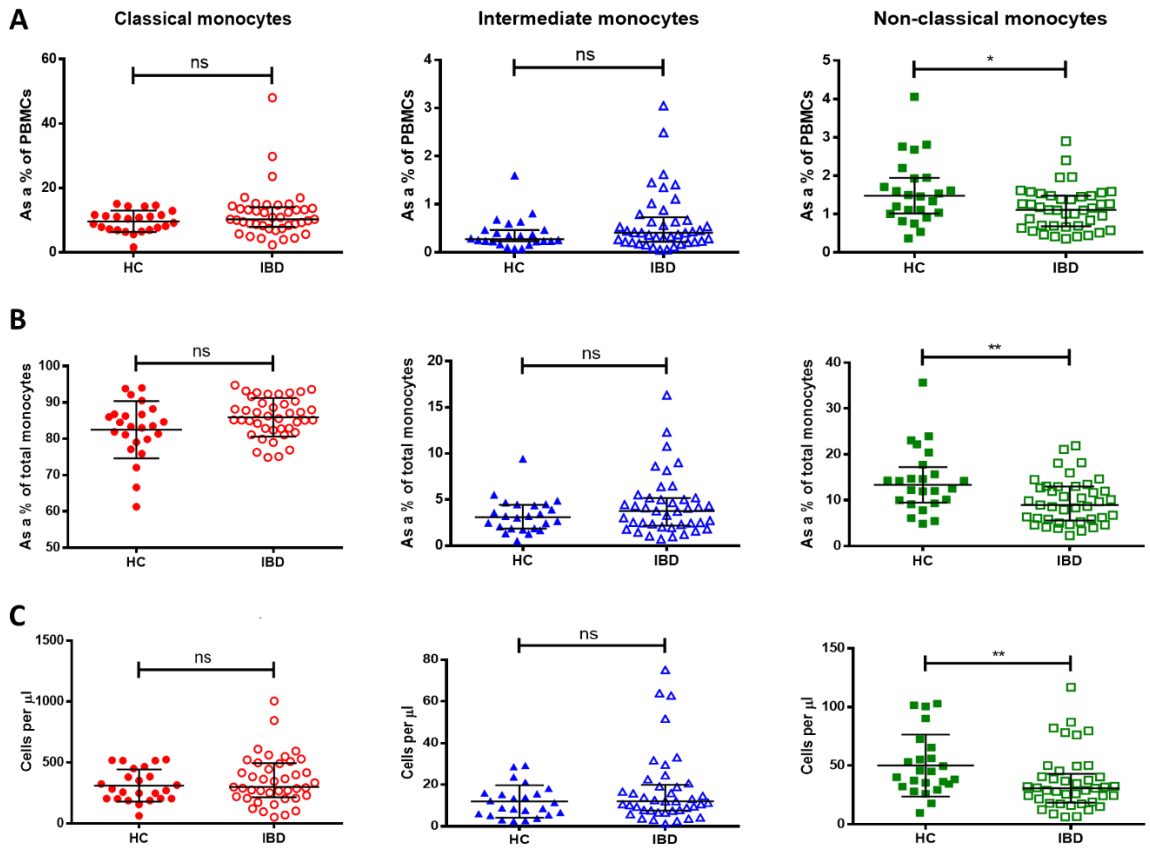

Figure 5.8: Monocyte subset distribution in health and IBD. Whole blood from healthy donors (n=24) and IBD patient (n=41) were labelled with anti-HLA-DR, anti-CD14, and anti-CD16 antibodies to distinguish the monocyte subsets before acquiring on the flow cytometer. Monocyte subset distribution was calculated as **A)** percentage of PBMCs, **B)** percentage of total monocyte, and **C)** absolute cell number. Mean and SD are displayed for normally distributed data sets, while median and IQR are displayed for non-normally distributed data sets. An unpaired T-tests was used to compare two groups of normally distributed data, while a Mann-Whitney test was used to compare two groups of data that were non-normally distributed. $p \leq 0.05$* $p \leq 0.01$** $p \leq 0.001$*** $p \leq 0.0001$****.

5.4.7 β7 is highly expressed in classical and intermediate monocytes

Poor regulation of the inflammatory activity of intermediate and non-classical monocytes may be of relevance in inflammatory disorders of the intestine, where IL-10 plays a critical role in the prevention of bacterial driven inflammation (Kühn et al., 1993). Schippers et al. 2015 showed that β7 integrin deficiency in mice was protective against DSS-induced colitis due to reduced monocyte recruitment, and injecting WT Ly6C^{hi} monocytes caused an aggravation of the colitis in these mice. This indicates a possible role of α4β7 in the recruitment of monocyte into the intestine. To test this, the expression levels of α4β7 was first measured on the monocyte subsets in 18 healthy individuals. The monocyte subsets in whole blood were labelled with anti-HLA-DR, anti-CD14, and anti-CD16 antibodies to distinguish the monocyte subsets, and anti-CD103 to distinguish between α4β7 and CD103β7, both of which would label with anti-β7 antibody (Figure 5.9 A). β7 expression was quantified as a percentage of cells positive for β7 and MFI calculated as MFI for staining with anti-β7 antibody minus MFI for staining with an isotype-matched control antibody.

A similar percentage (35-39%) of classical and intermediate monocytes were α4β7+ (identified as CD103-β7+) (Figure 5.9 C) but the level of expression was significantly higher ($p=0.0047$) on the intermediate cells (Figure 5.9 D). Relatively low β7 expression was detected on the non-classical monocytes (Figure 5.9 D), and significantly fewer non-classical monocytes were positive for α4β7 than classical monocytes or intermediate monocytes (both $p < 0.001$) (Figure 5.9 C). These data show that intermediate monocytes display the potential capacity to be recruited to the intestine in a α4β7-dependent manner, where the poor control of their inflammatory properties could contribute to intestinal inflammation.

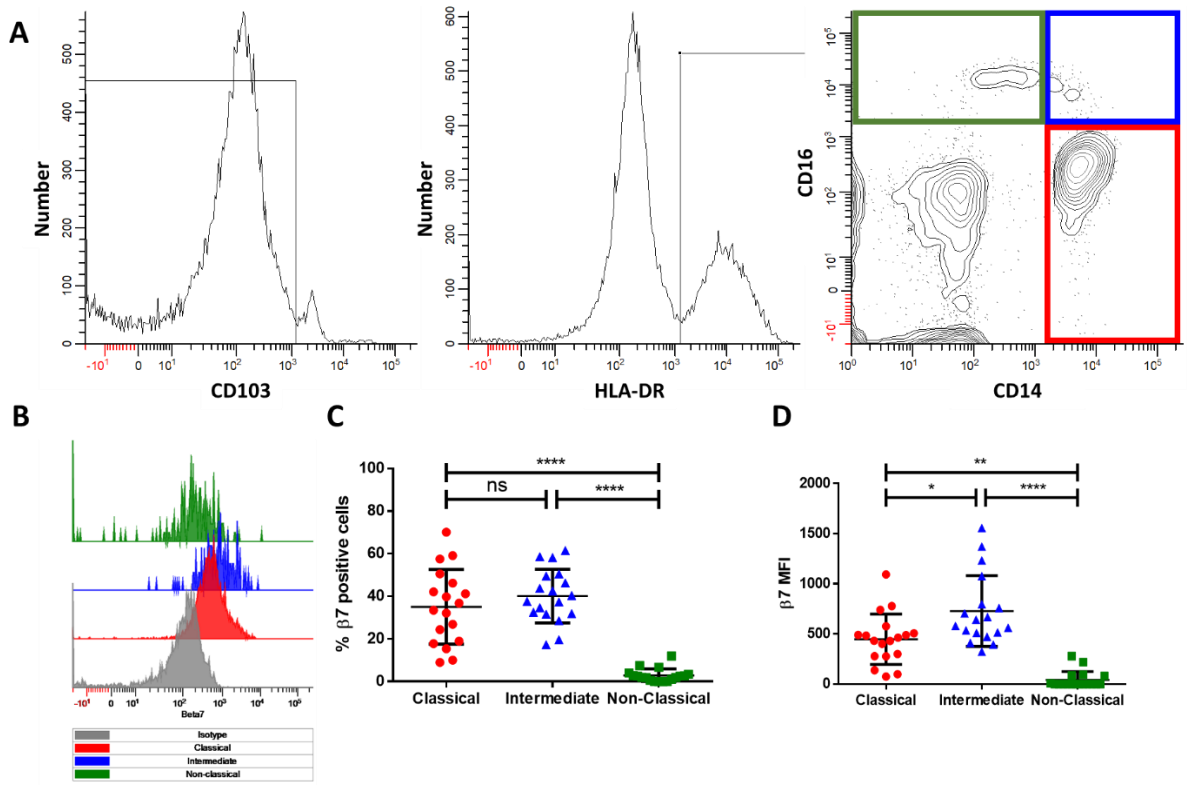

Figure 5.9: β7 expression on monocyte subsets in health. Whole blood from healthy donors (n=18) were labelled with anti-HLA-DR, anti-CD14, and anti-CD16 antibodies to distinguish the monocyte subsets (excluding CD103+ cells), and anti-β7 antibody before acquiring on the flow cytometer. **A)** gating strategy for assessing β7 expression on the monocyte subsets**. B)** representative histograms of β7 expression on the monocyte subset in relation to the isotype control for the total HLA-DR+ population (grey histogram) for illustration. β7 expression was quantified as **C)** percentage of cells positive for β7 and **D)** MFI calculated as MFI for staining with anti-β7 antibody minus MFI for staining with an isotype-matched control antibody for each monocyte subset in relation to their corresponding isotype control. Mean and SD are displayed for normally distributed data sets, while median and IQR are displayed for non-normally distributed data sets. Data were analysed statistically by Friedman test. $p \leq 0.05$* $p \leq 0.01$** $p \leq 0.001$*** $p \leq 0.0001$****.

5.4.8 β7 expression on the monocytes subsets does not differ between health and IBD

Next, expression levels of β7 on the monocyte subsets were compared between 18 healthy controls and 19 IBD patients with active disease (nine CD and ten UC). β7 expression was quantified as a percentage of cells positive for β7 (excluding CD103+ cells) and MFI calculated as MFI for staining with anti-β7 antibody minus MFI for staining with an isotype-matched control antibody.

No significant difference in either proportion of $\alpha 4\beta 7$+ monocytes or level of β7 expression was seen on any of the monocyte subsets between healthy controls and IBD patients. However, there was greater heterogeneity in the IBD group most notably in the non-classical monocytes where a few individuals had an increased frequency of $\alpha 4\beta 7$+ cells (Figure 5.10). Stratifying the IBD cohort into CD and UC patients or responders and non-responders did not reveal any significant association with disease type (Appendix 9). These data suggest that the loss of non-classical monocytes from the circulation of IBD patients is unlikely to be due to enhanced $\alpha 4\beta 7$-dependent recruitment to the intestine during inflammation, at least in the majority of individuals.

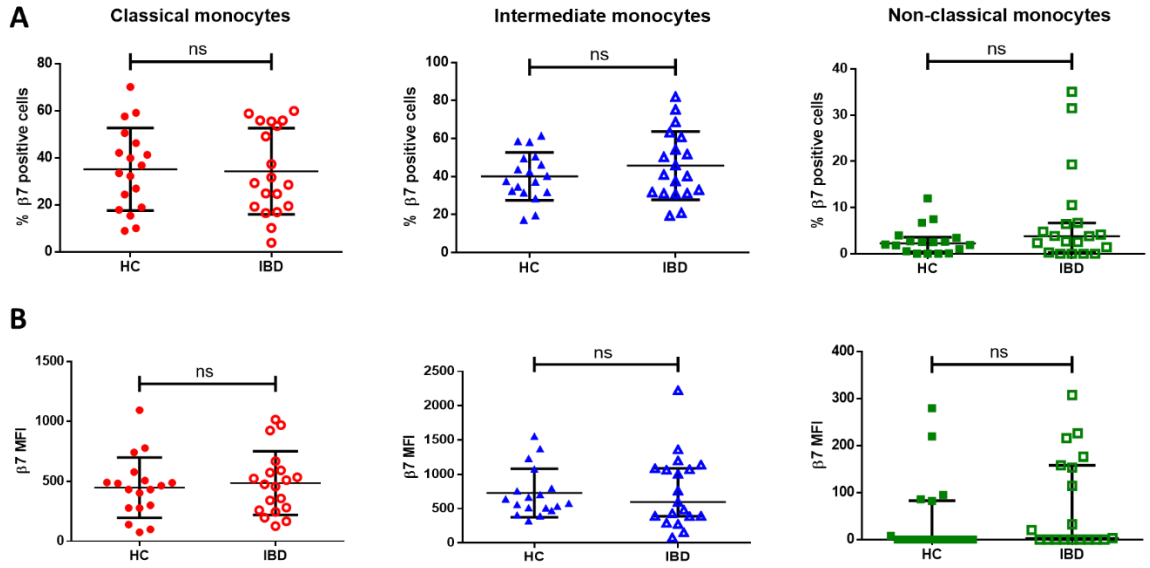

Figure 5.10: β7 expression on monocytes subsets in health and IBD. Whole blood from healthy donors (n=18) and IBD patient (n=19) were labelled with anti-HLA-DR, anti-CD14, and anti-CD16 antibodies to distinguish the monocyte subsets (excluding CD103+ cells), and β7 before acquiring on the flow cytometer. β7 expression was quantified as **A)** percentage of cells positive for β7 and **B)** MFI calculated as MFI for staining with anti-β7 antibody minus MFI for staining with an isotype-matched control antibody for each monocyte subset. Mean and SD are displayed for normally distributed data sets, while median and IQR are displayed for non-normally distributed data sets. An unpaired T-tests was used to compare two groups of normally distributed data, while a Mann-Whitney test was used to compare two groups of data that were non-normally distributed.

5.4.9 Blockade of α4β7 in IBD does not impact upon circulating monocytes

As previously described, monocytes have been implicated in intestinal inflammation using β7 integrin-deficient mice (Schippers et al. 2015). In support of this, the data showed that monocytes subsets express $\alpha4\beta7$. To assess the contribution of $\alpha4\beta7$-dependent monocyte recruitment to the intestine during inflammation, monocyte subset distribution was monitored in patients undergoing vedolizumab treatment (an $\alpha4\beta7$ blocking antibody). Whole blood from 19 IBD patients with active disease (nine CD and ten UC; seven responders and 10 non-responders) was collected at baseline and after two and six weeks of treatment. Monocyte subset distribution was assessed as the proportion of total PBMCs and total monocytes, and absolute cell number. Monocyte subset distribution was also assessed as a percentage of β7+ (excluding CD103+ cells) monocytes and β7+ monocytes per µL (Appendix 10a).

No significant change was seen in proportion or absolute cell number of any of the monocyte subsets (Figure 5.11 A, B, C) over the six weeks of vedolizumab treatment. There was a trend towards an increase in the absolute number of classical cells and non-classical monocytes over the six weeks of vedolizumab treatment. However, a larger cohort is required to confirm this trend. Stratifying the IBD cohort into CD and UC patients or responders and non-responders did not reveal any significant associations (Appendix 10b).

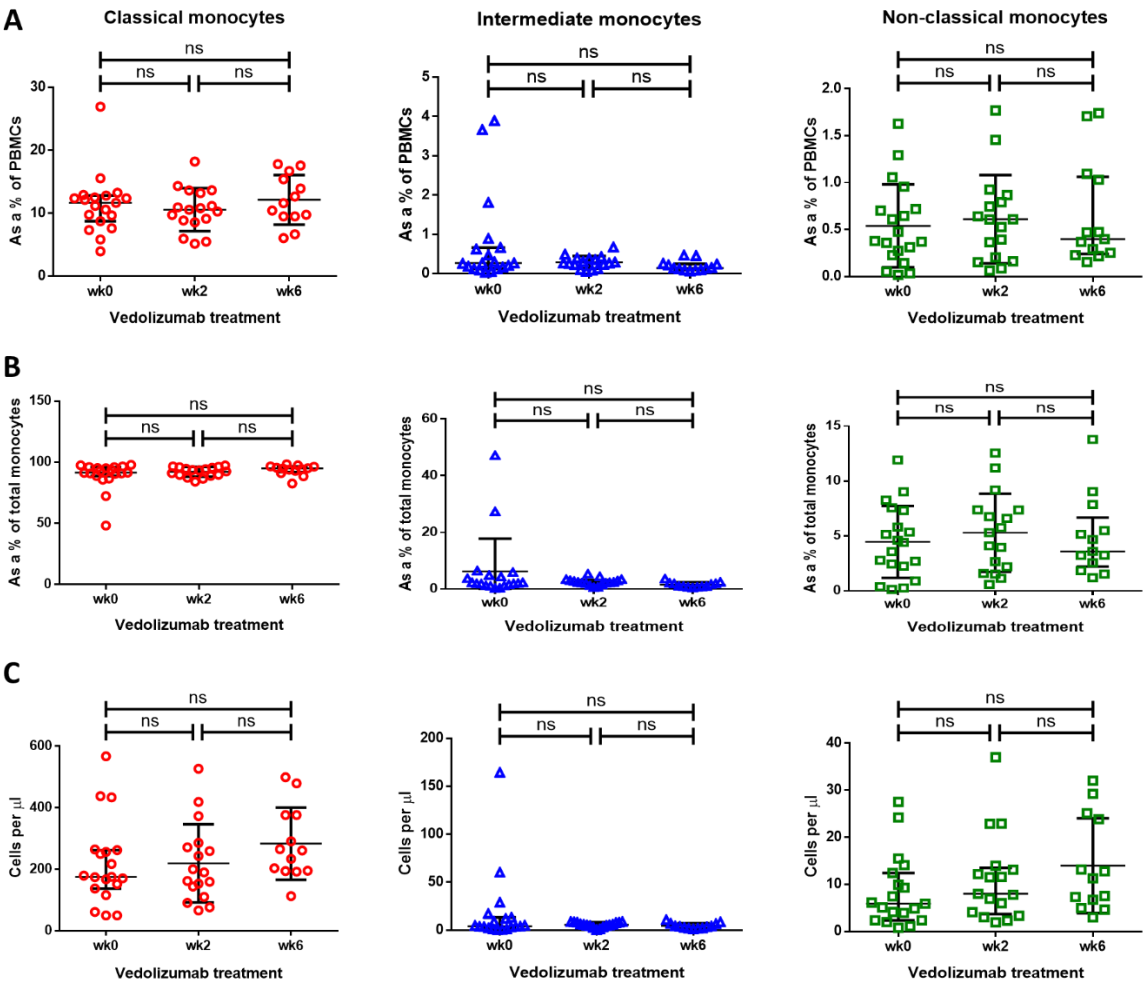

Figure 5.11: The effect of vedolizumab therapy on circulating monocyte subset distribution. Whole blood from IBD patients (n=19) starting vedolizumab treatment were labelled with anti-HLA-DR, anti-CD14, and anti-CD16 antibodies to distinguish the monocyte subsets before acquiring on the flow cytometer. Monocyte subset distribution and cell number were determined at baseline and after two and six weeks of treatment. Monocyte subset distribution was calculated as **A)** percentage of PBMCs, **B)** percentage of total monocyte, and **C)** absolute cell number. Mean and SD are displayed for normally distributed data sets, while median and IQR are displayed for non-normally distributed data sets. Data were analysed statistically by RM one-way ANOVA for normally distributed data sets, while a Friedman test was used for non-normally distributed data sets.

The presumed mechanism of action of vedolizumab is primarily to block effector T cell recruitment to the intestine. Therefore, we wished to determine whether an impact of vedolizumab on circulating T cells could be detected over the six weeks of treatment in this study. First, the distribution of β7+ (excluding CD103+ cells) CD45RA- T cells was compared between 16 healthy donors and 14 IBD patients with active disease. Next, the distribution of β7+CD45RA- T cells were assessed in the same 14 IBD patients at baseline and after two and six weeks of treatment.

A significant reduction in the number of β7 expressing CD8+ ($p = 0.0300$) and CD4+ ($p = 0.0138$) T cells compared with healthy controls was seen at baseline, which agrees with previous findings in IBD patients (Hart et al. 2004a; Hart et al. 2004b). Stratifying the IBD cohort into CD and UC did not reveal any significant associations (Appendix 11a).

There was no significant change in either population after two weeks or six weeks of vedolizumab therapy (Figure 5.12). Stratifying the IBD cohort into CD and UC or responders and non-responders did not reveal any significant associations (Appendix 11b).

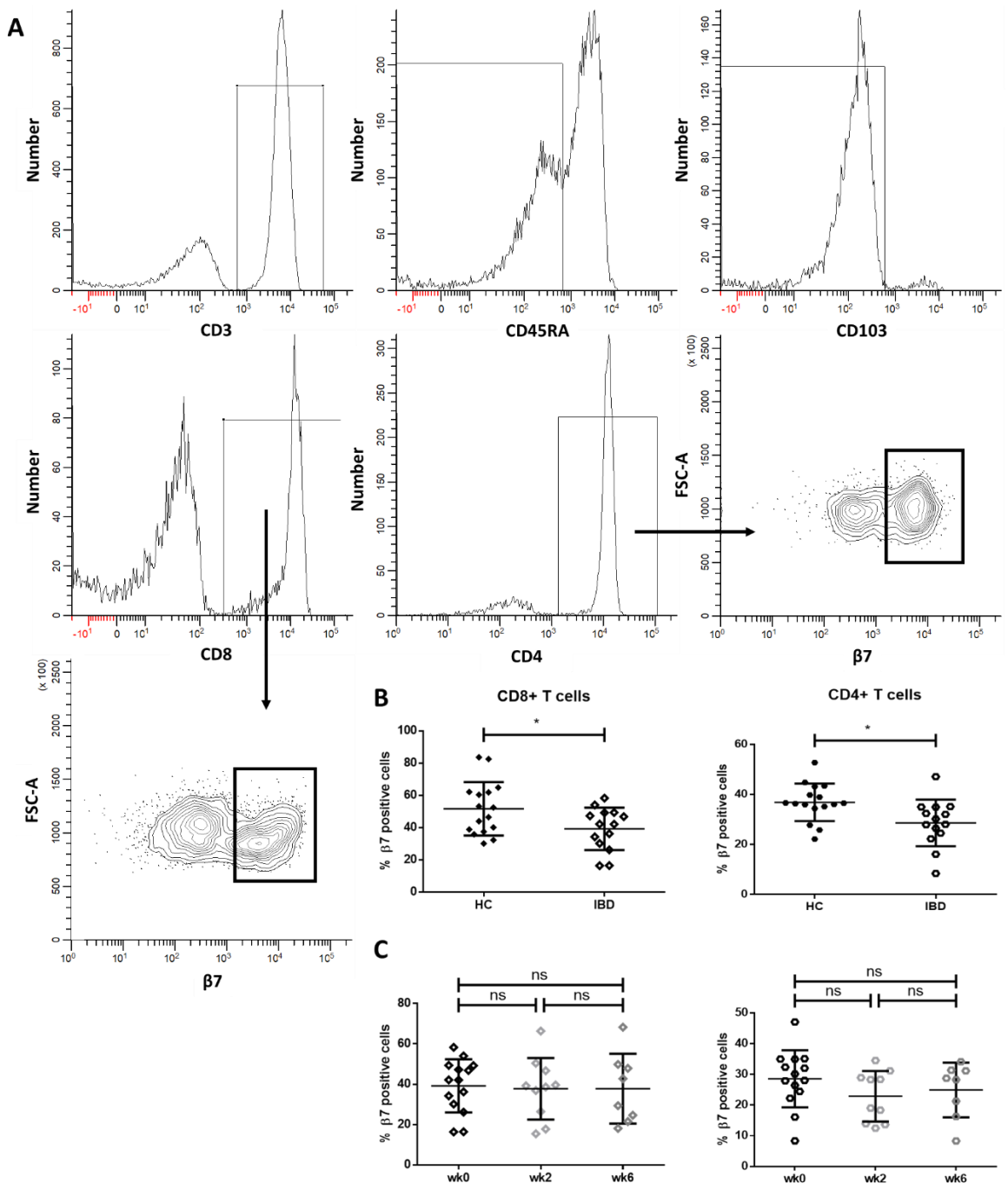

Figure 5.12: The effect of vedolizumab therapy on circulating β7+ CD4 and CD8 T cell distribution. Whole blood from healthy donors (n=16) and IBD patients (n=14) with active disease were labelled with anti-CD3, anti-CD45RA, anti-CD8, and anti-CD4 antibodies to distinguish CD45RA- CD8+ and CD4+ T cells (excluding CD103+ cells), and anti-β7 antibody before acquiring on the flow cytometer. The proportion of β7 expressing CD8+ and CD4+ T cells was calculated as a percentage of total T cells. **A)** gating strategy for assessing β7 expression on T cells**. B)** proportion of β7 expressing CD8+ and CD4+ T cells in health and disease. **C)** proportion of β7 expressing CD8+ and CD4+ T cells at baseline and after two and six weeks of treatment. Mean and SD are displayed for normally distributed data sets, while median and IQR are displayed for non-normally distributed data sets. Data were analysed statistically by RM one-way ANOVA for normally distributed data sets, while a Friedman test was used for non-normally distributed data sets. $p \leq 0.05$* $p \leq 0.01$** $p \leq 0.001$*** $p \leq 0.0001$****.

5.5 Discussion

The primary aim of this chapter was to determine differences in IL-10 responsiveness of monocyte subsets between healthy individuals and IBD patients, and identify any differences in signalling components in the IL-10 signalling pathway between health and IBD. In addition, monocyte subset distribution was also compared between healthy individuals and IBD patients, and a potential role for $\alpha4\beta7$ integrin in monocyte recruitment to the intestine explored.

Fate mapping techniques, as well as studies in CCR2-deficient mice, have shown that, at least in part, the intestinal Mϕ pool requires constant replenishment by circulating monocytes (Yona et al. 2013; Bain et al. 2014). During steady-state, newly arrived Ly6C^{hi} monocytes lose their inflammatory properties to give rise to regulatory Mϕs, which display characteristics, including constitutive IL-10 production and bacterial clearance without pro-inflammatory cytokine production, that would promote immune homeostasis (Bain et al. 2014). However, during inflammation, this pathway is disrupted, and the Ly6C^{hi} cells become arrested at an intermediary stage of differentiation resulting in an accumulation of cells that retain their ability to respond to TLR ligands; these inflammatory Mϕs are likely to be contributing to the inflammation (Bain et al. 2013). In humans, an expansion in the proportion of CD14+ Mϕs that retain their capacity to respond to TLR stimulation has been reported in CD patients (M. C. Grimm et al. 1995; Kamada et al. 2008; Lissner et al. 2015; Rugtveit et al. 1997; Thiesen et al. 2014), which resembles the model of intestinal inflammation described in mice. The signals responsible for the fate of the newly recruited monocytes are unknown. The studies reviewed in the introduction demonstrate that TGFβ and IL-10 act synergistically to imprint the regulatory phenotype of intestinal Mϕ.

There is increasing evidence in both mice and humans that systemic signals from the intestine during inflammation cause functional changes to circulating cells (Arts et al. 2018; Askenase et al. 2015; Christ et al. 2018; Mitroulis et al. 2018; Smith et al. 2009; Sanders et al. 2014). Together with the data that IL-10 has a critical non-redundant role in IL-10 KO mice and VEO-IBD patients, sparked the interest in

investigating IL-10 response of intestinal Mϕ and their precursors. Classical monocytes are said to be the human equivalent of LYC6^{hi} cells based on gene expression profiles (Ingersoll et al. 2010), therefore, classical monocytes are likely to be a major source of intestinal Mϕs (Bain et al. 2014). In the previous chapter, classical monocytes showed a robust response to IL-10, which suggests an important role for IL-10 in regulating their inflammatory properties once recruited to an IL-10 rich environment like the intestine. How this response changes in the context of intestinal inflammation was the subsequent area of interest.

First, the inflammatory capacity of the monocyte subsets was compared between healthy controls and IBD patients to ensure that IL-10 response was measured against the same inflammatory activity, as suggested by experiments in which IL-1β was measured, stronger responses are harder to inhibit. Indeed inflammatory signals from the intestine have been shown to affect the phenotype of monocytes from development in the BM (Askenase et al. 2015). However, there was no significant difference in the capacity of monocytes from healthy controls and IBD patients to produce either TNFα or IL-10 following LPS stimulation. A low frequency of monocytes produced IL-10 but not TNFα in the absence of stimulation but again the was no difference between cells from patients and controls. The findings reported here agree with Thiesen et al., 2014 and Begue et al., 2011 who also found no significant differences in pro-inflammatory cytokine production by individual monocyte subsets in healthy controls and CD patients.

A reduced response to IL-10 was found in classical monocytes of IBD patients. The release from IL-10 control may be a 'normal' feature of immune responses allowing a response to be mounted against a real challenge. However, a reduction in IL-10 response could favour the accumulation of inflammatory Mϕs, which may contribute to the sustainment of intestinal inflammation. The reduction in IL-10 response in circulating classical monocytes reveals that systemic signals, as well as the local environment, can have an impact on monocyte fate. This is in support of previous observations of systemic changes in monocytes during intestinal inflammation (Arts et al. 2018; Askenase et al. 2015;

Christ et al. 2018; Mitroulis et al. 2018; Smith et al. 2009; Sanders et al. 2014). Intermediate and non-classical monocytes showed no significant difference in their response to IL-10 between health and IBD. However, both of these subsets are relatively resistant to IL-10 inhibition in health compared with classical monocytes. Intermediate monocytes express CCR2 (Wong et al. 2011), indicating a potential capacity to be recruited to the intestine, via the CCR2-dependent process utilised by classical monocytes, where their pro-inflammatory properties and resistance to regulatory signals may favour differentiation into inflammatory Mϕs. However, the contribution of intermediate monocytes to the intestinal Mϕ pool and how this changes during inflammation has not been explored due to the lack of unique identifiers, as CD16 may be shed upon entry into the intestine making their identification challenging. Non-classical monocytes are likely to fulfil similar roles $Ly6C^{lo}$ cells, which have not yet been implicated in intestinal inflammation.

The reduced response to IL-10 in classical monocytes of IBD patients is an important observation. However, the study consists of small numbers and the magnitude of the difference in response to IL-10 between healthy individuals and IBD patients was also relatively small, therefore, a larger cohort is required to verify this finding. The genome of patients included in the cohort will be sequenced to test whether the donors express genetic variants along the IL-10R pathway that could impact IL-10 response. However, a reduced response to IL-10 was a common feature of the IBD patients studied here, such genetic variation is unlikely to be a significant contributor to the differences observed.

Proximal signalling components of the IL-10R signalling pathway were investigated for suboptimal activity in IBD patients that could explain the reduced IL-10 response in classical monocytes. In contrast to the functional response, classical monocytes showed enhanced expression of IL-10Rα in IBD patients. This again demonstrates systemic changes in monocytes caused by signals from the intestine during inflammation in support of previous observations (Arts et al. 2018; Askenase et al. 2015; Christ et al. 2018; Mitroulis et al. 2018; Smith et al. 2009; Sanders et al. 2014). The enhanced IL-10Rα expression in classical monocytes does not correlate with their functional response, providing

further evidence that the response to IL-10 is not determined by the level of receptor on the surface. The enhanced IL-10Rα expression may be an example of 'negative feedback' in which the immune system is attempting to control inflammation by upregulating the expression level of a receptor that respond to regulatory signals. However, if this is the case, this attempt by the immune system to enhance sensitivity to IL-10 seems to appear unsuccessful at least with regard to LPS-induced TNFα production, indicating the need to consider a defect further downstream. Phosphorylation of STAT3 is also enhanced in classical monocytes of IBD patients, which is not due to greater STAT3 availability since staining for T-STAT3 was equivalent. These data indicate that in IBD, phosphorylation of STAT3 in response to IL-10 exposure is further enhanced in classical monocytes as a result of IL-10Rα expression above the relatively low baseline level reported in Chapter 4. The expression levels of IL-10Rα on intermediate and non-classical monocytes does not differ between IBD patients and healthy controls. A failure to enhance IL-10R in the face of inflammation may indicate that these cells are poorly controlled and can actively contribute to the disease process. The capacity of intermediates and non-classical monocytes to phosphorylate STAT3 remains unchanged in IBD patients, which reflects the unaffected expression levels of the IL-10Rα in both subsets.

Differences in proximal signalling events do not explain the reduced response to IL-10 in classical monocytes in IBD, therefore, a target further downstream was investigated. As discussed in the previous chapter, a study by Kontoyiannis et al., 2001 speculated that the availability of a pool of pre-formed SOCS3 protein could be a source of rapid inhibition of inflammatory responses in the period during which STAT3 promotes gene expression and protein synthesis to generate new SOCS3 protein. Investigating SOCS3 protein levels directly was hindered by low cell numbers, and therefore mRNA expression at baseline was used as a potential surrogate measure. *SOCS3* mRNA levels showed a trend towards increased expression in IBD patients, which is consistent with the observed increase in IL-10Rα expression and STAT3 phosphorylation but does not provide a mechanism for the reduced response to IL-10 in classical monocytes of IBD patients. It would also be worthwhile to investigate the

level of IL-10 induced *SOCS3* mRNA or protein expression using pooled samples across donors to overcome the limitations of low cell numbers.

The signalling components investigated thus far do not provide a clear mechanism for the reduced response to IL-10 in classical monocytes of IBD patients, indicating that unknown mechanisms are regulating IL-10 responsiveness. A global phosphoproteomic analysis could be used to identify other proteins that are phosphorylated following exposure to IL-10 and any differences between cells from healthy individuals and IBD patients.

In humans, there is evidence that recruitment of monocytes is enhanced at sites of intestinal inflammation (M. Grimm et al. 1995) and this might be predicted to impact upon monocyte numbers or subset distribution in the circulation. To seek evidence of systemic changes to monocyte subset distribution, absolute cell numbers were compared between healthy controls and IBD patients. The observation that the non-classical monocytes, but not classical or intermediate cells, are significantly reduced in proportion and cell number in IBD patients, is in contrast to previous findings. Thiesen et al. 2013 and Grip et al., 2006 both reported an increase in the proportion of intermediate monocytes as a percentage of total monocytes but absolute cell numbers were not examined. Presenting the data as proportions and not absolute cell numbers means that the proportion of intermediate monocytes could be affected by changes in another subset. These conflicting observations could also be a result of the different gating strategies used to characterise the monocyte subsets: both Thiesen et al. 2013 and Grip et al., 2006 did not exclude HLA-DR negative populations, therefore, could have NK cell contamination in the CD16+ gate. Another possible explanation could be that different types of patients were analysed: the cohort selected by Thiesen et al. 2013 and Grip et al., 2006 were CD patients with active disease, while the IBD cohort in this study included a combination of CD and UC patients that were active or in inactive. However, stratification of these data into the individual subgroups did not show any significant differences based on disease type or activity or even treatment groups. This suggests that the systemic effects of intestinal inflammation are long-lasting and

persistent into subsequent periods of inactive, which may explain the relapsing pattern common in IBD patients. Fewer non-classical monocytes were also observed in a separate cohort of IBD patients before starting vedolizumab treatment. The replicability of this observation further supports the robust nature of this observation.

The reduction in circulating non-classical monocytes observed in IBD patients could be due to a number of reasons. One explanation may be that these cells are being recruited into the inflamed intestine as this population has been shown to be recruited into inflamed tissues, contributing initially to the inflammatory response before switching on reparative functions (Auffray et al. 2007). Another possible explanation for the loss of non-classical monocytes in blood could be that fewer classical monocytes are available to mature into non-classical monocytes. This could be explained by a surge in recruitment of monocytes into sites of intestinal inflammation (M. Grimm et al. 1995). No change in the abundance of classical monocytes was observed in IBD patients, which might have been expected if there was enhanced recruitment to the intestine. However, an increase in classical monocytes leaving the circulation could be compensated by enhanced monocyte development and release from the BM, in addition to arresting differentiation into non-classical monocytes. A rapid release of monocytes from the BM has been observed following systemic inflammation (Patel et al. 2017). The impact of intestinal inflammation on the half-life of the monocyte subsets has not been studied but enhanced cell death of non-classical monocytes in the IBD patients could also account for their reduced abundance. Alternatively, changes to the endothelial wall induced by intestinal inflammation may make the non-classical monocytes more adherent to the surface and appear less abundant in the blood. This adhesion to the endothelial wall has been demonstrated by the selective mobilisation of CD14+CD16++ monocytes by exercise (Steppich et al. 2000). The loss of non-classical monocytes from the circulation could have important implications for tissue repair, as this is their ultimate function after recruitment, which may perpetuate tissue damage during intestinal inflammation (Auffray et al. 2007). The implications of altered numbers of circulating Ly6C^{lo} monocytes has been demonstrated: mice fed a high-fiber diet showed enhanced generation of Ly6C^{lo}

monocytes and a subsequent increase in the numbers of alternatively activated Mϕs in the airways that displayed a limited capacity to produce CXCL1, which reduced neutrophil recruitment, thus limiting tissue immunopathology during infection (Trompette et al. 2018).

It is difficult to understand the implications of any changes seen in the immune composition of the circulating blood in IBD patients. Fate mapping is not accessible for human intestinal studies, therefore, investigating the impact of therapies that target immune cell trafficking to the intestine, by following the immune composition of circulating blood from patients undergoing this treatment, is one way of gaining information about the key molecules involved in recruitment of different cell populations under inflammatory conditions. In mice, CCL2-depend recruitment has been implicated using anti-CCR2 antibodies to ablate Ly6C^{hi} monocytes, which alleviated DSS-induced colitis (Zigmond et al. 2012). In humans, enhanced expression and production of CCL2 has been observed in IBD patients (Grimm et al. 1996). Monocytes recruited in an $\alpha4\beta7$-dependent manner has also been implicated in intestinal inflammation in studies using β7 integrin-deficient mice (Schippers et al. 2015). However, expression of $\alpha4\beta7$ by human monocyte subsets and its potential role in monocyte entry to the inflamed intestine had not been previously explored. The data presented in this thesis showed that classical and intermediate monocytes express $\alpha4\beta7$. However, the data does not show if the integrin is in an active conformation, and therefore measuring binding to mucosal vascular addressin cell adhesion molecule 1/MAdCAM-1 (direct leukocytes into mucosal and inflamed tissues) would be informative. To assess the possible contribution of $\alpha4\beta7$-dependent monocyte recruitment to the intestine during inflammation, monocyte subset distribution was monitored in patients undergoing vedolizumab treatment. The underlying assumption was that if blockade of $\alpha4\beta7$ with vedolizumab impacted on monocyte recruitment to the intestine this would impact on populations in the circulation. However, no significant change was seen in proportion or absolute cell number of any monocyte subset over the six weeks of vedolizumab treatment irrespective of clinical response. These data may be taken to indicate that $\alpha4\beta7$ may not play a major role in monocyte recruitment to the intestine during inflammation or, if it does, that there is redundancy which means that other pathways

can operate when $\alpha 4\beta 7$ is blocked. However, caution should be exercised before drawing this conclusion as no changes in blood T cells, the presumed primary target of Vedolizumab, were also observed over the course of the study. The assumption that blocking recruitment would lead to measurable changes in the blood may be incorrect, perhaps to compensatory homeostatic mechanisms or that such changes do occur but they take longer than six weeks, the last time-point analysed, to become evident. Patients achieve clinical remission after 14 weeks of vedolizumab therapy (Amiot et al. 2016; Shelton et al. 2015). An earlier time-point was chosen for our analysis in order to separate the direct effects of the drug on trafficking from later effects arising from resolving inflammation. Although, based on animal studies, intestinal monocyte-derived populations turnover rapidly (Bain et al. 2014), six weeks may have been too early to detect any effect. In future experiments, patients may need to be followed for a longer time period to see the impact of vedolizumab treatment on populations of circulating immune cells.

5.6 Conclusion

Classical monocytes showed a reduced response to IL-10 in IBD patients. As the main source of replenishment for intestinal Mϕs, the capacity to regulate the inflammatory properties of these precursors is important. The reduced response to IL-10 inhibition could favour the accumulation of inflammatory Mϕs, which may contribute to intestinal inflammation. Amongst the monocyte subsets, it is only the classical monocytes, which have a reduced response to IL-10, supporting the importance of this 'defect' to responses in the mucosa. Signalling components, including IL-10Rα expression, STAT3 phosphorylation, and *SOCS3* mRNA expression displayed differences between IBD patients and healthy control, supporting the concept that systemic changes occur in monocytes during intestinal inflammation but the direction of change (i.e. increase in IBD) was opposite to the functional response to IL-10, and therefore cannot explain the lack of response to IL-10 in IBD. Understanding how intestinal inflammation affects IL-10 responsiveness systemically in these cells and how this perpetuates intestinal inflammation may help generate new therapeutic targets.

Chapter 6: IL-10 response in intestinal Mo/moMϕs

6.1 Chapter summary

In the previous chapter, classical monocytes (CD14+) were shown to have a reduced response to IL-10 in IBD patients compared to healthy controls. The relevance of this finding in blood for CD14+ monocyte-derived cells in the intestinal mucosa was next explored. Firstly, Mo/moMϕs were identified in LPMCs extracted from intestinal biopsies. Expression of HLA-DR, CD14, and CD64 was used to distinguish MP populations: P1 (HLA-DR^{hi}CD14^{hi}CD64+), P2 (HLA-DR^{hi}CD14^{lo}CD64+), and P3 (HLA-DR^{hi}CD14-CD64-). The relative proportion of these Mo/moMϕs was compared between mucosa from non-IBD patients and inflamed mucosa from UC and CD patients. The distribution of the Mo/moMϕs in mucosa from non-IBD patients and inflamed mucosa from patients with UC were comparable, whereas inflamed mucosa from patients with CD had a significant increase in the proportion of P2 and decrease in P1.

Both P1 and P2 in mucosa from non-IBD patients produced TNFα in unstimulated cultures, and this response was significantly enhanced in both populations following LPS stimulation. The proportion of TNFα+ cells and the level of TNFα production (MFI) were both significantly higher in both unstimulated and LPS-stimulated P1 compared to P2. The magnitude of the increase in the level of TNFα production upon stimulation was also greater in P1 than P2. IL-10 at 2ng/ml inhibited TNFα production by both P1 and P2. In contrast to findings with classical blood monocytes where inhibition was only partial at this concentration, the response of P1 and P2 was completely inhibited by IL-10 in cells from 50% and 25% of samples respectively. There was also complete inhibition of TNFα production in the Mo/moMϕs in inflamed mucosa from patients with CD and UC patients, limiting the sensitivity of the assay and making it difficult to conclude with respect to differences in response to IL-10 between health and disease. Reducing the concentration of IL-10 would increase the sensitivity of the assay and allow for a more meaningful comparison of IL-10 responses.

6.2 Introduction

Human intestinal Mϕs are characterised by their expression of surface markers including CD64+, CX_3CR1^{hi}, and $MHCII^{hi}$ (reviewed by Mowat & Bain, 2011). Overlap in the expression of markers with DCs had previously made studying the role of intestinal Mϕs challenging. This has driven the use of multi-parameter analysis combining expression of surface markers with functional characteristics. The functional characteristic of intestinal Mϕs in humans include high levels of phagocytosis, bactericidal ability, and anergy to TLR activation (Smythies et al. 2005).

In mice, fate-mapping experiments revealed that monocytes are continuously recruited to the intestine to replenish at least some of the Mϕ pool in steady-state (Yona et al. 2013; Bain et al. 2014). In humans, turnover of Mϕ in the small intestine was determined by analysing tissue from pancreas transplant patients who receive a small segment of the duodenum along with the transplanted pancreas (Bujko et al. 2017). All donor-derived Mϕ subsets were completely replaced by recipient cells over time, although, distinct populations with different rates of replacement were identified, consistent with the mouse evidence for constant replenishment of at least some intestinal Mϕ.

Bain et al., 2013 also showed that the newly recruited $Ly6C^{hi}$ monocytes differentiate into Mϕ in a context-dependent manner. In the absence of inflammation, these newly recruited monocytes acquire properties as they mature into regulatory Mϕs, including constitutive IL-10 production and anergy to TLR activation. In the presence of inflammation, this process is disrupted, and the recruited monocytes get 'stuck' at an intermediate stage and retain their inflammatory properties. Similarly, in humans, phenotypic analysis of Mϕs from the human ileum was consistent with the maturation of $CD14^{hi}$ cells through intermediate stages to $CD14^{lo}$ cells (Bain et al. 2013). An accumulation of the intermediary population was observed in the inflamed ileum of CD patients, reflecting the observations in mice (Bain et al. 2013). Multiple studies have observed an accumulation of CD14+ cells in the inflamed mucosa of CD patients compared to healthy controls (Kamada et al. 2008; Lissner et al. 2015; Rugtveit et al. 1997; Thiesen et al. 2014). This is consistent with the concept that during

inflammation a disruption in monocyte cell differentiation into resident Mϕs occurs, perpetuating the intestinal inflammation. In addition, there is direct evidence that there is enhanced monocyte recruitment to the inflamed mucosa (Grimm *et al.*, 1995).

The environmental cues that determine monocyte differentiation into regulatory or inflammatory Mϕs are poorly understood. IL-10 and TGFβ have been shown to provide crucial signals during monocyte differentiation into resident Mϕs (Schridde et al. 2017; Shouval et al. 2014; Zigmond et al. 2014; Smythies et al. 2010). Importantly, Schriddle et al., 2017 showed, by comparing the global transcriptome of TGFβR-deficient and IL10R-deficient Mϕs, that TGFβ and IL-10 imprint distinct properties of intestinal Mϕs. Collectively, these studies showed that TGFβ and IL-10 play important non-redundant roles in regulating intestinal inflammation with Mϕs as targets.

There have been few studies on the factors that control the differentiation of Mϕs within the human intestine. TGFβ produced by stromal cells has been shown to be critical in inducing the regulatory properties of intestinal Mϕ during monocyte differentiation in vitro (Smythies et al. 2005). Individuals with LoF mutations in the IL-10R gene develop VEO-IBD and display no suppressive effect of IL10 in purified CD14+ monocytes and MDCs after stimulation (Begue et al. 2011; Glocker & Kotlarz 2009; Mao et al. 2012). These support the concept that IL-10 and TGFβ perform important non-redundant roles in regulating intestinal inflammation with unknown targets.

Identifying the factors that control the balance of inflammatory and regulatory functions in immune cells, can lead to new IBD therapies. For instance, T cells from inflamed mucosa displayed enhanced SMAD7 expression (Fantini et al. 2009), inhibiting their ability to respond to TGFβ, which has been targeted with an anti-sense drug (Mongersen) in order to restore responsiveness to TGFβ (Monteleone et al. 2015). Similarly understanding how IL-10 responsiveness is controlled in IBD patients could lead to therapeutic interventions involving the IL-10 signalling pathway.

The aim of the work described in this chapter was to identify MP populations in the human intestine and determine their response to IL-10 in health and disease.

6.3 Aims

1. Identify human intestinal MP populations.
2. Compare the distribution of these populations in non-IBD and inflamed IBD mucosa.
3. Determine the IL-10 responsiveness of intestinal Mo/moMϕs in health.
4. Compare the response to IL-10 in intestinal Mo/moMϕs from non-IBD and inflamed IBD mucosa.

6.4 Results

6.4.1 Identifying intestinal Mo/moMϕs

First, a gating strategy was developed to identify human intestinal Mo/moMϕs. LPMCs extracted from colonic biopsies from a patient with no history of IBD and no visible inflammation (non-IBD patient) were labelled with anti-CD45, anti-HLA-DR, and anti-CD14 antibodies. Leucocytes were gated based on CD45 expression (Figure 6.1 A). LPMCs were then gated based on FSC and SSC (Figure 6.1 B), excluding the dead cells using fixable dye (Appendix 12). Doublet discrimination was carried out (Figure 6.1 C and D). HLA-DR^{hi} expression was used to distinguish large APCs (Figure 3.1 E). Finally, CD14 marker expression was used to distinguish three intestinal large HLA-DR^{hi} populations: P1 (CD14^{hi}), P2 (CD14^{lo}), and P3 (CD14-) (Figure 3.1 F). Corresponding isotype controls were used to gate each marker (Appendix 13). The distribution of P1 and P2 will be compared between non-IBD, UC and CD patients with active disease in Figure 6.5.

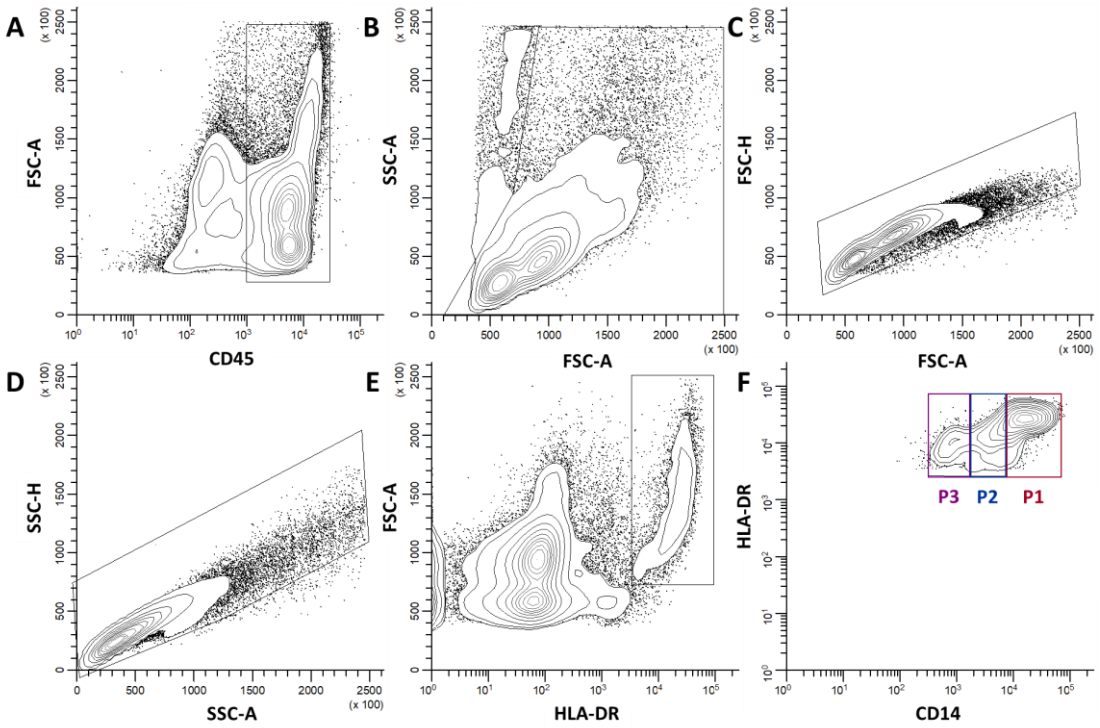

Figure 6.1: Gating strategy for the identification of human intestinal Mo/moMϕs. LPMCs extracted from colonic biopsies from a non-IBD patient were labelled with anti-CD45, anti-HLA-DR, and anti-CD14 antibodies; intestinal Mo/moMϕs were then identified by flow cytometry. **A)** leucocytes were gated based on CD45 expression. **B)** live LPMCs were gated based on FSC and SSC. **C, D)** doublet discrimination was carried out based on size and granularity. **E)** HLA-DR labelling was then used to distinguish large APCs. **F)** three intestinal Mo/moMϕs were distinguished based on their CD14 expression labelled P1, P2, and P3.

The phenotype of P1, P2, and P3 was investigated further using additional markers to confirm their identity and purity. LPMCs from a non-IBD patient where labelled with anti-CD45, anti-HLA-DR, and anti-CD14 antibodies to distinguish the intestinal Mo/moMϕs, and additional antibodies: anti-CD64, anti-CD206, anti-CCR2, and anti-CX_3CR1. Expression levels of each marker were compared for each population to the isotype control for the total HLA-DR+ population using overlaid histograms (Figure 6.2 A), and bar charts showing expression levels of each marker on the Mo/moMϕs in relation to their corresponding isotype control.

CD64 expression has been used to distinguish between intestinal Mo/moMϕs (CD64+) and DCs (CD64-) (Langlet et al. 2012; Tamoutounour et al. 2012). Both P1 and P2 express CD64 whereas P3 do not, suggesting that only P1 and P2 are Mo/moMϕs. CD206, CX_3CR1, and CCR2 were used as markers of MP maturation because CD206 and CX_3CR1 are upregulated during monocyte differentiation into intestinal Mϕs, and CCR2 is downregulated in mouse (reviewed by Mowat & Bain, 2011). However, all three markers are more highly expressed in P1 than P2. Collectively, these data suggest that P1 and P2 are MP populations but the direction of maturation cannot be clearly defined. The spread of the histograms indicates some contamination of the populations, which is expected with the overlap in marker expression between the APCs.

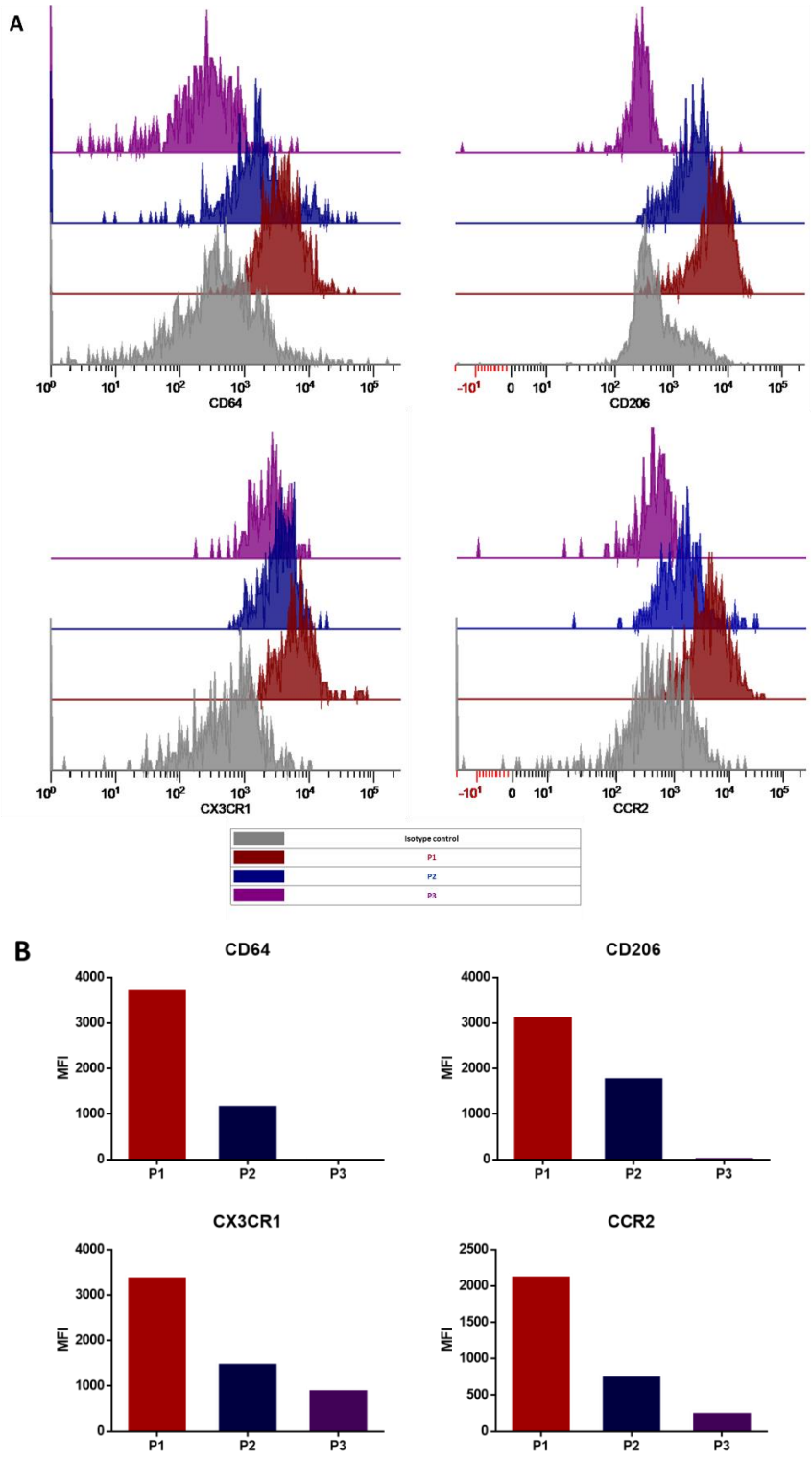

Figure 6.2: Characterisation of the human intestinal Mo/moMϕs. LPMCs extracted from colonic biopsies from a non-IBD patient (n=1) were labelled with anti-CD45, anti-HLA-DR, and anti-CD14 antibodies to distinguish the intestinal Mo/moMϕs. Additional antibodies were used to further characterise the intestinal Mo/moMϕs, including anti-CD64, anti-CD206, anti-CX_3CR1, and anti-CCR2. The sample was then acquired on the flow cytometer. **A)** overlays represent the expression levels of each marker on the Mo/moMϕs in relation to the isotype control for the total HLA-DR+ population (grey histogram) for illustration. **B)** expression levels of each marker on each Mo/moMϕs population in relation to its population specific isotype-matched control.

Next, the functional characteristics of the intestinal Mo/moMϕs were investigated. One functional characteristic of intestinal Mϕs is that they are highly phagocytic (Smythies et al. 2005), and therefore the phagocytic capacity of the intestinal Mo/moMϕs was investigated. LPMCs extracted from colonic biopsies from a non-IBD patient were incubated at 4°C (control) and 37°C in the presence of FITC-labelled microspheres 2.00µm (Polysciences Inc.) at a concentration of 10 microspheres per cell for 1.5 hours and detected via flow cytometry. Phagocytosis was quantified as the percentage of cells positive for FITC-labelled microspheres (above the control). P1 showed the highest proportion of phagocytic cells (Figure 6.3), indicating that P1 has a more Mϕ phenotype.

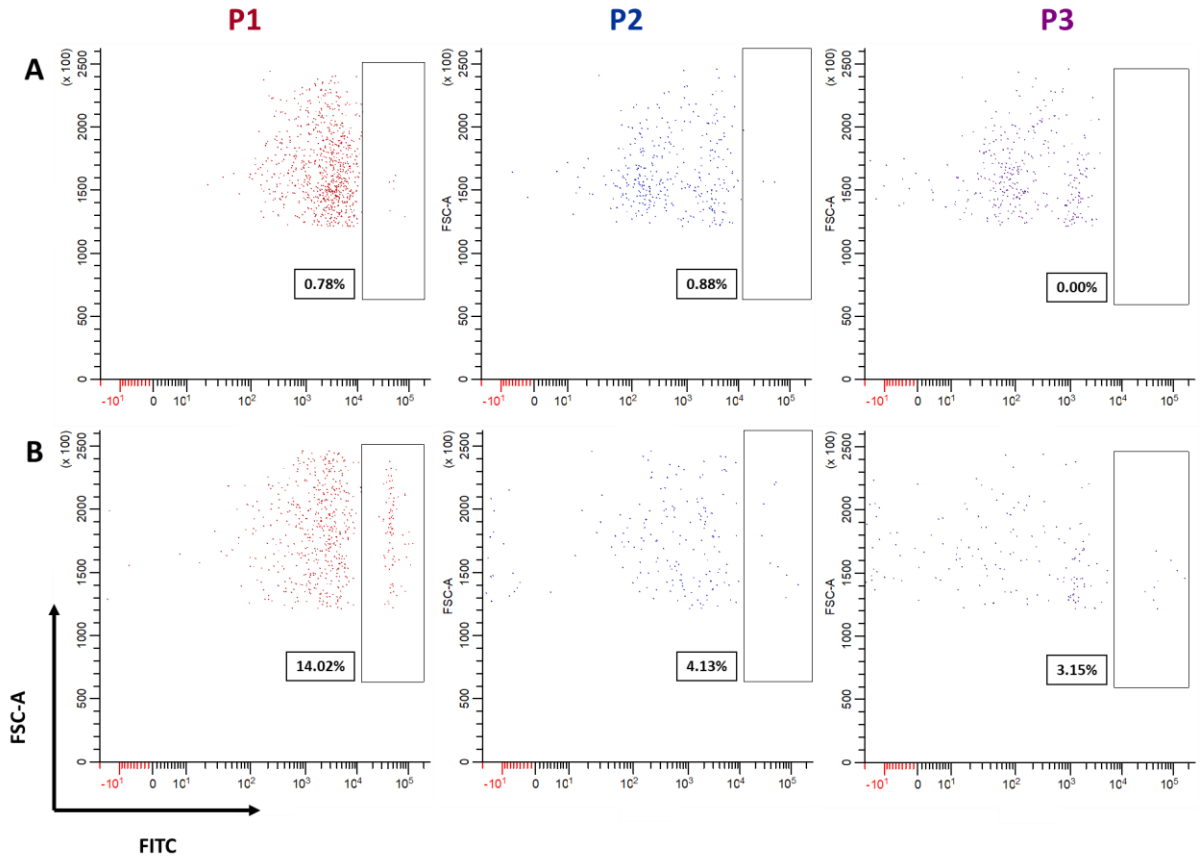

Figure 6.3: Phagocytic capacity of human intestinal Mo/moMϕs. LPMCs extracted from colonic biopsies from a non-IBD patient (n=1) were incubated at **A)** 4°C **B)** 37°C in the presence of FITC-labelled microspheres 2.00µm (Polysciences Inc.) at a concentration of 10 microspheres per cell for 1.5 hours. The LPMCs were then labelled with anti-CD45, anti-HLA-DR, and anti-CD14 antibodies to identify the intestinal Mo/moMϕs by flow cytometry.

The distribution of APC between P1, P2 and P3 was compared in LPMCs extracted from paired colonic and ileum endoscopic biopsies from the same non-IBD patient. There was a greater proportion of P1 cells in the LPMCs extracted from colonic biopsies than from ileal biopsies, which are the population of interest (Figure 6.4). In addition, colonic biopsies were more readily obtainable, and therefore were the focus of analyses going forward.

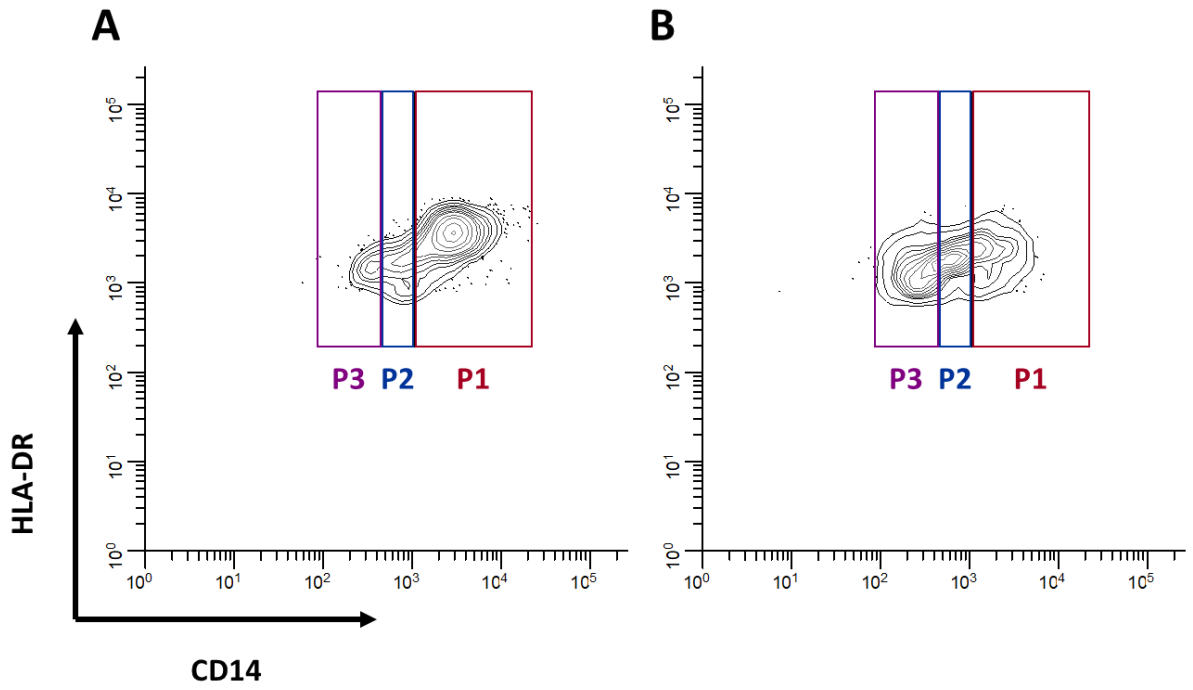

	Colon	Ileum
P1	72.89%	35.98%
P2	17.68%	27.63%
P3	7.95%	32.60%

Figure 6.4: Distribution of intestinal Mo/moMϕs from non-IBD colon vs ileum. LPMCs extracted from endoscopic biopsies from a non-IBD patient (n=1) were labelled with anti-CD45, anti-HLA-DR, and anti-CD14 antibodies to distinguish the intestinal Mo/moMϕs. The endoscopic biopsies were taken from **A)** the colon or **B)** the ileum.

6.4.2 P2 is increased proportionally in the inflamed mucosa of CD patients

The distribution of HLA-DR^{hi} cells between P1, P2, and P3 was compared between eight non-IBD patients, eight UC patients with active disease, and seven CD patients with active disease using LPMCs extracted from endoscopic biopsies. The distribution of the populations was assessed as a proportion of total HLA-DR^{hi} cells. The proportion of P1, P2 and P3 cells in colonic LPMC from non-IBD patients and UC patients with active disease was similar (Figure 6.5 A, B). However, P2 cells were enriched (p = 0.0016) at the expense of P1 cells (p = 0.0215) in CD patients with active disease (Figure 6.5 A, B).

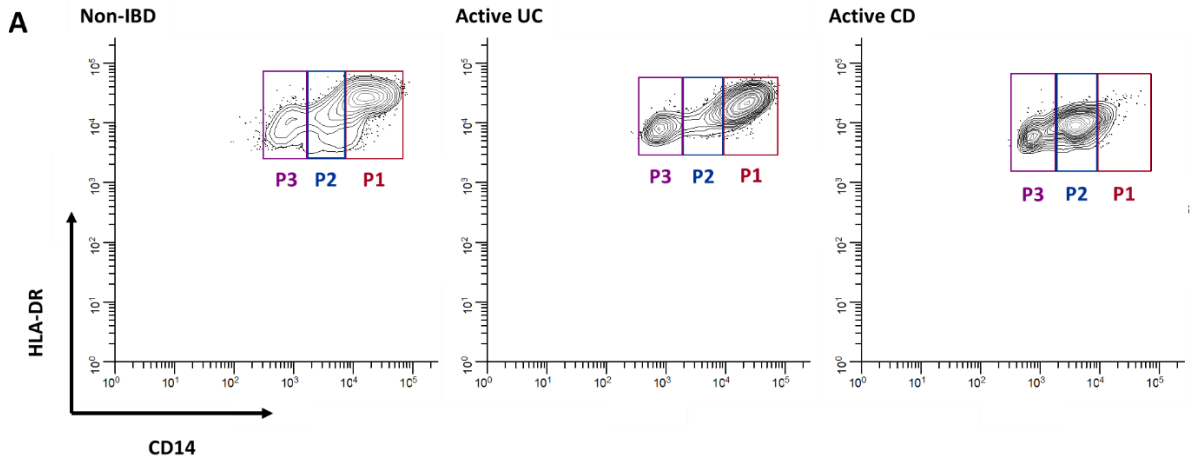

	HC	UC	CD
P1	64.36%	68.19%	16.42%
P2	18.45%	13.34%	48.54%
P3	16.82%	17.90%	34.63%

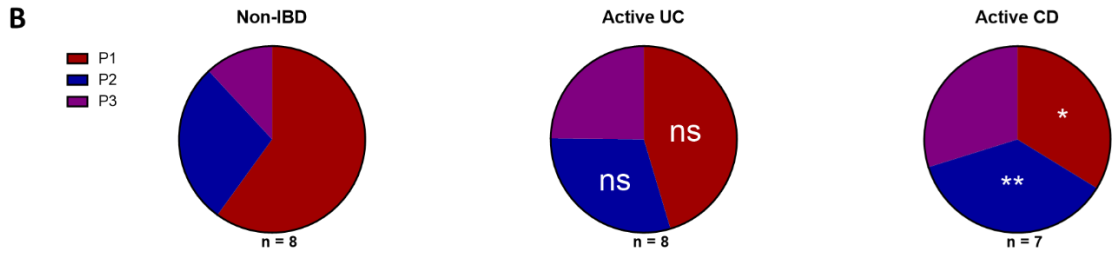

Figure 6.5: Distribution of intestinal Mo/moMϕs from non-IBD vs inflamed IBD colon. LPMCs extracted from endoscopic biopsies from non-IBD patients (n=8), UC patients (n=8) and CD patients (n=7) with active disease were labelled with anti-CD45, anti-HLA-DR, and anti-CD14 antibodies to distinguish the intestinal Mo/moMϕs before acquiring on the flow cytometer. The distribution of the populations was calculated as a percentage of total APCs. **A)** representative flow cytometry plots showing the distribution of intestinal Mo/moMϕs in non-IBD patients, CD and UC patients with active disease. **B)** distribution of intestinal Mo/moMϕs in non-IBD patients, CD and UC patients with active disease. CD and UC patients were compared to non-IBD patients for P1 and P2 using an ordinary one-way ANOVA. p ≤ 0.05* p ≤ 0.01** p ≤ 0.001*** p ≤ 0.0001****.

6.4.3 P1 have a higher capacity for TNFα production

The response of the intestinal Mo/moMϕs to LPS stimulation was compared in eight healthy individuals focusing on P1 and P2 but not P3 as this population was CD64 negative and unlikely to represent monocytes/Mϕs. LPMCs were stimulated with 1ng/ml LPS for three hours before staining for intracellular TNFα. TNFα production was quantified as the percentage of cells positive for TNFα (above the isotype control), and as a per cell level of TNFα production in the TNFα positive cells (MFI). Figure 6.6 A, B show representative flow cytometry plots of TNFα staining in P1 and P2 in unstimulated and LPS-stimulated cultures respectively. There was detectable TNFα production in unstimulated cultures of LPMC which was significantly upregulated upon LPS stimulation. In both unstimulated and LPS-stimulated cultures, TNFα production was greater in P1 than in P2 as assessed by either percent positive or MFI (Figure 6.6 C). The magnitude of the increase in TNFα upon LPS stimulation was greater in P1 as determined on a per cell basis (MFI) but not in terms of the proportion of cells making cytokine (Figure 6.6 D), and as a per cell level of TNFα production in the TNFα positive cells (MFI).

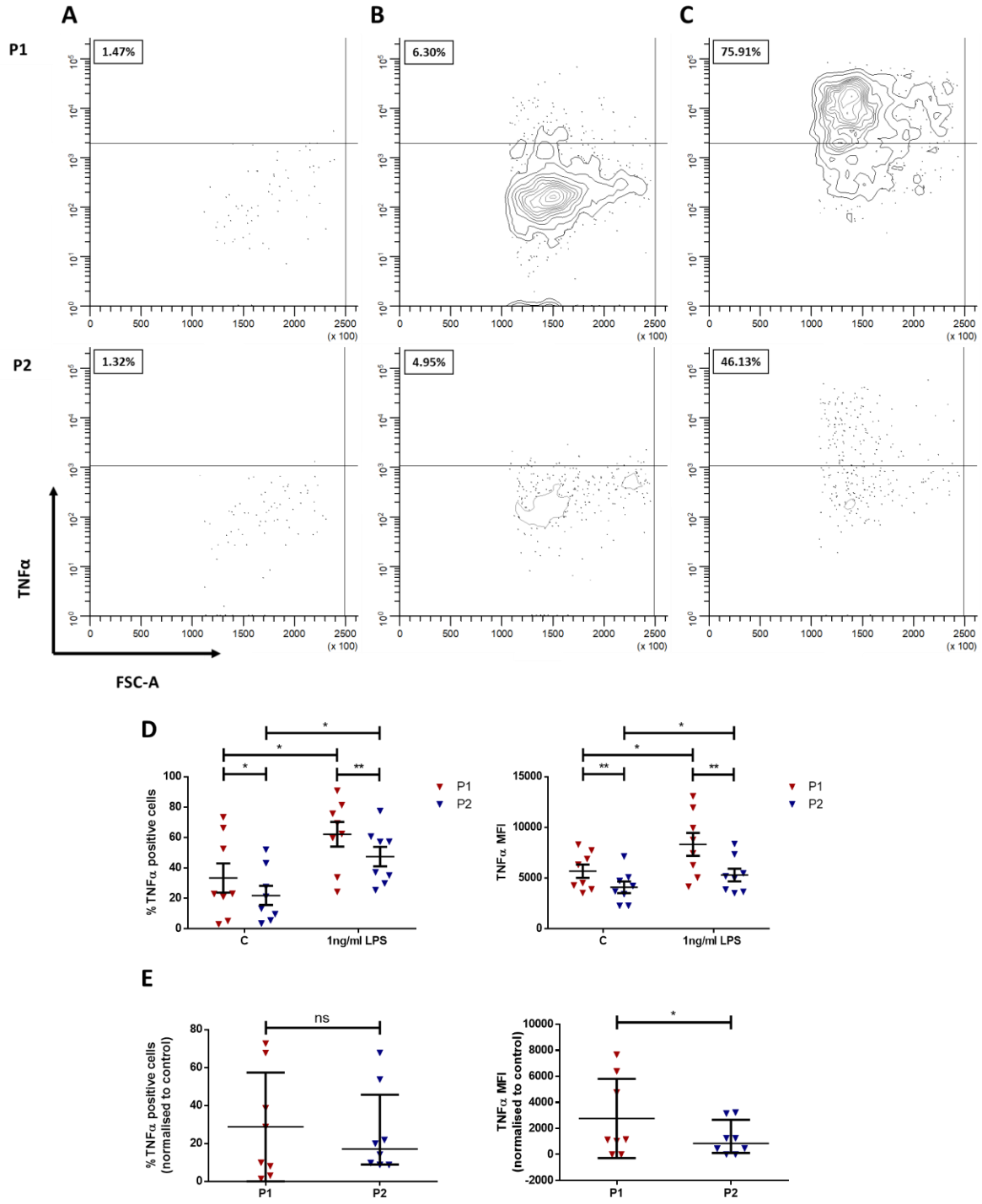

Figure 6.6: LPS-induced TNFα production by intestinal Mo/moMϕs from non-IBD colon. LPMCs extracted from endoscopic biopsies from non-IBD patients (n=8) were stimulated with 1ng/ml LPS for three hours in the presence of monensin and ADAM17 inhibitor (TMI-005). The LBMCs were labelled for anti-CD45, anti-HLA-DR, and anti-CD14 antibodies to distinguish the intestinal Mo/moMϕs, fixed, permeabilised, and stained intracellularly for TNFα before acquiring on the flow cytometer. Representative flow cytometry plots of **A)** isotype control for TNFα **B)** baseline and **C)** LPS-induced TNFα production. TNFα production was quantified as a percentage of cells positive MFI. **D)** TNFα production at baseline and upon LPS stimulation. **E)** TNFα production upon LPS stimulation minus baseline TNFα production. Median and IQR is displayed. A paired Wilcoxon tests was used to compare two groups of non-normally distributed data. $p \leq 0.05$* $p \leq 0.01$** $p \leq 0.001$*** $p \leq 0.0001$***.

6.4.4 The IL-10 response of Mo/moMϕs from non-IBD mucosa

The response of intestinal Mo/moMϕs to IL-10 was compared in eight non-IBD patients. Responses to IL-10 were measured by the inhibitory effect of IL-10 on LPS-induced TNFα production. Whole LPMCs were stimulated with 1ng/ml LPS with or without 2ng/ml IL-10, for three hours before staining for intracellular TNFα. Figure 6.7 A, B show representative flow cytometry plots of TNFα staining in P1 and P2 stimulated with LPS in the absence or presence of IL-10 respectively. IL-10 response was measured as percentage inhibition of LPS-induced TNFα production at 2ng/ml IL-10 (normalised to control; for raw values refer to Appendix 14).

The proportions of TNFα positive P1 and P2 were both reduced in the presence of IL-10. In four of eight P1 samples and two (overlapping) of eight P2 samples, LPS-induced TNFα production was completely inhibited in the presence of 2ng/ml IL-10. In contrast, responses of blood monocytes were only partially inhibited at the same concentration (Figure 6.7 C). This may indicate that CD14+ cells in the steady-state intestinal mucosa have a greater sensitivity to IL-10 than their circulating monocyte precursors.

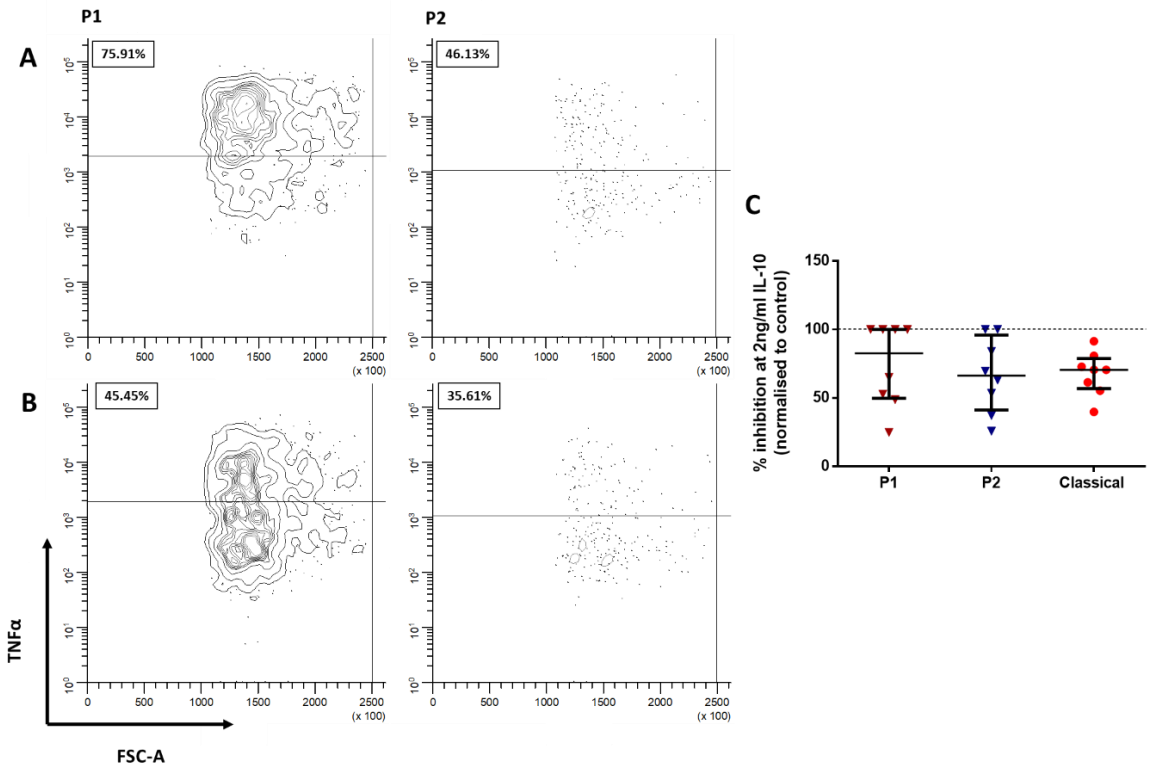

Figure 6.7: IL-10 responsiveness of intestinal Mo/moMϕs from non-IBD colon. LPMCs extracted from endoscopic biopsies from non-IBD patients (n=8) were stimulated with 1ng/ml LPS and 2ng/ml IL-10 for three hours in the presence of monensin and ADAM17 inhibitor (TMI-005). The LPMCs were labelled anti-CD45, anti-HLA-DR, and anti-CD14 antibodies to distinguish the intestinal Mo/moMϕs, fixed, permeabilised, and stained intracellularly for TNFα before acquiring on the flow cytometer. Representative flow cytometry plots showing TNFα production in P1 and P2 upon LPS stimulation **A)** without IL-10 and **B)** with 2ng/ml IL-10. Percentage inhibition of TNFα production at 2ng/ml IL-10 was calculated (minus baseline TNFα production). P1 and P2 from some patients showed 100% inhibition of TNFα production at 2ng/ml IL-10, and therefore statistical analysis of these data were not conducted. Median and IQR is displayed.

6.4. Comparing the IL-10 response of intestinal MPs from non-IBD and inflamed IBD mucosa

One aim of this chapter was to compare TNFα production in intestinal Mo/moMϕs and its ability to be inhibited by IL-10 in health and IBD. First, TNFα production was compared in P1 and P2 between health and IBD. Whole LPMCs from eight non-IBD patients, eight UC patients with active disease, seven CD patients with active disease, and four patients in remission (three UC and one CD) were cultured alone or stimulated with 1ng/ml LPS for three hours before staining for TNFα intracellularly. TNFα production was measured as a percentage of cells positive for TNFα, and as a per cell level of TNFα

production in the TNFα positive cells (MFI). Figure 6.8 A and C shows a trend towards increased production of TNFα by unstimulated cells from inflamed mucosa of CD patients but not UC patients compared to non-IBD patients, although this did not reach statistical significance with this small number of heterogeneous samples. This trend was most marked in P1 cells and was evident whether percentage positive or MFI was considered. There were no significant differences in the LPS-stimulated TNFα production in the Mo/moMϕs between non-IBD and UC or CD patients with active disease. However, this could be because LPS stimulation significantly ($p = 0.0002$ for P1; $p= 0.0011$ for P2) increased TNFα production in UC patients with active disease but not CD patients (data not shown), indicating Mo/moMϕs from CD patients may be already maximally activated.

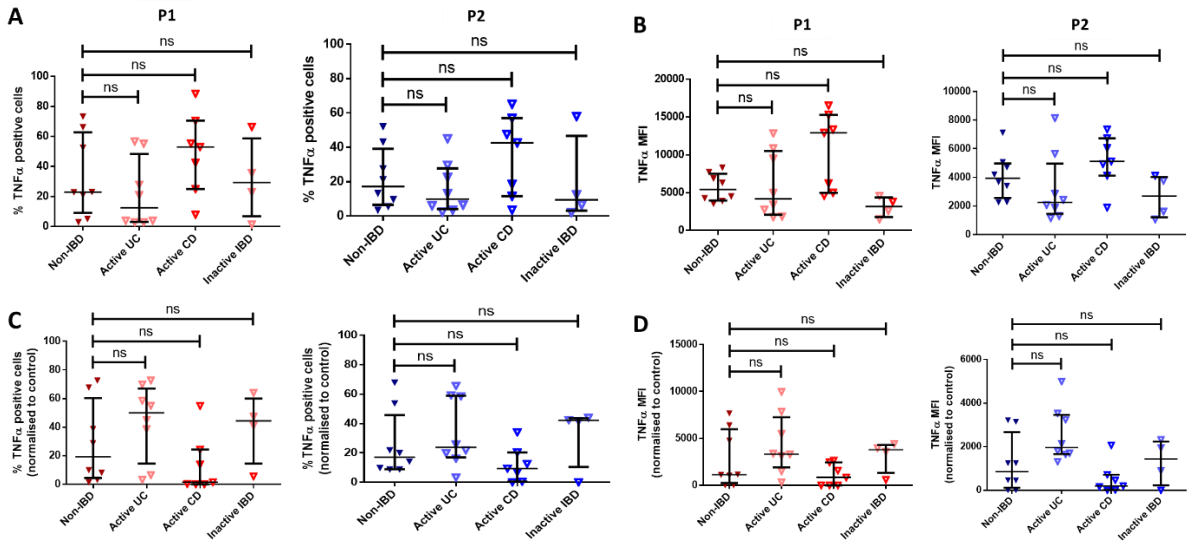

Figure 6.8: Endogenous and LPS-induced TNFα production by intestinal Mo/moMϕs from non-IBD and inflamed IBD colon. LPMCs extracted from biopsies from non-IBD patients (n=8), UC patients with active disease (n=8), CD patients with active disease (n=7), and four patients in remission (three UC and one CD) were stimulated with 1ng/ml LPS for three hours in the presence of monensin and ADAM17 inhibitor (TMI-005). The LPMCs were then labelled for anti-CD45, anti-HLA-DR, and anti-CD14 to antibodies distinguish the intestinal Mo/moMϕs, fixed, permeabilised, and stained intracellularly for TNFα before acquiring on the flow cytometer. TNFα production was quantified as a percentage of cells positive for TNFα, and as a per cell level of TNFα production in the TNFα positive cells (MFI). **A, B)** TNFα production by unstimulated P1 and P2. **C, D)** increase in TNFα production in P1 and P2 upon LPS stimulation. Median and IQR is displayed. Data were analysed statistically by Kruskal-Wallis test.

Next, the anti-inflammatory activity of the intestinal Mo/moMϕs was compared between non-IBD and inflamed IBD mucosa. There is reason to believe that there is enhanced production of IL-10 in the inflamed mucosa (detailed in the discussion), therefore, IL-10Rα blocking antibody was used to test if endogenous production of IL-10 had a limiting effect on TNFα production in unstimulated culture. In Chapter 3, this blocking antibody showed efficacy up to 10ng/ml IL-10. LPMCs from three non-IBD patients and three CD patients with active disease were cultured for three hours with or without IL-10Rα blocking antibody before staining for TNFα intracellularly. TNFα production was measured as a percentage of cells positive for TNFα, and as a per cell level of TNFα production in the TNFα positive cells (MFI). TNFα production in the presence or absence of IL-10Rα blocking antibody was compared. There was no significant difference in TNFα production in the presence of anti-IL-10Rα blocking antibody in either P1 or P2 cells from both non-IBD and inflamed CD mucosa (Figure 6.9). In addition, no IL-10 production by these populations could be detected using intracellular staining. Taken together, these observations suggest that over the timespan of these experiments, IL-10 production by P1, P2 or other cells in the culture does not impact significantly on TNFα production.

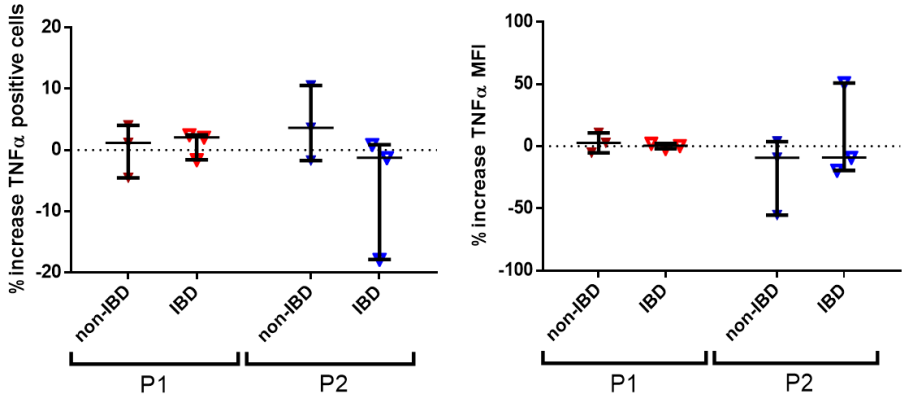

Figure 6.9: The effect of IL-10Rα-blocking antibody on TNFα production by P1 and P2. LPMCs extracted from endoscopic biopsies from non-IBD patients (n=3) and CD patients with active disease (n=3) were cultured for three hours with or without IL-10Rα blocking antibody in the presence of monensin. The LPMCs were then labelled for anti-CD45, anti-HLA-DR, and anti-CD14 antibodies to distinguish the intestinal Mo/moMϕs, fixed, permeabilised, and stained intracellularly for TNFα before acquiring on the flow cytometer. TNFα production was measured as a percentage of cells positive for TNFα, and as a per cell level of TNFα production in the TNFα positive cells (MFI). The difference in the proportion of TNFα positive cells and the percentage change in MFI was calculated for cultures with and without IL-10Rα blocking antibody. Median and IQR is displayed.

The response of intestinal Mo/moMϕs to IL-10 was compared between the eight non-IBD patients, eight UC patients with active disease, seven CD patients with active disease, and four patients in remission (three UC and one CD). LPMCs were stimulated with 1ng/ml LPS and with or without 2ng/ml IL-10 for three hours before staining for intracellular TNFα. IL-10 response was measured as percentage inhibition of LPS-induced TNFα production at 2ng/ml IL-10 (normalised to control; for raw values refer to Appendix 15).

P1 and P2 displayed enhanced sensitivity to IL-10 inhibition compared with blood monocytes, and multiple patients showed complete inhibition of TNFα production at 2ng/ml IL-10 in P1 and P2 (Figure 6.9 A, B). Thus, the high sensitivity of intestinal cells to IL-10 discussed above for cells isolated from non-IBD tissues was also evident in Mo/moMϕs from a number of IBD patients, which limited the ability to formally compare responsiveness between health and disease. Nonetheless, it is notable that the proportion of UC patients with active disease in which 2ng/ml IL-10 completely inhibited the TNFα responses was only half that of controls: 25% vs 50% for P1 cells and 12.5% versus 25% for P2 cells. For CD patients with active disease, these values were 71% and 57% for P1 and P2 respectively. Median levels of inhibition were also lower in cells from UC patients with active disease compared with non-IBD patients and CD patients with active disease. In addition, both P1 and P2 cells from the three UC patients in remission were poorly controlled by IL-10, similar to those from UC patients with active disease, whereas the response of both types of cell from a CD patient in remission was completely inhibited, similar to those from CD patients with active disease. Thus, the possibility that P1 and P2 cells have an altered response to IL-10 in the different IBD groups merits further investigation.

For patient information refer to Appendix 14.

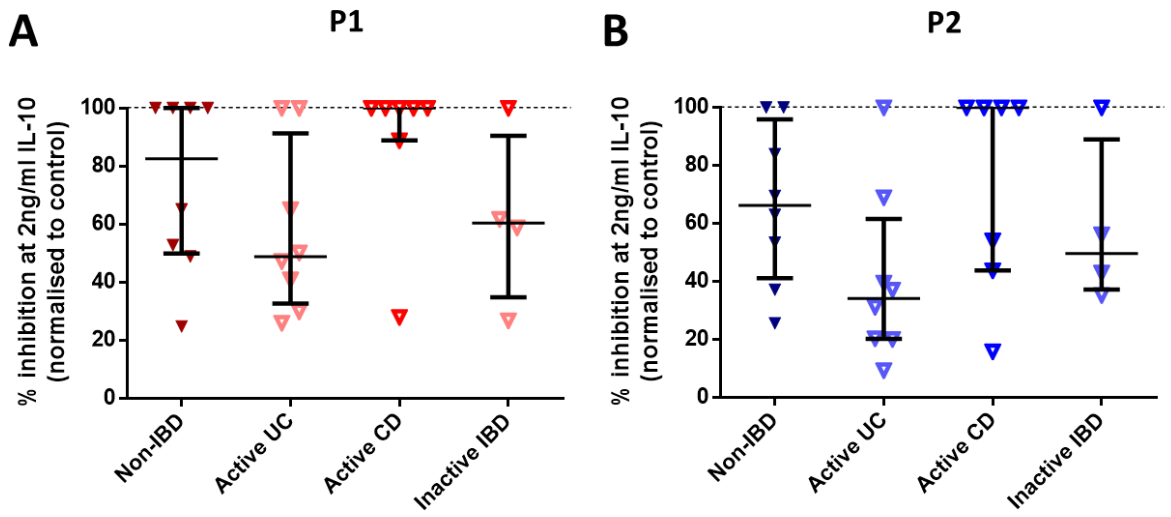

Figure 6.10: IL-10 responsiveness of intestinal Mo/moMϕs from non-IBD and inflamed IBD colon. LPMCs extracted from endoscopic biopsies from non-IBD patients (n=8), UC patients with active disease (n=8), CD patients with active disease (n=7), and four patients in remission (three UC and one CD) were stimulated with 1ng/ml LPS and 2ng/ml IL-10 for three hours in the presence of monensin and ADAM17 inhibitor (TMI-005). The LPMCs were labelled anti-CD45, anti-HLA-DR, and anti-CD14 antibodies to distinguish the intestinal Mo/moMϕs, fixed, permeabilised and stained intracellularly for TNFα before acquiring on the flow cytometer. Percentage inhibition of TNFα production at 2ng/ml IL-10 was calculated for **A)** P1 and **B)** P2. Median and IQR is displayed.

6.5 Discussion

This chapter aimed to assess the impact of the suboptimal response to IL-10 in CD14+ classical blood monocytes on CD14+ cells derived from them, in the intestinal mucosa

Fate mapping techniques, as well as studies in CCR2 deficient mice, have shown that at least part of the intestinal Mϕ pool requires constant replenishment by circulating monocytes (Bain et al. 2014; Yona et al. 2013). During steady-state, newly arrived monocytes lose their inflammatory properties to give rise to resident Mϕsthat promote immune homeostasis (Bain et al. 2014). During inflammation, an accumulation of cells that retain their inflammatory properties (inflammatory Mϕs) have been described in mice, which are likely to be contributing to the inflammation (Bain et al. 2013). In humans, an expansion in the proportion of CD14+ Mϕs that retain their capacity to respond to TLR stimulation has been reported in CD patients (Kamada et al. 2008; Lissner et al. 2015; Rugtveit et al. 1997; Thiesen et al. 2014; M. C. Grimm et al. 1995), resembling the models of intestinal inflammation described in mice. In addition, there is direct evidence that there is enhanced monocyte recruitment to the inflamed mucosa (Grimm et al. 1995).

Individual groups have defined human intestinal Mϕs using different methods. For example, Bain et al., 2013 defined $CD14^{hi}$ and $CD14^{lo}$ populations gated on CD45+Lin-CD103- cells, Bujko et al., 2017 further sub-grouped the Mϕ populations using CD11b expression, and Kamada et al., 2008 simply defined a population of CD33+ (MP marker) CD14+ cells. The lack of inconsistency in the criteria used to identify Mϕs makes it difficult to compare different studies directly.

The method chosen for characterising intestinal Mo/moMϕs was optimised from a collection of the work described. CD45 expression was used to distinguish immune cells from non-immune cells and aid in eliminating debris. Dead cells and doublets were eliminated using a viability dye and FSC/SSC plots. HLA-DR expression was then used to distinguish large APCs, including monocyte, Mϕs, DCs, and B cells. CD14 expression was finally used to distinguish populations of newly arrived monocytes and MDCs. Three populations were identified based on the level of CD14 expression: P1 ($CD14^{hi}$), P2

(CD14^{lo}), and P3 (CD14-). It has been suggested that CD14 is downregulated during monocyte differentiation into intestinal Mϕs as one mechanism by which inflammatory responses are dampened (Smith et al. 2001; Smythies et al. 2005). According to this view, P1 may be the newly arrived monocytes, and P2 and P3 represent the stages of monocyte differentiation. However, P1 displayed autofluorescence when gated on an empty channel, a feature previously reported in human Mϕ (Edelson et al. 1985; Li et al. 2012; Halldén et al. 1991), therefore, may appear to express higher CD14. Autofluorescence has previously been used to distinguish human alveolar Mϕ in tandem with antibody labelling (Havenith et al. 1993; Viksman et al. 1994). P1 and P2 were positive for CD64, suggesting that P1 and P2 represent MP cells. Bain et al., 2013 alternatively used CD103 to exclude DCs, which is less powerful then positively gating for monocytes and MDCs. P3 is unlikely to represent MP populations due to absent CD64 expression and are likely to be a heterogeneous population, including DCs and B cells.

The direction of a potential maturational pathway between P1 and P2 was explored by analysing additional markers: CD206, CX_3CR1, and CCR2, the expression of which are reported to change during monocyte differentiation into intestinal Mϕs (reviewed by Mowat & Bain, 2011). Enhanced expression of CX_3CR1 and downregulation in CCR2 expression has been reported during monocyte differentiation into intestinal Mϕs in mouse (Bain et al., 2013; Bain et al., 2014). However, in humans, there has been conflicting data: Bujko et al., 2017 assessed direction of maturation by comparing the transcriptional profile of blood monocytes to four MP populations (Mf1-4) and reported downregulation of both CX_3CR1 and CCR2 from Mf1 to Mf4. CD163, CD209, CD11b, and CD206 are upregulated during monocyte maturation into Mϕ in mice, and a reduction in their expression has been used interchangeably as an indicator of maturation (reviewed by Mowat & Bain 2011). However, all three markers tested were more highly expressed in P1 than P2. Collectively, these data suggest that P1 and P2 are MP populations but the direction of maturation cannot be clearly defined. The pro-inflammatory properties of the two populations will be discussed below.

The phagocytic capacity of the intestinal Mo/moMϕs was investigated because a functional characteristic of intestinal Mϕs is they are highly phagocytic (Smythies et al. 2005). P1 showed the highest phagocytic capacity, indicating that P1 has a more Mϕ phenotype. This is not consistent with the idea that CD14 is downregulated during monocyte differentiation into Mϕ (Smythies et al. 2005).

The distribution of the MP populations extracted from endoscopic biopsies was compared between the colon and the ileum. There was a greater proportion of P1 in the colon, and colonic biopsies are more readily accessible, therefore, colonic biopsies were used for subsequent experiments. Thiesen et al., 2014 also showed that was a greater proportion of HLA-DR+CD14+ cells in the uninflamed colon compared to the ileum. In mice, the higher rate of Mϕ replenishment in the large intestine compared to the small intestine is considered to be due to the higher commensal burden in the colon compared with the small intestine, which is relatively devoid of commensal bacteria (Bain et al., 2014; Ginhoux & Guilliams, 2016; Ginhoux & Jung, 2014; O'Hara & Shanahan, 2006).

The distribution of P1 and P2 was compared between non-IBD and inflamed mucosa from CD and UC patients. The distribution of P1 and P2 in non-IBD patients and UC patients with active disease were comparable, whereas CD patients with active disease displayed a significant increase in the proportion of P2 and a decrease in P1. Previous studies in CD patients reported an increase in the proportion of CD14+ Mϕs (Kamada et al. 2008; Lissner et al. 2015; Rugtveit et al. 1997; Thiesen et al. 2014; M. C. Grimm et al. 1995) but they did not distinguish $CD14^{hi}$ and $CD14^{lo}$ populations, therefore, the reported increase in CD14+ cells could be attributable to an accumulation of P2 cells. A weakness in proportional data is that a change in one population leads to an opposing effect on another population and it cannot give information about changes in cell numbers.

The inflammatory properties of P1 and P2 were measured by stimulating with LPS and detecting TNFα production. In contrast to blood monocytes, intestinal P1 and P2 both produced detectable TNFα in the absence of overt stimulation, which may reflect exposure during isolation or to activating components present in the intestine. Nonetheless, the addition of LPS significantly increased TNFα

production by both populations to a similar degree. This is not consistent with previous observations that human SI Mϕs did not produce pro-inflammatory cytokines in response to TLR stimulation (Smith et al. 2001; Smythies et al. 2005). However, both studies used counterflow centrifugal elutriation to purify SI Mϕs that were CD14- (Smith et al. 1997) and by definition CD14- cells were excluded from my analysis. CD14 is a co-receptor of TLR4, in the induction of pro-inflammatory responses (Dobrovolskaia & Vogel 2002), and in its absence response to LPS may be reduced or absent. P1 and P2 both express CD14, and this may explain their retained ability to respond to TLR4 activation and mandate active regulation by components such as IL-10 to prevent their inflammatory activation in the mucosa. Nonetheless, P1 had higher TNFα production, judged as the level of production in TNFα positive cells, in both unstimulated and LPS-stimulated cultures, suggesting these cells may have greater inflammatory potential, which may be consistent with the concept that these are newly recruited monocytes. Further characterisation of the Mo/moMϕs is required using additional markers and functional properties, such as bactericidal activity, to better define the populations and to resolve the currently conflicting information about potential development relationships.

The response of steady-state P1 and P2 cells to IL-10 was measured in cells from non-IBD patients. There were insufficient cells to test IL-10 across a range of concentration. Instead, a single concentration of 2ng/ml IL-10 was chosen because in earlier experiments on blood monocytes, this concentration caused an intermediate level of inhibition. However, in several intestinal samples, 2ng/ml IL-10 completely inhibited TNFα production. This made it difficult to compare responsiveness across different cell populations. Nonetheless, it is notable that, in this small sample, complete inhibition was more frequent with P1 than P2 cells (50% versus 25%). Thus, as with blood monocyte, the population with high pro-inflammatory potential is more sensitive to control by IL-10. These results indicate that intestinal Mo/moMϕs are more responsive to IL-10 than blood monocytes, and this may reflect an increased need to control their inflammatory activity in a microbe-rich environment.

Next, the pro-inflammatory capacity of P1 and P2 was compared between non-IBD patients and patients with active IBD by stimulating with LPS and measuring TNFα production. The proportion of TNFα producing cells and the level of TNFα production in unstimulated cultures and upon LPS stimulation did not differ between mucosa from non-IBD patients and inflamed mucosa from CD and UC patients in either P1 or P2. This is consistent with the findings in mouse where Bain et al., 2013 showed that the phenotype of the existing Mϕs did not change during intestinal inflammation, instead there was an accumulation of immature Mϕs which retain their inflammatory properties. However, studies in humans have shown enhanced production of pro-inflammatory cytokines by CD14+ cells from inflamed mucosa compared with non-inflamed: Kamada et al., 2008 showed that the CD14+ population isolated from the inflamed mucosa of CD patients had enhanced mRNA expression and production of pro-inflammatory cytokines, including TNFα and IFNγ, upon stimulation but that only IL-6 mRNA was enhanced in CD14+ cells isolated from the inflamed mucosa of UC patients. Ogino et al., 2013 showed enhanced production of inflammatory cytokines, including TNFα and IL-6, as well as upregulation of anti-inflammatory genes IL-10 and TGFβ, in the CD14+ population isolated from the non-inflamed mucosa of IBD patients compared to non-IBD patients, and this capacity was further enhanced in the inflamed mucosa of IBD patients. The contrast between the findings in this chapter and these two studies may be explained by TNFα production being measured via intracellular staining in this assay but mRNA expression and excreted cytokine was measured by Kamada et al., 2008 and Ogino et al., 2013. TNFα secretion is regulated at multiple levels.

The anti-inflammatory activity of the intestinal Mo/moMϕs was also compared between mucosa from non-IBD patients and inflamed mucosa from CD and UC patients by measuring IL-10 production. In mice, intestinal Mϕs display constitutive production of IL-10 (Bain et al. 2013; Krause et al. 2015; Rivollier et al. 2012). However, there is conflicting data on the constitutive production of IL-10 by human intestinal Mϕs. Bujko et al. 2017., did not detect IL-10 production by human jejunal Mϕs at baseline or upon TLR activation, which is in support of previous studies reporting a lack of IL-10 production by human jejunal Mϕs (Smythies et al. 2005; Smythies et al. 2010). In contrast, human

colonic Mϕs have been shown to produce IL-10 at baseline and upregulate upon activation (Kamada et al. 2008; Ogino et al. 2013). IL-10 producing Mϕs have been shown to be more frequent in the large intestine compared with small intestine in the mouse (Krause et al. 2015). If this is true in humans, it could account for the different findings reported with jejunal and colonic Mϕs. There is reason to believe that there is an increase in IL-10 production in the inflamed intestine. In humans, an increase in expression of mRNA for IL-10 has been observed in the CD14+ population isolated from the mucosa of CD patients compared with non-IBD patients (Ogino et al. 2013), which could reflect an increase in IL-10 production. To asses a potential role for IL-10 production in my cultures, an IL-10Rα blocking antibody was used to test whether endogenous IL-10 was affecting TNFα production by LPMCs. However, there was no increase in TNFα production in the presence of IL-10Rα blocking antibody in either P1 or P2 cells from non-IBD and inflamed IBD mucosa. Neither were IL-10 positive P1 or P2 cells detectable by intracellular staining. These data indicate that over the timespan of the cultures in these experiments, IL-10 production by CD14+ cells, or other populations is unlikely to influence TNFα production, and therefore the apparent increase in sensitivity to IL-10 in intestinal cells cannot be attributed to production within the culture.

Finally, the high sensitivity of intestinal Mo/moMϕs to IL-10 in healthy individuals was also reflected in IBD patients, suggesting that there is not a gross loss in IL-10 response of Mo/moMϕs in these active IBD patients. However, the sensitivity of the assay is reduced when responses of cells from donors are completely inhibited by IL-10 making it difficult to draw conclusions with respect to differences in response to IL-10 between health and disease. Nonetheless, it is notable that there is a trend suggesting that P1 and P2 from UC patients with active disease display a reduced response to IL-10 inhibition when compared with non-IBD patient and CD patients with active disease, and this pattern is reflected in the inactive IBD cohort. Reducing the concentration of IL-10 used in these experiments would increase the sensitivity of the assay and allow for a more meaningful comparison of IL-10 response between non-IBD patients and patients with active IBD.

6.6 Conclusion

The implications of a suboptimal response to IL-10 inhibition in classical monocytes was investigated in CD14+ monocyte-derived cells in the intestine. Two populations were identified based on CD14 expression: $CD14^{hi}$ (P1) and $CD14^{lo}$ (P2). Both populations spontaneously produce TNFα and production was enhanced with LPS stimulation. The intestinal populations were more sensitive to IL-10 control than blood monocytes, making it difficult to draw conclusions with respect to differences in response to IL-10 between the two populations and health and IBD. These experiments are being refined to increase sensitivity and allow meaningful comparisons.

Chapter 7: Final discussion and future work

The primary aim of the project was to identify MP populations in the blood and intestinal biopsies, determine their responsiveness to IL-10 and whether this response is altered in IBD patients, and finally begin to explore how such changes might contribute to the pathogenesis of IBD.

First, an assay that could measure IL-10 responsiveness in human monocyte subsets was developed. The three monocyte subsets were distinguished based on CD14 and CD16 expression: classical (CD14++CD16-), intermediate (CD14++CD16+), and non-classical (CD14+CD16++) monocytes. The assay for measuring IL-10 response involved LPS induction of TNFα production, which lead to an apparent loss of CD16+ cells. Shedding of the CD16 marker upon activation had previously been reported in NK cells, which could be blocked by an ADAM17 inhibitor (Romee et al. 2013). Therefore, an ADAM17 inhibitor was added to the cultures and CD16 expression was maintained upon activation, which enabled the responsiveness to IL-10 of all three monocyte subsets to be determined in parallel. CD16 is an activating Fc receptor for IgG (reviewed by Guilliams et al. 2014), therefore, the process of CD16 shedding may help limit ADCC or further stimulation by cross-linking immune complexes. The shedding of CD16 from the surface of monocytes upon activation also has important implications for the identification of monocyte-derived cells within the intestine and other tissues that are constantly exposed to foreign antigens. Caution should be applied when interpreting an absence of CD16 expression on cells in tissues as an absence of cells derived from intermediate or non-classical populations because CD16 may have been lost from the surface of such cells.

Induction of TNFα production with LPS was compared between the monocyte subsets. Intermediate monocytes displayed the highest TNFα production, followed by classical monocytes, and least responsive to TLR4 activation were the non-classical monocytes. The hierarchy of LPS response can in part be explained by CD14 expression as the co-receptor for TLR4 (Beutler et al., 2000). The finding that classical and intermediate monocytes are robust responders to TLR stimulation and non-classical monocytes are poorly activated, is generally consistent with previously published studies using similar

agonists (Belge et al. 2002; Boyette et al. 2017; Cros et al. 2010; Thiesen et al. 2014). However, Cros et al., 2010 showed that TLR7 and TLR8 agonists, not tested in the current study, are robust activators of non-classical monocytes and stimulate the production of TNFα, IL-6, and IL-1β. This indicates that under appropriate stimulation these cells have a greater capacity to produce pro-inflammatory cytokines than was previously appreciated.

The ability to inhibit LPS-induced TNFα production with IL-10 was then compared between monocyte subsets in healthy individuals. IL-10 inhibition of LPS-induced TNFα was greatest in classical monocytes, followed by intermediates, and least responsive were the non-classical monocytes despite low levels of TNFα production. The robust response of classical monocytes to IL-10 inhibition supports the concept that IL-10 is a critical mechanism by which their inflammatory properties can be controlled and may play an important role in acquiring regulatory properties during differentiation into intestinal Mϕs (Bain et al. 2013; Kayama et al. 2012; Shouval et al. 2014; Takada et al. 2010; Zigmond et al. 2014). The contribution of intermediate monocytes to the human intestinal Mϕ pool remains unclear due to the lack of unique identifiers, and the possibility that CD16 is shed upon entry into the intestine. The robust response of intermediate monocytes to TLR activation in combination with a suboptimal response to IL-10 inhibition may make them important contributors to bacterial driven inflammation, including of IBD. Although non-classical monocytes respond relatively poorly to LPS stimulation in comparison to classical and intermediate monocytes in the absence of added IL-10, their response is maintained in the presence of IL-10 and under these conditions is equivalent to the other two subsets. Auffray et al., 2007 showed that non-classical monocytes undergo rapid extravasation at sites of infection and contribute to the initial inflammatory response. A lack of response to IL-10 in the tissues could enhance this response. In the context of intestinal inflammation, non-classical monocytes entering the mucosa would be poorly regulated by IL-10 and may perpetuate the inflammation.

Next, the aim was to determine whether differences in monocytes subset responses to IL-10 were specific to the mode of activation (LPS) or functional readout (TNFα production). LPS signals down two

pathways: MyD88- and TRIF-dependent (Lu et al. 2008). LPS was compared to two stimulants chosen to target these signalling pathways: Pam_3CSK_4 triggers the MyD88 pathway, while Poly(I:C) activates TRIF. TNFα production was also compared to two additional readouts: IL-1β and IFNα induced by MyD88 and TRIF pathways respectively (Akira & Takeda 2004). Consistent with LPS-induced TNFα production, intermediate monocytes showed the highest cytokine production with all TLR agonists tested, followed by classical, and least responsive were the non-classical monocytes. Generally, the hierarchy of responses of the monocyte subsets to IL-10 inhibition of TNFα production is comparable between TLR agonists tested. The differential responses of the monocyte subsets to IL-10 inhibition was less evident when IL-1β and IFNα were used as readouts, most likely due to the limited sensitivity of the assay when the response was very high (IL-1β) or low (IFNα). Overall, these data show that the inflammatory properties of the monocyte subsets are not TLR-specific, and the capacity of IL-10 to inhibit TNFα production in the monocyte subset is also independent of the inducer.

Signalling components of the IL-10R signalling pathway were investigated to provide a possible explanation for the differences found in IL-10 response between monocyte subsets. These included IL-10Rα expression, STAT3 availability and phosphorylation, and SOCS3 mRNA expression. IL-10Rα expression was highest in intermediate monocyte and lowest in classical monocytes, which makes IL-10Rα expression a poor indicator of the ability of IL-10 to inhibit pro-inflammatory cytokine production. Relatively high expression of IL-10Rα on intermediate monocytes in combination with their robust response to TLR activation provides evidence that their phenotype is distinct from both classical and non-classical monocytes, and therefore challenges the concept that intermediate monocytes are merely a population transiting between classical and non-classical monocytes.

Classical and intermediate monocytes expressed high and equivalent levels of STAT3, while non-classical monocytes expressed lower levels of STAT3, which correlated well with levels of STAT3 phosphorylation upon IL-10 stimulation. This may explain why non-classical monocytes are less responsive to IL-10 than the other two subsets but does not explain the difference between classical

and intermediates. The difference in IL-10 response between classical and intermediate monocytes could be due to higher TNFα production in intermediate monocytes because as suggested by the experiment in which IL-1β was measured, stronger responses are harder to inhibit. In addition, PCR data show that classical monocytes also express higher levels of *SOCS3* mRNA at steady-state than both intermediate and non-classical monocytes. One role of SOCS3 protein is inhibiting the NFκB pathway, therefore, increased expression may provide a mechanism behind enhanced IL-10 responsiveness. Investigating SOCS3 protein levels directly was hindered by low cell numbers, and therefore mRNA expression at baseline was used as a potential surrogate measure. SOCS3 protein levels remain to be assessed, and pooling of samples across donors could be used to overcome the limitations of low cell numbers in future experiments. It would also be worthwhile to investigate the level of IL-10 induced *SOCS3* mRNA or protein expression.

The IL-10 responsiveness of the monocytes subsets was compared between healthy individuals and patients with active IBD to determine whether this response is altered in the presence of intestinal inflammation. Classical monocytes were the only subset that displayed a reduced response to IL-10 in IBD patients compared with healthy controls. This may have important implications in IBD as fate-mapping experiments in mice point to classical monocytes as the origin of intestinal Mϕ (Bain et al. 2014). Bain et al. 2013 demonstrated a context-dependent differentiation of newly arrived monocytes in mice. The inflammatory properties of the newly arrived monocytes are downregulated during differentiation into resident Mϕs in steady-state. However, during intestinal inflammation, this pathway is disrupted causing an accumulation of cells that retain their ability to respond to TLR ligands, and these inflammatory Mϕs are likely to perpetuate the inflammation (Bain et al. 2013). In humans, an expansion in the proportion of CD14+ Mϕs that retain their capacity to respond to TLR stimulation has been reported in CD patients (M. C. Grimm et al. 1995; Kamada et al. 2008; Lissner et al. 2015; Rugtveit et al. 1997; Thiesen et al. 2014), which resembles the situation described in intestinal inflammation in mice. The signals responsible for the fate of the newly recruited monocytes are poorly understood. The studies described previously by Zigmond et al., 2014 and Shouval et al., 2014 indicate

that IL-10 has an important non-redundant role during monocyte differentiation into 'regulatory' Mϕ. In support of this, classical monocytes showed a robust response to IL-10, suggesting an important role for IL-10 in regulating their inflammatory properties. The reduction in IL-10 response could favour the accumulation of inflammatory Mϕs, which may contribute to the sustainment of intestinal inflammation. In vitro models, such as those used by Smythies et al. 2005, could be used to further investigate the role of IL-10 in during monocyte maturation into intestinal Mϕ.

There is increasing evidence in both mice and humans that systemic signals from the intestine during inflammation cause functional changes to circulating cells (Arts et al. 2018; Askenase et al. 2015; Christ et al. 2018; Mitroulis et al. 2018; Sanders et al. 2014; Smith et al. 2009). This formed the rationale for studying blood monocytes, as the likely precursors of intestinal Mϕ. The reduction in IL-10 response observed in circulating classical monocytes of IBD patients is consistent with the concept that systemic signals, as well as the local environment, can have an impact on monocyte fate.

Signalling components of the IL-10R signalling pathway were investigated to explore the possible mechanisms behind the reduced response to IL-10 in classical monocytes from IBD patients. The reduced response to IL-10 was despite increased IL-10Rα expression. Higher expression of Il-10Rα may explain the enhanced capacity to phosphorylate STAT3 following IL-10 stimulation in classical monocytes from IBD patients despite comparable levels of T-STAT3 within the cell. In addition, baseline *SOCS3* mRNA levels showed a trend towards increased expression in IBD. These IBD-associated changes may demonstrate negative feedback mechanisms conditioned to return the immune system to steady-state. However, the signalling components investigated thus far do not provide a mechanism for the reduced response to IL-10 in classical monocytes of IBD patients, indicating that unknown mechanisms are regulating IL-10 responsiveness. Global phosphorylation analysis could be used to look at IL-10 signalling components globally and compare health and disease to expose changes that may account for the reduced response.

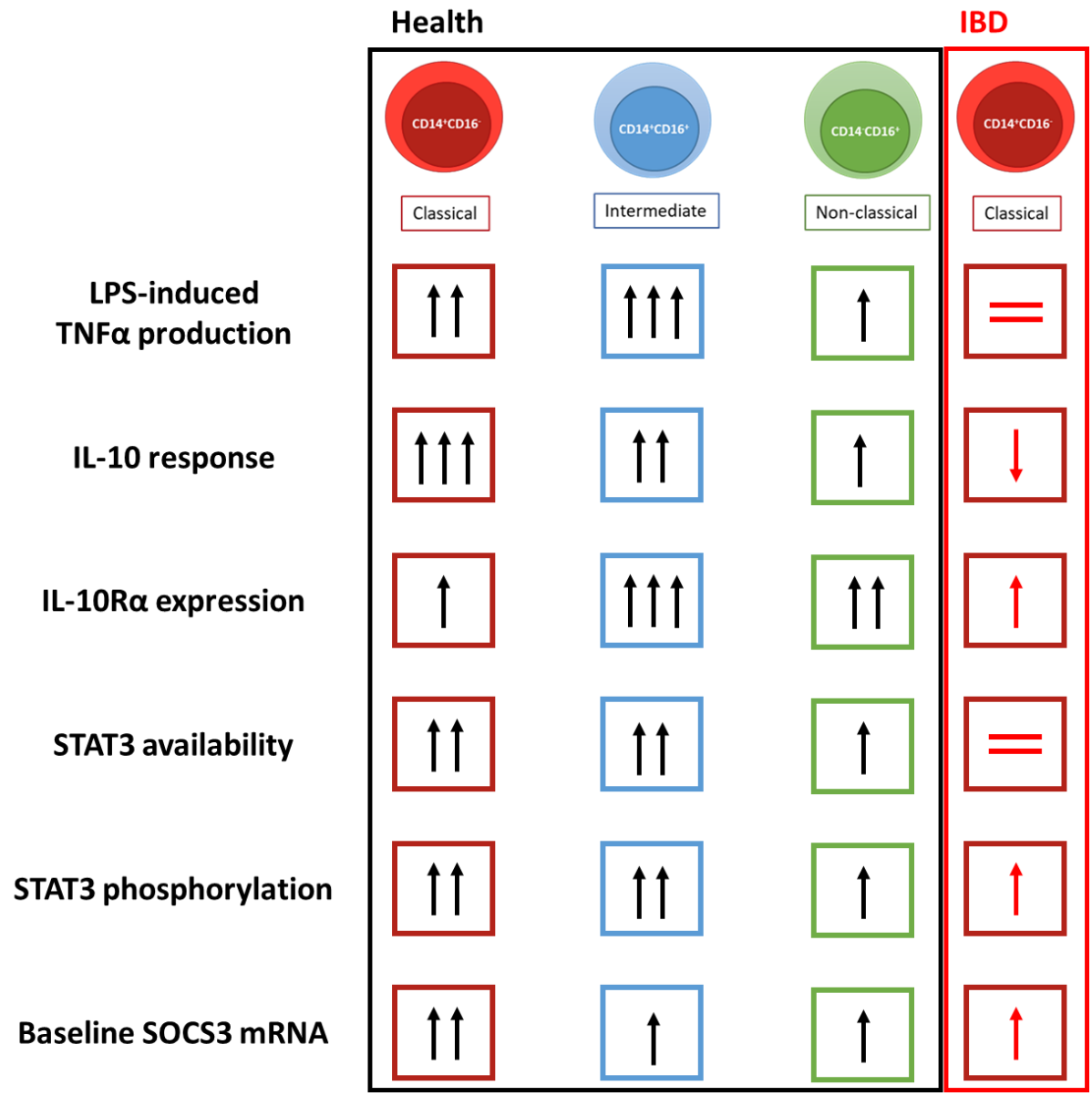

Figure 7: Summary Diagram.

The distribution of the monocyte subsets in health and IBD was investigated. Non-classical monocytes, but not classical or intermediate cells, were significantly reduced in proportion and cell number in IBD patients in two separate cohorts. This is in contrast to Thiesen et al. 2013 and Grip et al., 2006 who both reported an increase in the proportion of intermediate monocytes in CD patients. The contrasting results could be because different gating strategies were used to identify the monocyte subsets.

The loss of non-classical monocytes in circulating blood could be due to increased recruitment to the inflamed intestine as this population has been shown to be recruited into inflamed tissues, initially

contributing to the inflammatory response before switching on reparative functions (Auffray et al. 2007). Alternatively, changes to the endothelial wall induced by intestinal inflammation may make the non-classical monocytes more adherent to the surface and appear less abundant in the blood. Enhanced death of non-classical monocytes in the IBD patients could account for fewer circulating cells but the impact of intestinal inflammation on the half-life of the monocyte subsets has not been studied. Another possible explanation for the loss of non-classical monocytes in circulating blood could be that fewer classical monocytes are available to mature into non-classical cells due to enhanced recruitment into the inflamed intestine (Grimm *et al.*, 1995). Regardless of the precise mechanism, any loss of non-classical monocytes from the circulation could have important implications for tissue repair as this is their ultimate function after recruitment (Auffray et al. 2007). Reduced recruitment of reparative monocytes could contribute to tissue damage and inflammation in IBD.

The implications of a suboptimal response to IL-10 inhibition observed in classical monocytes was investigated in CD14+ monocyte-derived cells in the intestine. First, these cell populations were identified in LPMCs extracted from intestinal biopsies. Expression of HLA-DR, CD14, and CD64 was used to distinguish two CD14-expressing populations both of which expressed the Mo/Mϕ marker CD64: P1 (HLA-DR^{hi}CD14^{hi}CD64+) and P2 (HLA-DR^{hi}CD14^{lo}CD64+).

LPS-induced TNFα production was measured using LPMCs extracted from intestinal biopsies from non-IBD patients. Both P1 and P2 were responsive to LPS stimulation but less than in blood monocytes, which supports the concept that inflammatory responses of newly arrived monocytes are regulated. In contrast to blood monocytes, intestinal P1 and P2 produced detectable TNFα in the absence of LPS, which may reflect the constant exposure to external antigens in the intestine. Addition of LPS significantly increased TNFα production by both populations to a similar degree. In both unstimulated and LPS-stimulated cultures, TNFα production was greater in P1 than in P2 as assessed by either percent positive or MFI, which suggests these cells have greater inflammatory potential indicating newly recruited monocytes. However, P1 was more phagocytic than P2 indicating that P1 has a more

Mϕ phenotype. Further characterisation of the two populations is required using functional properties such as bactericidal activity. Although P2 expressed less CD14, their capacity to respond to LPS was not diminished, which is not consistent with the concept that newly arrived monocytes downregulate TLR expression and become anergic to activation during maturation into intestinal Mϕ (Smith et al. 2001; Smythies et al. 2005). However, it is not known that P2 is derived from P1.

TNFα production at baseline and upon LPS stimulation did not differ in P1 and P2 between non-IBD and inflamed IBD mucosa. This compliments the findings by Bain et al., 2013 in mice that showed the phenotype of the resident Mϕ did not change, instead, there is an accumulation of immature Mϕ which retain their inflammatory properties. However, in humans, studies have shown enhanced production of pro-inflammatory cytokines in CD14+ cells from inflamed mucosa compared to non-inflamed (Kamada et al. 2008; Ogino et al. 2013). The contrasting results could be because Kamada et al., 2008 measured secreted cytokine and Ogino et al., 2013 measured mRNA expression.

The distribution of P1 and P2 was compared between non-inflamed and inflamed mucosa. The distribution of P1 and P2 in non-IBD patients and patients with active UC were comparable but patients with active CD displayed a significant increase in the proportion of P2 and a decrease in P1. This is in contrast to previous findings in CD patients that showed an increase in the proportion of CD14+ Mϕs (Grimm *et al.*, 1995; Rugtveit *et al.*, 1997; Kamada *et al.*, 2008; Thiesen *et al.*, 2014; Lissner *et al.*, 2015). The contradicting results could be due to the lack of consistent markers used to characterise intestinal Mϕ populations in humans.

Finally, the capacity of IL-10 to inhibit LPS-induced TNFα production was measured in P1 and P2 using 2ng/ml IL-10 chosen on the basis of experiments carried out on blood monocytes. However, in multiple samples, there was 100% inhibition, and therefore it was difficult to conclude with respect to differences in IL-10 response between P1 and P2. These data may also indicate that intestinal CD14+ cells have an enhanced response to IL-10 compared with circulating monocytes, their putative precursors. Whether this enhanced response to IL-10 is directly due to greater sensitivity to lL-10 itself

or because the lower response to LPS observed with intestinal cells is more readily inhibited cannot be distinguished currently. There was no evidence that IL-10 production by intestinal cells in the culture contributed. A lower concentration of IL-10 is required to increase the sensitivity of the assay and allow meaningful comparisons between health and IBD.

Overall, this thesis has demonstrated that IL-10 is a critical mechanism by which the inflammatory properties of classical monocytes can be controlled but it may play a less prominent role in the control of responses by other subsets. Understanding the environmental cues determining the fate of monocyte-derived cells in the intestine and how these cues differ between health and disease is likely to be a key area for future research. Modulating monocyte maturation to favour differentiation into regulatory Mϕ may provide new therapeutic targets for treating IBD.

References

Abraham, C. & Medzhitov, R., 2011. Interactions between the host innate immune system and microbes in inflammatory bowel disease. *Gastroenterology*, 140(6), pp.1729–1737. Available at: http://dx.doi.org/10.1053/j.gastro.2011.02.012.

Abreu, M.T., 2010. Toll-like receptor signalling in the intestinal epithelium: How bacterial recognition shapes intestinal function. *Nature Reviews Immunology*, 10(2), pp.131–143. Available at: http://dx.doi.org/10.1038/nri2707.

Adrain, C. et al., 2012. Tumor necrosis factor signaling requires iRhom2 to promote trafficking and activation of TACE. *Science*, 335(6065), pp.225–228. Available at: http://www.pubmedcentral.nih.gov/articlerender.fcgi?artid=3272371&tool=pmcentrez&rendertype=abstract.

Akira, S., 2000. Roles of STAT3 defined by tissue-specific gene targeting. *Oncogene*, 19(21), pp.2607–2611.

Akira, S. & Takeda, K., 2004. FOCUS ON TLR SIGNALLING. *Nature Reviews Immunology*, 4(July), pp.499–511.

Alex, P. et al., 2009. Distinct cytokine patterns identified from multiplex profiles of murine DSS and TNBS-induced colitis. *Inflammatory Bowel Diseases*, 15(3), pp.341–352.

Amiot, A. et al., 2016. Effectiveness and Safety of Vedolizumab Induction Therapy for Patients With Inflammatory Bowel Disease. *Clinical Gastroenterology and Hepatology*, 14(11), p.1593–1601.e2. Available at: https://www.sciencedirect.com/science/article/pii/S1542356516001646 [Accessed July 1, 2018].

Ancuta, P. et al., 2003. Fractalkine Preferentially Mediates Arrest and Migration of CD16 $^{+}$ Monocytes. *The Journal of Experimental Medicine*, 197(12), pp.1701–1707. Available at: http://www.jem.org/lookup/doi/10.1084/jem.20022156.

Anderson, C.A. et al., 2011. Meta-analysis identifies 29 additional ulcerative colitis risk loci, increasing the number of confirmed associations to 47. *Nature Genetics*, 43(3), pp.246–252.

Annunziato, F. et al., 2007. Phenotypic and functional features of human Th17 cells. *The Journal of Experimental Medicine*, 204(8), pp.1849–1861. Available at: http://www.jem.org/lookup/doi/10.1084/jem.20070663.

Antoniou, E. et al., 2016. The TNBS-induced colitis animal model: An overview. *Annals of Medicine and Surgery*, 11, pp.9–15. Available at: http://dx.doi.org/10.1016/j.amsu.2016.07.019.

Appleby, L.J. et al., 2013. Sources of heterogeneity in human monocyte subsets. *Immunology Letters*, 152(1), pp.32–41. Available at: http://dx.doi.org/10.1016/j.imlet.2013.03.004.

Arts, R.J.W. et al., 2018. BCG Vaccination Protects against Experimental Viral Infection in Humans through the Induction of Cytokines Associated with Trained Immunity. *Cell Host and Microbe*, 23(1), p.89–100.e5. Available at: https://doi.org/10.1016/j.chom.2017.12.010.

Arya, M. et al., 2005. Basic principles of real-time quantitative PCR. *Expert review of molecular diagnostics*, 5(2), pp.209–19. Available at: http://www.ncbi.nlm.nih.gov/pubmed/15833050.

Askenase, M.H. et al., 2015. Bone-Marrow-Resident NK Cells Prime Monocytes for Regulatory Function during Infection. *Immunity*, 42(6), pp.1130–1142. Available at: http://dx.doi.org/10.1016/j.immuni.2015.05.011.

Auffray, C. et al., 2007. Monitoring of Blood Vessels and Tissues by a Population of Monocytes with Patrolling Behavior. *Science*, 317, pp.666–670.

Backhed, F. et al., 2005. Host-Bacterial Mutualism in the Human Intestine. *Science*, 307(5717), pp.1915–1920. Available at: http://www.sciencemag.org/cgi/doi/10.1126/science.1104816.

Baillie, J.K. et al., 2017. *Analysis of the human monocyte-derived macrophage transcriptome and response to lipopolysaccharide provides new insights into genetic aetiology of inflammatory bowel disease*,

Bain, C.C. et al., 2014. Constant replenishment from circulating monocytes maintains the macrophage pool in the intestine of adult mice. *Nature Immunology*, 15(10), pp.929–937. Available at: http://www.nature.com/doifinder/10.1038/ni.2967.

Bain, C.C. et al., 2013. Resident and pro-inflammatory macrophages in the colon represent alternative context-dependent fates of the same Ly6Chi monocyte precursors. *Mucosal Immunology*, 6(3), pp.498–510. Available at: http://www.nature.com/doifinder/10.1038/mi.2012.89.

Baldwin, A.S., 1996. THE NF-κB AND IκB PROTEINS : New Discoveries and Insights. *Annu. Rev. Immunol*, (14), pp.649–681.

Baumgart, D.C. & Carding, S.R., 2007. Inflammatory bowel disease: cause and immunobiology. *The Lancet*, 369, pp.1627–1640. Available at: https://ac.els-cdn.com/S0140673607607508/1-s2.0-S0140673607607508-main.pdf?_tid=d1e9d92e-1d87-454b-bba4-61b0a517fca3&acdnat=1527261831_1ee054d186ec6db2edf739bfb0648597 [Accessed May 25, 2018].

Baumgart, D.C. & Sandborn, W.J., 2012. Crohn's disease. *Lancet*, 380, pp.1590–1601.

Baumgart, D.C. & Sandborn, W.J., 2007. Inflammatory bowel disease : clinical aspects and established and evolving therapies. *The Lancet*, 369, pp.1641–1657.

Bazil, V. & Strominger, J.L., 1991. Shedding as a mechanism of down-modulation of CD14 on stimulated human monocytes. *The Journal of immunology*, 147(5), pp.1567–1574.

Begue, B. et al., 2011. Defective IL10 Signaling Defining a Subgroup of Patients With Inflammatory Bowel Disease. *The American Journal of Gastroenterology*, 106(8), pp.1544–1555. Available at: http://www.nature.com/doifinder/10.1038/ajg.2011.112.

Belge, K.-U. et al., 2002. The proinflammatory CD14+CD16+DR++ monocytes are a major source of TNF. *Journal of immunology*, 168, pp.3536–3542.

Belkaid, Y. & Harrison, O.J., 2017. Review Homeostatic Immunity and the Microbiota. *Immunity*, 46(4), pp.562–576. Available at: http://dx.doi.org/10.1016/j.immuni.2017.04.008.

Benjamin, J.L. et al., 2012. Smokers with active Crohn's disease have a clinically relevant dysbiosis of the gastrointestinal microbiota. *Inflammatory Bowel Diseases*, 18(6), pp.1092–1100. Available at: http://www.ncbi.nlm.nih.gov/pubmed/22102318 [Accessed May 25, 2018].

Berg, D.J. et al., 1996. Enterocolitis and colon cancer in interleukin-10-deficient mice are associated with aberrant cytokine production and CD4+Th1-like responses. *Journal of Clinical Investigation*, 98(4), pp.1010–1020.

Beutler, B., 2000. Tlr4: Central component of the sole mammalian LPS sensor. *Current Opinion in Immunology*, 12(1), pp.20–26.

Bigley, V. et al., 2011. The human syndrome of dendritic cell, monocyte, B and NK lymphoid

deficiency. *The Journal of Experimental Medicine*, 208(2), pp.227–234. Available at: http://www.jem.org/lookup/doi/10.1084/jem.20101459.

Biswas, S.K. & Lopez-Collazo, E., 2009. Endotoxin tolerance: new mechanisms, molecules and clinical significance. *Trends in Immunology*, 30(10), pp.475–487.

Biswas, S.K. & Mantovani, A., 2010. Macrophage plasticity and interaction with lymphocyte subsets: Cancer as a paradigm. *Nature Immunology*, 11(10), pp.889–896. Available at: http://dx.doi.org/10.1038/ni.1937.

Boehm, U. et al., 1997. Cellular Responses To Interferon-γ. *Annual review of immunology*, 15, pp.749–95.

Boring, L. et al., 1997. Impaired monocyte migration and reduced type 1 (Th1) cytokine responses in C-C chemokine receptor 2 knockout mice. *Journal of Clinical Investigation*, 100(10), pp.2552–2561.

Boudeau, J. et al., 1999. Invasive Ability of an Escherichia coli Strain Isolated from the Ileal Mucosa of a Patient with Crohn's Disease. *INFECTION AND IMMUNITY*, 67(9), pp.4499–4509. Available at: http://iai.asm.org/content/67/9/4499.full.pdf [Accessed May 25, 2018].

Bouma, G. & Strober, W., 2003. The immunological and genetic basis of inflammatory bowel disease. *Nature reviews. Immunology*, 3(7), pp.521–33. Available at: http://www.ncbi.nlm.nih.gov/pubmed/12876555 [Accessed August 29, 2014].

Boyette, L.B. et al., 2017. Phenotype, function, and differentiation potential of human monocyte subsets. *PloS one*, 12(4), pp.1–20.

Brandl, K. et al., 2007. MyD88-mediated signals induce the bactericidal lectin RegIIIγ and protect mice against intestinal *Listeria monocytogenes* infection. *The Journal of Experimental Medicine*, 204(8), pp.1891–1900. Available at: http://www.jem.org/lookup/doi/10.1084/jem.20070563.

Brockmann, L. et al., 2017. IL-10 Receptor Signaling Is Essential for Tr1 Cell Function In Vivo. *The Journal of Immunology*, 198, pp.1130–1141.

Bujko, A. et al., 2017. Transcriptional and functional profiling defines human small intestinal macrophage subsets. *The Journal of Experimental Medicine*, 215(3), p.jem.20170057. Available at: http://www.jem.org/lookup/doi/10.1084/jem.20170057.

Butovsky, O. et al., 2014. Identification of a unique TGF-β-dependent molecular and functional signature in microglia. *Nature Neuroscience*, 17(1), pp.131–143.

Cadwell, K. et al., 2008. A key role for autophagy and the autophagy gene Atg16l1 in mouse and human intestinal Paneth cells. *Nature*, 456(November), pp.259–264.

Caprilli, R., Lapaquette, P. & Darfeuille-Michaud, A., 2010. Eating the enemy in Crohn's disease. An old theory revisited. *Journal of Crohn's and Colitis*, 4(4), pp.377–383. Available at: http://dx.doi.org/10.1016/j.crohns.2010.05.007.

Cara, C.J. et al., 2004. Reviewing the mechanism of action of thiopurine drugs: towards a new paradigm in clinical practice. *Medical science monitor*, 10(11), pp.247–254.

Cheong, C. et al., 2011. Microbial stimulation fully differentiates monocytes to DC-SIGN/ CD209+ dendritic cells for immune T cell areas. *Cell*, 143(3), pp.416–429.

Christ, A. et al., 2018. Western Diet Triggers NLRP3-Dependent Innate Immune Reprogramming. *Cell*, 172(1–2), p.162–175.e14.

Clapp, D.W., Baley, J.E. & Gerson, S.L., 1989. Gestational age-dependent changes in circulating hematopoietic stem cells in newborn infants. *The Journal of laboratory and clinical medicine*, 113(4), pp.422–7. Available at: http://www.ncbi.nlm.nih.gov/pubmed/2703757 [Accessed April 8, 2018].

Colombel, J.-F. et al., 2018. Effect of tight control management on Crohn's disease (CALM): a multicentre, randomised, controlled phase 3 trial. *Lancet (London, England)*, 390(10114), pp.2779–2789. Available at: http://linkinghub.elsevier.com/retrieve/pii/S0140673617326417 [Accessed May 31, 2018].

Cooney, R. et al., 2010. NOD2 stimulation induces autophagy in dendritic cells influencing bacterial handling and antigen presentation. *Nature Medicine*, 16(1), pp.90–97. Available at: http://dx.doi.org/10.1038/nm.2069.

Covert, M.W., 2005. Achieving Stability of Lipopolysaccharide-Induced NF-kB Activation. *Science*, 309(5742), pp.1854–1857. Available at: http://www.sciencemag.org/cgi/doi/10.1126/science.1112304.

Cros, J. et al., 2010. Human CD14dim Monocytes Patrol and Sense Nucleic Acids and Viruses via TLR7 and TLR8 Receptors. *Immunity*, 33, pp.375–386. Available at: http://linkinghub.elsevier.com/retrieve/pii/S1074761310003171.

Darfeuille-Michaud, A. et al., 2004. High prevalence of adherent-invasive Escherichia coli associated with ileal mucosa in Crohn's disease. *Gastroenterology*, 127(2), pp.412–421.

Davies, L.C. et al., 2013. Tissue-resident macrophages. *Nature Immunology*, 14(10), pp.986–995.

Denning, T.L. et al., 2007. Lamina propria macrophages and dendritic cells differentially induce regulatory and interleukin 17-producing T cell responses. *Nature Immunology*, 8(10), pp.1086–1094.

Desjardins, P., Joel, B. & Allen, M., 2009. Microvolume Protein Concentration Determination using the NanoDrop 2000c Spectrometer. *Journal of Visualized Experiments*, 10(1610), pp.8–10. Available at: http://www.ncbi.nlm.nih.gov/pmc/articles/PMC3157846/.

Dobrovolskaia, M.A. & Vogel, S.N., 2002. Toll receptors, CD14, and macrophage activation and deactivation by LPS. *Microbes and Infection*, 4(9), pp.903–914.

Donnelly, R.P., Dickensheets, H. & Finbloom, D.S., 1999. The Interleukin-10 Signal Transduction Pathway and Regulation of Gene Expression in Mononuclear Phagocytes. *Journal of Interferon & Cytokine Research*, 19(6), pp.563–573. Available at: http://www.liebertonline.com/doi/abs/10.1089/107999099313695.

Duricova, D. et al., 2014. Age-related differences in presentation and course of inflammatory bowel disease: An update on the population-based literature. *Journal of Crohn's and Colitis*, 8(11), pp.1351–1361.

Edelson, J.D. et al., 1985. Autofluorescence of alveolar macrophages: Problems and potential solutions. *Medical Hypotheses*, 17(4), pp.403–407. Available at: https://www.sciencedirect.com/science/article/pii/0306987785900994 [Accessed July 26, 2018].

Enzan, H., 1986. ELECTRON MICROSCOPIC STUDIES OF MACROPHAGES IN EARLY HUMAN YOLK SACS. *Pathology International*, 36(1), pp.49–64. Available at: http://doi.wiley.com/10.1111/j.1440-1827.1986.tb01460.x [Accessed March 22, 2018].

Epelman, S. et al., 2014. Embryonic and adult-derived resident cardiac macrophages are maintained

through distinct mechanisms at steady state and during inflammation. *Immunity*, 40(1), pp.91–104. Available at: http://dx.doi.org/10.1016/j.immuni.2013.11.019.

Fantini, M.C. et al., 2009. Smad7 Controls Resistance of Colitogenic T Cells to Regulatory T Cell-Mediated Suppression. *Gastroenterology*, 136(4), p.1308–1316.e3. Available at: http://dx.doi.org/10.1053/j.gastro.2008.12.053.

Fingerle, B.G. et al., 2018. The Novel Subset of CD14+/CD16+ Blood Monocytes I s Expanded in Sepsis Patients. *Blood*, 82(10), pp.3170–3176.

Fogg, D.K. et al., 2006. A Clonogenic Bone Marrow Progenitor Specific for Macrophages and Dendritic Cells. *Science*, 311(March), pp.83–88.

Ford, A.C. et al., 2011. Efficacy of 5-Aminosalicylates in Crohn's Disease: Systematic Review and Meta-Analysis. *The American Journal of Gastroenterology*, 106(4), pp.617–629. Available at: http://www.nature.com/articles/ajg201171 [Accessed December 17, 2018].

Fournier, B.M. & Parkos, C.A., 2012. The role of neutrophils during intestinal inflammation. *Mucosal Immunology*, 5(4), pp.354–366. Available at: http://dx.doi.org/10.1038/mi.2012.24.

Franke, A. et al., 2010. Genome-wide meta-analysis increases to 71 the number of confirmed Crohn's disease susceptibility loci. *Nature genetics*, 42(12), pp.1118–1125. Available at: http://www.pubmedcentral.nih.gov/articlerender.fcgi?artid=3299551&tool=pmcentrez&rendertype=abstract.

Fuss, I.J. et al., 1996. Disparate CD4+ lamina propria (LP) lymphokine secretion profiles in inflammatory bowel disease. Crohn's disease LP cells manifest increased secretion of IFN-gamma, whereas ulcerative colitis LP cells manifest increased secretion of IL-5. *The Journal of experimental medicine*, 157, pp.1261–1270.

Fuss, I.J. et al., 2004. Nonclassical CD1d-restricted NKT cells that produce IL-13 characterized an atypical Th2 response in ulcerative colitis. *J Clin Invest*, 113(10), pp.2–9. Available at: http://www.ncbi.nlm.nih.gov/pubmed/15146247.

Gasche, C. et al., 2003. Novel variants of the IL-10 receptor 1 affect inhibition of monocyte TNF-alpha production. *Journal of immunology*, 170, pp.5578–5582.

Geissmann, F., Jung, S. & Littman, D.R., 2003. Blood monocytes consist of two principal subsets with distinct migratory properties. *Immunity*, 19(1), pp.71–82.

Geremia, A. & Arancibia-Cárcamo, C. V., 2017. Innate lymphoid cells in intestinal inflammation. *Frontiers in Immunology*, 8(OCT), pp.1–13.

Ginhoux, F. et al., 2010. Fate Mapping Analysis Reveals That Adult Microglia Derive from Primitive Macrophages. *Science*, 701(November), pp.841–845.

Ginhoux, F. & Guilliams, M., 2016. Tissue-Resident Macrophage Ontogeny and Homeostasis. *Immunity*, 44(3), pp.439–449. Available at: http://dx.doi.org/10.1016/j.immuni.2016.02.024.

Ginhoux, F. & Jung, S., 2014. Monocytes and macrophages: developmental pathways and tissue homeostasis. *Nature reviews. Immunology*, 14(6), pp.392–404. Available at: http://www.ncbi.nlm.nih.gov/pubmed/24854589 [Accessed July 13, 2014].

Girardin, S.E. et al., 2003. Nod2 Is a General Sensor of Peptidoglycan through Muramyl Dipeptide (MDP) Detection *. *The Journal of Biological Chemistry*, pp.8869–8873.

Glocker, E. & Kotlarz, D., 2009. Inflammatory Bowel Disease and Mutations Affecting the Interleukin-10 Receptor. *The NEW ENGLAND JOURNAL of Medicine*, 361, pp.2033–2045. Available at:

http://www.nejm.org/doi/full/10.1056/nejmoa0907206.

Godin, I. & Cumano, A., 2005. Of birds and mice: hematopoietic stem cell development. *The International Journal of Developmental Biology*, 49(2–3), pp.251–257. Available at: http://www.intjdevbiol.com/paper.php?doi=041945ig.

Graham, D.B. & Xavier, R.J., 2013. From genetics of inflammatory bowel disease towards mechanistic insights. *Trends in Immunology*, 34(8), pp.371–378. Available at: http://dx.doi.org/10.1016/j.it.2013.04.001.

Grainger, J.R. et al., 2013. Inflammatory monocytes regulate pathologic responses to commensals during acute gastrointestinal infection. *Nature Medicine*, 19(6), pp.713–721. Available at: http://dx.doi.org/10.1038/nm.3189.

Granlund, A. van B. et al., 2013. Whole Genome Gene Expression Meta-Analysis of Inflammatory Bowel Disease Colon Mucosa Demonstrates Lack of Major Differences between Crohn's Disease and Ulcerative Colitis. *PLoS ONE*, 8(2).

Grimm, M. et al., 1995. Direct evidence of monocyte recruitment to inflammatory bowel disease mucosa. *Journal of Gastroenterology and Hepatology*, 10(4), pp.387–395. Available at: http://doi.wiley.com/10.1111/j.1440-1746.1995.tb01589.x [Accessed May 9, 2018].

Grimm, M.C. et al., 1996. Enhanced expression and production of monocyte chemoattractant protein-1 in inflammatory bowel disease mucosa. *Journal of Leukocyte Biology*, 59(6), pp.804–812.

Grimm, M.C. et al., 1995. Evidence for a CD14+ population of monocytes in inflammatory bowel disease mucosa-implications for pathogenesis. *Clinical experimental immunology*, 100, pp.291–297.

Grip, O. et al., 2006. Increased subpopulations of CD16(+) and CD56(+) blood monocytes in patients with active Crohn's disease. *Inflammatory bowel diseases*, 12, pp.1–7. Available at: http://www.ncbi.nlm.nih.gov/pubmed/17260384 [Accessed February 9, 2015].

Grundtner, P. et al., 2009. The IL-10R1 S138G loss-of-function allele and ulcerative colitis. *Genes and immunity*, 10, pp.84–92.

Guilliams, M. et al., 2013. Alveolar macrophages develop from fetal monocytes that differentiate into long-lived cells in the first week of life via GM-CSF. *The Journal of Experimental Medicine*, 210(10), pp.1977–1992. Available at: http://www.jem.org/lookup/doi/10.1084/jem.20131199.

Guilliams, M., Bruhns, P., et al., 2014. The function of Fcγ receptors in dendritic cells and macrophages. *Nature reviews. Immunology*, 14(2), pp.94–108. Available at: http://www.ncbi.nlm.nih.gov/pubmed/24445665.

Guilliams, M., Ginhoux, F. & Jakubzick, C., 2014. Dendritic cells, monocytes and macrophages: a unified nomenclature based on ontogeny. *Nature Reviews …*, 14(August), pp.571–576. Available at: http://www.nature.com/nri/journal/v14/n8/abs/nri3712.html [Accessed November 7, 2014].

Guindi, M. & Riddell, R.H., 2004. Indeterminate colitis. *Journal of Clinical Pathology*, 57(12), pp.1233–1244.

Hadis, U. et al., 2011. Intestinal Tolerance Requires Gut Homing and Expansion of FoxP3+ Regulatory T Cells in the Lamina Propria. *Immunity*, 34(2), pp.237–246.

Halfvarson, J. et al., 2003. Inflammatory bowel disease in a Swedish twin cohort: A long- term follow-up of concordance and clinical characteristics. *Gastroenterology*, 124(7), pp.1767–1773.

Halldén, G. et al., 1991. Quenching of intracellular autofluorescence in alveolar macrophages permits analysis of fluorochrome labelled surface antigens by flow cytofluoremetry. *Journal of Immunological Methods*, 142(2), pp.207–214. Available at: https://www.sciencedirect.com/science/article/pii/002217599190108R?via%3Dihub [Accessed July 26, 2018].

Hanauer, S.B., 2006. Inflammatory Bowel Disease : Epidemiology , Pathogenesis , and Therapeutic Opportunities. *Inflammatory Bowel Diseases*, 12(January), pp.3–8.

Hann, M.I., Bodger, M.P. & Hoffmann, A. V., 1983. Development of Pluripotent Hematopoietic Progenitor Cells in the Human Fetus. *Blood*, 62(1), pp.118–123.

Hanna, R.N. et al., 2011. The transcription factor NR4A1 (Nur77) controls bone marrow differentiation and the survival of Ly6C- monocytes. *Nature Immunology*, 12(8), pp.778–785.

Hans, W. et al., 2000. The role of the resident intestinal flora in acute and chronic dextran sulfate sodium-induced colitis in mice. *European journal of gastroenterology & hepatology*, 12(3), pp.267–73. Available at: http://www.ncbi.nlm.nih.gov/pubmed/10750645 [Accessed March 19, 2018].

Hansen, R. et al., 2012. Microbiota of De-Novo Pediatric IBD: Increased Faecalibacterium Prausnitzii and Reduced Bacterial Diversity in Crohn's But Not in Ulcerative Colitis. *The American Journal of Gastroenterology*, 107, pp.1913–1922. Available at: https://www.nature.com/articles/ajg2012335.pdf [Accessed May 25, 2018].

Hart, A.L. et al., 2005. Characteristics of intestinal dendritic cells in inflammatory bowel diseases. *Gastroenterology*, 129(1), pp.50–65.

Hart, A.L. et al., 2004a. Prospective evaluation of intestinal homing memory T cells in ulcerative colitis. *Inflammatory Bowel Diseases*, 10(5), pp.496–503.

Hart, A.L. et al., 2004b. Quantitative and functional characteristics of intestinal-homing memory T cells : analysis of Crohn ' s disease patients and healthy controls. *Clinical experimental immunology*, 135, pp.137–145.

Hashimoto, D. et al., 2013. Tissue-resident macrophages self-maintain locally throughout adult life with minimal contribution from circulating monocytes. *Immunity*, 38(4), pp.792–804.

Havenith, C.E.G. et al., 1993. Separation of alveolar macrophages and dendritic cells via autofluorescence: phenotypical and functional characterizatior. *Journal of Leukocyte Biology*, 53(5), pp.504–510. Available at: http://doi.wiley.com/10.1002/jlb.53.5.504 [Accessed July 26, 2018].

Heazlewood, C.K. et al., 2008. Aberrant mucin assembly in mice causes endoplasmic reticulum stress and spontaneous inflammation resembling ulcerative colitis. *PLoS Medicine*, 5(3), pp.0440–0460.

Heller, F. et al., 2002. Oxazolone colitis, a Th2 colitis model resembling ulcerative colitis, is mediated by IL-13-producing NK-T cells. *Immunity*, 17(5), pp.629–638.

Hoeffel, G. et al., 2012. Adult Langerhans cells derive predominantly from embryonic fetal liver monocytes with a minor contribution of yolk sac–derived macrophages. *The Journal of Experimental Medicine*, 209(6), pp.1167–1181. Available at: http://www.jem.org/lookup/doi/10.1084/jem.20120340.

Honda, K. et al., 2005. IRF-7 is the master regulator of type-I interferon-dependent immune responses. *Nature*, 434(April), pp.772–777.

Hooper, L. V. & MacPherson, A.J., 2010. Immune adaptations that maintain homeostasis with the intestinal microbiota. *Nature Reviews Immunology*, 10(3), pp.159–169.

Hori, S., Nomura, T. & Sakaguchi, S., 2002. Control of Regulatory T Cell Development by the Transcription Factor Foxp3. *Science*, 299, pp.1057–1061.

Hoshi, N. et al., 2012. MyD88 signalling in colonic mononuclear phagocytes drives colitis in IL-10 deficient mice. *Nature Communications*, 3(1120), pp.1–18.

Hovhannisyan, Z. et al., 2011. Characterization of interleukin-17-producing regulatory T cells in inflamed intestinal mucosa from patients with inflammatory bowel diseases. *Gastroenterology*, 140(3), pp.957–965. Available at: http://dx.doi.org/10.1053/j.gastro.2010.12.002.

Hudcovic, T. et al., 2001. The Role of Microflora in the Development of Intestinal Inflammation: Acute and Chronic Colitis Induced by Dextran Sulfate in Germ-Free and Conventionally Reared Immunocompetent and Immunodeficient Mice. *Folia Microbiologica*, 46(6), pp.565–572.

Hue, S. et al., 2006. Interleukin-23 drives innate and T cell–mediated intestinal inflammation. *The Journal of Experimental Medicine*, 203(11), pp.2473–2483. Available at: http://www.jem.org/lookup/doi/10.1084/jem.20061099.

Hueber, W. et al., 2012. Secukinumab, a human anti-IL-17A monoclonal antibody, for moderate to severe Crohn's disease: Unexpected results of a randomised, double-blindplacebo- controlled trial. *Gut*, 61(12), pp.1693–1700.

Huff, K.R. et al., 2011. Extracellular matrix-associated cytokines regulate CD4+ effector T-cell responses in the human intestinal mucosa. *Mucosal Immunology*, 4(4), pp.420–427. Available at: http://www.nature.com/doifinder/10.1038/mi.2010.86.

Hugot, J. et al., 2001. Association of NOD2 leucine-rich repeat variants with susceptibility to Crohn ' s disease. *Nature*, pp.599–603.

Hviid, A., Svanstro, H. & Frisch, M., 2011. Antibiotic use and inflammatory bowel diseases in childhood. *Gut*, 60, pp.49–54.

Ingersoll, M. et al., 2010. Comparison of gene expression profiles between human and mouse monocyte subsets. *Blood*, 115(3), pp.10–20. Available at: http://bloodjournal.hematologylibrary.org/content/115/3/e10.short.

Inohara, N. et al., 2003. Host Recognition of Bacterial Muramyl Dipeptide Mediated through NOD2. *The Journal of Biological Chemistry*, pp.5509–5513.

Ip, W.K.E. et al., 2017. Anti-inflammatory effect of IL-10 mediated by metabolic reprogramming of macrophages. *Science*, 356(6337), pp.513–519.

Italiani, P. & Boraschi, D., 2014. From monocytes to M1/M2 macrophages: Phenotypical vs. functional differentiation. *Frontiers in Immunology*, 5(OCT), pp.1–22.

Jakubzick, C. et al., 2013. Minimal differentiation of classical monocytes as they survey steady-state tissues and transport antigen to lymph nodes. *Immunity*, 39(3), pp.599–610. Available at: http://dx.doi.org/10.1016/j.immuni.2013.08.007.

Jia, T. et al., 2008. Additive Roles for MCP-1 and MCP-3 in CCR2-Mediated Recruitment of Inflammatory Monocytes during Listeria monocytogenes Infection. *The Journal of Immunology*, 180(10), pp.6846–6853. Available at: http://www.jimmunol.org/cgi/doi/10.4049/jimmunol.180.10.6846.

Joeris, T. et al., 2017. Diversity and functions of intestinal mononuclear phagocytes. *Mucosal*

Immunology, 10(4), pp.845–864. Available at: http://www.nature.com/articles/mi201722 [Accessed May 31, 2018].

Joffre, O.P. et al., 2012. Cross-presentation by dendritic cells. *Nature Reviews Immunology*, 12, pp.557–569. Available at: www.nature.com/reviews/immunol [Accessed August 9, 2018].

Johansson, M.E. V., Larsson, J.M.H. & Hansson, G.C., 2011. The two mucus layers of colon are organized by the MUC2 mucin, whereas the outer layer is a legislator of host-microbial interactions. *PNAS*, 108(Supplement_1), pp.4659–4665. Available at: http://www.pnas.org/cgi/doi/10.1073/pnas.1006451107.

Johansson, M.E. V et al., 2008. The inner of the two Muc2 mucin-dependent mucus layers in colon is devoid of bacteria. *Pnas*, 105(39), pp.15064–15069. Available at: http://www.ncbi.nlm.nih.gov/pubmed/18806221%5Cnhttp://www.pubmedcentral.nih.gov/articlerender.fcgi?artid=PMC2567493.

Jones, G.-R. et al., 2018. Dynamics of Colon Monocyte and Macrophage Activation During Colitis. *Frontiers in Immunology*, 9(November), p.2764. Available at: https://www.frontiersin.org/article/10.3389/fimmu.2018.02764/full.

Jostins, L. et al., 2012. Host-microbe interactions have shaped the genetic architecture of inflammatory bowel disease. *Nature*, 491(7422), pp.119–24. Available at: http://www.pubmedcentral.nih.gov/articlerender.fcgi?artid=3491803&tool=pmcentrez&rendertype=abstract [Accessed July 9, 2014].

Jurjus, A.R., Khoury, N.N. & Reimund, J.M., 2004. Animal models of inflammatory bowel disease. *Journal of Pharmacological and Toxicological Methods*, 50(2), pp.81–92.

Kagan, J.C. et al., 2008. TRAM couples endocytosis of Toll-like receptor 4 to the induction of interferon-β. *Nature Immunology*, 9(4), pp.361–368.

Kamada, N. et al., 2008. Unique CD14+ intestinal macrophages contribute to the pathogenesis of Crohn disease via IL-23/IFN-γ axis. *Journal of clinical investigations*, 118(6), pp.2269–2280.

Kanitakis, J. et al., 2011. Self-renewal capacity of human epidermal Langerhans cells: Observations made on a composite tissue allograft. *Experimental Dermatology*, 20(2), pp.145–146.

Kawamura, S. et al., 2017. Identification of a Human Clonogenic Progenitor with Strict Monocyte Differentiation Potential: A Counterpart of Mouse cMoPs. *Immunity*, 46(5), p.835–848.e4. Available at: http://dx.doi.org/10.1016/j.immuni.2017.04.019.

Kayama, H. et al., 2012. Intestinal CX3C chemokine receptor 1high (CX3CR1high) myeloid cells prevent T-cell-dependent colitis. *Proceedings of the National Academy of Sciences*, 109(13), pp.5010–5015. Available at: http://www.pnas.org/cgi/doi/10.1073/pnas.1114931109.

Kenny, E.E. et al., 2012. A genome-wide scan of ashkenazi jewish crohn's disease suggests novel susceptibility loci. *PLoS Genetics*, 8(3), pp.1–10.

Kim, Y.G. et al., 2011. The Nod2 Sensor Promotes Intestinal Pathogen Eradication via the Chemokine CCL2-Dependent Recruitment of Inflammatory Monocytes. *Immunity*, 34(5), pp.769–780.

Kitajima, S. et al., 2001. Dextran Sodium Sulfate-Induced Colitis in Germ-Free IQI/Jic Mice. *Experimental Animals*, 50(5), pp.387–395. Available at: http://joi.jlc.jst.go.jp/JST.JSTAGE/expanim/50.387?from=CrossRef.

Kleer, I. De et al., 2014. Ontogeny of myeloid cells. *Frontiers in Immunology*, 5(423), pp.1–11.

Knoll, R.L. et al., 2016. Gut microbiota differs between children with Inflammatory Bowel Disease

and healthy siblings in taxonomic and functional composition: a metagenomic analysis. *American Journal of Gastrointestinal and Liver Physiology*, 312, pp.G327–G339. Available at: https://www.physiology.org/doi/pdf/10.1152/ajpgi.00293.2016 [Accessed May 25, 2018].

Kojima, R. et al., 2004. Oxazolone-Induced Colitis in BALB/C Mice: a New Method to Evaluate the Efficacy of Therapeutic Agents for Ulcerative Colitis. *Journal of Pharmacological Sciences*, 96(3), pp.307–313. Available at: http://joi.jlc.jst.go.jp/JST.JSTAGE/jphs/FP0040214?from=CrossRef.

Kole, A. & Maloy, K.J., 2014. Control of Intestinal Inflammation by Interleukin-10. In *Interleukin-10 in Health and Disease*. Springer, Berlin, Heidelberg, pp. 19–38. Available at: http://link.springer.com/10.1007/978-3-662-43492-5_2 [Accessed March 23, 2018].

Kontoyiannis, D. et al., 1999. Impaired On/Off Regulation of TNF Biosynthesis in Mice Lacking TNF AU-Rich Elements: Implications for Joint and Gut-Associated Immunopathologies. *Immunity*, 10, pp.387–398. Available at: http://www.cell.com/immunity/pdf/S1074-7613(00)80038-2.pdf [Accessed April 3, 2018].

Kotenko, S. V. et al., 1997. Identification and functional characterization of a second chain of the interleukin-10 receptor complex. *The EMBO journal*, 16(19), pp.5894–903. Available at: http://www.ncbi.nlm.nih.gov/pubmed/9312047%5Cnhttp://www.pubmedcentral.nih.gov/articlerender.fcgi?artid=PMC1170220.

Krause, P. et al., 2015. IL-10-producing intestinal macrophages prevent excessive antibacterial innate immunity by limiting IL-23 synthesis. *Nature Communications*, 6(May), pp.1–12. Available at: http://dx.doi.org/10.1038/ncomms8055.

Kühn, R. et al., 1993. Interleukin-10-deficient mice develop chronic enterocolitis. *Cell*, 75, pp.263–274.

van de Laar, L. et al., 2016. Yolk Sac Macrophages, Fetal Liver, and Adult Monocytes Can Colonize an Empty Niche and Develop into Functional Tissue-Resident Macrophages. *Immunity*, 44(4), pp.755–768. Available at: http://dx.doi.org/10.1016/j.immuni.2016.02.017.

De Lange, K.M. et al., 2017. Genome-wide association study implicates immune activation of multiple integrin genes in inflammatory bowel disease. *Nature Genetics*, 49(2), pp.256–261. Available at: http://dx.doi.org/10.1038/ng.3760.

Langlet, C. et al., 2012. CD64 Expression Distinguishes Monocyte-Derived and Conventional Dendritic Cells and Reveals Their Distinct Role during Intramuscular Immunization. *The Journal of Immunology*, 188(4), pp.1751–1760. Available at: http://www.jimmunol.org/cgi/doi/10.4049/jimmunol.1102744.

Lawrence, T., 2009. The nuclear factor NF-kappaB pathway in inflammation. *Cold Spring Harbor perspectives in biology*, 1(6), pp.1–10.

Lee, J.C. et al., 2017. Genome-wide association study identifies distinct genetic contributions to prognosis and susceptibility in Crohn's disease. *Nature Genetics*, 49, pp.1–9. Available at: http://www.nature.com/doifinder/10.1038/ng.3755.

Lee, P.Y. et al., 2013. Ly6 family proteins in neutrophil biology. *Journal of leukocyte biology*, 94(4), pp.585–94. Available at: http://www.ncbi.nlm.nih.gov/pubmed/23543767.

Levin, A.D., Wildenberg, M.E. & van den Brink, G.R., 2016. Mechanism of action of anti-TNF therapy in inflammatory bowel disease. *Journal of Crohn's & colitis*, pp.1–9. Available at: http://ecco-jcc.oxfordjournals.org/content/early/2016/02/17/ecco-jcc.jjw053.abstract.

Levitt, M.D. et al., 1999. Detoxification of hydrogen sulfide and methanethiol in the cecal mucosa.

Journal of Clinical Investigation, 104(8), pp.1107–1114.

Li, F. et al., 2012. Autofluorescence contributes to false-positive intracellular Foxp3 staining in macrophages: A lesson learned from flow cytometry. *Journal of Immunological Methods*, 386(1–2), pp.101–107. Available at: https://www.sciencedirect.com/science/article/pii/S0022175912002657?via%3Dihub [Accessed July 26, 2018].

Lindsay, J.O. et al., 2003. Local delivery of adenoviral vectors encoding murine interleukin 10 induces colonic interleukin 10 production and is therapeutic for murine colitis. *Gut*, 52(7), pp.981–987.

Lisi, S. et al., 2011. Advances in the understanding of the Fc gamma receptors-mediated autoantibodies uptake. *Clinical and Experimental Medicine*, 11(1), pp.1–10.

Lissner, D. et al., 2015. Monocyte and M1 Macrophage-induced Barrier Defect Contributes to Chronic Intestinal Inflammation in IBD. *Inflammatory Bowel Diseases*, 21(6), pp.1297–1305.

Liu, Z. et al., 1999. Hyperexpression of CD40 Ligand (CD154) in Inflammatory Bowel Disease and Its Contribution to Pathogenic Cytokine Production. *The Journal of Immunology*, 163(7), pp.4049–4057.

Livak, K.J. & Schmittgen, T.D., 2001. Analysis of relative gene expression data using real-time quantitative PCR and the 2(-Delta Delta C(T)) Method. *Methods (San Diego, Calif.)*, 25(4), pp.402–8. Available at: http://www.ncbi.nlm.nih.gov/pubmed/11846609 [Accessed January 20, 2014].

Lu, Y.C., Yeh, W.C. & Ohashi, P.S., 2008. LPS/TLR4 signal transduction pathway. *Cytokine*, 42(2), pp.145–151.

Ma, T.Y. et al., 2004. TNFa-induced increase in intestinal epithelial tight junction permeability requires NF- B activation. *AJP: Gastrointestinal and Liver Physiology*, 286(3), p.367G–376. Available at: http://ajpgi.physiology.org/cgi/doi/10.1152/ajpgi.00173.2003.

MacPherson, A.J. et al., 2008. The immune geography of IgA induction and function. *Mucosal Immunology*, 1(1), pp.11–22.

Magnusson, M.K. et al., 2016. Macrophage and dendritic cell subsets in IBD: ALDH+cells are reduced in colon tissue of patients with ulcerative colitis regardless of inflammation. *Mucosal Immunology*, 9(1), pp.171–182.

Mahid, S.S. et al., 2006. Smoking and Inflammatory Bowel Disease: A Meta-analysis. *Mayo Clinic Proceedings*, 81(11), pp.1462–1471. Available at: https://www.sciencedirect.com/science/article/pii/S0025619611612536?via%3Dihub [Accessed May 25, 2018].

Mahida, Y.R., Wu, K.C. & Jewell, D.P., 1989. Respiratory burst activity of intestinal macrophages in normal and inflammatory bowel disease. *Gut*, 30(10), pp.1362–1370. Available at: http://gut.bmj.com/cgi/doi/10.1136/gut.30.10.1362.

Makita, S. et al., 2004. CD4+ CD25bright T Cells in Human Intestinal Lamina Propria as Regulatory Cells. *The Journal of Immunology*, 173(5), pp.3119–3130. Available at: http://www.jimmunol.org/lookup/doi/10.4049/jimmunol.173.5.3119.

Malefyt, R. et al., 1991. Interleukin 10(IL-10) Inhibits Cytokine Synthesis by Human Monocytes: An Autoregulatory Role of IL-10 Produced by Monocytes. *Journal of Experimental Medicine*, 174(November), pp.1209–1220.

Manichanh, C. et al., 2006. Reduced diversity of faecal microbiota in Crohn's disease revealed by a

metagenomic approach. *Gut*, 55, pp.205–211. Available at: http://gut.bmj.com/content/gutjnl/55/2/205.full.pdf [Accessed May 25, 2018].

Manichanh, C. et al., 2012. The gut microbiota in IBD. *Nature Reviews Gastroenterology & Hepatology*, 9(10), pp.599–608. Available at: http://www.nature.com/articles/nrgastro.2012.152 [Accessed May 25, 2018].

Mannon, P.J. et al., 2004. Anti–Interleukin-12 Antibody for Active Crohn's Disease. *New England Journal of Medicine*, 351(20), pp.2069–2079. Available at: http://www.nejm.org/doi/abs/10.1056/NEJMoa033402.

Mao, H. et al., 2012. Exome sequencing identifies novel compound heterozygous mutations of IL-10 receptor 1 in neonatal-onset Crohn's disease. *Genes and Immunity*, 13(5), pp.437–442. Available at: http://www.nature.com/doifinder/10.1038/gene.2012.8.

Marlow, G.J., van Gent, D. & Ferguson, L.R., 2013. Why interleukin-10 supplementation does not work in Crohn's disease patients. *World journal of gastroenterology : WJG*, 19(25), pp.3931–41. Available at: http://www.pubmedcentral.nih.gov/articlerender.fcgi?artid=3703179&tool=pmcentrez&rendertype=abstract [Accessed January 9, 2015].

Martin, H.M. et al., 2004. Enhanced Escherichia coli adherence and invasion in Crohn's disease and colon cancer. *Gastroenterology*, 127(1), pp.80–93.

Mass, E. et al., 2016. Specification of tissue-resident macrophages during organogenesis. *Science*, 4238(6304), p.1114.

Maul, J. et al., 2005. Peripheral and intestinal regulatory CD4+CD25highT cells in inflammatory bowel disease. *Gastroenterology*, 128(7), pp.1868–1878.

Mazzini, E. et al., 2014. Oral Tolerance Can Be Established via Gap Junction Transfer of Fed Antigens from CX3CR1+ Macrophages to CD103+ Dendritic Cells. *Immunity*, 40(2), pp.248–261. Available at: http://dx.doi.org/10.1016/j.immuni.2013.12.012.

McGovern, D.P.B. et al., 2010. Genome-wide association identifies multiple ulcerative colitis susceptibility loci. *Nature genetics*, 42(4), pp.332–337.

Melgar, S. et al., 2005. Acute colitis induced by dextran sulfate sodium progresses to chronicity in C57BL / 6 but not in BALB / c mice : correlation between symptoms and inflammation. *American Journal of Gastrointestinal and Liver Physiology*, 288, pp.1328–1338.

Melgar, S. et al., 2008. Validation of murine dextran sulfate sodium-induced colitis using four therapeutic agents for human inflammatory bowel disease. *International Immunopharmacology*, 8(6), pp.836–844.

Mildner, A. et al., 2017. Genomic Characterization of Murine Monocytes Reveals C/EBPβ Transcription Factor Dependence of Ly6C−Cells. *Immunity*, 46(5), p.849–862.e7.

Mirza Muhammad Adnan, 2011. Comparison between Crohn Disease and Ulcerative Colitis. *MBBS Medicine (Humanity First)*. Available at: http://medicinembbs.blogspot.co.uk/2011/01/comparison-between-crohn-disease-and.html [Accessed May 7, 2018].

Mitroulis, I. et al., 2018. Modulation of Myelopoiesis Progenitors Is an Integral Component of Trained Immunity. *Cell*, 172(1–2), p.147–161.e12.

Molander, P. et al., 2013. Achievement of deep remission during scheduled maintenance therapy with TNFα-blocking agents in IBD. *Journal of Crohn's and Colitis*, 7(9), pp.730–735. Available at:

http://dx.doi.org/10.1016/j.crohns.2012.10.018.

Molawi, K. et al., 2014. Progressive replacement of embryo-derived cardiac macrophages with age. *The Journal of Experimental Medicine*, 211(11), pp.2151–2158. Available at: http://www.jem.org/lookup/doi/10.1084/jem.20140639.

Molodecky, N.A. et al., 2012. Increasing incidence and prevalence of the inflammatory bowel diseases with time, based on systematic review. *Gastroenterology*, 142(1), p.46–54.e42. Available at: http://dx.doi.org/10.1053/j.gastro.2011.10.001.

Monteleone, G. et al., 1997. Interleukin 12 is expressed and actively released by Crohn's disease intestinal lamina propria mononuclear cells. *Gastroenterology*, 112(4), pp.1169–1178.

Monteleone, G. et al., 2015. Mongersen, an Oral SMAD7 Antisense Oligonucleotide, and Crohn's Disease. *New England Journal of Medicine*, 372, pp.1104–1113. Available at: http://www.nejm.org/doi/abs/10.1056/NEJMoa1407250.

Moore, K.W. et al., 2001. Interleukin-10 and the Interleukin-10 Receptor. *Annual Review of Immunology*, 19(1), pp.683–765. Available at: http://www.annualreviews.org/doi/abs/10.1146/annurev.immunol.19.1.683.

Morrissey, P.J. et al., 1993. CD4+ T cells that express high levels of CD45RB induce wasting disease when transferred into congenic severe combined immunodeficient mice. Disease development is prevented by cotransfer of purified CD4+ T cells. *The Journal of experimental medicine*, 178(July), pp.237–244.

Mosser, D.M. & Edwards, J.P., 2009. Exploring the full spectrum of macrophage activation David. *Nature Reviews Immunology*, 8(12), pp.958–969.

Mosser, D.M. & Zhang, X., 2008. Interleukin-10: New perspectives on an old cytokine. *Immunological Reviews*, 226, pp.205–218.

Mowat, A.M. & Bain, C.C., 2011. Mucosal Macrophages in Intestinal Homeostasis and Inflammation. *Journal of Innate Immunity*, 3(6), pp.550–564. Available at: http://www.karger.com/doi/10.1159/000329099.

Nathan, C. & Cunningham-Bussel, A., 2013. Beyond oxidative stress: an immunologist's guide to reactive oxygen species. *Nature Reviews Cancer*, 13(2), pp.83–96.

Nemoto, H. et al., 2012. Reduced Diversity and Imbalance of Fecal Microbiota in Patients with Ulcerative Colitis. *Digestive Diseases and Sciences*, 57, pp.2955–2964. Available at: https://link.springer.com/content/pdf/10.1007%2Fs10620-012-2236-y.pdf [Accessed May 25, 2018].

Nenci, A. et al., 2007. Epithelial NEMO links innate immunity to chronic intestinal inflammation. *Nature*, 446(7135), pp.557–561.

Neurath, M.F. et al., 2002. The Transcription Factor T-bet Regulates Mucosal T Cell Activation in Experimental Colitis and Crohn's Disease. *The Journal of Experimental Medicine*, 195(9), pp.1129–1143. Available at: http://www.jem.org/lookup/doi/10.1084/jem.20011956.

Ng, S.C. et al., 2013. Geographical variability and environmental risk factors in inflammatory bowel disease. *Gut*, 62(4), pp.630–649.

Nockher, W.A., Chemistry, C. & Universita, L., 1998. Expanded CD14+CD16+ Monocyte Subpopulation in Patients with Acute and Chronic Infections Undergoing Hemodialysis. *Infection and iImunity*, 66(6), pp.2782–2790.

O'Hara, A.M. & Shanahan, F., 2006. The gut flora as a forgotten organ. *EMBO Reports*, 7(7), pp.688–693.

Ogino, T. et al., 2013. Increased Th17-inducing activity of CD14+CD163lowmyeloid cells in intestinal lamina propria of patients with Crohn's disease. *Gastroenterology*, 145(6), p.1380–1391.e1. Available at: http://dx.doi.org/10.1053/j.gastro.2013.08.049.

Ogura, Y. et al., 2001. A frameshift mutation in NOD2 associated with susceptibility to Crohn ' s disease. *Journal of Biological Chemistry*, 411(May), pp.603–606.

Okayasu, I. et al., 1990. A novel method in the induction of reliable experimental acute and chronic ulcerative colitis in mice. *Gastroenterology*, 98(3), pp.694–702. Available at: https://www.sciencedirect.com/science/article/pii/001650859090290H [Accessed March 19, 2018].

Oppmann, B. et al., 2000. Novel p19 protein engages IL-12p40 to form a cytokine, IL-23, with biological activities similar as well as distinct from IL-12. *Immunity*, 13(5), pp.715–725.

Ordás, I. et al., 2012. Ulcerative colitis. *Lancet*, 380, pp.1606–1619.

Parrello, T. et al., 2000. Up-regulation of the IL-12 receptor beta 2 chain in Crohn's disease. *The Journal of Immunology*, 165(12), pp.7234–7239. Available at: http://www.ncbi.nlm.nih.gov/pubmed/11120856%5Cnhttp://www.jimmunol.org/content/165/12/7234.full.pdf.

Parronchi, P. et al., 1997. Type 1 T-helper cell predominance and interleukin-12 expression in the gut of patients with Crohn's disease. *The American journal of pathology*, 150(3), pp.823–832.

Passlick, B., Flieger, D. & Ziegler-Heitbrock, L., 1989. Identification and characterisation of a Novel Monocyte Subpopulation in Human Peripheral Blood. *Blood*, 74(7), pp.2527–2534.

Patel, A.A. et al., 2017. The fate and lifespan of human monocyte subsets in steady state and systemic inflammation. *Journal of Experimental Medicine*, 214(6), pp.1–15. Available at: http://jem.rupress.org/content/early/2017/06/09/jem.20170355.

Paul, W.E. & Zhu, J., 2010. How are TH2-type immune responses initiated and amplified? *Nat Rev Immunol*, 10(4), pp.225–235. Available at: http://www.uniprot.org [Accessed August 9, 2018].

Perše, M. & Cerar, A., 2012. Dextran sodium sulphate colitis mouse model: Traps and tricks. *Journal of Biomedicine and Biotechnology*, 2012, pp.1–13.

Peterson, L.W. & Artis, D., 2014. Intestinal epithelial cells: regulators of barrier function and immune homeostasis. *Nature reviews. Immunology*, 14(3), pp.141–53. Available at: http://www.nature.com/nri/journal/v14/n3/pdf/nri3608.pdf%5Cnhttp://www.nature.com/nri/journal/v14/n3/pdf/nri3608.pdf?WT.ec_id=NRI-201403%5Cnhttp://dx.doi.org/10.1038/nri3608%5Cnhttp://www.ncbi.nlm.nih.gov/pubmed/24566914.

Piccirillo, C.A. et al., 2002. CD4+ CD25+ Regulatory T Cells Can Mediate Suppressor Function in the Absence of Transforming Growth Factor β1 Production and Responsiveness. *The Journal of Experimental Medicine*, 196(2), pp.237–246. Available at: http://www.jem.org/lookup/doi/10.1084/jem.20020590.

Plantinga, M. et al., 2013. Conventional and Monocyte-Derived CD11b+ Dendritic Cells Initiate and Maintain T Helper 2 Cell-Mediated Immunity to House Dust Mite Allergen. *Immunity*, 38(2), pp.322–335. Available at: http://dx.doi.org/10.1016/j.immuni.2012.10.016.

Platt, A.M. et al., 2010. An Independent Subset of TLR Expressing CCR2-Dependent Macrophages

Promotes Colonic Inflammation. *The Journal of Immunology*, 184(12), pp.6843–6854. Available at: http://www.jimmunol.org/cgi/doi/10.4049/jimmunol.0903987.

Polito, J.M. et al., 1996. Crohn's disease: influence of age at diagnosis on site and clinical type of disease. *Gastroenterology*, 111(3), pp.580–586.

Poritz, L.S. et al., 2007. Loss of the Tight Junction Protein ZO-1 in Dextran Sulfate Sodium Induced Colitis. *Journal of Surgical Research*, 140(1), pp.12–19.

Pull, S.L. et al., 2004. *Activated macrophages are an adaptive element of the colonic epithelial progenitor niche necessary for regenerative responses to injury*, Available at: www.pnas.orgcgidoi10.1073pnas.0405979102 [Accessed December 17, 2018].

Pütsep, K. et al., 2000. Germ-free and colonized mice generate the same products from enteric prodefensins. *Journal of Biological Chemistry*, 275(51), pp.40478–40482.

Qualls, J.E., 2006. Suppression of experimental colitis by intestinal mononuclear phagocytes. *Journal of Leukocyte Biology*, 80(4), pp.802–815. Available at: http://www.jleukbio.org/cgi/doi/10.1189/jlb.1205734.

Reinecker, H.C. et al., 1993. Enhanced secretion of tumour necrosis factor-alpha, IL-6, and IL-1 beta by isolated lamina propria mononuclear cells from patients with ulcerative colitis and Crohn's disease. *Clinical and Experimental Immunology*, 94(1), pp.174–181. Available at: http://eutils.ncbi.nlm.nih.gov/entrez/eutils/elink.fcgi?dbfrom=pubmed&id=8403503&retmode=ref&cmd=prlinks%5Cnpapers3://publication/uuid/DFB27BD1-EEA9-40D0-AF96-62080DF12B51.

Rescigno, M. et al., 2001. Dendritic cells express tight junction proteins and penetrate gut epithelial monolayers to sample bacteria. *Nature Immunology*, 2(4), pp.361–367.

Rhen, T. & Cidlowski, J. a, 2005. Anti-inflammatory action of glucocorticoids--new mechanisms for old drugs. *The New England journal of medicine*, 353, pp.1711–1723.

Riley, J.K. et al., 1999. Interleukin-10 Receptor Signaling through the JAK-STAT Pathway. *The Journal of biological chemistry*, 274(23), pp.16513–16521.

Rivollier, A. et al., 2012. Inflammation switches the differentiation program of Ly6Chi monocytes from antiinflammatory macrophages to inflammatory dendritic cells in the colon. *The Journal of Experimental Medicine*, 209(1), pp.139–155. Available at: http://www.jem.org/lookup/doi/10.1084/jem.20101387.

Romee, R. et al., 2013. NK cell CD16 surface expression and function is regulated by a disintegrin and metalloprotease-17 (ADAM17). *Blood*, 121(18), pp.3599–3608.

Rossol, M. et al., 2012. The CD14 bright CD16+ Monocyte Subset Is Expanded in Rheumatoid Arthritis and Promotes Expansion of the Th17 Cell Population. *ARTHRITIS & RHEUMATISM*, 64(3), pp.671–677.

Rovedatti, L. et al., 2009. Differential regulation of interleukin 17 and interferon γ production in inflammatory bowel disease. *Gut*, 58(12), pp.1629–1636.

Rugtveit, J. et al., 1997. Cytokine profiles differ in newly recruited and resident subsets of mucosal macrophages from inflammatory bowel disease. *Gastroenterology*, 112(5), pp.1493–1505.

Sandborn, W.J. et al., 2008. A Randomized Trial of Ustekinumab, a Human Interleukin-12/23 Monoclonal Antibody, in Patients With Moderate-to-Severe Crohn's Disease. *Gastroenterology*, 135(4), pp.1130–1141.

Sanders, T.J. et al., 2014. Increased Production of Retinoic Acid by Intestinal Macrophages Contributes to Their Inflammatory Phenotype in Patients With Crohn ' s Disease. *Gastroenterology*, 146(5), pp.1278–1286. Available at: http://www.sciencedirect.com/science/article/pii/S0016508514001486%5Cnhttp://www.ncbi.nlm.nih.gov/pubmed/24503130.

Schakel, K. et al., 2006. Human 6-Sulfo LacNAc-Expressing Dendritic Cells Are Principal Producers of Early Interleukin-12 and Are Controlled by Erythrocytes. *Immunity*, 24(6), pp.767–777.

Schippers, a et al., 2015. β7-Integrin exacerbates experimental DSS-induced colitis in mice by directing inflammatory monocytes into the colon. *Mucosal immunology*, 9(2), pp.527–538. Available at: http://www.ncbi.nlm.nih.gov/pubmed/26349655.

Schlitt, A. et al., 2004. Cell Signalling and Vessel Remodelling CD14 + CD16 + monocytes in coronary artery disease and their relationship to serum TNF- α levels. *Thrombosis and Haemostasis*, (Sept), pp.419–424.

Schmitz, M. et al., 2002. Native human blood dendritic cells as potent effectors in antibody-dependent cellular cytotoxicity. *Blood*, 100(4), pp.1502–4. Available at: http://www.ncbi.nlm.nih.gov/pubmed/12149240.

Schridde, A. et al., 2017. Tissue-specific differentiation of colonic macrophages requires TGFβ receptor-mediated signaling. *Mucosal Immunology*, 10(6), pp.1387–1399. Available at: http://dx.doi.org/10.1038/mi.2016.142.

Schulz, O. et al., 2009. Intestinal CD103 $^{+}$, but not CX3CR1 $^{+}$, antigen sampling cells migrate in lymph and serve classical dendritic cell functions. *The Journal of Experimental Medicine*, 206(13), pp.3101–3114. Available at: http://www.jem.org/lookup/doi/10.1084/jem.20091925.

Selve, N. & Wöhrmann, T., 1992. Intestinal inflammation in TNBS sensitized rats as a model of chronic inflammatory bowel disease. *Mediators of Inflammation*, 1(2), pp.121–126.

Serbina, N. V. & Pamer, E.G., 2006. Monocyte emigration from bone marrow during bacterial infection requires signals mediated by chemokine receptor CCR2. *Nature Immunology*, 7(3), pp.311–317.

Shalova, I.N. et al., 2017. CD16 Regulates TRIF-Dependent TLR4 Response in Human Monocytes and Their Subsets. *The Journal of Immunology*, 188, pp.1–10.

Shaw, M.H. et al., 2012. Microbiota-induced IL-1β, but not IL-6, is critical for the development of steady-state TH17 cells in the intestine. *The Journal of Experimental Medicine*, 209(2), pp.251–258. Available at: http://www.jem.org/lookup/doi/10.1084/jem.20111703.

Shaw, T.N. et al., 2018. Tissue-resident macrophages in the intestine are long lived and defined by Tim-4 and CD4 expression. *The Journal of Experimental Medicine*, p.jem.20180019. Available at: http://www.jem.org/lookup/doi/10.1084/jem.20180019.

Shelton, E. et al., 2015. Efficacy of Vedolizumab as Induction Therapy in Refractory IBD Patients. *Inflammatory Bowel Diseases*, 21(12), pp.2879–2885. Available at: https://academic.oup.com/ibdjournal/article/21/12/2879-2885/4579258 [Accessed July 1, 2018].

Shiloh, M.U. et al., 1999. Phenotype of mice and macrophages deficient in both phagocyte oxidase and inducible nitric oxide synthase. *Immunity*, 10(1), pp.29–38.

Shouval, D.S. et al., 2014. Interleukin-10 Receptor Signaling in Innate Immune Cells Regulates Mucosal Immune Tolerance. *Immunity*, 40(5), pp.706–719.

Simon, J.M. et al., 2016. Alterations to chromatin in intestinal macrophages link IL-10 deficiency to inappropriate inflammatory responses. *European Journal of Immunology*, 46(8), pp.1912–1925.

Singh, H. et al., 2016. Vedolizumab: A novel anti-integrin drug for treatment of inflammatory bowel disease. *Journal of Natural Science, Biology and Medicine*, 7(1), p.4. Available at: http://www.jnsbm.org/text.asp?2016/7/1/4/175016.

Van der Sluis, M. et al., 2006. Muc2-Deficient Mice Spontaneously Develop Colitis, Indicating That MUC2 Is Critical for Colonic Protection. *Gastroenterology*, 131(1), pp.117–129.

Smith, A.M. et al., 2009. Disordered macrophage cytokine secretion underlies impaired acute inflammation and bacterial clearance in Crohn's disease. *The Journal of Experimental Medicine*, 206(9), pp.1883–1897. Available at: http://www.jem.org/lookup/doi/10.1084/jem.20091233.

Smith, P.D. et al., 2011. Intestinal macrophages and response to microbial encroachment. *Mucosal immunology*, 4(1), pp.31–42. Available at: http://www.pubmedcentral.nih.gov/articlerender.fcgi?artid=3821935&tool=pmcentrez&rendertype=abstract.

Smith, P.D. et al., 2001. Intestinal macrophages lack CD14 and CD89 and consequently are down-regulated for LPS- and IgA-mediated activities. *Journal of immunology (Baltimore, Md. : 1950)*, 167(5), pp.2651–2656.

Smith, P.D. et al., 1997. Isolation and purification of CD14-negative mucosal macrophages from normal human small intestine. *Journal of Immunological Methods*, 202(1), pp.1–11. Available at: https://www.sciencedirect.com/science/article/pii/S0022175996002049 [Accessed July 26, 2018].

Smith, P.D., Ochsenbauer-Jambor, C. & Smythies, L.E., 2005. Intestinal macrophages: Unique effector cells of the innate immune system. *Immunological Reviews*, 206, pp.149–159.

Smythies, L.E. et al., 2005. Human intestinal macrophages display profound inflammatory anergy despite avid phagocytic and bacteriocidal activity. *Journal of Clinical Investigation*, 115(1), pp.66–75.

Smythies, L.E. et al., 2010. Inflammation anergy in human intestinal macrophages is due to Smad-induced IκBα expression and NF-κB inactivation. *Journal of Biological Chemistry*, 285(25), pp.19593–19604.

Sokol, H. et al., 2008. Faecalibacterium prausnitzii is an anti-inflammatory commensal bacterium identified by gut microbiota analysis of Crohn disease patients. *PNAS*, 105(43), pp.16731–16736. Available at: http://www.pnas.org/content/pnas/105/43/16731.full.pdf [Accessed May 25, 2018].

Steidler, L. et al., 2000. Treatment of Murine Colitis by Lactococcus lactis Secreting Interleukin-10. *Science*, 289(5483), pp.1352–1355. Available at: http://www.sciencemag.org/cgi/doi/10.1126/science.289.5483.1352.

Steppich, B. et al., 2000. Selective mobilization of CD14+CD16+ monocytes by exercise. *American Journal of Physiology - Cell Physiology*, 279(3), pp.C578–C586. Available at: http://ajpcell.physiology.org/content/279/3/C578%5Cnhttp://ajpcell.physiology.org/content/279/3/C578.full.pdf%5Cnhttp://ajpcell.physiology.org/content/279/3/C578.short%5Cnhttp://www.ncbi.nlm.nih.gov/pubmed/10942707.

Strauch, U.G. et al., 2005. Influence of intestinal bacteria on induction of regulatory T cells: Lessons from a transfer model of colitis. *Gut*, 54(11), pp.1546–1552.

Strober, W. & Fuss, I.J., 2011. Proinflammatory cytokines in the pathogenesis of inflammatory bowel diseases. *Gastroenterology*, 140(6), pp.1756–1767. Available at: http://dx.doi.org/10.1053/j.gastro.2011.02.016.

Sugimoto, C. et al., 2015. Differentiation Kinetics of Blood Monocytes and Dendritic Cells in Macaques: Insights to Understanding Human Myeloid Cell Development. *The Journal of Immunology*, 195(4), pp.1774–1781. Available at: http://www.jimmunol.org/cgi/doi/10.4049/jimmunol.1500522.

Sunderkotter, C. et al., 2004. Subpopulations of Mouse Blood Monocytes Differ in Maturation Stage and Inflammatory Response. *The Journal of Immunology*, 172(7), pp.4410–4417. Available at: http://www.jimmunol.org/cgi/doi/10.4049/jimmunol.172.7.4410.

Suzuki, K. et al., 2004. Aberrant expansion of segmented filamentous bacteria in IgA-deficient gut. *PNAS*, 101(7), pp.1981–1986. Available at: http://www.pnas.org/lookup/doi/10.1073/pnas.0307317101.

Szabo, S.J. et al., 2003. MOLECULAR MECHANISMS REGULATING TH1 IMMUNE RESPONSES. *Annu. Rev. Immunol*, 21, pp.713–58. Available at: www.annualreviews.org [Accessed August 9, 2018].

Takada, Y. et al., 2010. Monocyte Chemoattractant Protein-1 Contributes to Gut Homeostasis and Intestinal Inflammation by Composition of IL-10–Producing Regulatory Macrophage Subset. *The Journal of Immunology*, 184(5), pp.2671–2676. Available at: http://www.jimmunol.org/lookup/doi/10.4049/jimmunol.0804012.

Tamoutounour, S. et al., 2012. CD64 distinguishes macrophages from dendritic cells in the gut and reveals the Th1-inducing role of mesenteric lymph node macrophages during colitis. *European Journal of Immunology*, 42, pp.3150–3166.

Tamoutounour, S. et al., 2013. Origins and Functional Specialization of Macrophages and of Conventional and Monocyte-Derived Dendritic Cells in Mouse Skin. *Immuni*, 39, pp.925–938. Available at: http://dx.doi.org/10.1016/j.immuni.2013.10.004 [Accessed March 27, 2018].

Tavian, M. & Peault, B., 2005. Embryonic development of the human hematopoietic system. *The International Journal of Developmental Biology*, 49(2–3), pp.243–250. Available at: http://www.intjdevbiol.com/paper.php?doi=041957mt.

Thiesen, S. et al., 2014. CD14hiHLA-DRdim macrophages, with a resemblance to classical blood monocytes, dominate inflamed mucosa in Crohn's disease. *Journal of leukocyte biology*, 95, pp.531–41. Available at: http://www.ncbi.nlm.nih.gov/pubmed/24212097.

Tian, H. & Cronstein, B.N., 2007. Understanding the mechanisms of action of methotrexate: Implications for the treatment of rheumatoid arthritis. *Bulletin of the NYU Hospital for Joint Diseases*, 65(3), pp.168–173.

Travassos, L.H. et al., 2009. Articles Nod1 and Nod2 direct autophagy by recruiting ATG16L1 to the plasma membrane at the site of bacterial entry. *Nature Immunology*, 11(1), pp.55–62. Available at: http://dx.doi.org/10.1038/ni.1823.

Trompette, A. et al., 2018. Dietary Fiber Confers Protection against Flu by Shaping Ly6c−Patrolling Monocyte Hematopoiesis and CD8+T Cell Metabolism. *Immunity*, 48(5), p.992–1005.e8.

Tsou, C.L. et al., 2007. Critical roles for CCR2 and MCP-3 in monocyte mobilization from bone marrow and recruitment to inflammatory sites. *Journal of Clinical Investigation*, 117(4), pp.902–909.

Tzeng, D.Y. et al., 1985. Platelet-Derived Growth Factor Promotes Human Peripheral Monocyte

Activation. *Blood*, 66(1), pp.179–183.

Uhlig, H.H. et al., 2006. Characterization of Foxp3+CD4+CD25+ and IL-10-Secreting CD4+CD25+ T Cells during Cure of Colitis. *The Journal of Immunology*, 177(9), pp.5852–5860. Available at: http://www.jimmunol.org/cgi/doi/10.4049/jimmunol.177.9.5852.

Uhlig, H.H. et al., 2006. Differential Activity of IL-12 and IL-23 in Mucosal and Systemic Innate Immune Pathology. *Immunity*, 25(2), pp.309–318.

Uhlig, H.H., 2013. Monogenic diseases associated with intestinal inflammation: implications for the understanding of inflammatory bowel disease. *Gut*, 62(12), pp.1795–1805. Available at: http://www.ncbi.nlm.nih.gov/pubmed/24203055.

Vavricka, S.R. et al., 2015. Extraintestinal manifestations of inflammatory bowel disease. *Inflammatory Bowel Diseases*, 21(8), pp.1982–1992.

Ventham, N.T. et al., 2013. Beyond gene discovery in inflammatory bowel disease: The emerging role of epigenetics. *Gastroenterology*, 145(2), pp.293–308. Available at: http://dx.doi.org/10.1053/j.gastro.2013.05.050.

Vermeire, S., Assche, G. Van & Rutgeerts, P., 2004. C-reactive protein as a marker for inflammatory bowel disease. *Inflammatory bowel diseases*, 10(5), pp.661–665.

Verrier, B. et al., 2006. Small Intestinal Lamina Propria Transepithelial Pathogen Uptake into the. *The Journal of Immunology*, 176(10), pp.2465–2469. Available at: http://www.jimmunol.org/content/176/4/2465 [Accessed December 17, 2018].

Viksman, M.Y. et al., 1994. Application of a flow cytometric method using autofluorescence and a tandem fluorescent dye to analyze human alveolar macrophage surface markers. *Journal of Immunological Methods*, 172(1), pp.17–24. Available at: https://www.sciencedirect.com/science/article/pii/0022175994903743?via%3Dihub [Accessed July 26, 2018].

Wang, X., Ouyang, Q. & Luo, W.J., 2004. Oxazolone-induced murine model of ulcerative colitis. *Chinese Journal of Digestive Diseases*, 5(4), pp.165–168.

Watanabe, T. et al., 2004. NOD2 is a negative regulator of Toll-like receptor 2 – mediated T helper type 1 responses. *Nature Immunology*, 5(8), pp.800–808.

Weber, B. et al., 2011. CX3CR1 defines functionally distinct intestinal mononuclear phagocyte subsets which maintain their respective functions during homeostatic and inflammatory conditions. *European Journal of Immunology*, 41(3), pp.773–779.

Wei, W. et al., 2017. Microbiota-specific Th17 cells: Yin and Yang in regulation of inflammatory bowel disease. *inflamatory Bowels Diseases*, 22(6), pp.1473–1482.

Wenzel, U.A. et al., 2014. Spontaneous colitis in Muc2-deficient mice reflects clinical and cellular features of active ulcerative colitis. *PLoS ONE*, 9(6), pp.1–12.

Wilson, N.J. et al., 2007. Development, cytokine profile and function of human interleukin 17-producing helper T cells. *Nature Immunology*, 8(9), pp.950–957.

Witowski, J., Książek, K. & Jörres, A., 2004. Interleukin-17: A mediator of inflammatory responses. *Cellular and Molecular Life Sciences*, 61(5), pp.567–579.

Wong, K.L. et al., 2011. Gene expression profiling reveals the defining features of the classical, intermediate, and nonclassical human monocyte subsets. *Blood*, 118(5), pp.16–31. Available at: http://www.ncbi.nlm.nih.gov/pubmed/21653326.

Wynn, T.A., Chawla, A. & Pollard, J.W., 2013. Macrophage biology in development, homeostasis and disease. *Nature*, 496(7446), pp.445–55. Available at: http://www.pubmedcentral.nih.gov/articlerender.fcgi?artid=3725458&tool=pmcentrez&rendertype=abstract.

Yang, W.S. et al., 2018. ADAM17-Mediated Ectodomain Shedding of Toll-Like Receptor 4 as a Negative Feedback Regulation in Lipopolysaccharide-Activated Aortic Endothelial Cells. *Cellular Physiology and Biochemistry*, 45(5), pp.1851–1862.

Yang, Z. et al., 2008. NOD2 Transgenic Mice Exibit Enhanced MDP-Mediated Down-Regulation of TLR2 Responses and Resistance to Colitis Induction. *Gastroenterology*, 257(5), pp.2432–2437.

Yang, Z. et al., 1996. Soluble CD14 and LPS-binding protein from bovine serum enable bacterial LPS-mediated cytotoxicity and activation of bovine vascular endothelial cell in vitro. *Journal of Leukocyte Biology*, 59(Feb), pp.241–247.

Yasukawa, H. et al., 2003. IL-6 induces an anti-inflammatory response in the absence of SOCS3 in macrophages. *Nature Immunology*, 4(6), pp.551–556.

Yona, S. et al., 2013. Fate Mapping Reveals Origins and Dynamics of Monocytes and Tissue Macrophages under Homeostasis. *Immunity*, 38(1), pp.79–91. Available at: http://dx.doi.org/10.1016/j.immuni.2012.12.001.

Yu, X. et al., 2017. The Cytokine TGF-β Promotes the Development and Homeostasis of Alveolar Macrophages. *Immunity*, 47(5), p.903–912.e4. Available at: https://doi.org/10.1016/j.immuni.2017.10.007.

Zawada, A.M. et al., 2011. SuperSAGE evidence for CD14 ++CD16 + monocytes as a third monocyte subset. *Blood*, 118(12), pp.50–62.

Zheng, Y. et al., 2008. Interleukin-22 mediates early host defense against attaching and effacing bacterial pathogens. *Nature Medicine*, 14(3), pp.282–289.

Ziegler-heitbrock, L. et al., 2014. Nomenclature of monocytes and dendritic cells in blood Nomenclature of monocytes and dendritic cells in blood. *Blood*, 116(16), pp.5–7.

Zigmond, E. et al., 2012. Article Ly6Chi Monocytes in the Inflamed Colon Give Rise to Proinflammatory Effector Cells and Migratory Antigen-Presenting Cells. *Immunity*, 37, pp.1076–1090. Available at: http://dx.doi.org/10.1016/j.immuni.2012.08.026 [Accessed August 5, 2018].

Zigmond, E. et al., 2014. Macrophage-Restricted Interleukin-10 Receptor Deficiency, but Not IL-10 Deficiency, Causes Severe Spontaneous Colitis. *Immunity*, 40(5), pp.720–733.

Appendix

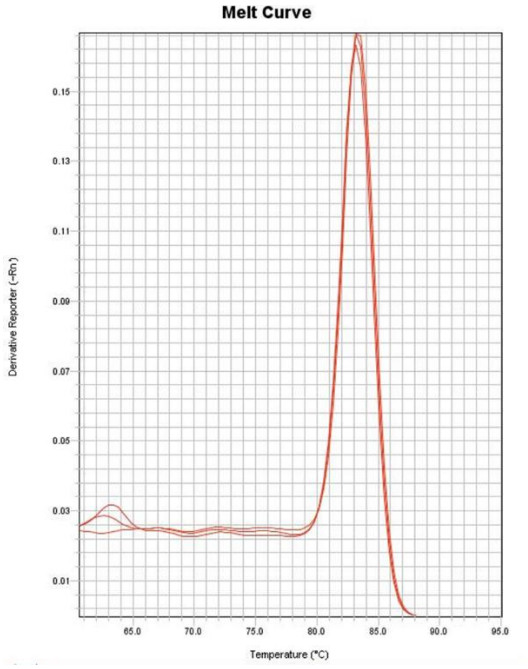

Appendix 1: Example of a melt curve. Purity of the amplified product was verified by melt curve analysis. For the SOCS3 amplified product there is a single discrete change in fluorescence at a specific temperature indicating a pure product.

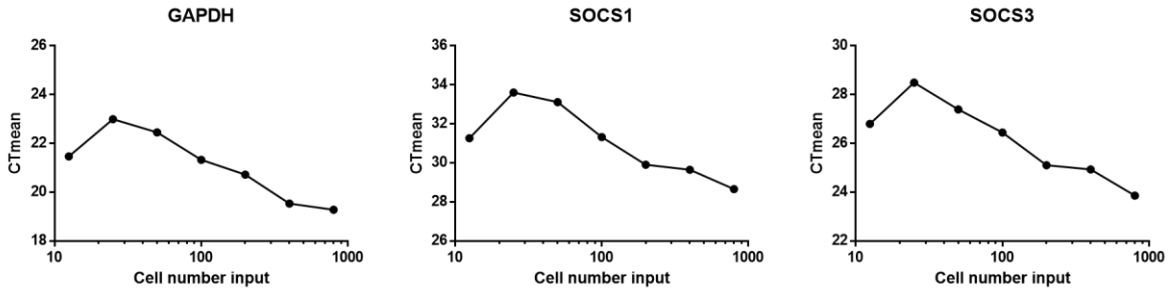

Appendix 2: Titration of cell number input. Whole PBMCs from a healthy donor were labelled with anti-HLA-DR, anti-CD14, and anti-CD16 antibodies to distinguish the monocyte subsets before sorting on the FACS Aria (BD). $1x10^6$ classical monocytes were sorted and titrated (800,000-12,500 cells) down past the cell number present in the experimental samples to be analysed (>50,000 cells) and showed a reliable deltaCT could be calculated above 25,000 cells.

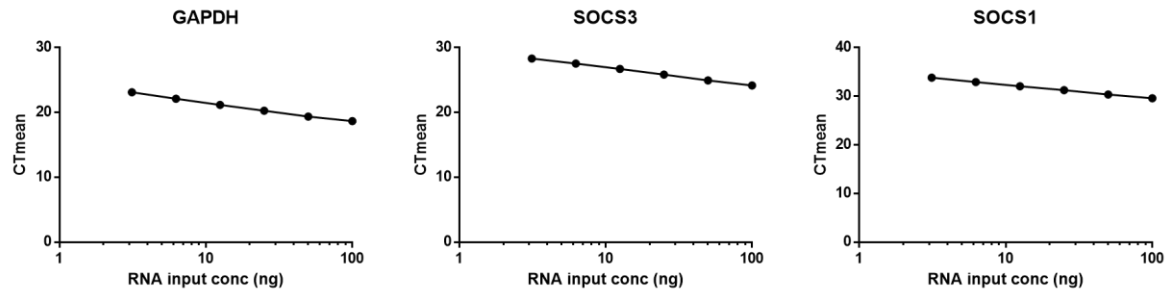

Appendix 3: Titration of RNA input concentration. Whole PBMCs from a healthy donor were labelled with anti-HLA-DR, anti-CD14, and anti-CD16 antibodies to distinguish the monocyte subsets before sorting on the FACS Aria (BD). $1x10^6$ classical monocytes were sorted and the concentration of RNA measured using Nanodrop. A titration of a known concentration of RNA (100-3.125ng/µL) was used to determine the lowest RNA concentration that allowed calculation of a reliable deltaCT, and showed a reliable deltaCT could still be calculated at the lowest concentration of RNA tested.

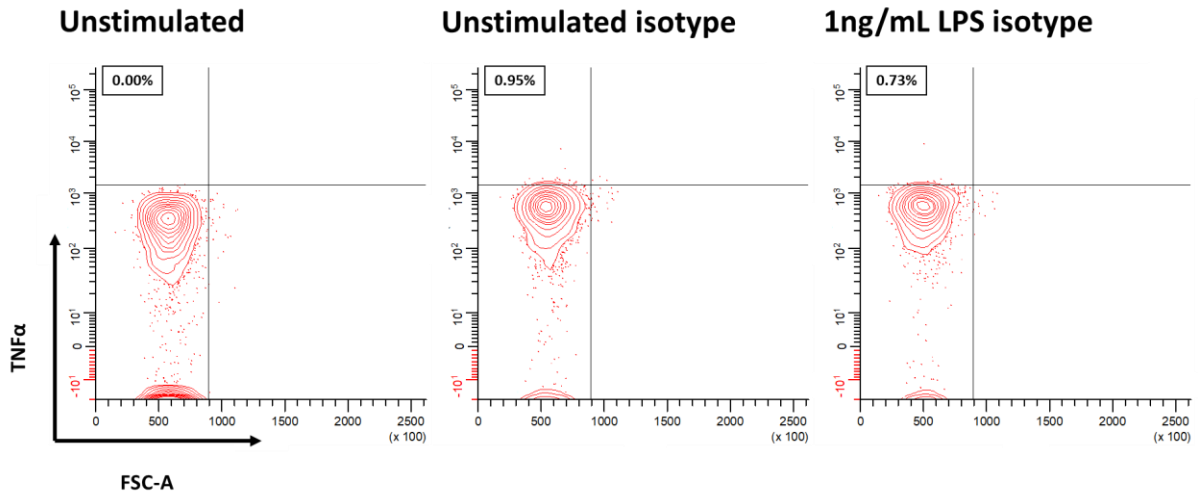

Appendix 4a: Representative flow cytometry plots of TNFα isotype controls. Healthy donor PBMCs were stimulated or not with 1ng/ml LPS for three hours in the presence of monensin. The PBMCs were then labelled for anti-HLA-DR, anti-CD14, and anti-CD16 antibodies to distinguish the monocytes subsets, fixed, permeabilised and labelling intracellularly with corresponding isotype controls for anti-TNFα antibody before acquiring on the flow cytometer.

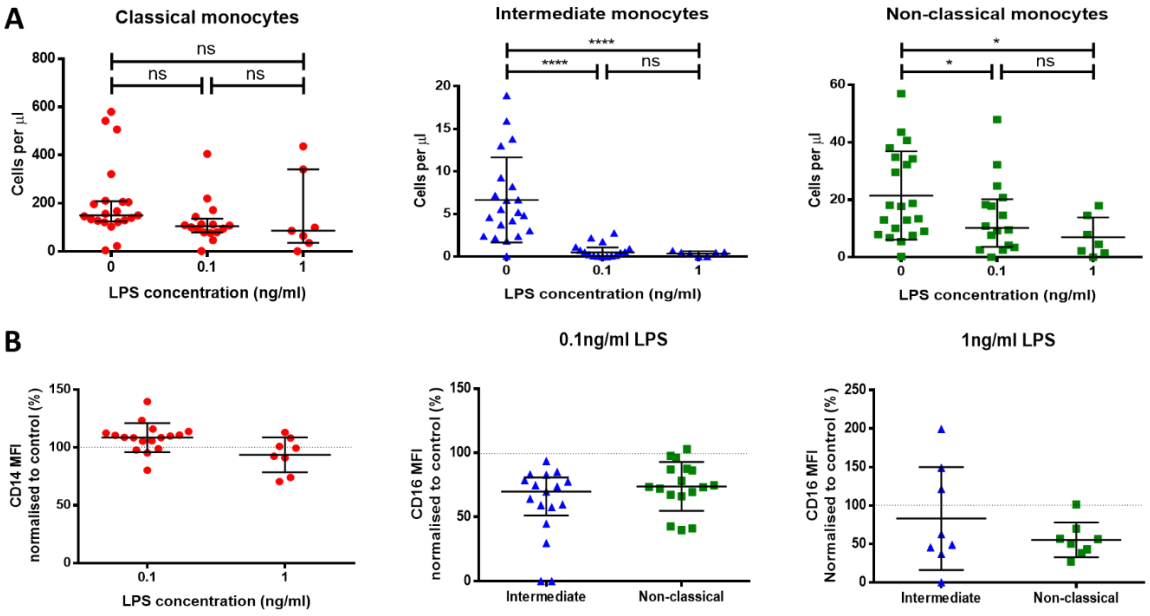

Appendix 4b: Marker expression and cell numbers of monocyte subsets upon LPS stimulation. Healthy donor PBMCs (n=21) were stimulated with LPS (0.1/1ng/ml) for three hours in the presence of monensin. The PBMCs were then labelled with anti-HLA-DR, anti-CD14, and anti-CD16 antibodies to distinguish the monocytes subsets before acquiring on the flow cytometer. **A)** absolute cell numbers of classical, intermediate, and non-classical monocytes upon stimulation with 0.1/1ng/ml LPS. Median and IQR is displayed for non-normally distributed data sets. The data were analysed statistically by Kruskal-Wallis test. $p \leq 0.05$* $p \leq 0.01$** $p \leq 0.001$*** $p \leq 0.0001$***. **B)** level of CD14 and CD16 marker expression (MFI) on the monocyte subsets upon stimulation with 0.1/1ng/ml LPS normalised to control (where unstimulated cells represent 100% expression).

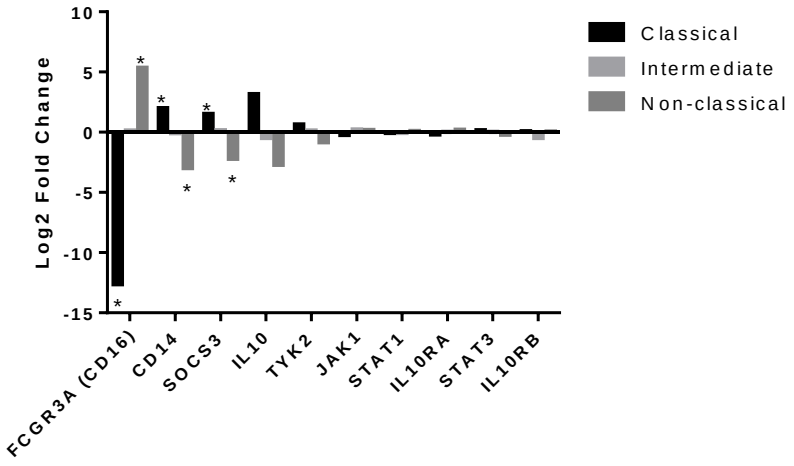

Appendix 5: Analysis of 10x ChromiumTM Single Cell 5' and 3' gene expression data using LoupeTM cell browser (10X genomics). The monocyte subsets were identified on the basis of CD14 and CD16 gene expression. Expression levels of selective genes along the IL-10R pathway were analysed in the monocyte subsets.

	CD	UC	IC
n = 31	21	8	2
Active disease			
n = 15	10	5	0
Inactive disease			
n = 16	11	3	2
Medication			
Steroids	5		
Immune modulators (IM)	18		
Anti-TNFα	7		
None of the above	7		

Appendix 6a: Patient data. Several IBD patients were receiving combination therapies at the time of blood collection.

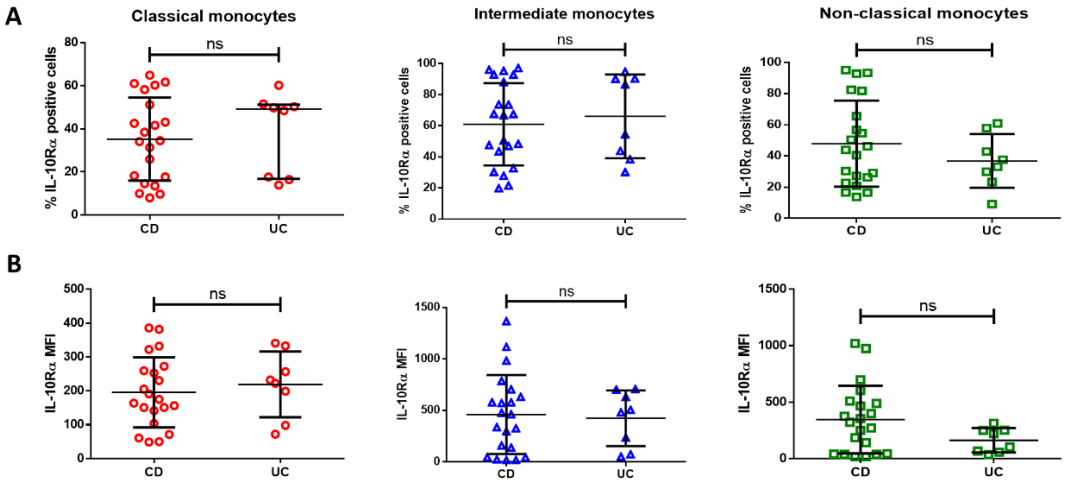

Appendix 6b: Stratification of IL-10Rα expression data from IBD cohort into CD vs UC. Whole blood from 21 CD and 8 UC patients were labelled with anti-HLA-DR, anti-CD14, and anti-CD16 antibodies to distinguish the monocyte subsets, and IL-10Rα before acquiring on the flow cytometer. IL-10Rα expression was quantified as **A)** percentage of cells positive for IL-10Rα and **B)** MFI calculated as MFI for staining with anti-IL-10Rα antibody minus MFI for staining with an isotype-matched control antibody for each monocyte subset. Mean and SD are displayed for normally distributed data sets, while median and IQR are displayed for non-normally distributed data sets. An unpaired T-tests was used to compare two groups of normally distributed data, while a Mann-Whitney test was used to compare two groups of data that were non-normally distributed.

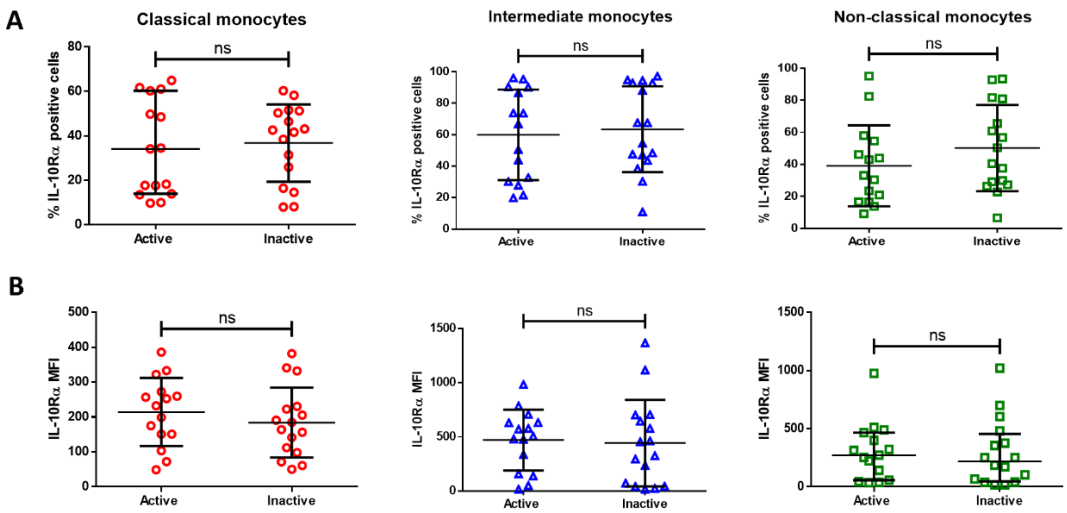

Appendix 6c: Stratification of IL-10Rα expression data from IBD cohort into active vs inactive. Whole blood from 15 active and 16 inactive patients were labelled with anti-HLA-DR, anti-CD14, and anti-CD16 antibodies to distinguish the monocyte subsets, and IL-10Rα before acquiring on the flow cytometer. IL-10Rα expression was quantified as **A)** percentage of cells positive for IL-10Rα and **B)** MFI calculated as MFI for staining with anti-IL-10Rα antibody minus MFI for staining with an isotype-matched control antibody for each monocyte subset. Mean and SD are displayed for normally distributed data sets, while median and IQR are displayed for non-normally distributed data sets. An unpaired T-tests was used to compare two groups of normally distributed data, while a Mann-Whitney test was used to compare two groups of data that were non-normally distributed.

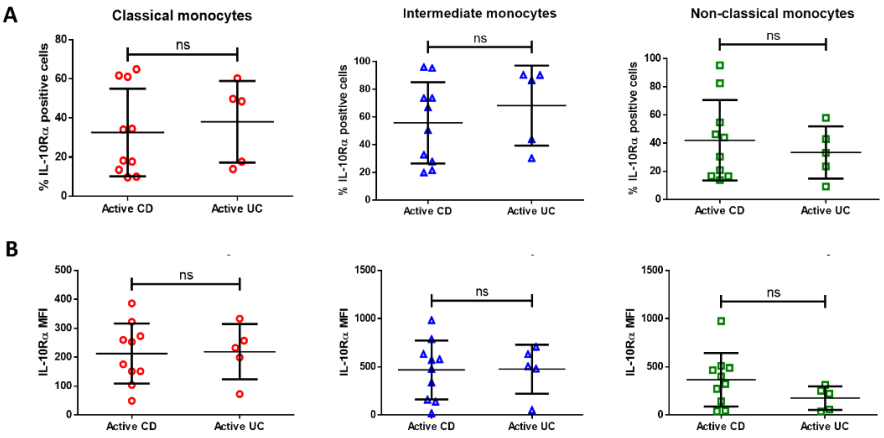

Appendix 6d: Stratification of IL-10Rα expression data from IBD cohort into active CD vs active UC. Whole blood from 10 active CD and 5 active UC patients were labelled with anti-HLA-DR, anti-CD14, and anti-CD16 antibodies to distinguish the monocyte subsets, and IL-10Rα before acquiring on the flow cytometer. IL-10Rα expression was quantified as **A)** percentage of cells positive for IL-10Rα and **B)** MFI calculated as MFI for staining with anti-IL-10Rα antibody minus MFI for staining with an isotype-matched control antibody for each monocyte subset. Mean and SD are displayed for normally distributed data sets, while median and IQR are displayed for non-normally distributed data sets. An unpaired T-tests was used to compare two groups of normally distributed data, while a Mann-Whitney test was used to compare two groups of data that were non-normally distributed.

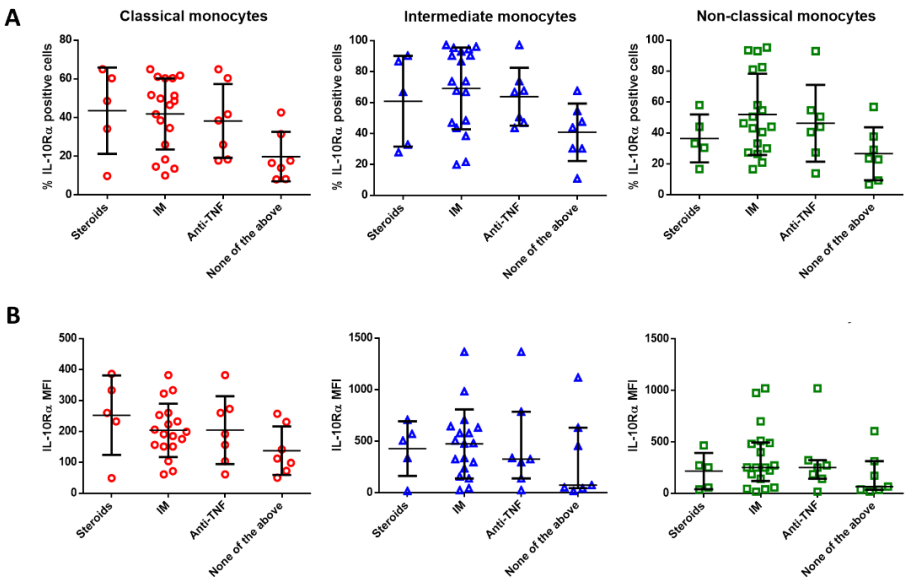

Appendix 6e: Stratification of IL-10Rα expression data from IBD cohort into treatment groups. Whole blood from 5 patients on steroids, 18 on IM, 7 on anti-TNFα, and 7 on none of the above treatments were labelled with anti-HLA-DR, anti-CD14, and anti-CD16 antibodies to distinguish the monocyte subsets, and IL-10Rα before acquiring on the flow cytometer. IL-10Rα expression was quantified as **A)** percentage of cells positive for IL-10Rα and **B)** MFI calculated as MFI for staining with anti-IL-10Rα antibody minus MFI for staining with an isotype-matched control antibody for each monocyte subset. Mean and SD are displayed for normally distributed data sets, while median and IQR are displayed for non-normally distributed data sets. An unpaired one-way ANOVA for normally distributed data sets, while a Kruskal-Wallis test was used to compare two groups of unpaired data that were non-normally distributed.

	CD	UC	IC
n = 41	28	11	2
Active disease			
n = 20	12	8	0
Inactive disease			
n = 21	16	3	2
Medication			
Steroids	5		
IM	23		
Anti-TNFα	8		
None of the above	11		

Appendix 7a: Patient data. Several IBD patients were receiving combination therapies at the time of blood collection.

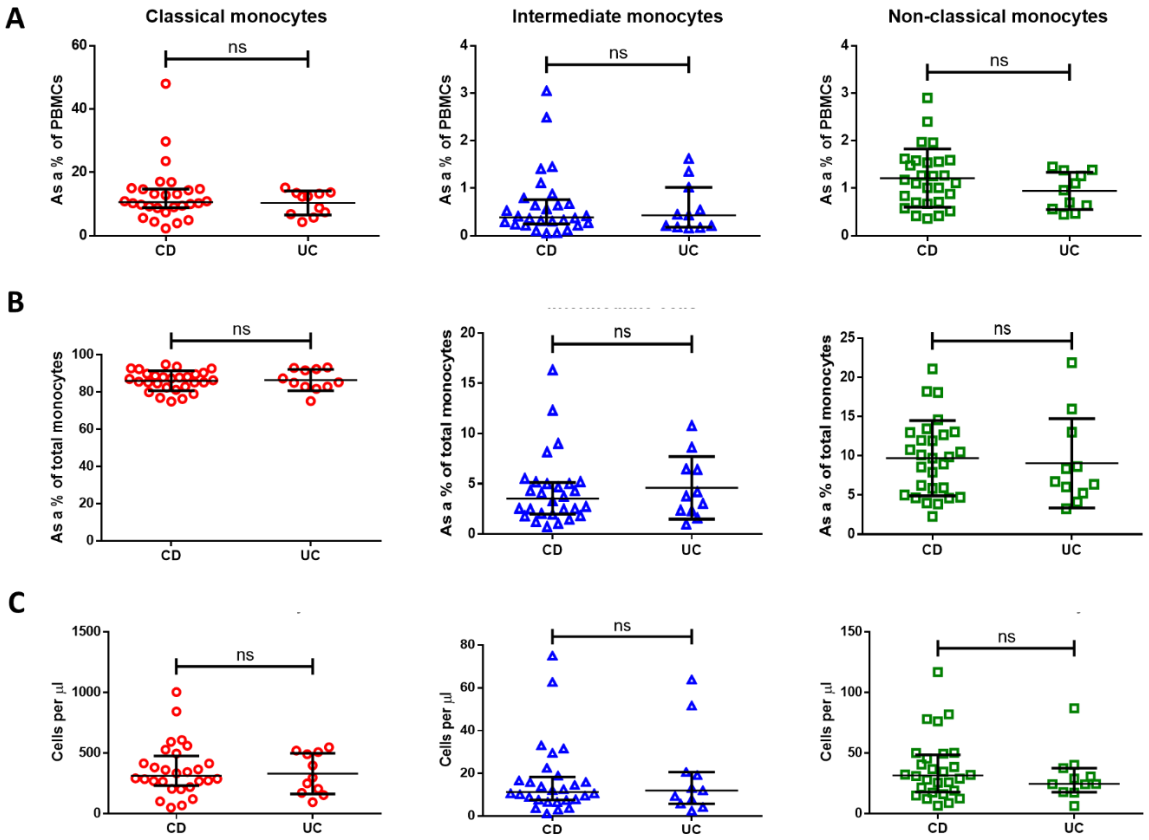

Appendix 7b: Stratification of monocyte subset distribution data from IBD cohort into CD vs UC. Whole blood from 28 CD and 11 UC patients were labelled with anti-HLA-DR, anti-CD14, and anti-CD16 antibodies to distinguish the monocyte subsets before acquiring on the flow cytometer. Monocyte subset distribution was calculated as **A)** percentage of PBMCs, **B)** percentage of total monocyte, and **C)** absolute cell number. Mean and SD are displayed for normally distributed data sets, while median and IQR are displayed for non-normally distributed data sets. An unpaired T-tests was used to compare two groups of normally distributed data, while a Mann-Whitney test was used to compare two groups of data that were non-normally distributed.

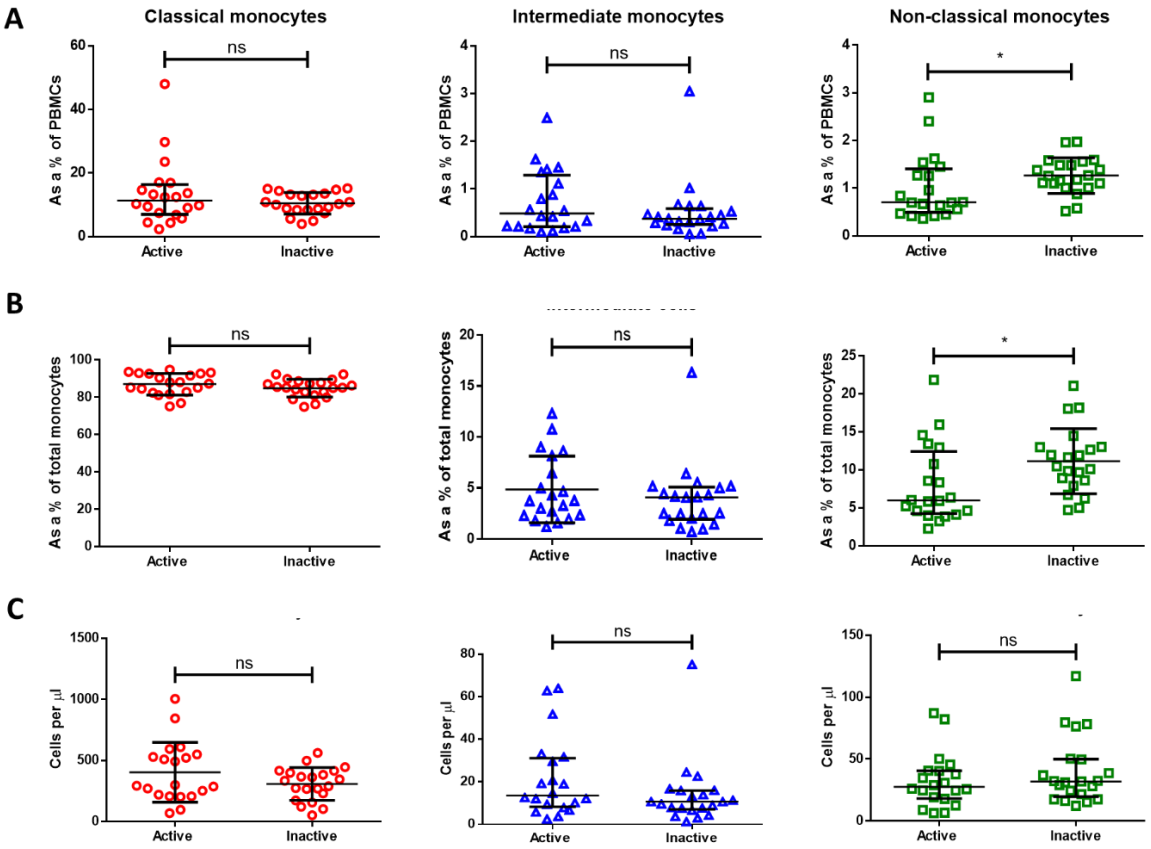

Appendix 7c: Stratification of monocyte subset distribution data from IBD cohort into active vs inactive. Whole blood from 21 active and 20 inactive patients were labelled with anti-HLA-DR, anti-CD14, and anti-CD16 antibodies to distinguish the monocyte subsets before acquiring on the flow cytometer. Monocyte subset distribution was calculated as **A)** percentage of PBMCs, **B)** percentage of total monocyte, and **C)** absolute cell number. Mean and SD are displayed for normally distributed data sets, while median and IQR are displayed for non-normally distributed data sets. An unpaired T-tests was used to compare two groups of normally distributed data, while a Mann-Whitney test was used to compare two groups of data that were non-normally distributed.

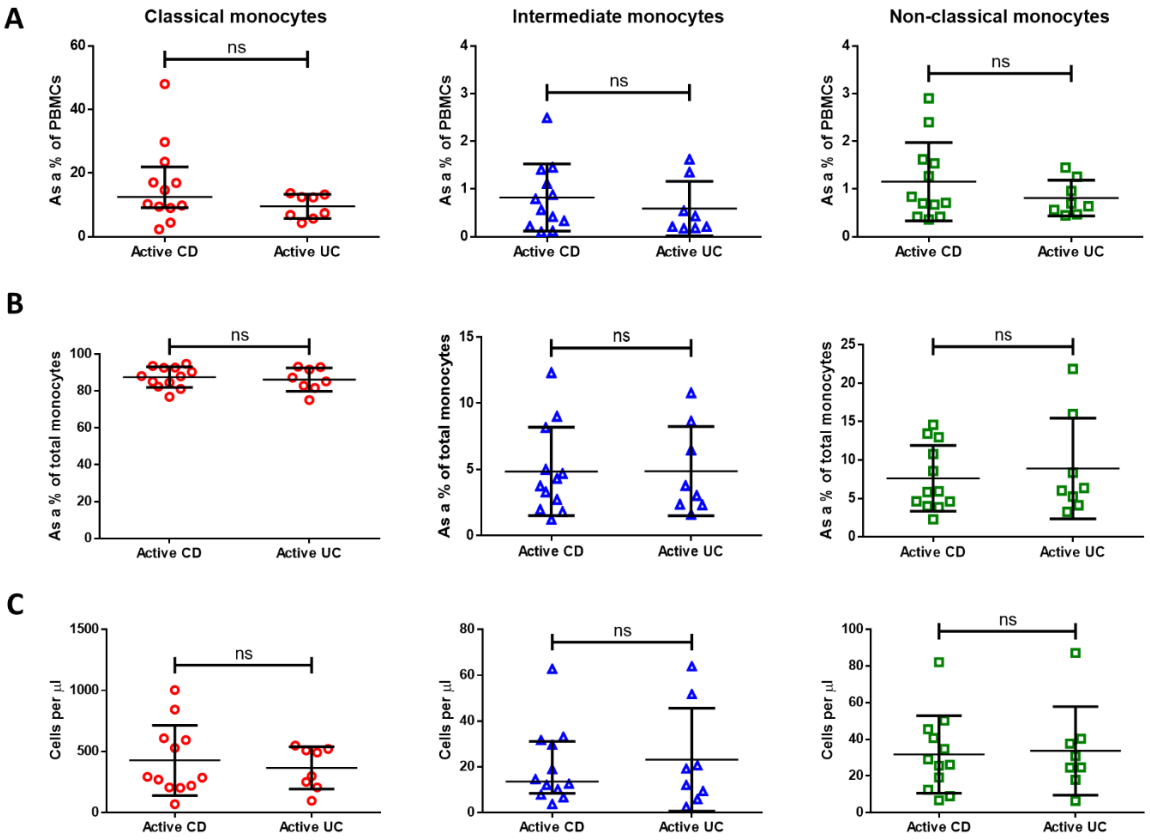

Appendix 7d: Stratification of monocyte subset distribution data from IBD cohort into active CD vs active UC. Whole blood from 12 active CD and 8 active UC patients were labelled with anti-HLA-DR, anti-CD14, and anti-CD16 antibodies to distinguish the monocyte subsets before acquiring on the flow cytometer. Monocyte subset distribution was calculated as **A)** percentage of PBMCs, **B)** percentage of total monocyte, and **C)** absolute cell number. Mean and SD are displayed for normally distributed data sets, while median and IQR are displayed for non-normally distributed data sets. An unpaired T-tests was used to compare two groups of normally distributed data, while a Mann-Whitney test was used to compare two groups of data that were non-normally distributed.

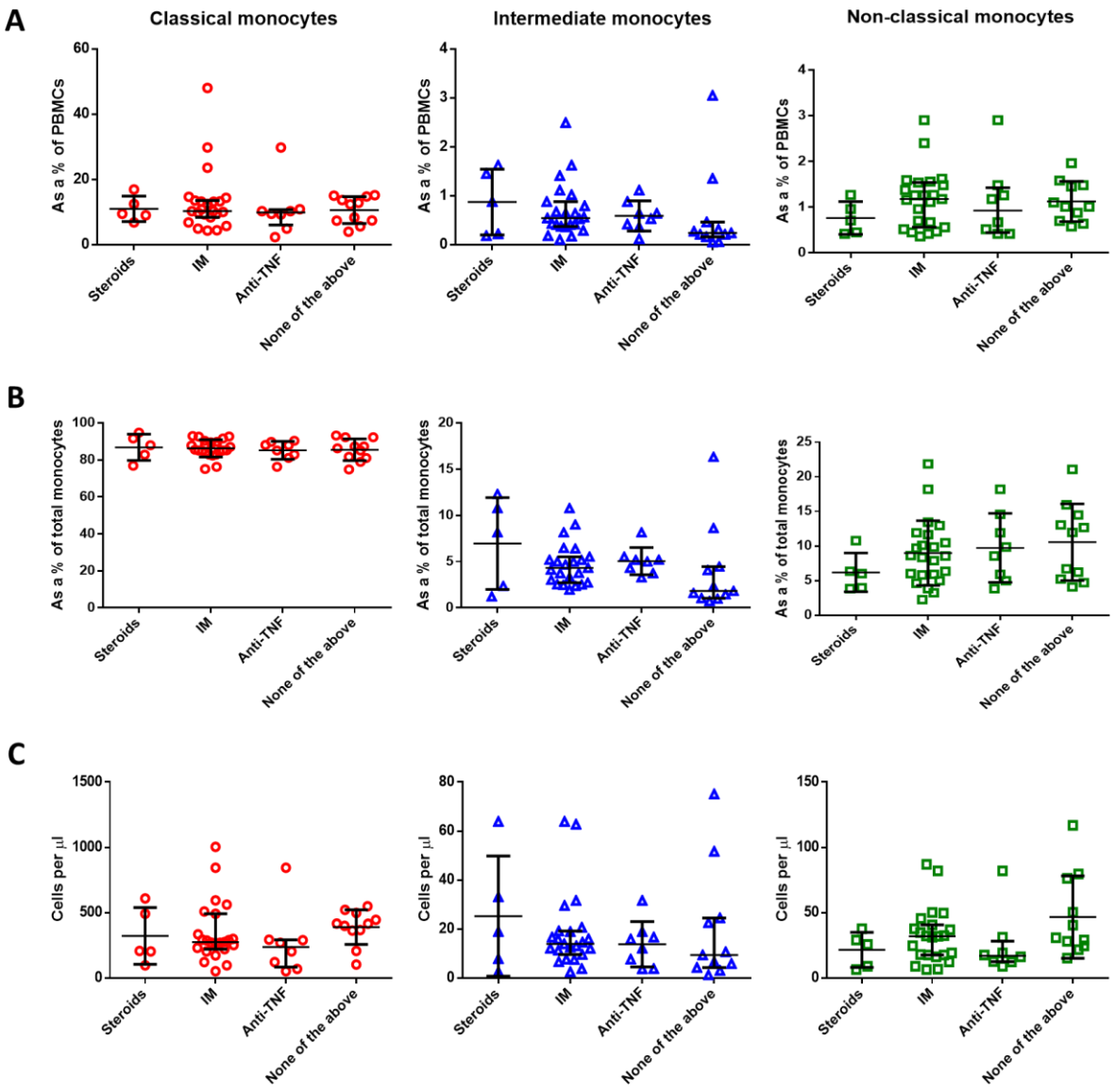

Appendix 7e: Stratification of monocyte subset distribution data from IBD cohort into treatment groups. Whole blood from 5 patients on steroids, 23 on IM, 8 on anti-TNFα, and 11 on none of the above treatments were labelled with anti-HLA-DR, anti-CD14, and anti-CD16 antibodies to distinguish the monocyte subsets before acquiring on the flow cytometer. Monocyte subset distribution was calculated as **A)** percentage of PBMCs, **B)** percentage of total monocyte, and **C)** absolute cell number. Mean and SD are displayed for normally distributed data sets, while median and IQR are displayed for non-normally distributed data sets. An unpaired one-way ANOVA for normally distributed data sets, while a Kruskal-Wallis test was used to compare two groups of unpaired data that were non-normally distributed.

	CD	UC
n = 19	9	10
Active disease		
n = 19	9	10
Responders		
n = 8	2	6
Non-responders		
n = 11	7	4
Medication		
Steroids	4	
IM	4	
Anti-TNFα	0	
None of the above	11	

Appendix 8a: Patient data. Several IBD patients were receiving combination therapies at the time of blood collection.

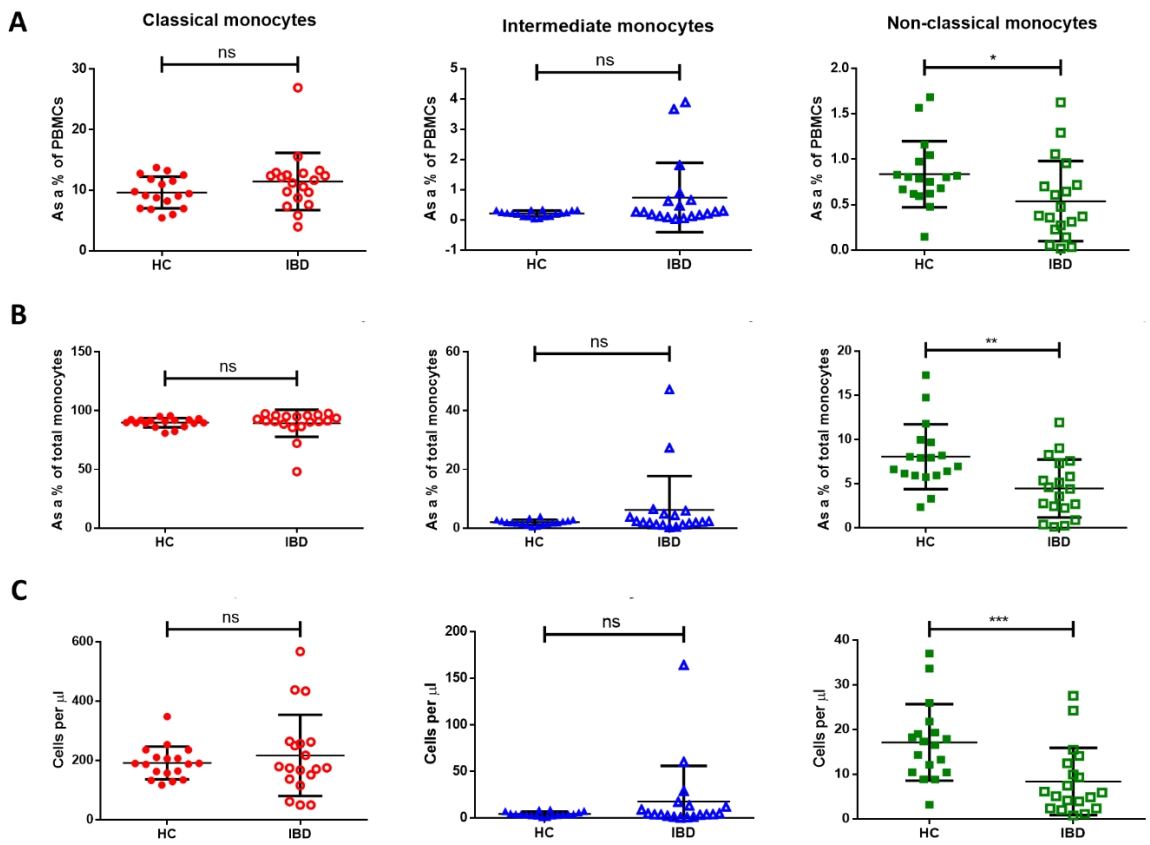

Appendix 8b: Monocyte subset distribution in health and IBD. Whole blood from 18 healthy controls and 19 IBD patients with active disease were labelled with anti-HLA-DR, anti-CD14, and anti-CD16 antibodies to distinguish the monocyte subsets before acquiring on the flow cytometer. Monocyte subset distribution was calculated as **A)** percentage of PBMCs, **B)** percentage of total monocyte, and **C)** absolute cell number. Mean and SD are displayed for normally distributed data sets, while median and IQR are displayed for non-normally distributed data sets. An unpaired T-tests was used to compare two groups of normally distributed data, while a Mann-Whitney test was used to compare two groups of data that were non-normally distributed. $p \leq 0.05$* $p \leq 0.01$** $p \leq 0.001$*** $p \leq 0.0001$****.

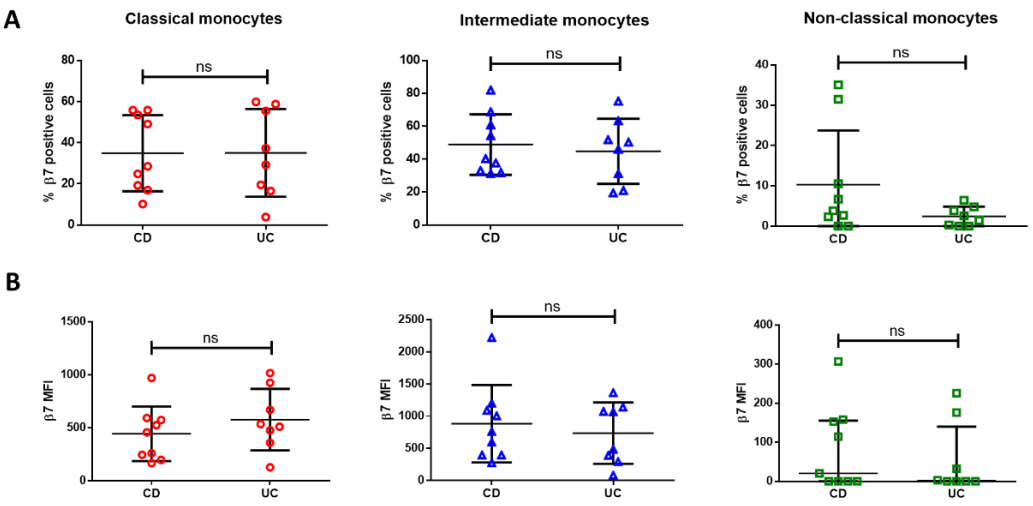

Appendix 9a: Stratification of monocyte subset distribution data from IBD cohort into active CD vs active UC. Whole blood from 9 CD and 8 UC patients were labelled with anti-HLA-DR, anti-CD14, and anti-CD16 antibodies to distinguish the monocyte subsets (excluding CD103+ cells), and β7 before acquiring on the flow cytometer. β7 expression was quantified as **A)** percentage of cells positive for β7 and **B)** MFI calculated as MFI for staining with anti-β7 antibody minus MFI for staining with an isotype-matched control antibody for each monocyte subset. Mean and SD are displayed for normally distributed data sets, while median and IQR are displayed for non-normally distributed data sets. An unpaired T-tests was used to compare two groups of normally distributed data, while a Mann-Whitney test was used to compare two groups of data that were non-normally distributed.

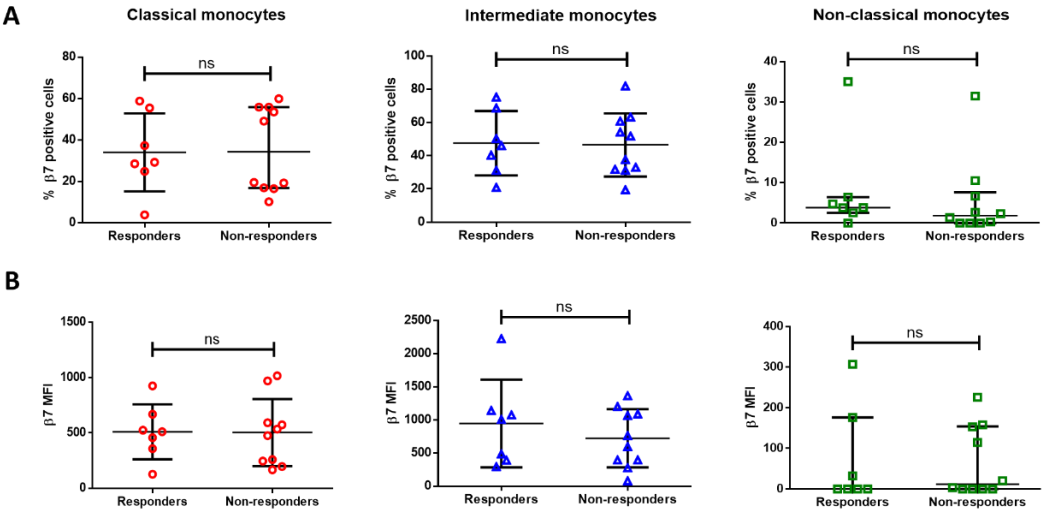

Appendix 9b: Stratification of monocyte subset distribution data from IBD cohort into responders vs non-responders. Whole blood from 7 responders and 10 non-responders were labelled with anti-HLA-DR, anti-CD14, and anti-CD16 antibodies to distinguish the monocyte subsets (excluding CD103+ cells), and β7 before acquiring on the flow cytometer. β7 expression was quantified as **A)** percentage of cells positive for β7 and **B)** MFI calculated as MFI for staining with anti-β7 antibody minus MFI for staining with an isotype-matched control antibody for each monocyte subset. Mean and SD are displayed for normally distributed data sets, while median and IQR are displayed for non-normally distributed data sets. An unpaired T-tests was used to compare two groups of normally distributed data, while a Mann-Whitney test was used to compare two groups of data that were non-normally distributed.

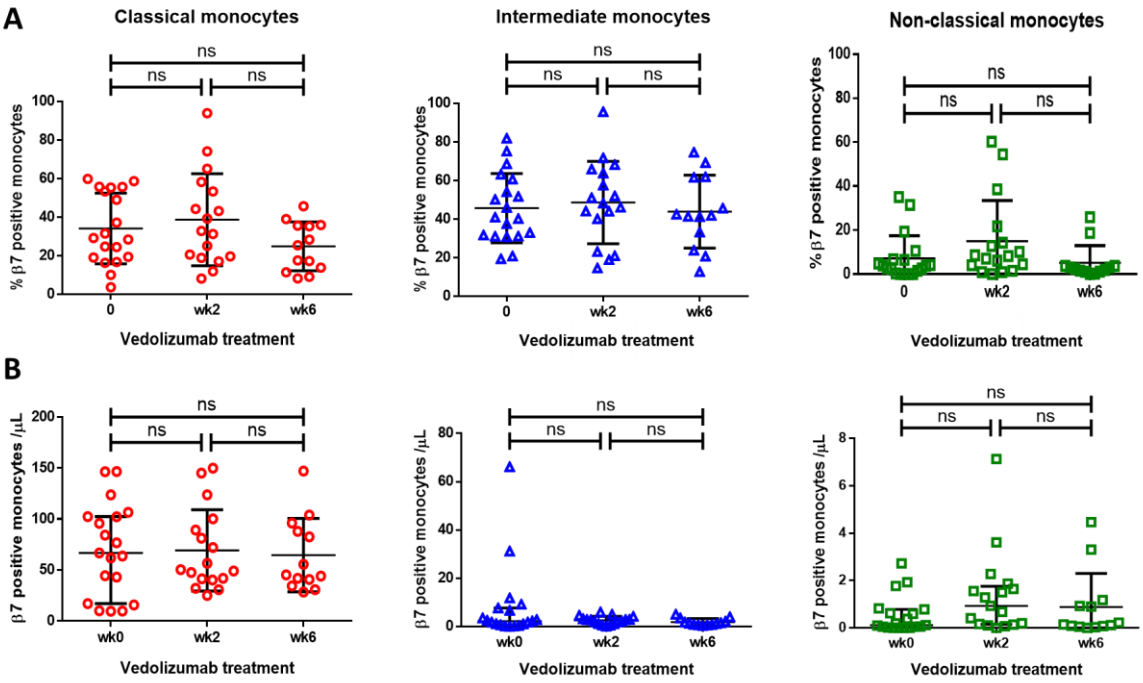

Appendix 10a: The effect of vedolizumab therapy on circulating β7+ monocyte subset distribution. Whole blood from 19 IBD patients (n=19) starting vedolizumab treatment were labelled with anti-HLA-DR, anti-CD14, and anti-CD16 antibodies to distinguish the monocyte subsets (excluding CD103+ cells), and anti-β7 antibody before acquiring on the flow cytometer. Monocyte subset distribution and cell number were determined at baseline and after two and six weeks of treatment. The proportion of β7 expressing monocytes cells was calculated as a **A)** percentage of β7 positive monocytes **B)** β7 positive monocytes per µL. Mean and SD are displayed for normally distributed data sets, while median and IQR are displayed for non-normally distributed data sets. Data were analysed statistically by RM one-way ANOVA for normally distributed data sets, while a Friedman test was used for non-normally distributed data sets.

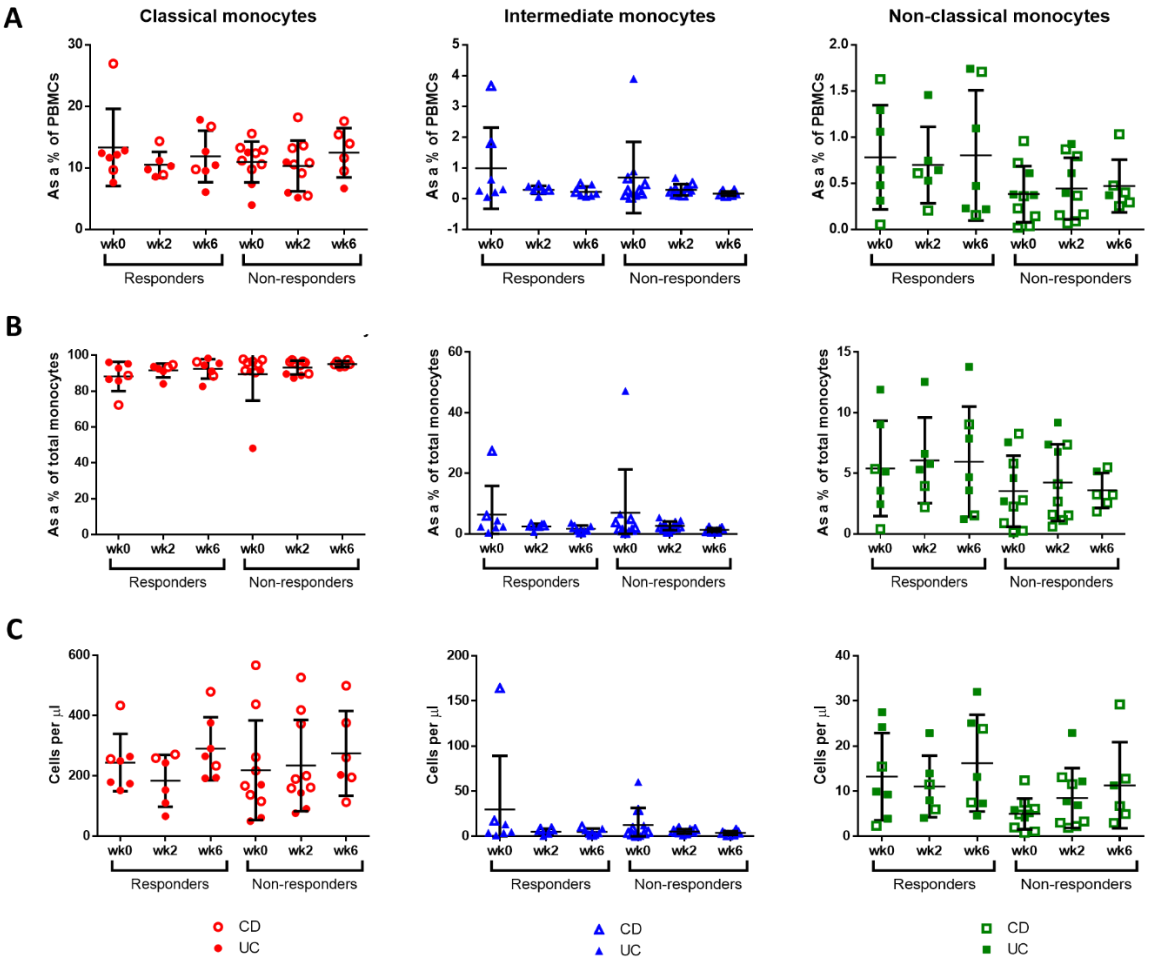

Appendix 10a: Stratification of monocyte subset distribution data from IBD cohort into responders vs non-responders. Whole blood from 19 IBD patients (7 responders and 10 non-responders) starting vedolizumab treatment were labelled with anti-HLA-DR, anti-CD14, and anti-CD16 antibodies to distinguish the monocyte subsets before acquiring on the flow cytometer. Monocyte subset distribution and cell number were determined at baseline and after two and six weeks of treatment. Monocyte subset distribution was calculated as **A)** percentage of PBMCs, **B)** percentage of total monocyte, and **C)** absolute cell number. Mean and SD are displayed for normally distributed data sets, while median and IQR are displayed for non-normally distributed data sets. An unpaired one-way ANOVA for normally distributed data sets, while a Kruskal-Wallis test was used to compare two groups of unpaired data that were non-normally distributed.

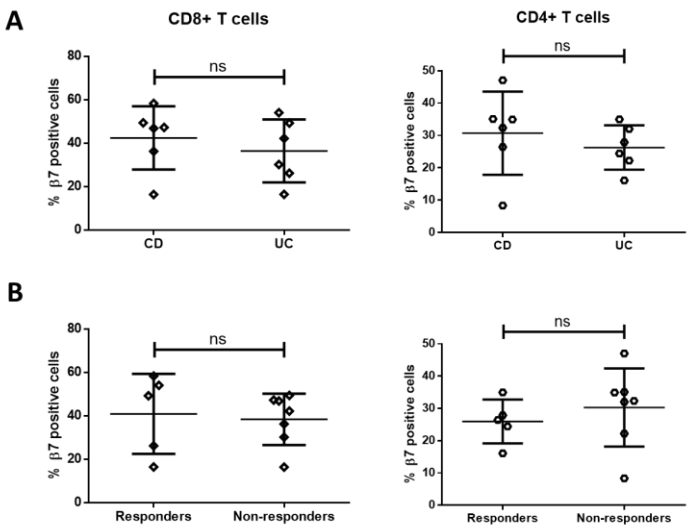

Appendix 11a: Stratification of circulating β7+ CD4 and CD8 T cell distribution data from IBD cohort into responders vs non-responders. Whole blood from 12 IBD patients (6 CD and 6 UC or 5 responders and 7 non-responders) were labelled with anti-CD3, anti-CD45RA, anti-CD8, and anti-CD4 antibodies to distinguish effector memory (CD45RA-) CD8+ and CD4+ T cells (excluding CD103+ cells), and anti-β7 antibody before acquiring on the flow cytometer. The proportion of β7 expressing CD8+ and CD4+ T cells was calculated as a percentage of total T cells. **A)** proportion of β7 expressing CD8+ and CD4+ T cells at baseline in CD and UC patients. **B)** proportion of β7 expressing CD8+ and CD4+ T cells at baseline in responders and non-responders. Mean and SD are displayed for normally distributed data sets, while median and IQR are displayed for non-normally distributed data sets. An unpaired T-tests was used to compare two groups of normally distributed data, while a Mann-Whitney test was used to compare two groups of data that were non-normally distributed.

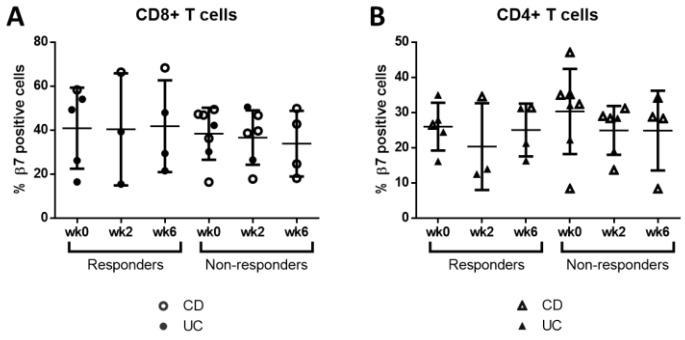

Appendix 11b: Stratification of circulating β7+ CD4 and CD8 T cell distribution data from IBD cohort on vedolizumab therapy into responders vs non-responders. Whole blood from 5 responders and 7 non-responders were labelled with anti-CD3, anti-CD45RA, anti-CD8, and anti-CD4 antibodies to distinguish effector memory (CD45RA-) CD8+ and CD4+ T cells (excluding CD103+ cells), and anti-β7 antibody before acquiring on the flow cytometer. The proportion of β7 expressing CD8+ and CD4+ T cells was calculated as a percentage of total T cells. **A)** proportion of β7 expressing CD8+ T cells at baseline and after two and six weeks of treatment. **B)** proportion of β7 expressing CD4+ T cells at baseline and after two and six weeks of treatment. Mean and SD are displayed for normally distributed data sets, while median and IQR are displayed for non-normally distributed data sets. A RM one-way ANOVA for normally distributed data sets, while a Friedman test was used to compare two groups of paired data that were non-normally distributed.

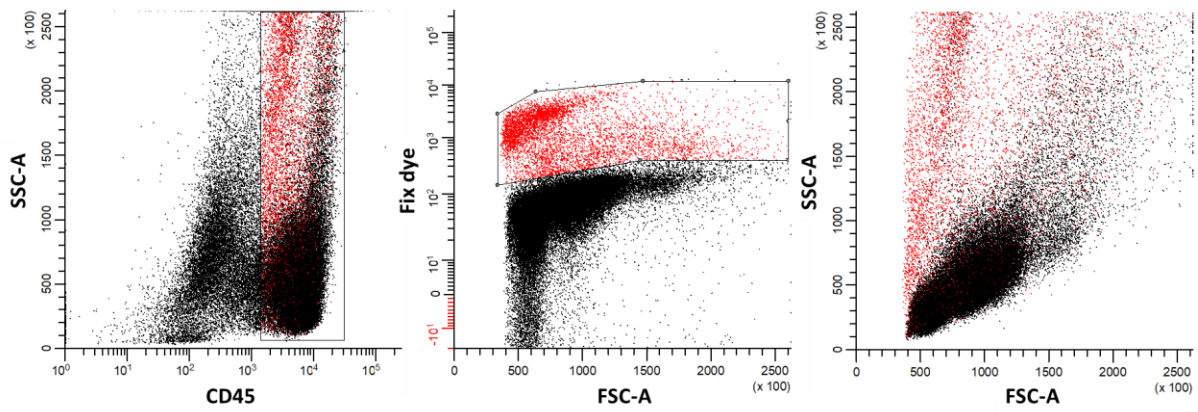

Appendix 12: Measuring cell viability. LPMCs extracted from colonic biopsies from a non-IBD patient (n=1) were labelled with anti-CD45 antibody before adding the viability dye at a final dilution of 1:10,000 and incubated for 30min in the dark. The sample was then acquired on the flow cytometer.

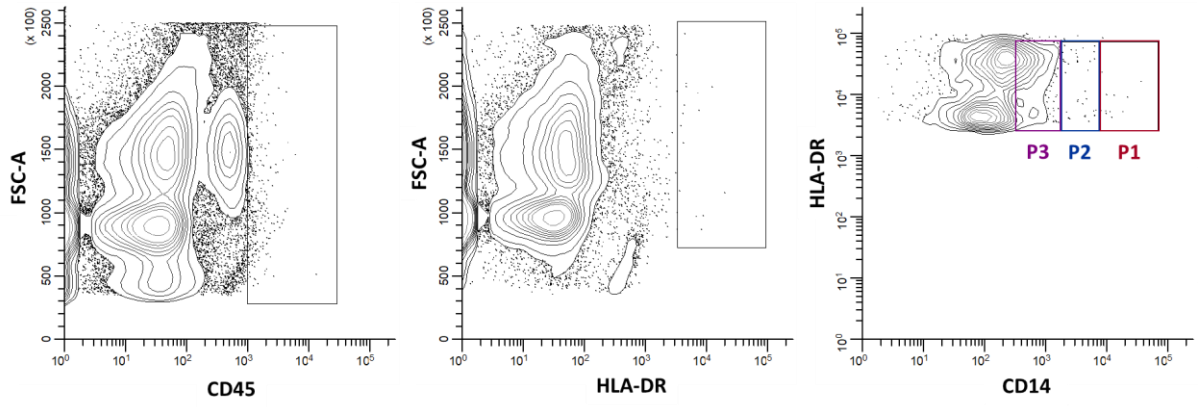

Appendix 13: Representative flow cytometry plots of isotype controls. LPMCs extracted from colonic biopsies from a non-IBD patient were labelled with corresponding isotype controls for anti-CD45, anti-HLA-DR, and anti-CD14 antibodies. The sample was then acquired on the flow cytometer.

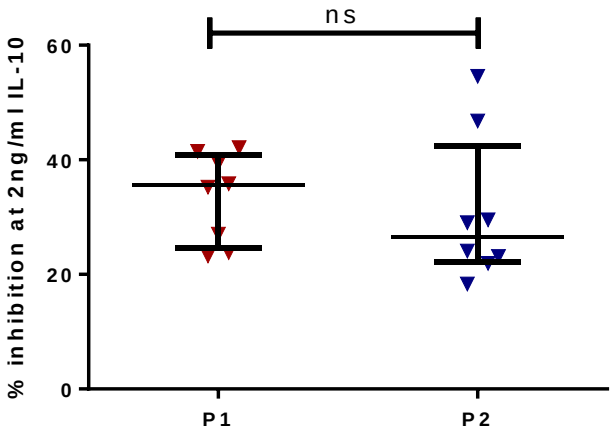

Appendix 14: Raw values for IL-10 response in Mo/moMϕs from non-IBD colon. LPMCs extracted from endoscopic biopsies from non-IBD patients (n=8) were stimulated with 1ng/ml LPS and 2ng/ml IL-10 for three hours in the presence of monensin and ADAM17 inhibitor (TMI-005). The LPMCs were labelled anti-CD45, anti-HLA-DR, and anti-CD14 antibodies to distinguish the intestinal Mo/moMϕs, fixed, permeabilised, and stained intracellularly for TNFα before acquiring on the flow cytometer. Percentage inhibition of TNFα production at 2ng/ml IL-10 was calculated. Median and IQR is displayed. A paired Wilcoxon tests was used to compare two groups of non-normally distributed data.

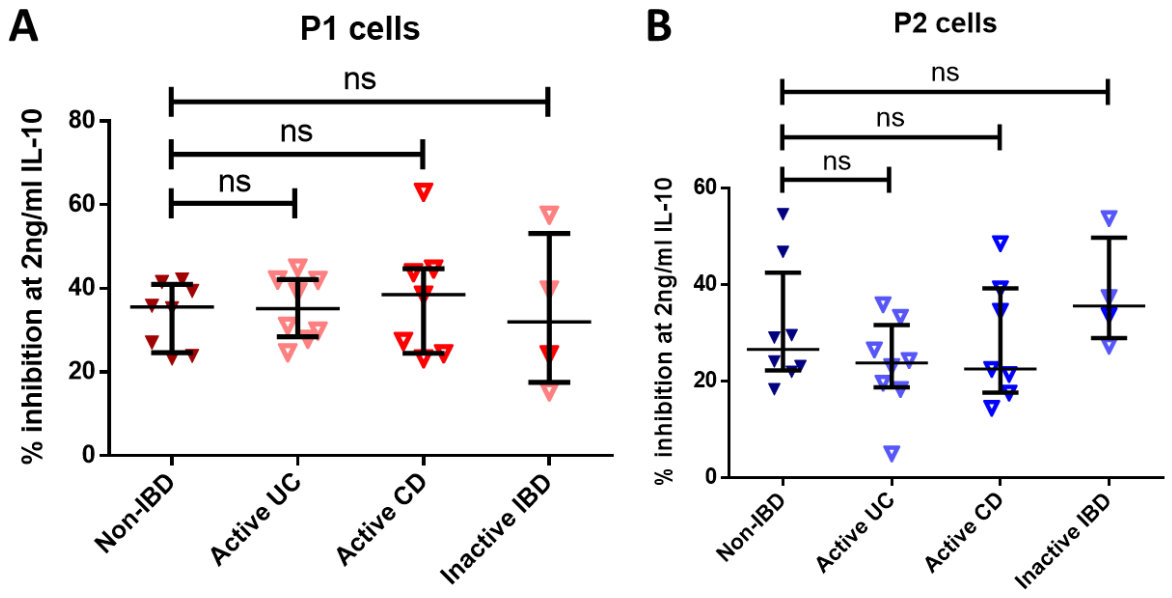

Appendix 15: Raw values for IL-10 response in Mo/moMϕs from non-IBD and inflamed IBD colon. LPMCs extracted from endoscopic biopsies from non-IBD patients (n=8), UC patients with active disease (n=8), CD patients with active disease (n=7), and four patients in remission (three UC and one CD) were stimulated with 1ng/ml LPS and 2ng/ml IL-10 for three hours in the presence of monensin and ADAM17 inhibitor (TMI-005). The LPMCs were labelled anti-CD45, anti-HLA-DR, and anti-CD14 antibodies to distinguish the intestinal Mo/moMϕs, fixed, permeabilised and stained intracellularly for TNFα before acquiring on the flow cytometer. Percentage inhibition of TNFα production at 2ng/ml IL-10 was calculated for **A)** P1 and **B)** P2. Median and IQR is displayed. Data were analysed statistically by Kruskal-Wallis test.

	CD	UC
n = 19	9	10
Active disease		
n = 15	8	7
Inactive disease		
n = 4	1	3
Medication		
Steroids	3	
IM	14	
Anti-TNFα	5	
None of the above	2	

Appendix 16: Patient data. Several IBD patients were receiving combination therapies at the time of biopsy collection.

Limitations

Chapter 3:

- Some of the negative findings were not verified (n=1).
- Did not measure soluble CD16 or CD14.
- Did not measure TNFα production as secretion levels by ELISA.

Chapter 4 & 5:

- IL-10Rα expression was measured as the subunit specific to the IL-10R. However, IL-10Rβ is the signal transducer, and therefore its expression level could have an impact on IL-10 signalling.
- STAT3 phosphorylation was measured at 15 minutes, however, the kinetics were not investigated using timepoint analysis in the monocytes. The peak of STAT3 phosphorylation could have occurred earlier and differed between the monocyte subsets.
- Baseline *SOCS3* mRNA expression was used as a potential surrogate measure for protein levels in the monocyte subsets. It would be informative to also compare the level of IL-10 induced *SOCS3* mRNA expression between the monocyte subsets.
- A reduced response to IL-10 in classical monocytes was observed in IBD patients. However, the study consists of small numbers and the magnitude of the difference in response to IL-10 between healthy individuals and IBD patients was also relatively small, therefore, a larger cohort is required to verify this finding.
    - The genome of patients included in the cohort were not sequenced to test whether the donors express genetic variants along the IL-10R pathway that could impact IL-10 response. However, a reduced response to IL-10 was a common feature of the IBD patients studied here, such genetic variation is unlikely to be a significant contributor to the differences observed.

Chapter 6:

- A difference in the distribution of P1 and P2 was observed between the colon and the ilium therefore, biopsies were restricted to the colon. However, there could be a gradient from the ascending colon to the rectum. The majority of biopsies from UC patients were taken in the sigmoid colon, whilst from the CD patients the majority of biopsies were taken from the ascending colon, which could account for the difference in distribution of P1 and P2 between CD and UC patients. However, non-IBD biopsies were taken from across the colon, and therefore, a gradient cannot account for the difference in distribution of P1 and P2 between non-IBD and CD patients.
- LPMCs were not harvested using trypsin, therefore, cells were likely to have been lost due to adherence to the plate. There could be variation in the adherence of P1 and P2, as well as between non-IBD and IBD samples.
- Live/dead stain was not included in the panel.